DELHI POLYTECHNIC
LIBRARY

CLASS NO. 621.4

BOOK NO. ~~St 24 I~~ STA

ACCESSION NO. 15,105

INDUCTION HEATING

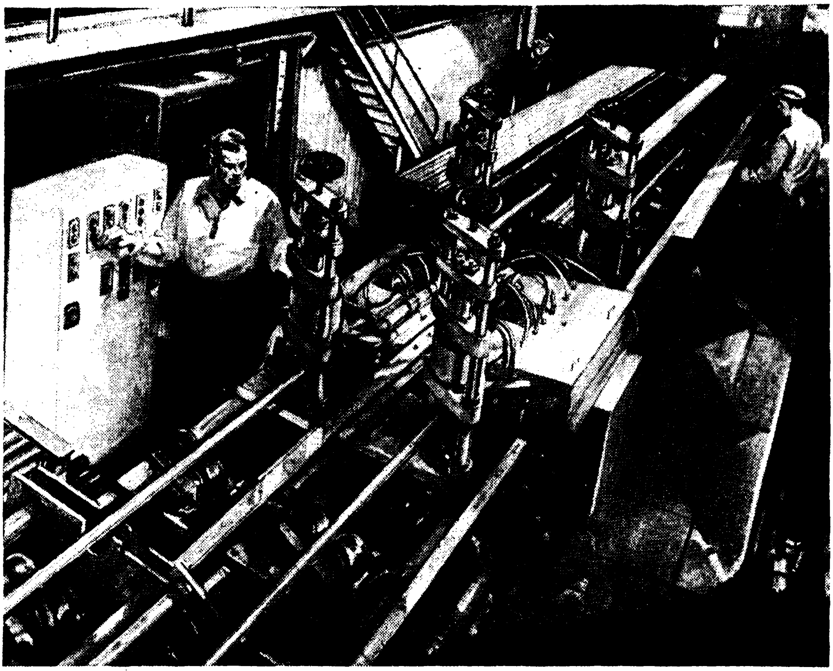

An application of induction heating with 9,600 cycles in the continuous heat-treatment of cold-finished steel bars. (*Jones and Laughlin Steel Corporation.*)

INDUCTION HEATING

by

N. R. STANSEL

Fellow, American Institute of Electrical Engineers
Author of "Industrial Electric Heating"
Electric Heating and Welding, Section 18, of Knowlton, "Standard Handbook for Electrical Engineers"
Electric Furnaces in Section 7 of Marks, "Mechanical Engineers' Handbook"

FIRST EDITION

McGRAW-HILL BOOK COMPANY, Inc.
NEW YORK TORONTO LONDON
1949

INDUCTION HEATING

Copyright, 1949, by the McGraw-Hill Book Company, Inc. Printed in the United States of America. All rights reserved. This book, or parts thereof, may not be reproduced in any form without permission of the publishers.

THE MAPLE PRESS COMPANY, YORK, PA.

PREFACE

The aim of this book is to present the electrical and thermal principles of the use of eddy currents for heating service and to show how these principles are applied in practice. The text is supported by measurements to provide a factual basis for the work.

The derivations of the equations in the text are not given. Those interested in the theoretical basis of induction heating can find these derivations in the references. Practically every equation is accompanied by a curve to show visually the consequences of varying its parameter.

The most important data required for applications of induction heating are the resistivity values of metals at the temperatures specified for heat applications. An effort to supply at least a part of this need has been made. There are many gaps in data of this kind, particularly in the field of alloys.

The frequency for an induction-heating application is a joint technical and economic problem. The economic component of this problem is expressed herein as the use of certain frequencies which, because of usage, are termed standard frequencies for this service.

The importance of the design of the primary coil, inductor, or work coil, of induction-heating apparatus is emphasized from the viewpoint of practice. Theoretically this design is individual, yet a coil of good design is effective over a considerable range of operating conditions.

The primary merit of induction heating is the development of heat within the mass of the charge. It thus provides a new technique to tackle old problems in the use of heat in manufacturing.

The coreless induction furnace for melting metals—the first large-scale use of induction heating with frequencies above 60 cycles—is one of the few industrial tools in which no change in design has been found to be either necessary or desirable. This correctness of design and the experience gained by its use made it comparatively easy to extend induction heating to many other applications.

The courtesies of the companies that supplied the photographs for illustrations are acknowledged in the legends. The author expresses his appreciation of the cooperation of the engineers of the following organizations: Ajax Electrothermic Corporation, Trenton, N.J.; Ajax Electric Furnace Corporation, Philadelphia, Pa.; Ajax Engineering Corporation; Trenton, N.J.; The Budd Company—Induction Heating *Division, Detroit, Mich.; The Ohio Crankshaft Company—Toco* Division, Cleveland, Ohio; The Scomet Engineering Company, New York, N.Y.; and Chase Brass and Copper Company, Inc., Waterbury, Conn. It is also a pleasure to record the interest and helpfulness of the author's associates in the General Electric Company.

N. R. Stansel

Schenectady, N.Y.
April, 1949

CONTENTS

PREFACE v

CHAPTER I. INTRODUCTION 1

Historical Note—Assemblies for Induction Heating—Shape of Charge—The Magnetic Field—Flux and Current Distributions—Cardinal Relations—Reference Dimension—Index Ratio—Eddy-current Watts—Frequency—Standard Frequencies—Service.

CHAPTER II. HEAT 10

Temperature Scales—Methods of Heating—Heat Cycle—Effects of Heat—Conductivity—Resistivity—Metals—Alloys—Nonferrous Alloys—Iron and Carbon Steels—Carbon—Glass—The Magnetic Property—Magnetization Curves—Permeability—Effect of Hardness—Thermal Properties—Thermal Conductivity—Thermal Diffusivity—Heat Development—Magnetic Charges—Hysteresis and Frequency—Hysteresis and Temperature—Hysteresis in Induction Heating—Eddy-current Watts—Shape Factors—Shape Effect—Directional Effect—Cross-flux Watts—Heat Concentration—Current Density—Heating Density—Volume V_p—Heat Development in Volume V_p—Temperature Rise—Mass Effect—Surface-volume Ratio—Equilibrium Temperature—Log of a Heat Cycle—Heat Content—Heat Loss.

CHAPTER III. INDUCTION HEATERS—CLASS A SERVICE 48

Charges—Rated Index Ratio—Primary Coils—Examples of Coils—Instrumentation—Auxiliary Devices—Illustrations.

CHAPTER IV. CIRCUIT EQUATIONS 61

Single-phase Load—Circuits—Equations—Resistance—Primary Circuit—Optimum Radial Thickness—Loaded Coil—Capacitance—Secondary Circuit—Effective Resistance, R—Reactance—Primary Circuit—Effect of Charge—Effective Reactance, X—Effective Impedance, Z—Electrical Efficiency—Conversion Efficiency—Number of Turns—Corrective Factors—Hollow Cylindrical Charge—Charge with a Rectangular Section—Resistance—Primary Circuit—Secondary Circuit—Effective Resistance—Volt-amperes—Primary Circuit—Secondary Circuit—Effective Volt-amperes—Calculations—Measurements—Data—Examples.

CHAPTER V. CIRCUIT ANALYSIS 84

Charge Resistivity—Secondary Resistance—Effective Values—Power Factor—Electrical Efficiency—Solid Cylindrical Charge—Charge with Rectangular Section—Hollow Cylindrical Charge—Power—Basic Principle—Heating a Nonmagnetic Charge—Air-gap Ratio—The Magnetic

Property—Heating Magnetic Charges—Frequency—Effective Values—Power Ratio—Power Factor—Electrical Efficiency—Thin-wall Tubes—Base Frequency—Current—Voltage—Volt-amperes.

CHAPTER VI. APPLICATIONS—CLASS A SERVICE 107

Operating Conditions—Thin and Thick Bodies—Mass Heating—Selection of Frequency—Lower Limit Frequencies—Standard Frequencies—Protection—Plant Economics—Heating Rates—Internal Stress—Typical Heating Rates—Power Density—Heating Metals for Forming—Forging—Upsetting—Surface Heating—Surface Hardening—Internal Hardening—Illustrations of Surface Hardening—Installations, Class A Service—Brazing and Soldering—Degassing Tubes—Heating Aluminum for Upsetting—Heating Steel for Forging—Heating Steel for Hardening and Tempering—Internal Heating.

CHAPTER VII. MELTING METALS—CLASS B SERVICE 132

Metal Classification—Charges—Pouring Temperatures—Melting Furnaces—Coreless Induction Furnace—Crucibles—Primary Coils—Frame—Platform Furnaces—Floor-level Furnaces—Lift-coil Furnaces—Vacuum Furnaces—Standard Furnaces—Floor Plan—Installations—Service—Special Services—Artificial Atmospheres—Operation—Operating Periods—Charging—Filling Coefficient—Aftercharging—Stirring—Melting Rates—Losses—Conversion Efficiency—Over-all Efficiency—Operating Data—Electrical Features—Circuit—Special Features—Frequency—Standard Frequencies—Rated Index Ratios—Power-time Relation—Submerged Resistor Furnace—Operation Data—Melting Aluminum—Continuous Melting Furnaces.

CHAPTER VIII. POWER CIRCUIT CONDUCTORS—MACHINE FREQUENCIES . . 160

Heating of Conductors—Alternating-current Ratings—Insulated Conductors—Resistance and Inductance—Resistivity of Copper—Alternating-current Resistance—Inductance—Solid Round Conductors—Hollow Round Conductors—Hollow Square Conductors—Comparison of Hollow Round Conductors and Hollow Square Conductors—Flat Bars on Edge—Coaxial Conductors—Electrical Separation of Bare Conductors—Selection of Conductors.

REFERENCES 183

APPENDIXES 185

INDEX 209

CHAPTER I

INTRODUCTION

Induction heating is the use of the principle of electromagnetic induction for heating service. The mass to be heated, which must be of conductive material, is exposed to an alternating (or varying) magnetic flux. The currents thus induced in the mass flow wholly within the mass. Such currents are termed eddy currents. Hence, the term eddy-current heating sometimes applied to this use of the i^2r effect.

Historical Note. The background of induction heating was established by the contributions of Oliver Heaviside[1]* (1884) and of J. J. Thomson[2] (1892) to the theory of the eddy-current phenomenon.

Heaviside considered the development of heat by eddy currents in the core of an alternating-current solenoid. He showed that there is a transformation from the electromagnetic energy of the coil to heat in the core and that this transformation is directional, normal to the directions of the alternating magnetic flux. The exposition is somewhat difficult to follow. The excerpt below is indicative of the method of treatment.

"The transmission of energy takes place from places of greater to places of less force irrespective of sign, and the rate of transference is proportional to the rate of decrease of the density of the magnetic energy in the direction of transference. This remarkable simple property, which applies to every part of the core at every moment according to which the transmission of magnetic energy whilst induced currents are lasting is determined solely by the space variation of its density, is not a general property of induction in conductors."

Thomson's main interest in eddy currents was the loss caused by these currents in the cores of transformers. He stated:

"In my paper 'On the Discharge of Electricity through Exhausted Tubes without Electrodes' I had occasion to investigate the absorption of energy by a piece of iron placed near a primary coil through which the rapidly alternating currents produced by the discharge of a Leyden

---

* Superior numbers refer to items in the list of cited references beginning on p. 183.

jar were passing. In the following paper I apply this investigation to determine the rate of heat production by eddy currents in the iron plates of an ordinary transformer."

The opposite viewpoint, the use of eddy currents for heating service, is expressed in early proposals and patents. However, but little progress in this art was made until 1916 when E. F. Northrup[3] began the development of the coreless (or high-frequency) induction furnace for metal-melting service. Thus a new tool for the metallurgical industry was created. An outgrowth of that development is the use of induction heating for many other applications of heat to metals and alloys.

ASSEMBLIES FOR INDUCTION HEATING

The term assembly as used herein denotes an arrangement of parts for the exposure of the mass to be heated—the charge—to alternating (or varying) magnetic flux. There are a number of these assemblies in use. Those most common are

1. A coil around the charge as indicated in Fig. 1. If the charge is to be melted, a refractory container (crucible) is required and the coil is placed around the container.

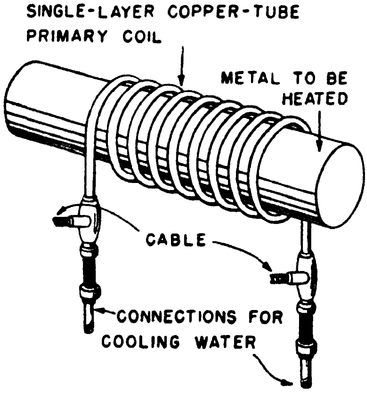
SINGLE-LAYER COPPER-TUBE PRIMARY COIL
METAL TO BE HEATED
CABLE
CONNECTIONS FOR COOLING WATER

Fig. 1. Typical assembly for induction heating.

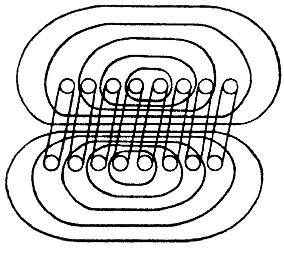

Fig. 2. Conventional diagram of the magnetic field of a coil.

2. A coil in the bore of a hollow charge.
3. A coil with the charge adjacent to the side or to one end.

Shape of Charge. A charge of any shape can be heated by eddy currents. Shape alone does not affect the principle involved. It only introduces the complication of its geometry.

The Magnetic Field. The conventional diagram of Fig. 2 represents the magnetic field established by a current in a coil. A photograph of a field thus produced is shown in Fig. 3.

It will be noted that the direction of the magnetic flux within a coil is parallel, approximately, to the longitudinal axis of the coil. Thus, with a charge in a coil, as indicated by the sectional diagram of Fig. 4, the directions of alternating magnetic flux are likewise parallel to the lateral surface of the charge. (This parallelism is sometimes expressed with reference to induction heating by the term longitudinal flux.) The resultant eddy currents in the charge will, from symmetry, be circles whose centers are on the longitudinal axis of the coil and charge.

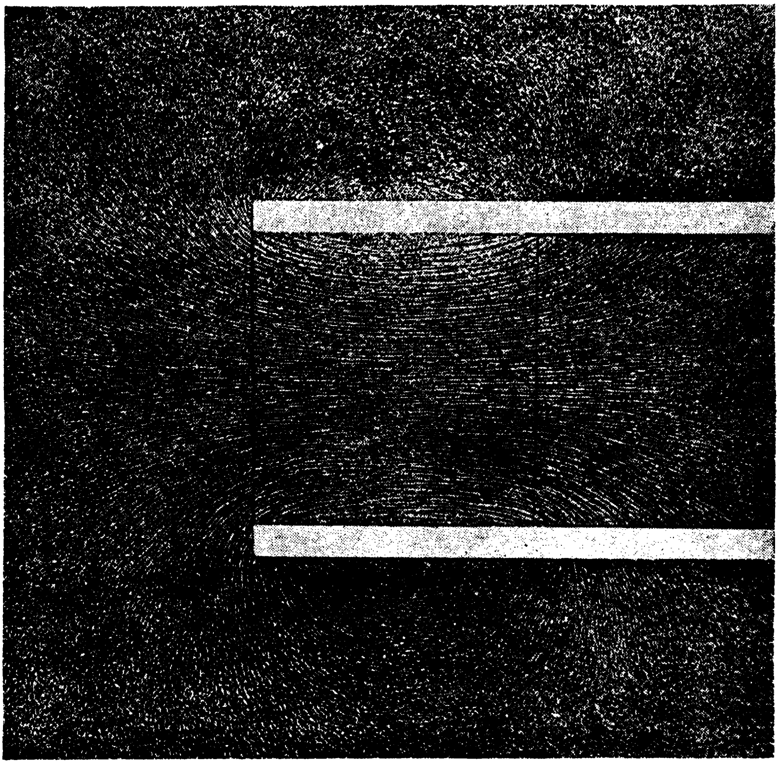

FIG. 3. The magnetic field of a coil as shown by iron filings. (*Benische.*)

Flux and Current Distributions. The currents induced in the charge will alter the strength of the magnetizing force. Hence, this force will have different values in the mass at different distances from and normal to its lateral surface. Consider a conducting mass of either circular or rectangular section, Fig. 5*a* or 5*b*, and assume that there is an alternating magnetic flux at and parallel to the lateral surface of the mass.

Let Φ_m denote the value of this flux at the lateral surface of the mass. This flux induces an emf e_w in the elementary circuit dx which, for a sinusoidal wave form, is represented by a vector lagging 90 deg behind the flux vector (see Fig. 6). The emf e_w produces a current i_w which in turn produces a flux Φ_w. Hence, the eddy-current circuit possesses inductance corresponding to the flux Φ_w, and the current i_w lags behind the voltage e_w.

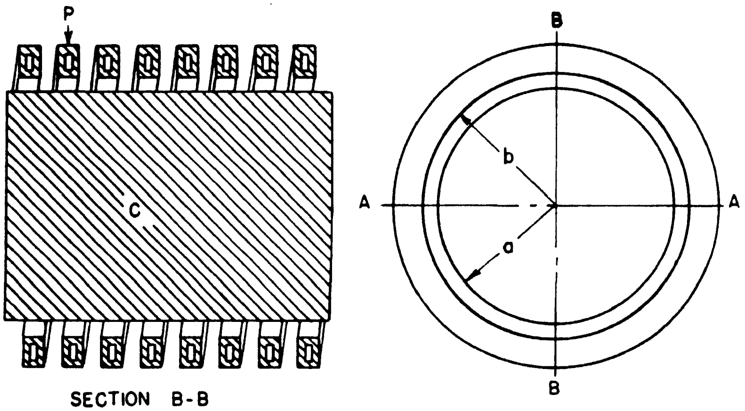

FIG. 4. Section of an assembly with a solid cylindrical charge.

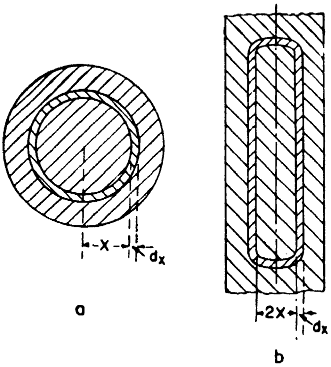

FIG. 5. Sections of charges (see Fig. 6).

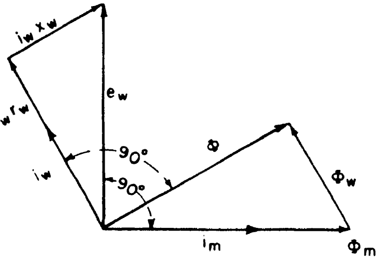

FIG. 6. Vector diagrams of alternating magnetic flux, current, and voltage in a conducting mass (see Fig. 5).

The resultant flux of Φ_m and Φ_w is Φ. Thus the effect of all the eddy currents in the mass is to cause (1) the resultant flux to lag behind the magnetizing current i_m and (2) the flux to be reduced from Φ_m to Φ.

The diagrams of Figs. 5 and 6 together with the brief explanation thereof are from a more complete exposition of the theory of eddy currents in the 1913 edition of "Theory and Calculation of Electric Currents," by La Cour and Bragstad, published by Longmans, Green & Co. Inc.

This progressive reduction of alternating magnetic flux in a mass is illustrated by Fig. 7, a reproduction from a paper by Ewing.[4] Sections of three thicknesses of steel sheets are represented. The lengths of the sheets are parallel to the directions of the alternating magnetic flux at the surfaces of the sheets. The symbols are

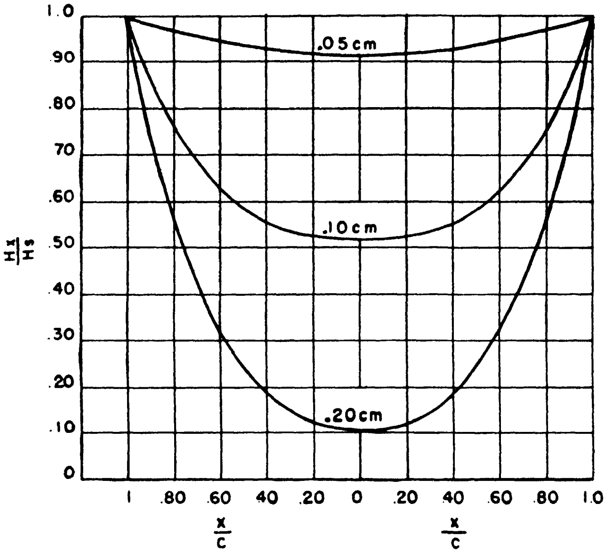

FIG. 7. Intensities of alternating magnetic flux across the sections of steel sheets. Frequency, 100 cycles. (*Ewing.*)

c = one-half the sheet thickness
H_x = intensity of magnetizing force within mass at various distances x from its longitudinal axis
H_s = intensity of magnetizing force at surfaces of sheets

The graphs of Fig. 7 show the relative intensities of the magnetic flux across the sections of the sheets. For example, at $x = 50$ per cent of one-half the thickness of the 0.20-cm sheet, the flux intensity is 25 per cent of the surface intensity.

Thus, with a given frequency the intensity of the magnetic flux across the sheet section varies with the thickness of the sheet. This distribution in the case of the 0.05-cm sheet is nearly uniform. That of the 0.10-cm sheet is much less so, and the flux in the 0.20-cm sheet is confined largely to the near-surface zones.

Cardinal Relations. The factors that determine the distribution of alternating magnetic flux and of the resultant eddy currents in the mass of a charge are

1. The electric and magnetic properties of the material
2. The frequency
3. The dimension of the charge that is normal to the directions of the alternating magnetic flux. This dimension, termed the base dimension of the charge, for different shapes of charges is as follows:

Solid cylindrical charge = radius
Charge with rectangular section = one-half the thickness
Hollow charge = wall thickness

The relations of these factors are expressed by the four equations that follow.

Reference Dimension. This dimension is a fraction of the base dimension and is measured from the lateral surface of the charge, as indicated in Fig. 8. The value of this dimension, designated by the symbol p, is given by the ratio

$$p = \frac{\sqrt{\rho_a 10^9}}{2\pi \sqrt{2} \sqrt{\mu f}} \quad \text{cm} \qquad (1)$$

or

$$p = \frac{3{,}560 \sqrt{\rho_a}}{\sqrt{\mu f}} \quad \text{cm} \qquad (1a)$$

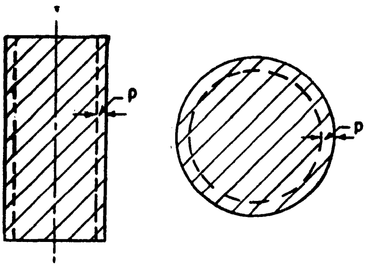

FIG. 8. Reference dimension diagrams.

where ρ_a = resistivity of the material of the charge, ohm-cm^3
μ = permeability of the material of the charge
f = frequency, cycles

Index Ratio. This term denotes the ratio of the base dimension and the reference dimension of the charge; thus:
Solid cylindrical charge (Fig. 9),

$$\text{Index ratio } \Delta = \frac{a}{p} \qquad (2)$$

Hollow charge (Fig. 9),

$$\text{Index ratio } \Lambda = \frac{\sqrt{2}\, t}{p} \qquad (3)$$

Charge with rectangular section (Fig. 9),

$$\text{Index ratio } \nabla = \frac{\sqrt{2}\, c}{p} \qquad (4)$$

These ratios are the parameters of the equations of induction-heating circuits according to shape of the charge in each case.

Eddy-current Watts. Thomson[2] showed that a near-uniform distribution of alternating magnetic flux in the core of a transformer is necessary for a low value of eddy-current watts in the core and that this uniformity requires that the core be made up of thin sheets (laminations). Ewing[4] gave values of the eddy-current watts in steel sheets (the steel of his day) with a given frequency. These data are presented in Table 1. The corresponding values of the index ratio are added to his data. The values of the table should be compared with the flux distribution curves of Fig. 7.

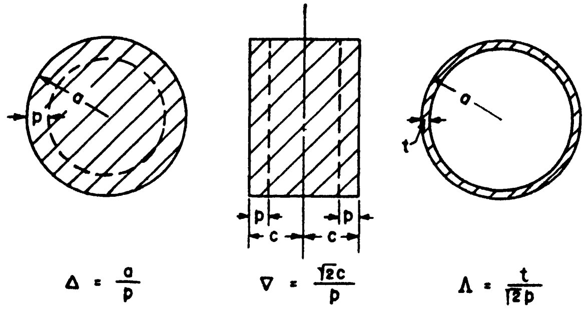
p
a
p
p
c
c
a
t
$\Delta = \frac{a}{p}$
$\nabla = \frac{\sqrt{2}c}{p}$
$\Lambda = \frac{t}{\sqrt{2}p}$

FIG. 9. Index-ratio diagrams.

Thus the use of thin sheets for transformer cores was established. This is expressed here with reference to Table 1 as the use of a low value of the index ratio.

TABLE 1. EDDY-CURRENT WATTS IN STEEL SHEETS

Frequency = 100 cycles
Flux density = 4,000 gausses
Resistivity = 10×10^{-6} ohm-cm^3
Permeability = 2,000

Thickness of sheet, cm	Watts per lb	Index ratio
0.20 (0.079 in.)	3.35	5.70
0.15 (0.059 in.)	2.50	4.20
0.10 (0.0395 in.)	1.41	2.83
0.05 (0.0197 in.)	0.39	1.41
0.025 (0.010 in.)	0.097	0.70

The investigations of Thomson[2] and Ewing[4] also established the principle of a nonuniform flux distribution, which is a comparatively high value of the index ratio, for induction heating.

Frequency. If the object is to minimize the eddy-current watts with a given frequency in a metal part, there may be a choice of materials and a choice of the base dimension of the part; for example, in the selection of the steel and of the thickness of the sheets for the core of a transformer.

In induction heating the base dimension of the charge, its resistivity, and its permeability are given values. Hence, frequency is the only factor of choice to obtain the needed comparatively high value of the index ratio.

Standard Frequencies. It will be found that there is in each case a range of frequencies from which to make the technical selection. Economics dictate the use of a standard frequency within this range. Thus each application of induction heating is (1) a study of the technical requirements and (2) the selection of a standard frequency for the service.

The frequencies in general use for induction heating are

1. *Rotating Machines.* Frequencies of 960, 3,000, and 9,600 cycles are used with generators driven by 60-cycle motors. These frequencies because of usage, are termed standard frequencies. Other machine frequencies above 60 cycles in use to some extent for this service are 480, 600, and 2,000 cycles.

2. *Spark-gap Apparatus.* This designation refers to apparatus that produces damped oscillations by a discharge across a gap. The nominal frequency is usually within the range 20 to 80 kilocycles. The design is such that there is considerable latitude in the selection of the nominal frequency, and no one frequency within the range noted can be considered as standard.

3. *Electric Oscillators.* Economics and the technique of induction heating with electronic frequencies usually dictate a frequency within the range 200 to 500 kilocycles. Around 450 kilocycles is regarded as more or less standard. An exception is equipment with mercury-vapor tubes, which is limited to frequencies below 2,000 cycles.

Inasmuch as the designation standard frequency is based on economics, any frequency that is practicable and not now termed standard will become a standard frequency when its use justifies that designation.

Service. The unique feature of induction heating is the use of the i^2r effect (internal heat development) without terminals attached to, or electrodes in contact with, the charge. That feature and the stipulation that the charge be a conductive material define generally the field of this method of heating.

The following classification is used herein:

Class A Service. Heating conductive materials (mainly metals and alloys) to temperatures below the melting points. The subdivisions of this service are (1) mass heating, such as heating metals for forging. The term "through heating" also applies to this service. The object is a uniform temperature throughout the mass of the charge. (2) Surface heating, where the heat effect is required only in the near-surface zone of the charge. The term "zonal heating" also is applicable. The principal use of surface heating is for hardening steel. Equipments for Class A service are termed induction heaters.

Class B Service. Melting metals and alloys. Equipments for this service are termed induction furnaces.

CHAPTER II

HEAT

In most industrial uses of heat there is an optimum temperature for each application. The importance of this exactness varies with the nature of the material of the charge and with the object of the heat application.

Temperature Scales. Both the centigrade and the Fahrenheit scale are in general use. The relations are

$$\text{Temperature C} = \frac{\text{F} - 32}{1.80} \qquad (5)$$

$$\text{Temperature F} = 1.80\text{C} + 32 \qquad (6)$$

A conversion chart for these scales is given in Fig. 10.

Absolute Temperatures.

Centigrade scale,

$$K = C + 273 \qquad \text{deg abs} \qquad (7)$$

Fahrenheit scale,

$$R = F + 460 \qquad \text{deg abs} \qquad (8)$$

Methods of Heating. The two methods of heating with reference to handling the charge are

Stationary Heating. The charge is stationary during the heat application. The term batch heating is also in current use.

Continuous Heating. The charge is heated while in motion. The term progressive heating is another term for this method.

Heat Cycle. This term denotes the time period during which the charge is exposed to the magnetic flux. In stationary heating, the heat cycle corresponds to current on and current off. In continuous heating, the heat cycle is the time period during which a unit lateral-surface area of the charge is exposed to the magnetic flux.

Effects of Heat. We are concerned mainly with the effects of heat on the electric, magnetic, and thermal properties of materials that are conductors.

Conductivity. The unit of electrical conductivity is the reciprocal of the unit of resistivity, that is, reciprocal ohm-centimeter cube.

The term conductor is applied to materials that have conductivities

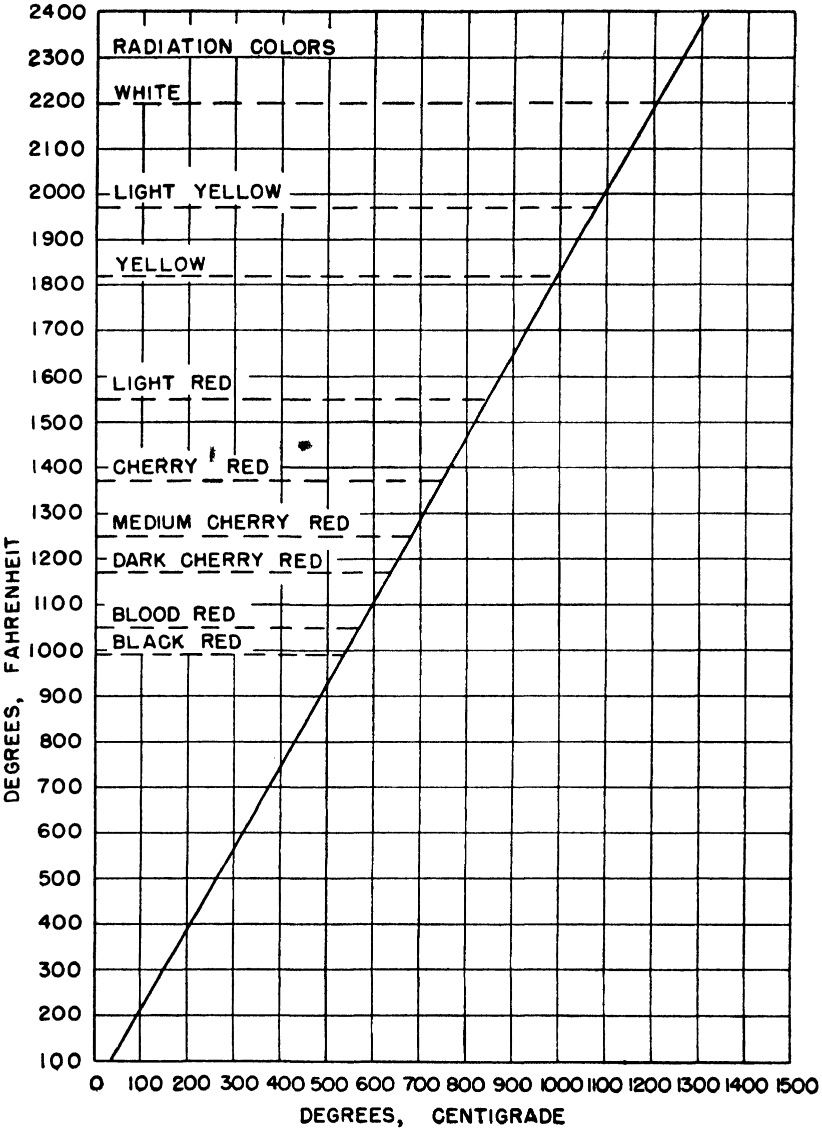

FIG. 10. Temperature conversion chart.

equal to or greater than 1,000 reciprocal ohm-centimeter cube. The scale begins with graphitic carbon (graphite), which has a conductivity at room temperature around this limit value, and extends through the metals. The high-conductivity metals are silver, copper, gold, and aluminum. The low-conductivity common metals are mercury, antimony, and lead.

RESISTIVITY

Metals. The resistivities of the metals while in the solid state increase with rise of temperatue, that is, the temperature coefficients of resistivity are positive. The rate of increase of resistivity may or may not be linear, depending on the particular metal and on the range of temperature under consideration. An illustration is found in the resistivity-temperature relation of nickel shown in Fig. 11.

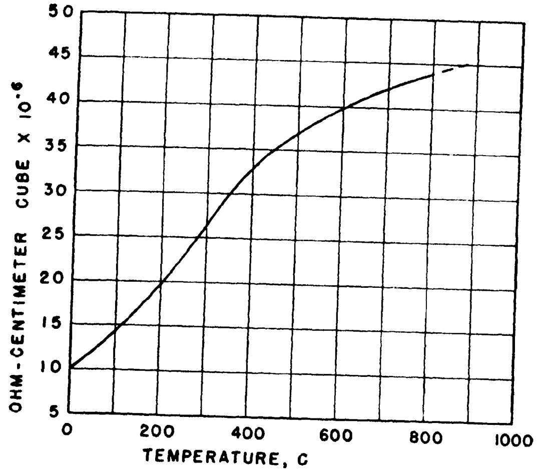

FIG. 11. Resistivity-temperature curve of nickel.

There are three types of behavior of metals at and above the melting points:

1. The resistivity approximately doubles and the resistivity temperature coefficients above the melting point are positive. Examples are aluminum, copper, and lead. This behavior is illustrated by the resistivity temperature graphs of aluminum and copper shown in Fig. 12.

2. The resistivity about doubles, and the resistivity temperature coefficients above the melting point are at first negative followed with rising temperature to positive. Examples are zinc and cadmium.

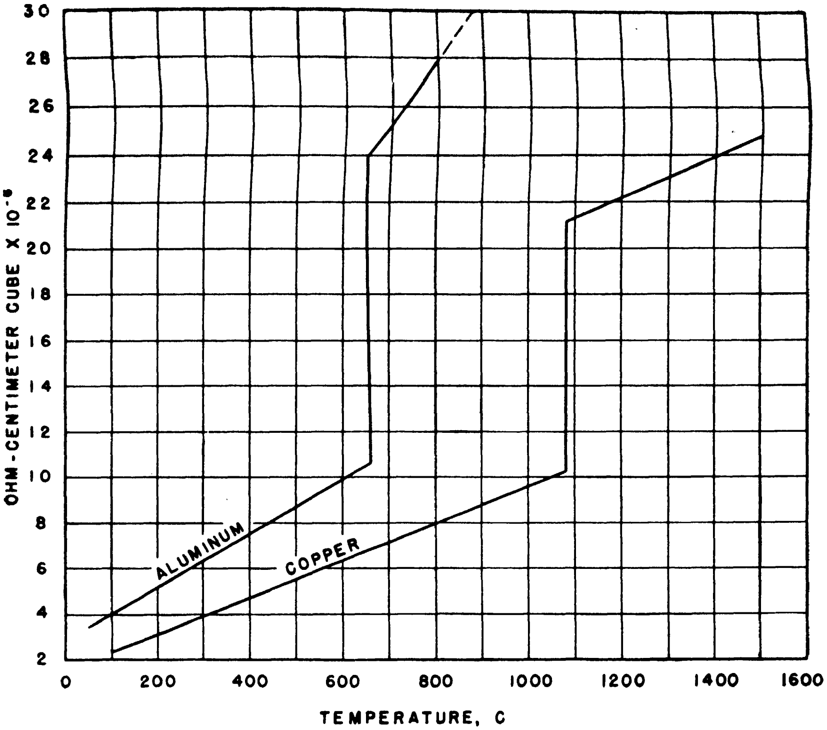

FIG. 12. Resistivity-temperature curves of aluminum and copper.

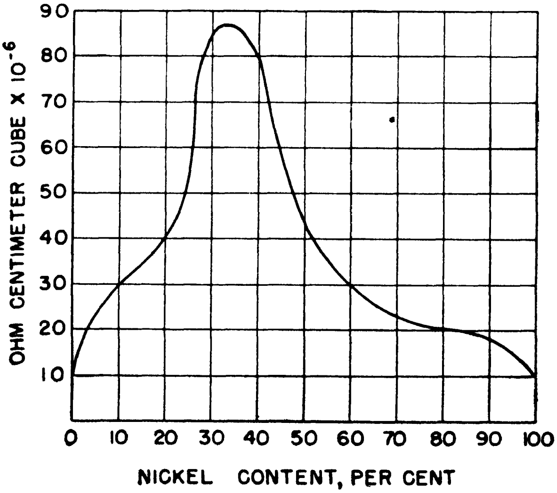

FIG. 13. Resistivity-composition relations of the iron-nickel alloy system.

3. The resistivity abruptly decreases and thereafter steadily increases. Examples are antimony and bismuth.

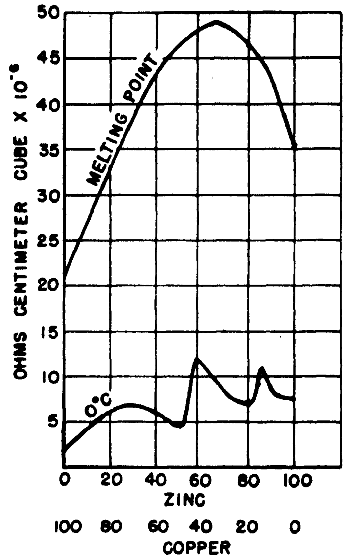

Fig. 14. Relative values of the resistivities of the copper-zinc alloys.

Alloys. The resistivity of an alloy at a given temperature depends on the natures of the component metals and on their proportions. Each alloy is an individual study. This is illustrated by the resistivity composition diagram of the iron-nickel alloy system shown in Fig. 13; also by the graphs of the relative values of the resistivities of copper-zinc alloys in the solid state (room temperature) and in the liquid state, as determined by Tama,[5] Fig. 14.

In many cases, the resistivity of an alloy in the solid state depends on its prior heat-treatment. An example is the effect of hardening steel, by heating and quenching, on its resistivity as given below. The following are average values of the resistivity of four bars of 1.11 to 1.25 carbon steel at room temperature:

$$\text{Before hardening} = 18.73 \times 10^{-6}\ \text{ohm-cm}^3$$
$$\text{After hardening} = 27.7 \times 10^{-6}\ \text{ohm-cm}^3$$

The effect of a heat-treatment, generally annealing, on the resistivity of a nonferrous alloy is variable, depending on the particular alloy.

Cold working increases the resistivity of a metal at or near room temperature. This applies likewise to alloys. As a rule this increase of resistivity disappears with heating, but there are some exceptions. For example, the resistivity of a cold-worked nickel-chromium alloy is increased to some extent by heating.

Thus stated, resistivity values of a given alloy may vary, sometimes widely, depending on the conditions pertaining to prior heat-treatment and to cold working.

Nonferrous Alloys. Data on the resistivities of nonferrous alloys above room temperature are few. One example is the resistivity temperature curve of a copper-zinc alloy with the composition 63 Cu, 34.58 Zn, 2.42 Sb, from data by Northrup[6] shown in Fig. 15. It will be noted that the resistivity values extend beyond the melting point, an unusual case.

Some additional data on the resistivities of nonferrous alloys are given in Appendix *B*.

Iron and Carbon Steels. The resistivity temperature curves of iron and 1 per cent carbon steel in the solid state are shown in Fig. 16. The resistivities of this class of steels with intermediate carbon contents lie between the values of these curves.

Effect of Grain Size. The resistivity of a steel at room temperature decreases to some extent with decrease of grain size. This is illustrated by the two following photomicrographs (Figs. 17*a* and 17*b*) and measured values of resistivity of a SAE 1045 steel.

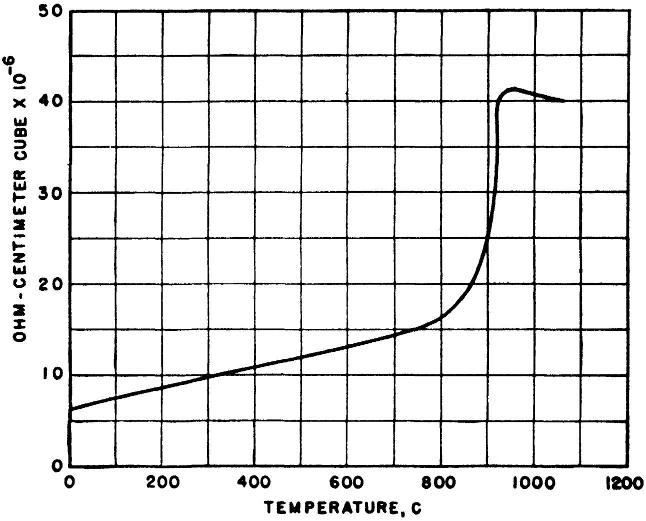

FIG. 15. Resistivity-temperature curve of a brass (see text).

Figure 17*a* shows the steel as received. The average grain size is about No. 3 ASTM. Resistivity at room temperature is 20×10^{-6} ohm-cm^3.

Figure 17*b* shows the steel after being annealed. Average grain size is about No. 8 ASTM. Resistivity at room temperature 18.9×10^{-6} ohm-cm^3.

Stainless Steel (18:8). The resistivity temperature curve of a specimen of this steel in the solid state is shown in Fig. 18.

Silicon Steels. The resistivities of silicon steels according to the silicon content at room temperature are shown in Fig. 19*a*. Resistivity temperature curves of this class of steels in the solid state are shown in Fig. 19*b*.

Additional data on the resistivities of ferrous alloys in the solid state are given in Appendix *C*.

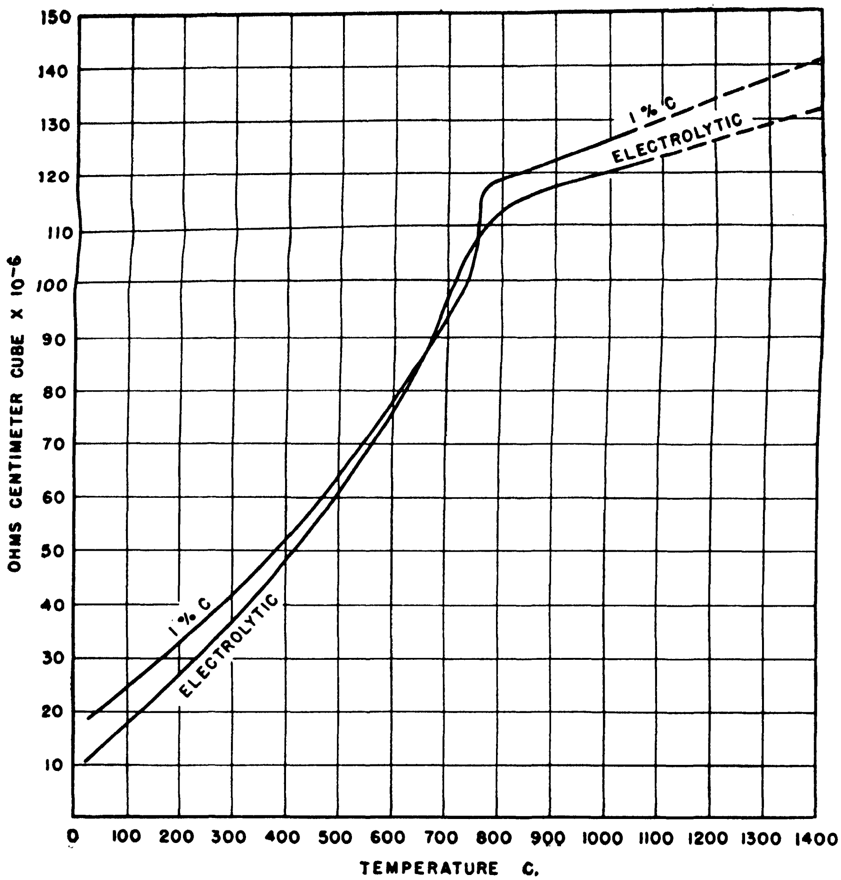

FIG. 16. Resistivity-temperature curves of iron and carbon steel.

Liquid Steel. The resistivity of a steel in the liquid state depends on its composition and its temperature. The only data that are known are the values estimated from indirect measurements. These are within the range 150×10^{-6} to 250×10^{-6} ohm-cm^3 for miscellaneous steels at pouring temperatures.

Carbon. The variations in resistivity with temperature of two forms of carbon are shown by the graphs of Fig. 20. Values of the resistivities of different forms of solid carbon at 20°C are given in Table 2. Values of the resistivities of amorphous carbon and graphite in porous form from a paper by Vosburgh[7] are given in Table 3.

Glass. In the solid state glass is a nonconductor, but it approaches the conductor specification when liquid. Resistivity temperature curves of three kinds of glass from a paper by Guyer[8] are shown in Fig. 21.

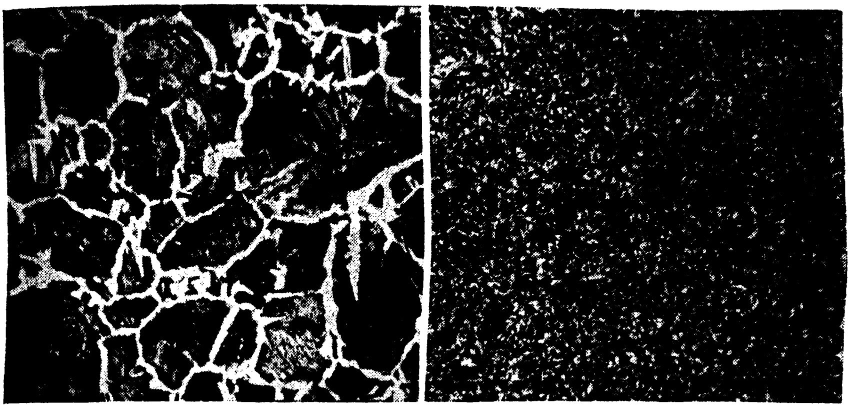

FIG. 17. Photomicrographs (X100) of SAE 1045 steel (a) before annealing, (b) after annealing.

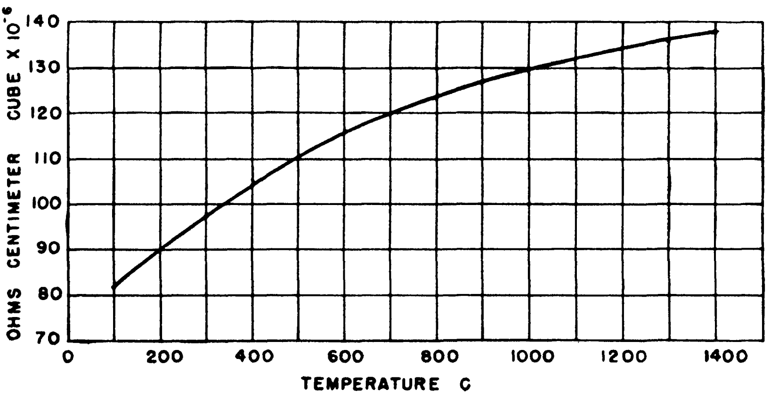

FIG. 18. Resistivity-temperature curve of stainless steel (18:8).

THE MAGNETIC PROPERTY

The magnetic property of a ferromagnetic alloy depends on

1. Its chemical composition
2. Its crystal structure—grain size and orientation
3. Its temperature

Magnetization Curves. The reference for a charge of magnetic material should be its alternating-current excitation curve, peak values. However, since that curve more or less coincides with the direct-current magnetization curve of the material as saturation is approached, the latter curve is generally the reference in induction-heating practice.

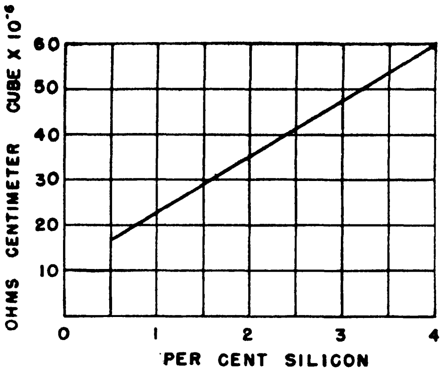

Fig. 19*a*. Resistivities of silicon steels at room temperature.

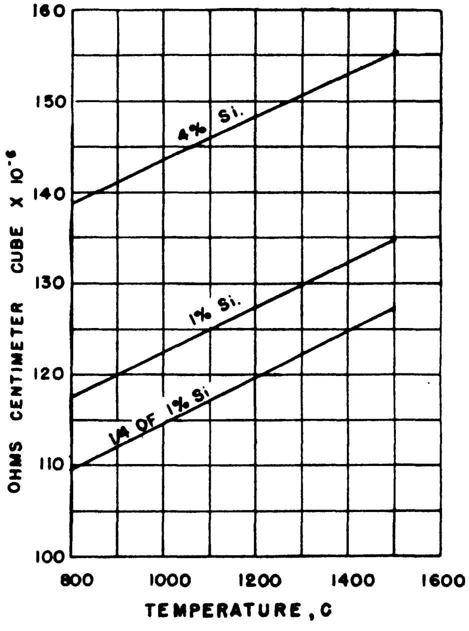

Fig. 19*b*. Resistivity-temperature curves of silicon steels.

Table 2. Resistivities of Solid Carbon at 20°C
(National Carbon Company)

Form	*Resistivity, Ohm-cm^3*
Carbon, coke base	0.0035–0.0046
Carbon, anthracite base	0.0033–0.0066
Carbon, lampblack base, gas-baked	0.0058–0.0081
Carbon, lampblack base, graphitized	0.0046–0.0066
Graphite	0.0008–0.0013

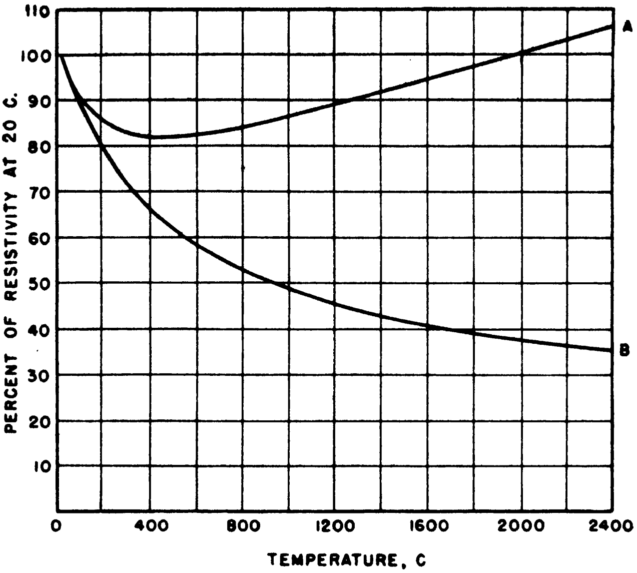

FIG. 20. Variations of resistivity with temperature of two forms of carbon. (*A*) Graphitized coke-base carbon. (*B*) Graphitized lampblack-base carbon. (*National Carbon Company.*)

Examples of the two types of curves are given in Fig. 22*a*. The alternating-current excitation curves of that illustration are for 60 cycles. The magnetic induction below saturation decreases with increase of frequency as shown by the curves of Fig. 22*b*.

TABLE 3. RESISTIVITIES OF POROUS FORMS OF CARBON AND GRAPHITE AT 20°C (48 per cent effective porosity)

Average pore diameter, micron	Resistivity, ohm-cm[3]	
	Carbon	Graphite
0.0013	0.0178	0.0031
0.0019	0.0178	0.0031
0.0027	0.0145	0.0030
0.0039	0.0178	0.0045
0.0055	0.0178	0.0051
0.0075	0.0203	0.0051

Typical Magnetization Curves. The magnetization curve of a particular steel is not often at hand. The reference usually must be to a curve typical of that class of material. Typical direct-current

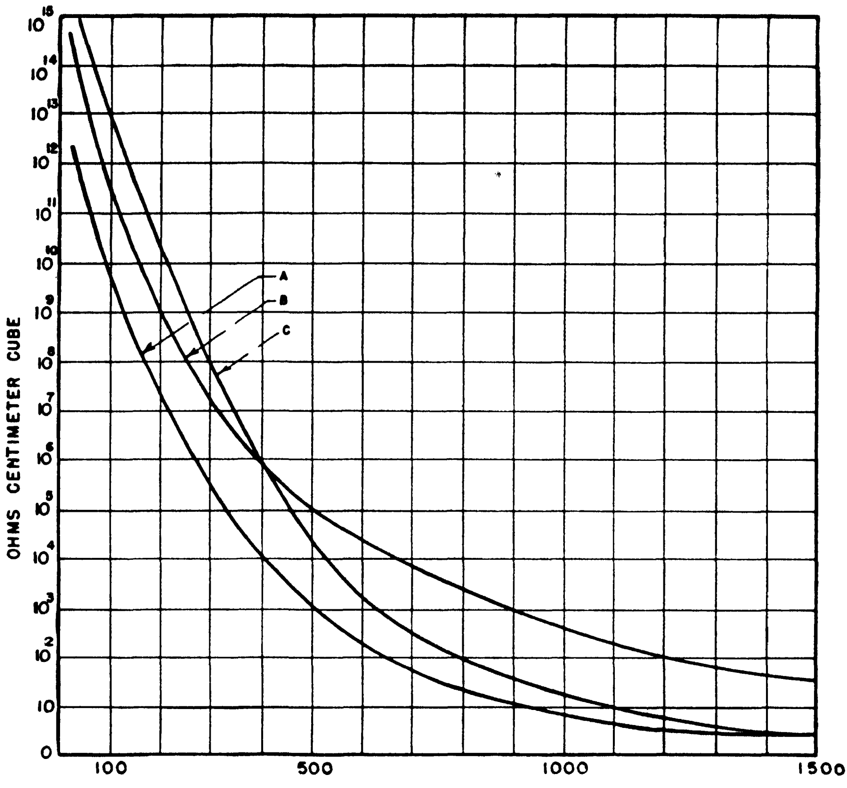

Fig. 21. Resistivity-temperature curves of glass. (*A*) Lime glass. (*B*) Borosilicate glass. (*C*) Lead glass.

Table 4. Compositions of the Materials of Fig. 24

Number	Carbon, per cent	Manganese, per cent
1	0.08–0.13	0.60–0.90
2	0.08–0.13	0.30–0.50
3	0.18–0.23	0.40–0.60
4	0.18–0.23	0.40–0.60
5	0.43–0.50	0.60–0.90
6	0.10	1.20
9	0.015 max	0.60 max
7	Ingot iron	C + Mn 0.10, max
8	Common iron	C 0.10 max, Mn 0.60 max

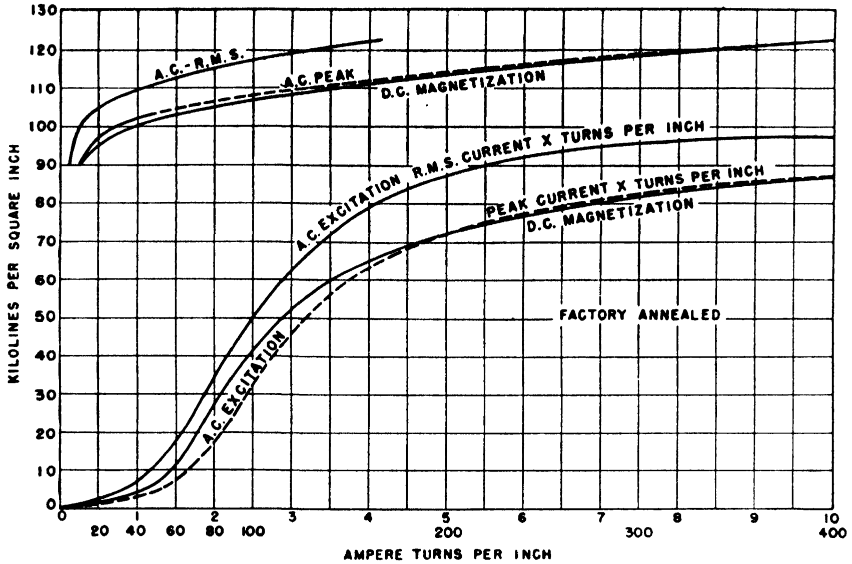

FIG. 22*a*. Direct-current magnetization curves and 60-cycle alternating-current excitation curves of a low-carbon steel.

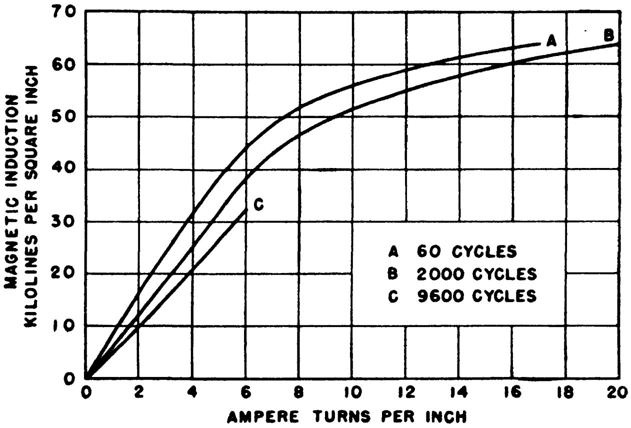

FIG. 22*b*. Alternating-current excitation curves, rms values, of a silicon steel.

magnetization curves of a number of common alloys are given in Fig. 23. The graphs of Fig. 24 are typical direct-current magnetization curves of some carbon steels and two irons. The compositions of these materials are given in Table 4.

Representative values of the magnetizing force H and the intrinsic induction β at saturation with reference to the carbon content of steel are given in Table 5.

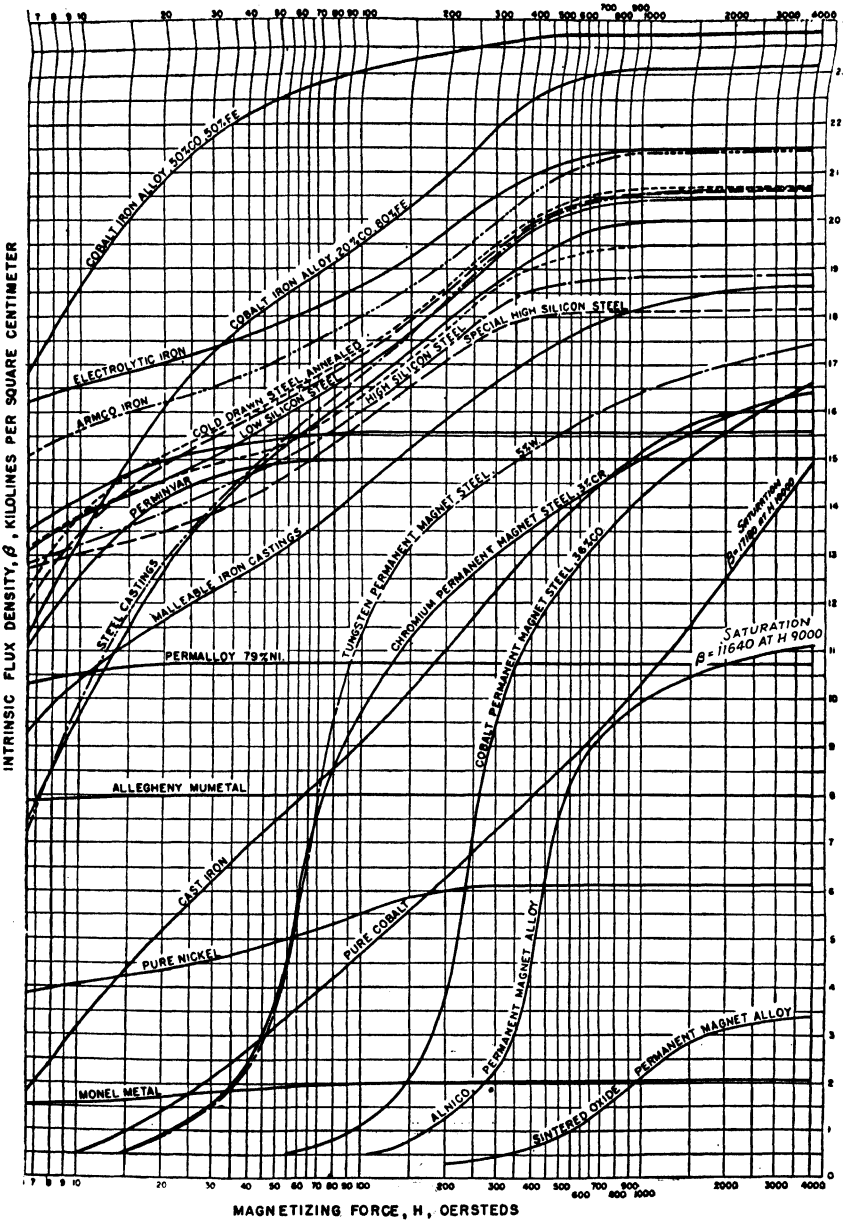

FIG. 23. Direct-current magnetization curves of various magnetic materials.

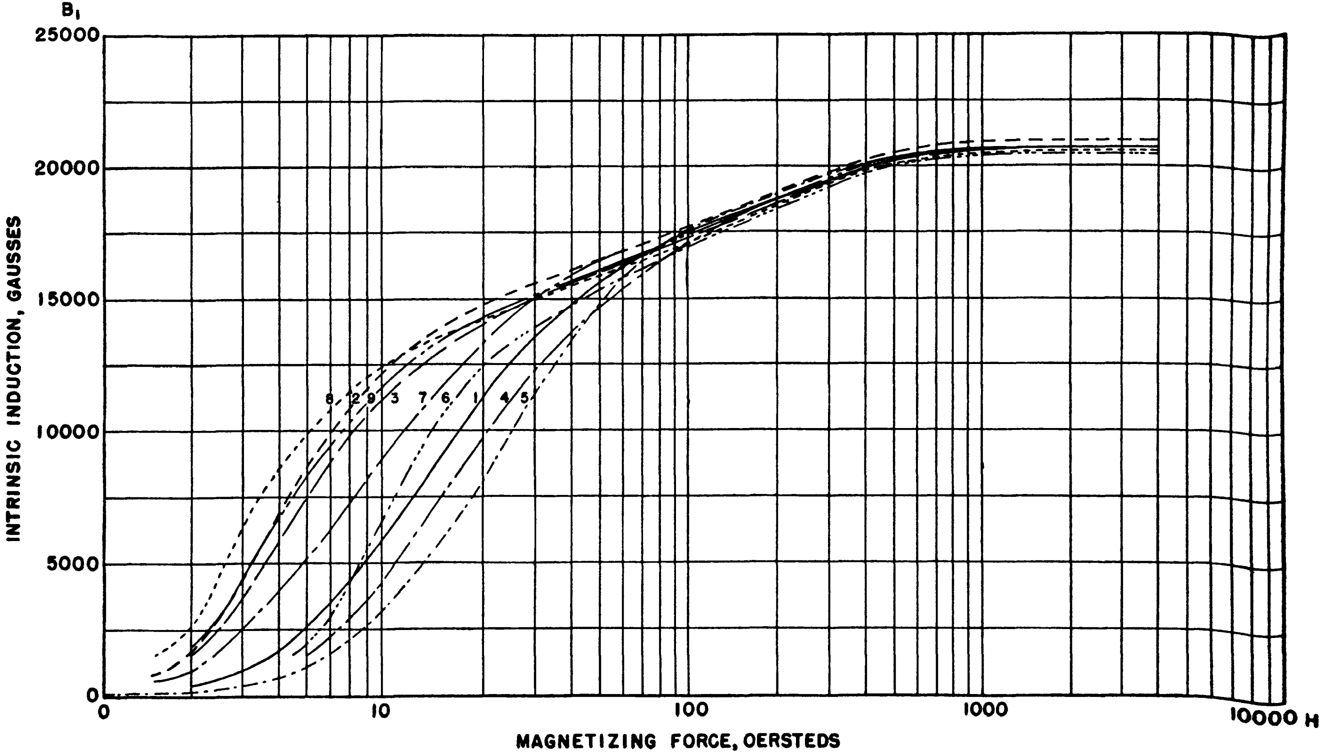

FIG. 24. Direct-current magnetization curves of some carbon steels (see Table 4).

TABLE 5. SATURATION VALUES, CARBON STEELS

Carbon, per cent	H, oersteds	β, gausses
0.02	1,000	21,000
0.40	1,100–1,500	20,000
0.85–1.25	2,500	19,500
1.11–1.25	2,500	13,600

NOTE 1.
Gausses × 6.5416 = lines per square inch
Oersteds × 2.0213 = ampere-turns per inch

Permeability. The factor that indicates how much magnetic flux is produced in a material by a given magnetizing force is permeability. This factor is the ratio

$$\mu = \frac{\beta + H}{H} = \frac{B}{H} \tag{9}$$

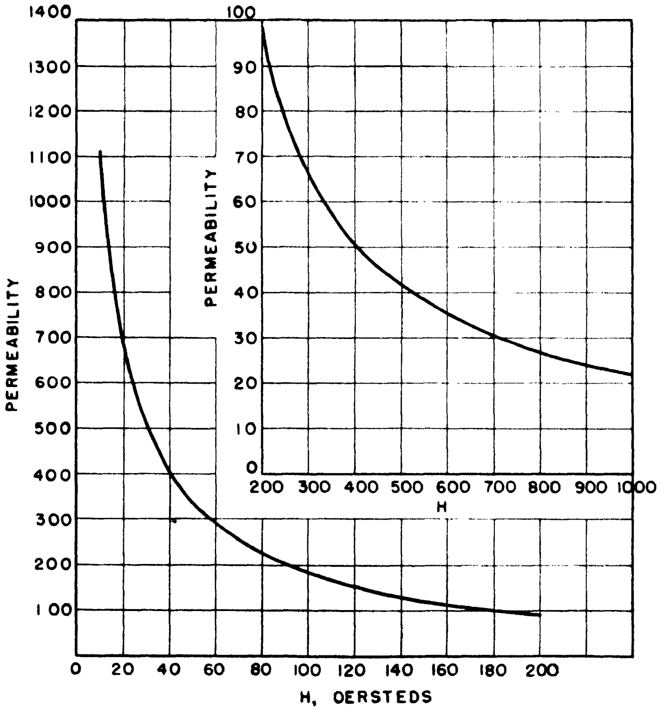

FIG. 25. Typical permeability curve of low-carbon steel.

where β = intrinsic induction, gausses
B = total induction, gausses
H = magnetizing force, oersteds

A typical permeability curve of low-carbon steel at room temperature is given in Fig. 25. In every case the permeability curve of an alloy of a given composition depends on the crystal structure of the alloy.

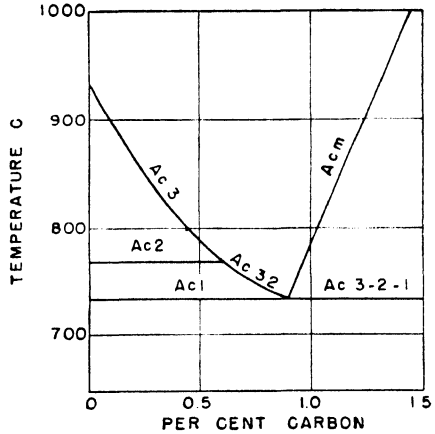

Fig. 26. Curie-point diagram of carbon steel.

Permeability and Temperature. The magnetic property of an iron-carbon alloy is but little affected by heat until its temperature approaches the value shown by the lines AC 2, AC 3-2, and AC 3-2-1 on the diagram of Fig. 26. At that temperature, known as the Curie point, the permeability becomes unity. This transformation from the magnetic to the nonmagnetic state is more or less abrupt, as indicated by Fig. 27.

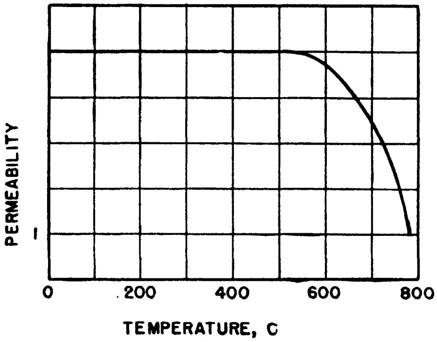

Fig. 27. Effect of heat on the permeability of carbon steel.

Other metallic elements added to an iron-carbon alloy change the Curie point values by small percentages. Examples are the increases caused by molybdenum and silicon and the decreases caused by manganese and nickel.

Effect of Hardness. The magnetic property of a steel is affected adversely by hardness. This is illustrated by the average values of

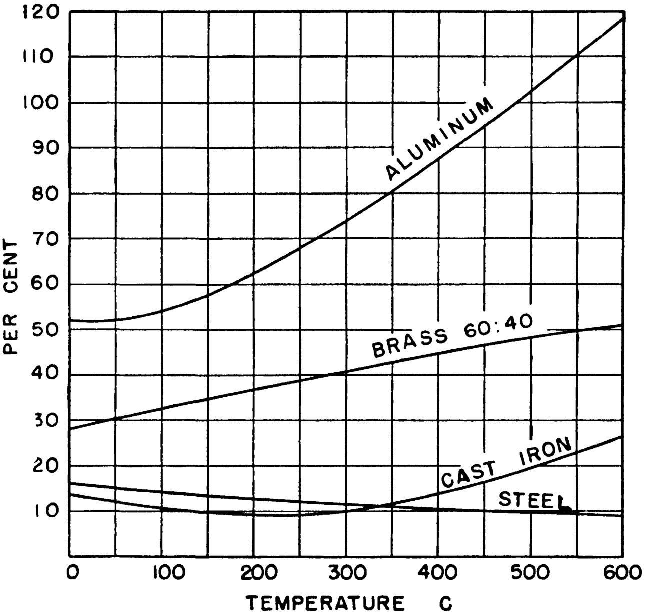

FIG. 28a. Relative thermal conductivities of some metals over a range of temperature.

B and H of the four bars of 1.11 to 1.25 carbon steel noted in a previous paragraph with reference to the effect of hardness on resistivity. These values for room temperature are

Before hardening, $H = 100$ oersteds, $B = 14{,}500$ gausses
After hardening, $H = 100$ oersteds, $B = 11{,}625$ gausses

This effect of hardness can be removed by heat-treatment.

THERMAL PROPERTIES

Thermal Conductivity. The relative thermal conductivities of aluminum, a brass, cast iron, and carbon steel expressed as percentages of the thermal conductivity of copper are shown in Fig. 28*a*. Three specific examples of the thermal conductivity-temperature relation are shown in Fig. 28*b*. The materials are

1. Iron, 99.60 Fe, 0.25 Mo
2. Boiler plate, 0.25–0.30 C, 0.80 Mn
3. Tool steel, 1.11 C, 0.15–0.35 Mn

These graphs also show the effect of the carbon content of a ferrous alloy on its thermal conductivity. Additional data on the thermal conductivities of metals and alloys are given in Appendixes *B* and *C*.

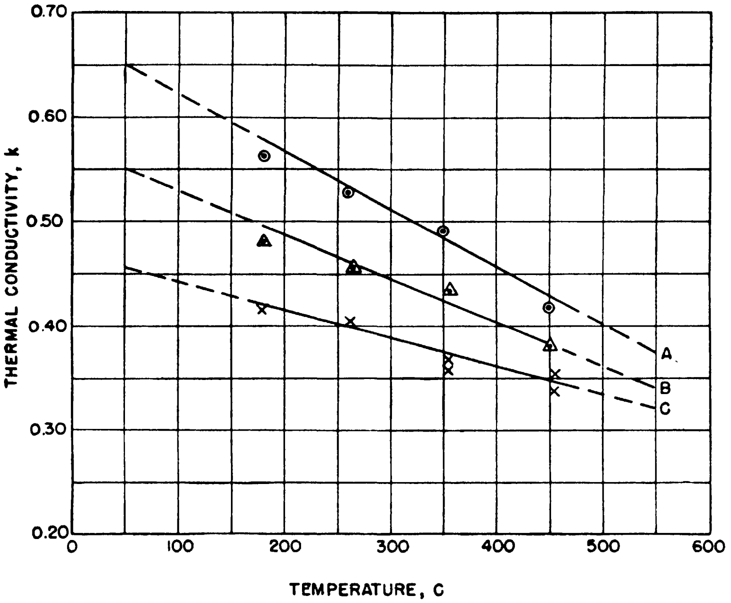

FIG. 28*b*. Thermal conductivity-temperature relations of three materials (see text). k = watts per sq cm for 1 cm length per °C.

Thermal Diffusivity. The ratio of the thermal conductivity of a material to its heat content per unit volume is called its diffusivity.

$$\text{Thermal diffusivity} = \frac{k}{ds} \tag{10}$$

where k = thermal conductivity, cgs unit
d = density, cgs unit
s = specific heat

Thermal diffusivity has the same role in temperature flow as thermal conduction has in heat flow. All other conditions being the same, the rates of heating of two materials will be faster for the material that has the higher thermal diffusivity. The room temperature values of the thermal diffusivities of some of the metals are given in Table 6.

TABLE 6

Metal	*Thermal Diffusivity, Cgs Unit*
Silver	1.737
Copper	1.133
Aluminum	0.826
Zinc	0.402
Steel	0.173
Nickel	0.152

The thermal diffusivity of a metal varies with its temperature. However, this variation is due mainly to variations of thermal conductivity and of specific heat, which in most cases offset each other so that, in general, thermal diffusivity is regarded as independent of temperature.

HEAT DEVELOPMENT

Magnetic Charges. The rate of heat development in a magnetic material at a temperature well below its Curie point, and exposed to an alternating magnetic flux, has two components: hysteresis watts (a magnetic effect) and eddy-current watts. The percentages of these components vary with the material, its temperature, the grain size, the base dimension of the part, the flux density, and the frequency.

An example of the total watts and the percentages of the hysteresis watts and the eddy-current watts in a carbon steel are given in Table 7.

TABLE 7. RATES OF HEAT DEVELOPMENT IN 0.10 CARBON STEEL SHEETS AT ROOM TEMPERATURE
(Flux density, 10,000 gausses; frequency, 60 cycles)

Thickness of sheet, in.	Total watts per lb	Per cent hysteresis watts	Per cent eddy-current watts
0.014	1.43	58	42
0.025	2.05	38	62
0.034	3.64	44	55
0.044	5.25	33	67

The separation of the hysteresis watts and eddy-current watts was made by the two-frequency method.

Hysteresis and Frequency. The value of the hysteresis watts per cycle is practically constant with frequencies that give low values of the index ratio. This is illustrated by Fig. 29. With higher frequencies the hysteresis watts per cycle decrease with increase of frequency and become negligible with high values of the index ratio.

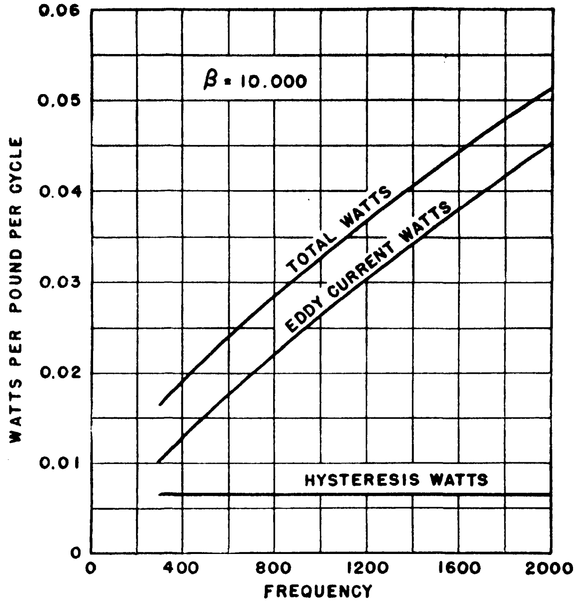

Fig. 29. Effects of frequency on hysteresis watts and on eddy-current watts in carbon steel with low values of the index ratio. Room temperature.

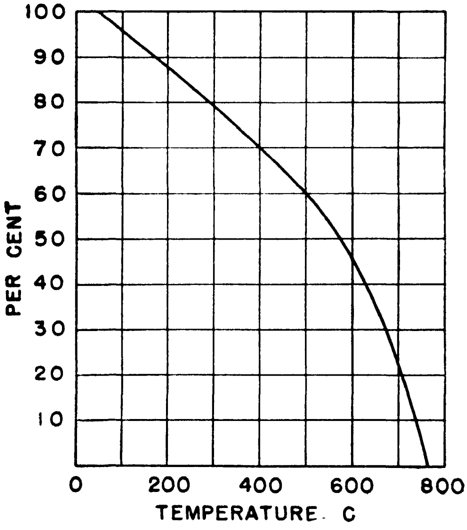

Fig. 30. Effect of heat on the hysteresis watts in carbon steel.

Hysteresis and Temperature. The rate of heat development by hysteresis decreases with rise of temperature of the charge, as indicated in Fig. 30.

Hysteresis in Induction Heating. Under the conditions of induction heating—high flux densities and comparatively high frequencies—the hysteresis effect is relatively small. This together with the fact that the hysteresis watts decrease with rise of temperature makes hysteresis a generally unimportant factor in induction-heating practice. The effect may be important in heating a magnetic material to a low temperature.

Eddy-current Watts. The general equation for the rate of heat development by eddy currents in a conducting mass (the charge) that is exposed to a uniform and sinusoidal alternating magnetic flux, the directions of which are parallel to the lateral surface of the charge, is

$$P = \frac{H^2 \sqrt{\mu f} \sqrt{\rho_a 10^9}\, lS}{10^7} \quad \text{watts} \tag{11}$$

where H = magnetizing force (crest value), oersteds
μ = permeability of the material
f = frequency, cycles
ρ_a = resistivity of material, ohm-cm^3
l = length of charge, cm
S = shape factor of charge

The value of the magnetizing force is

$$H = \frac{4\pi N \sqrt{2}\, i}{10l} \quad \text{oersteds} \tag{12}$$

where N = number of turns in coil around charge
i = current in coil, amp
l = length of coil over turns, cm

Example 1. $N = 75$, $i = 100$ amp, $l = 28$ cm, $H = 475$ oersteds, B from Fig. 24 = 20,475 gausses, $\mu = 43$.

NOTE 2. The values of μ and ρ_a in Eq. (11) correspond to the mean temperature of the path of the current in the charge.

NOTE 3. If the magnetizing force H is higher than is required to produce saturation in a charge of magnetic material, the values of β and H that correspond to saturation are used in Eq. (9) to determine the value of μ in Eq. (11).

Example 2. A charge of 0.40 C steel, magnetizing force $H = 2{,}060$ oersteds. The magnetizing force required to produce saturation (see Table 5) is 1,250 oersteds. Intrinsic induction β at saturation is 20,000 gausses.

$$\mu = \frac{21{,}250}{1{,}250} = 17$$

Shape Factors. The expressions for the shape factors of three common shapes of charges are given in the paragraphs that follow.

Solid Cylindrical Charges.

$$S = \frac{aF_r}{4\sqrt{2}} \tag{13}$$

where a = radius of charge, cm

$$F_r = \text{resistance function} = \frac{\text{ber}\,\Delta\,\text{ber}'\,\Delta + \text{bei}\,\Delta\,\text{bei}'\,\Delta}{(\text{ber}\,\Delta)^2 + (\text{bei}\,\Delta)^2} \tag{14}$$

Δ = index ratio

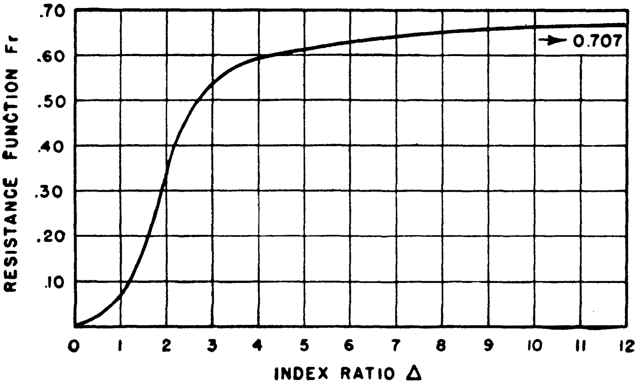

FIG. 31. Resistance function F_r for solid cylindrical charge.

A graph of values of the function F_r for values of the index ratio is given in Fig. 31.

The value of the shape factor Eq. (13) substituted in Eq. (11) gives

$$P = \frac{H^2 \sqrt{\mu f}\,\sqrt{\rho_a 10^9}\,alF_r}{4\sqrt{2} \times 10^7} \quad \text{watts} \tag{15}$$

or

$$P = \frac{H^2 \rho_a 10^9 l}{16\pi \times 10^7}\,\Delta F_r \quad \text{watts} \tag{15a}$$

The value of H in Eq. (12) substituted in Eq. (15) gives

$$P = \frac{4\pi^2 \sqrt{2}\,\sqrt{\mu f}\,\sqrt{\rho_a 10^9} N^2 a i^2 F_r}{l \times 10^9} \quad \text{watts} \tag{15b}$$

or, in more convenient form,

$$P = \frac{2\pi\rho_a N^2 i^2}{l}\,\Delta F_r \qquad \text{watts} \tag{15c}$$

The equation for the unit rate of heat development in a solid cylindrical charge is obtained by dividing Eq. (15) by the volume of the charge, $\pi a^2 l$; thus,

$$P_{\text{cm}^3} = \frac{H^2\sqrt{\mu f}\,\sqrt{\rho_a 10^9}\,F_r}{4\pi\sqrt{2}a \times 10^7} \qquad \text{watts per cm}^3 \tag{16}$$

Hollow Cylindrical Charges.

$$S = \frac{aM_r}{8} \tag{17}$$

$$M_r = \frac{(\sinh\Lambda + \sin\Lambda) + 2k^2(\sinh\Lambda - \sin\Lambda) + 2k(\cosh\Lambda - \cos\Lambda)}{(\cosh\Lambda - \cos\Lambda) + 2k^2(\cosh\Lambda + \cos\Lambda) + 2k(\sinh\Lambda + \sin\Lambda)} \tag{18}$$

where Λ = index ratio, Eq. (3)

$$k = \frac{2t}{(a - t)\Lambda} \tag{19}$$

t = wall thickness, cm

Since the value of the function M_r of a charge of a given material for a given frequency is determined by the radial dimensions a and t, there is an individual graph of the relations of this function and the index ratio for each set of a and t dimensions of charges of a given material.

Two examples of these graphs are given in Fig. 32. The data are

Graph 1	*Graph* 2
a = 3.175 cm	a = 3.175 cm
t = 0.333 cm	t = 0.086 cm
$\rho_a = 1.90 \times 10^{-6}$ ohm-cm³	$\rho_a = 6.8 \times 10^{-6}$ ohm-cm³
μ = 1.0	μ = 1.0

The value of the shape factor from Eq. (17) is substituted in Eq. (11) to obtain

$$P = \frac{H^2\sqrt{\mu f}\,\sqrt{\rho_a 10^9}\,alM_r}{8 \times 10^7} \qquad \text{watts} \tag{20}$$

This equation was derived by Oatley[9] for thin-wall cylindrical tubes. It is applicable with reasonable accuracy to all assemblies with hollow cylindrical charges and external primary coils.

The applicability of Eq. (20) to assemblies with hollow cylindrical charges and internal primary coils has not been determined.

The value of H in Eq. (12), substituted in Eq. (20), gives

$$P = \frac{4\pi^2 \sqrt{\mu f}\,\sqrt{\rho_a 10^9}\,N^2\,aM_r i^2}{l \times 10^9} \quad \text{watts} \qquad (20a)$$

For values of $\Lambda \geqslant 3.0$, Eq. (20a) is identical with the corresponding equation for a solid cylindrical charge of the same material and with the same radius.

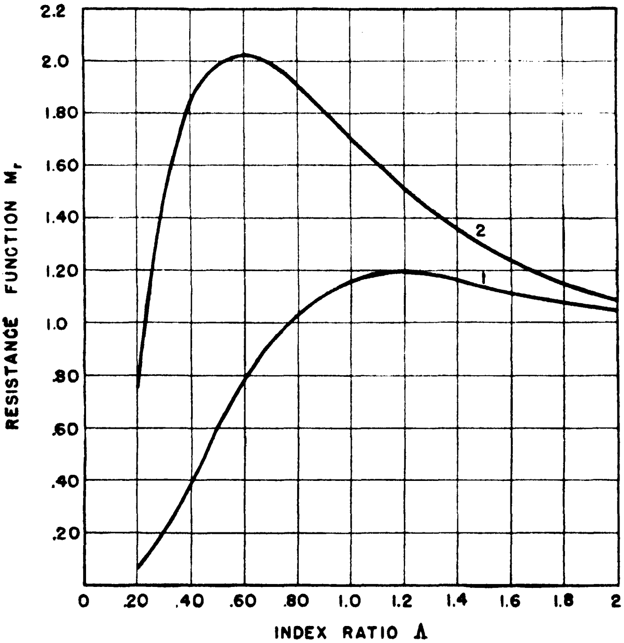

FIG. 32. Resistance functions M_r for two hollow cylindrical charges (see text).

Rectangular Charges, Plates and Sheets. Both sides exposed to longitudinal alternating magnetic flux.

$$S = \frac{w_a G_r}{8\pi} \qquad (21)$$

where w_a = width of charge, cm

G_r = resistance function $= \dfrac{\sinh \nabla - \sin \nabla}{\cosh \nabla + \cos \nabla}$ (22)

∇ = index ratio

A graph of values of this function for values of the index ratio is given in Fig. 33. For values of $\nabla \geqslant 2\pi$, the value of G_r is 1.0.

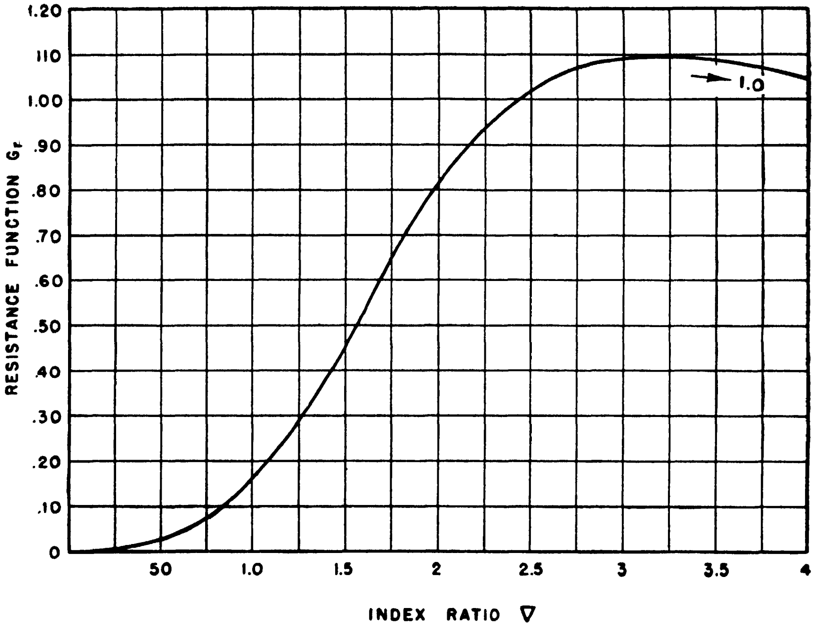

FIG. 33. Resistance function G_r for charge with rectangular section.

The value of the shape factor, Eq. (21), is substituted in Eq. (11) to obtain

$$P = \frac{H^2 \sqrt{\mu f}\,\sqrt{\rho_a 10^9}\, w_a l G_r}{8\pi \times 10^7} \quad \text{watts} \qquad (23)$$

The value of H from Eq. (12), substituted in Eq. (23) gives

$$P = \frac{4\pi \sqrt{\mu f}\,\sqrt{\rho_a 10^9}\, N^2 w_a i^2 G_r}{l \times 10^9} \quad \text{watts} \qquad (23a)$$

The equation for the unit rate of heat development in a charge with a rectangular section is obtained by dividing Eq. (23) by the volume of the charge, $2lw_a c$; thus,

$$P_{\text{cm}^3} = \frac{H^2 \sqrt{\mu f}\,\sqrt{\rho_a 10^9}\, G_r}{16\pi c \times 10^7} \quad \text{watts per cm}^3 \qquad (24)$$

where c = one-half thickness of charge, cm

Shape Effect. The effect of the shape of the charge on the rate of heat development by eddy currents is illustrated by the use of the ratio of Eqs. (24) and (16).

$$\frac{P_{\text{cm}^3\text{ plate}}}{P_{\text{cm}^3\text{ cylinder}}} = \frac{aG_r}{2\sqrt{2}\,cF_r} \tag{25}$$

The numerical values of the index ratios of these two shapes of charges—plate and solid cylinder—are the same when one-half the thickness of the plate is equal to the radius of the cylinder divided by $\sqrt{2}$, that is, $c = a/\sqrt{2}$. Hence, for this relation of dimensions,

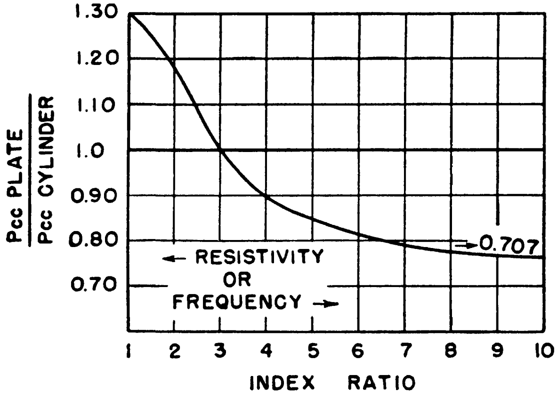

FIG. 34. Relative rates of heat development by eddy currents in two shapes of charges.

$$\frac{P_{\text{cm}^3\text{ plate}}}{P_{\text{cm}^3\text{ cylinder}}} = \frac{G_r}{2F_r} \rightarrow 0.707 \tag{26}$$

A graph of Eq. (26) for values of the common index ratio is given in Fig. 34. We see from this graph that, with values of the common index ratio below 3.0, the rate of heat development is greater in a charge with a rectangular section. Also that the opposite is the case with values of the common index ratio above 3.0.

Directional Effect. The magnetization curves of steel sheets obtained with the magnetization along the rolling direction (with the grain) and with the magnetization across the rolling direction (across the grain) differ because of the differences in the random orientations of the crystals with respect to the direction of magnetization. An illustration is given in Fig. 35.

The resistivities of the material measured in these two directions are the same. However, the eddy-current watts with a given flux density are greater with the magnetization across the grain.

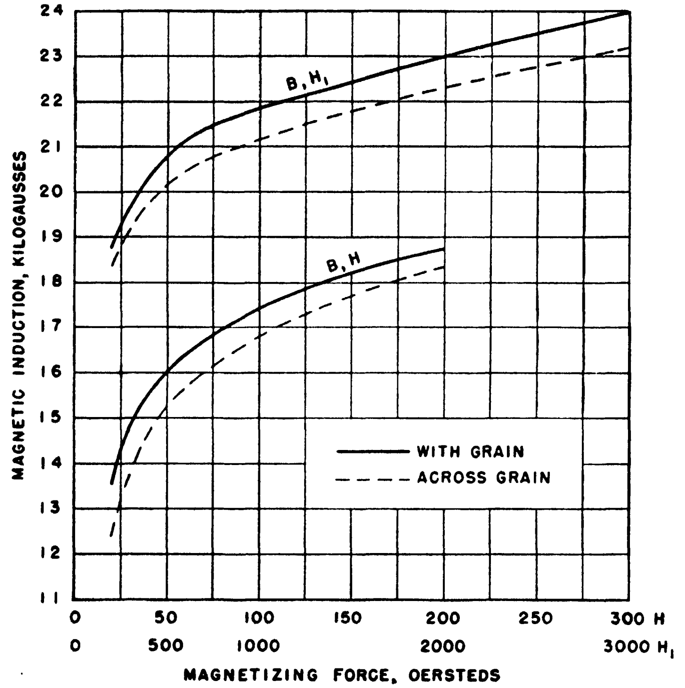

FIG. 35. Direct-current magnetization curves along and across the grain of a 0.15 carbon-steel sheet.

Cross-flux Watts. Measured values of eddy-current watts in sheets of magnetic material generally exceed the values calculated by Eq. (23). This difference varies with materials, with the magnetizing force, and with the method of measurement, including the method of obtaining the magnetization curve. If the measurement of eddy-current watts is made with the magnetization in the rolling direction, the measured values in carbon-steel sheets usually are 30 to 40 per cent greater than the values calculated on the basis of a typical magnetization curve. Higher percentages are obtained with silicon-steel sheets.

This difference between measured and calculated values is attributed to cross fluxes in the material due to variations in the permeabilities of the grains which, in turn, depend on the orientations of the crystals with respect to the direction of the resultant magnetization;

hence, the term cross-flux watts. This effect is much less pronounced in solid cylindrical charges of magnetic material. It may be present in some degree depending on the orientations of the near-surface crystals.

HEAT CONCENTRATION

The distribution of heat development by eddy currents in a charge is the same as that of the magnetic flux and the currents induced therein. This distribution, for brevity, is termed heat concentration.

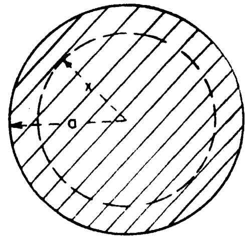

FIG. 36. Diagram relating to heat concentration.

Current Density. The relative current density in a solid cylindrical charge at radius x (see Fig. 36) is

$$Cd = \frac{1}{p}\left[\frac{(\text{ber}'\, x/p)^2 + (\text{bei}'\, x/p)^2}{(\text{ber}\,\Delta)^2 + (\text{bei}\,\Delta)^2}\right]^{1/2} \text{ amp per sq cm} \qquad (27)$$

Heating Density. The values of relative heating density corresponding to the current density values are the squares of the current density values. The graphs of Fig. 37 show values of the relative current density and relative heating density for a solid charge with 4 cm radius and with the reference dimension to give the index ratio 4.0. In each case the value of the ordinate at $[a - (p/2)]$ is 100 per cent. The data for Fig. 38 are the same as for Fig. 37 with the exception that the frequency is four times that for Fig. 37. Thus the index ratio of Fig. 38 is 8.0. These two illustrations show that the heat concentration in a given charge can be made as desired by the selection of the frequency.

Volume V_p. The degree of concentration of heat development by eddy currents in a charge is expressed as the percentage of the total watts in the charge that is developed in the annular zone, which has a radial thickness equal to the reference dimension, p. This annular zone, designated by the symbol V_p (see Fig. 39), has the volume

$$V_p = \pi p(2a - p)l \qquad (28)$$

The ratio of volume V_p and the volume of the charge is

$$\begin{aligned} \frac{V_p}{V_c} &= \frac{p}{a}\left(2 - \frac{p}{a}\right) \\ &= \frac{1}{\Delta}\left(2 - \frac{1}{\Delta}\right) \end{aligned} \qquad (29)$$

A graph of this ratio for values of the index ratio is given in Fig. 40.

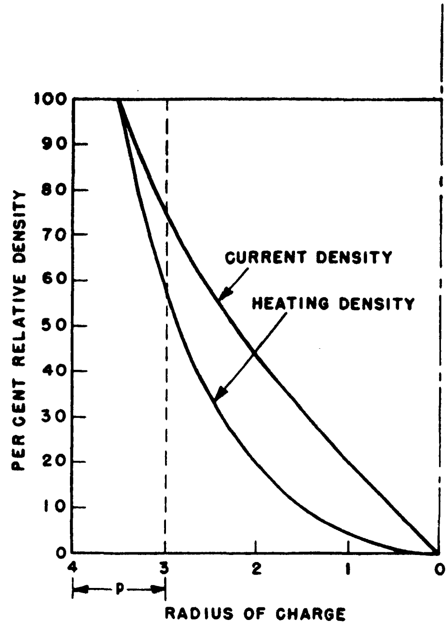

FIG. 37. Relative values of current density and heating density in a solid cylindrical charge. Index ratio, 4.0.

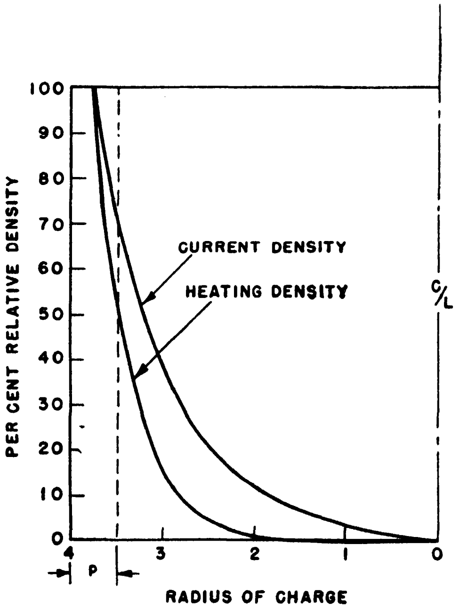

FIG. 38. Relative values of current density and heating density in a solid cylindrical charge. Index ratio, 8.0.

Heat Development in Volume V_p. The rate of heat development in the annular zone V_p is the total watts in the charge minus the watts in the core of the charge; this core being defined by the radius $(a - p)$. This rate is

$$P_v = (P_c - P_{(a-p)}) \qquad \text{watts} \tag{30}$$

The equation for the rate of heat development in the core of a charge is

$$P_{(a-p)} = \frac{H^2\rho_a 10^9(a-p)l}{16\pi p \times 10^7} \left[\frac{\left(\text{ber}\,\frac{a-p}{p}\,\text{ber}'\,\frac{a-p}{p}\right) + \left(\text{bei}\,\frac{a-p}{p}\,\text{bei}'\,\frac{a-p}{p}\right)}{(\text{ber}\,\Delta)^2 + (\text{bei}\,\Delta)^2}\right] \text{watts} \tag{31}$$

or, since $(a - p)/p = \Delta - 1$,

$$P_{(a-p)} = \frac{H^2\rho_a 10^9 l}{16\pi \times 10^7}(\Delta - 1) \left[\frac{(\text{ber}\,\Delta - 1\;\text{ber}'\,\Delta - 1) + (\text{bei}\,\Delta - 1\;\text{bei}'\,\Delta - 1)}{(\text{ber}\,\Delta)^2 + (\text{bei}\,\Delta)^2}\right] \text{watts} \tag{31a}$$

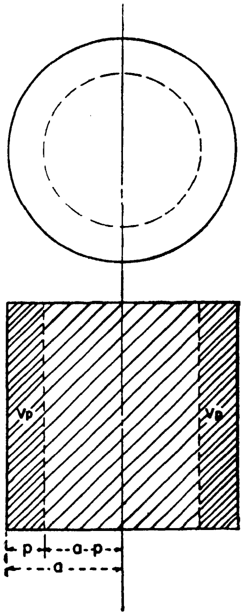

Fig. 39. Diagram relating to volume V_p.

The percentage of the total watts in the charge that is developed in volume V_p from Eqs. (15a) and (31a) is

$$\frac{P_c - P_{(a-p)}}{P_c} = 1 - \left\{\frac{\Delta - 1}{\Delta}\left[\frac{(\text{ber}\,\Delta - 1\;\text{ber}'\,\Delta - 1) + (\text{bei}\,\Delta - 1\;\text{bei}'\,\Delta - 1)}{(\text{ber}\,\Delta\;\text{ber}'\,\Delta) + (\text{bei}\,\Delta\;\text{bei}'\,\Delta)}\right]\right\} \tag{32}$$

Values of these percentages for values of the index ratio are given in Fig. 41.

The heat concentration expressed by Eq. (32) is the condition when the mass of the charge is at a uniform temperature—the temperature that corresponds to the value of resistivity used in Eqs. (15a) and (31a).

The relations shown by Figs. 40 and 41 are considered together in Table 8. For example, with the index ratio 4 approximately 79 per cent of the heat development occurs in the annular zone, which constitutes 44 per cent of the volume of the charge.

Temperature Rise. If there were no loss of heat from the charge during the heat cycle, the initial radial temperature gradient in the charge would be as indicated by curve *A* of Fig. 42. This temperature gradient is more like curve *B* of Fig. 42 because of the loss of heat from the surfaces of the charge. As the heating is continued, the radial temperature gradient becomes less and less as heat is absorbed by the charge.

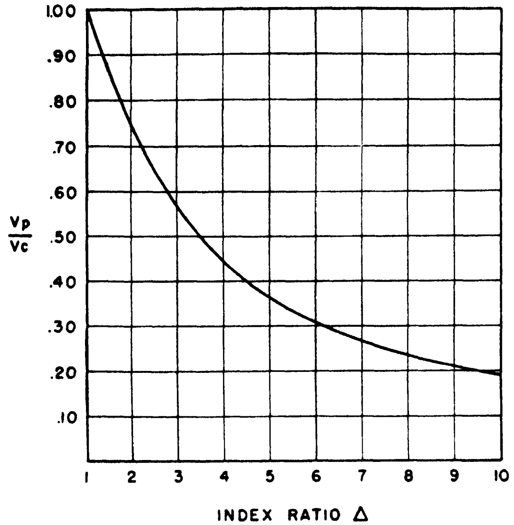

FIG. 40. Ratio of volume V_p and the volume of a solid cylindrical charge.

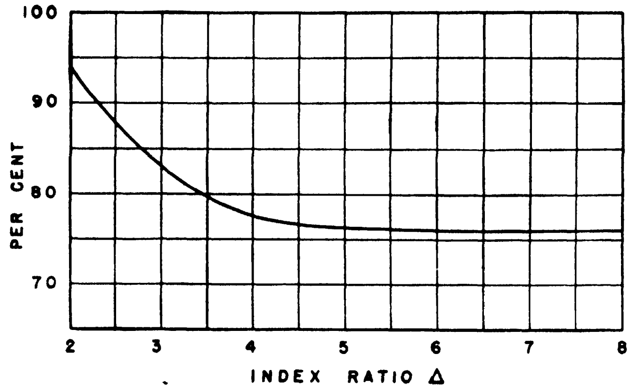

FIG. 41. Percentage of the heat development in volume, V_p.

Mass Effect. The rate of rise of temperature of the charge as a whole for a given applied voltage is determined by the electrical efficiency, the rate of heat loss, the thermal properties of the material, and the surface-volume ratio of the charge. This last determinant expresses the mass effect of the charge.

TABLE 8

Index ratio	Watts, per cent in volume V_p	V_p/V_c
2	98	0.75
3	84	0.56
4	79	0.44
5	76.5	0.36
6	76	0.30
7	76	0.26
8	76	0.23
10	76	0.19

Surface-volume Ratio. This relation is the ratio of the lateral-surface area of the charge and its volume.

Solid cylindrical charge, end areas neglected,

$$\frac{\text{Lateral-surface area}}{\text{Volume}} = \frac{2\pi al}{\pi a^2 l} = \frac{2}{a} \qquad (33)$$

where a = radius of charge
l = its length

Charge with a rectangular section, edge and end areas neglected,

$$\frac{\text{Lateral-surface area}}{\text{Volume}} = \frac{2w_a l}{2cw_a l} = \frac{1}{c} \qquad (34)$$

where w_a = width of charge
l = its length
c = one-half thickness

Graphs of Eqs. (33) and (34) for a range of base dimensions are shown in Figs. 43a and 43b.

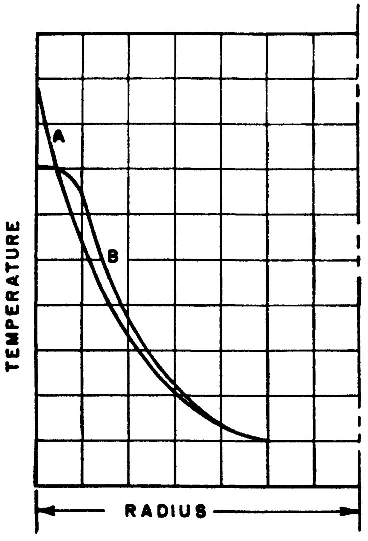

FIG. 42. Initial temperature gradient in a charge.

With charges having small base dimensions (radius or one-half thickness) the lateral-surface area is of prime importance, and the thermal diffusivity is relatively unimportant as regards heating.

the base dimension increases, this relation changes and the thermal diffusivity becomes the controlling factor in the heating of the charge.

Equilibrium Temperature. With constant applied voltage, the mean temperature of the path of the current in the charge will rise to the value at which the sum of the rate of heat dissipation from the charge surface and the i^2r watts in the coil around the charge is equal to the watts input to the coil. That temperature is the equilibrium temperature of the charge in a given assembly with given values of voltage and frequency. Disregarding the drop in temperature in the near-surface zone of the charge, the equilibrium temperature corresponds to uniform distribution of temperature throughout the mass of the charge.

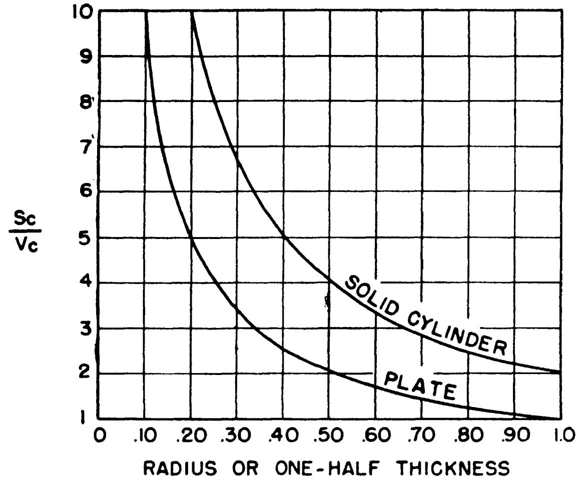

FIG. 43a. Surface-volume relations of two shapes of charges.

The heat cycle may end before the equilibrium temperature is attained. In such cases equalization of temperature in the mass of the charge is left to thermal conduction within the mass.

Log of a Heat Cycle. A record from practice is given in Table 9 and Fig. 44. These data pertain to the stationary heating of a solid cylindrical carbon-steel billet. The graph of Fig. 44 is the record of the temperature readings at the center of the billet.

Dimensions:	
Diameter	2 in.
Length	12¼ in.
Lateral-surface area	77 sq in.
Weight	11⅞ lb
Heat cycle	110 sec
Frequency	9,600 cycles

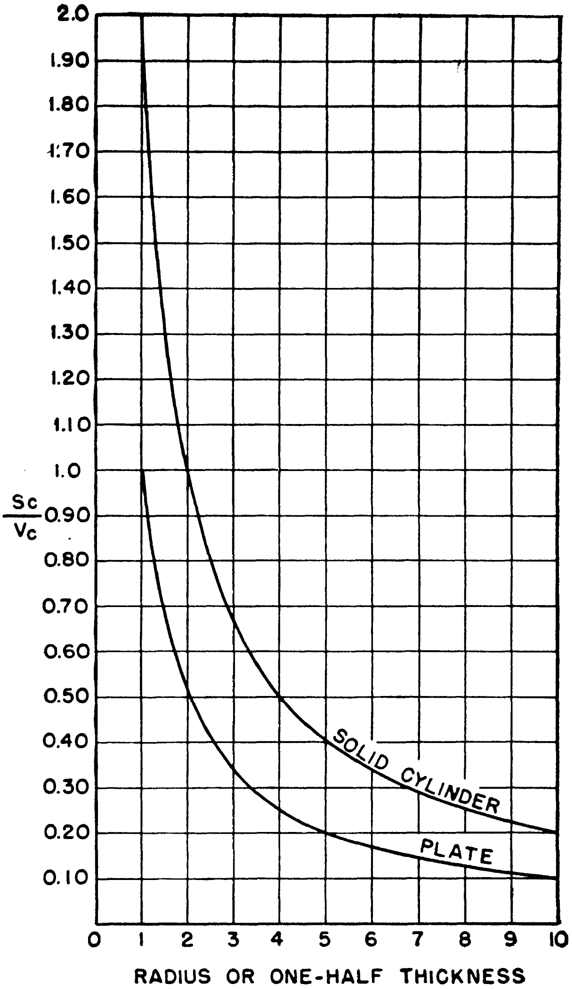

FIG. 43*b*. Surface-volume relations of two shapes of charges.

TABLE 9. LOG OF HEAT CYCLE, SEE FIG. 44

Time, sec	Volts	Kw	Time, sec	Volts	Kw
0	420	78	70	490	80
10	440	80	80	485	80
20	340	52	90	480	79
30	305	33	100	480	79
40	290	22	110	480	79
50	490	81	Power off		
60	490	81			

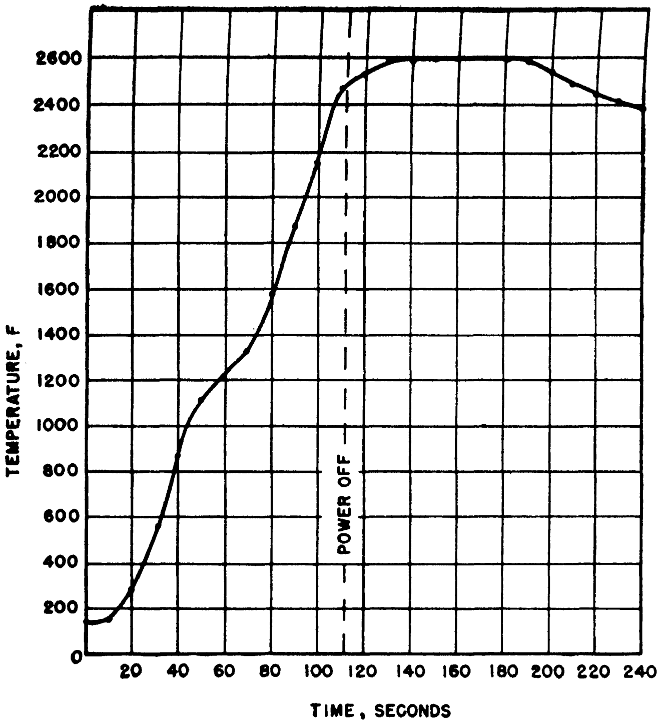

FIG. 44. Temperatures at the center of a solid cylindrical steel charge during and after the heat cycle (see Table 9).

Heat Content. The unit quantity of heat absorbed by a mass for a given rise of temperature t' deg is

Centigrade scale,

$$q = \frac{s_m(t' \times 1.80)}{3.412} + L \quad \text{watthours per lb} \tag{35}$$

Fahrenheit scale,

$$q = \frac{s_m t'}{3.412} + L \quad \text{watthours per lb} \tag{35a}$$

where s_m = mean specific heat of material over range of temperature t'
L = latent heat, if any, watthours per lb

NOTE 4. One watthour = 3.412 Btu.

The heat contents of the metals up to and above the melting points are given in Figs. 45 and 46. A value of kilowatt-hours per ton (2,000 lb) divided by 2 gives watthours per pound.

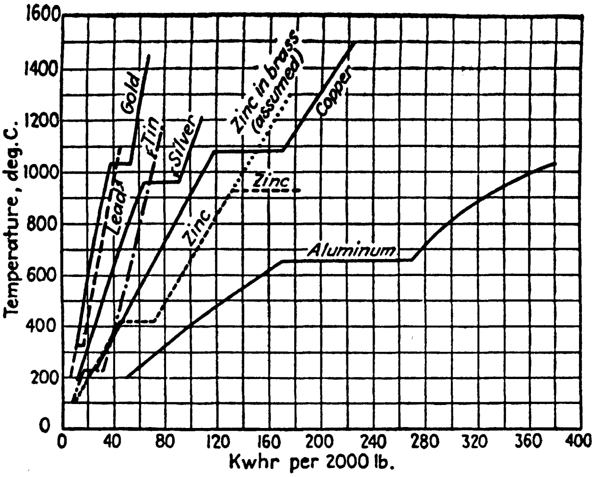

Fig. 45. Heat contents of metals.

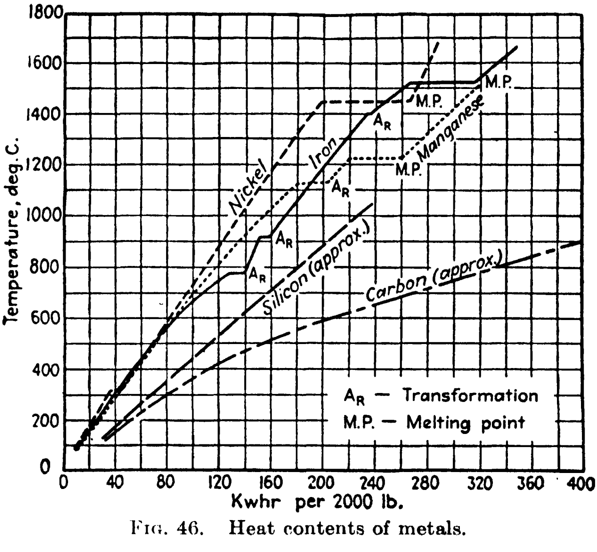

Fig. 46. Heat contents of metals.

The heat content of an alloy can be obtained by adding the heat contents of the component metals in accordance with the proportions by weight of the components. A table of the heat contents of various carbon steels is given in Appendix *D*.

It is of interest to note that, in heating steel to 1400°C, approximately one-half of the total heat absorbed is required to raise the temperature of the steel to the Curie point.

Heat Loss. With few exceptions in induction-heating practice charges are heated either in open air or in a protective gas atmosphere. Thus these charges lose heat by radiation and by convection during the heat cycle. If the charge is a part of a body, for example, the end of a shaft, there is also a loss of heat by conduction to the cold mass of the body. The large part of the heat loss at temperatures common in the heating of metals is by radiation.

Radiation. The rate of heat loss by radiation is

$$P_{\text{rad}} = 0.57\psi(T_s^4 - T_a^4)\,10^{-11} \quad \text{watts per sq cm} \tag{36}$$

or

$$P_{\text{rad}} = 3.68\psi(T_s^4 - T_a^4)10^{-11} \quad \text{watts per sq in.} \tag{37}$$

where ψ = emissivity coefficient of surface
T_s = absolute temperature of surface, K
T_a = absolute temperature of surroundings, K

Emissivity coefficients vary as widely as the natures of the surfaces vary. Also in a given case this coefficient increases with rise of temperature. The emissivity coefficient of a smooth polished surface is lower than that of a rough surface. Hence, the use of a gas atmosphere to prevent oxidation of a metal surface during heating is also advantageous as regards heat loss by radiation from the surface.

If we take $\psi = 0.81$ as representative of the average value of the emissivity coefficient of metals heated in open air and neglect the value of the temperature of the surroundings in Eqs. (36) and (37), these equations become

$$P_{\text{rad}} = 0.47T_s^4 \times 10^{-11} \quad \text{watts per sq cm} \tag{36a}$$

and

$$P_{\text{rad}} = 3.0T_s^4 \times 10^{-11} \quad \text{watts per sq in.} \tag{37a}$$

Values obtained by Eqs. (36*a*) and (37*a*) for a range of temperatures are given in Fig. 47.

Convection. The rate of loss of heat by natural convection in still air from a hot body depends on the difference of temperature between the body and the surrounding air and on the size and shape of the body. For average conditions in induction heating, the natural convection component of the rate of heat loss from the charge is

$$P_c = 1.86(t')^{1.25} \times 10^{-4} \quad \text{watts per sq cm} \tag{38}$$

or

$$P_c = 12(t')^{1.25} \times 10^{-4} \quad \text{watts per sq in.} \tag{39}$$

The use of a protective gas atmosphere may increase the convection component of the heat loss from the charge due to the movement of the gas past the surfaces of the charge.

Total Heat Loss. The value of the emissivity coefficient used to obtain Eqs. (36*a*) and (37*a*) is liberal for most cases in induction-heating practice. Hence, inasmuch as the natural convection component of the heat loss in this practice is comparatively small, the graphs of Fig. 47 represent fairly well the rates of heat loss from charges heated in open air.

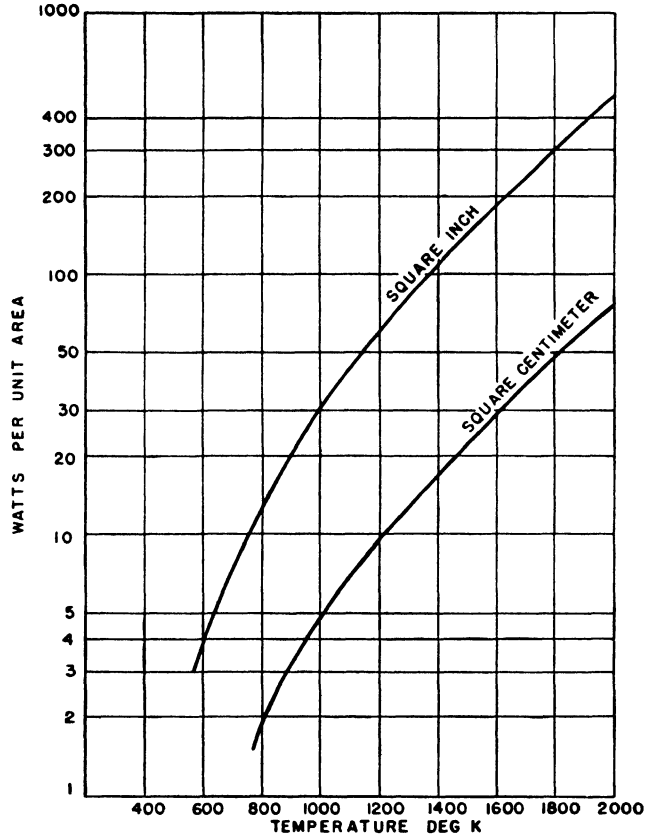

FIG. 47. Rates of heat dissipation by radiation from the surface of a charge. Emissivity coefficient, 0.81.

Thermal Efficiency. The ratio of the heat absorbed by a charge and the sum of that value and the heat loss from the charge during the heat cycle expresses the thermal efficiency of the heating operation.

CHAPTER III

INDUCTION HEATERS—CLASS A SERVICE

An induction heater comprises a primary coil, or inductor, supports for the charge and coil, the instruments, gauges, and other auxiliary devices required for that application, a mechanism for handling the charge if required, and an enclosure. Generally, space is provided in the enclosure for capacitors and the associated switching devices for power-factor correction. Also in some cases the power apparatus for the unit is mounted within the enclosure.

Charges. An induction heater is designed with reference to a type of charge and to the method of heating, stationary or continuous as the case may be.

A full charge is defined by the relation: axial length of charge equal to the length of the primary coil over the turns; that is,

$$l_a = l_b = l$$

A charge of less length is termed a part charge. Unless otherwise noted for a particular case, the references herein are to full charges.

If a charge is a part of a body, for example, the end of a shaft, the mass of the body outside of the primary coil is of concern only with respect to the heat loss from the charge to the cold mass of the body. In the special case of heating steel for hardening, the mass of the body outside of the coil has an effect on the heat pattern developed in the charge.

The term "long charge" refers to a charge with a length many times its diameter; "short charge" is equally indefinite. The distinction begins to apply when the ratio of length and diameter is about 6.0.

Rated Index Ratio. The values of charge resistivity and permeability that correspond to the maximum temperature of the charge during the heat cycle, the frequency, and the base dimension of the charge are the factors of the rated index ratio of the charge in stationary heating applications.

In continuous heating the mean values of charge resistivity and permeability during the heat cycle, the frequency, and the base dimension of the charge are the factors of the rated index ratio.

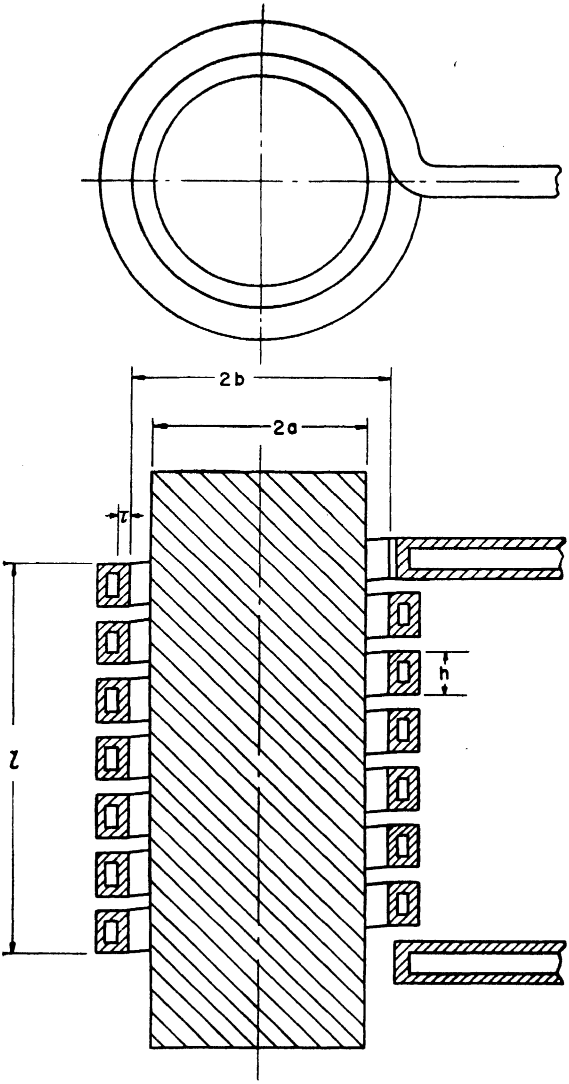

FIG. 48. Section of an assembly with a solid cylindrical charge.

Primary Coils. These coils—sometimes termed inductors, sometimes work coils—are almost invariably of the single-layer design illustrated by Fig. 48. This design is based on the following considerations:

1. The strength of the magnetic field is proportional to the ampere-turns of the coil. The heating effect of the current in the coil conductor—neglecting the space required for turn insulation—is

independent of the number of turns and number of layers. For example, if a given coil space were filled with two layers instead of one, there would be for the same number of ampere-turns, twice the number of turns, four times the coil resistance, and one-half the current.

2. The insulation of the coil becomes more and more of a problem as the number of layers is increased.

3. If the coil has more than one layer, its heating is increased by inductive action between layers.

4. The single-layer coil has the minimum electrical radius (the mean radius of the path of the current in the coil). This radius should be as small as conditions will permit.

5. The coil must be protected against the elevated temperature of the charge. This protection is obtained generally by the use of tubular conductors and water cooling. A single-layer coil is best suited for this method of protection.

6. The simplicity of the construction of the single-layer coil alone is sufficient reason for its use.

Types of Coils. There are four types of primary coils:

1. The multiturn cylindrical coil
2. The single-turn coil
3. The flat or pancake coil
4. Coils of special shapes, each generally made to conform to the contour of a nonsymmetrical charge

The last three types can be regarded as modifications of the multiturn coil, which is used as the reference type.

Length of Coil. The length of the charge defines the length of a primary coil for stationary heating. The length of a primary coil for continuous heating is fixed by the speed of movement of the charge and the required rate of heating.

Coil Diameter. The inside diameter of a primary coil must be sufficient for coil insulation, for guides and supports for the charge, and for handling the charge into and out of the coil. There is no electrical restriction on the maximum outside diameter of a primary coil.

Number of Turns. The desired relation of volts and amperes for the coil is the basis of the selection of the number of turns in a primary coil. As a rule the use of a standard, and not high, voltage is desirable. With a large number of turns per unit length of the coil, the provision for water cooling may be difficult; this may impose a limit on the maximum number of turns.

Taps. Coil windings may be provided with taps. These serve for adjustment of coil length to charge length and for the use of the primary coil as an autotransformer (with capacitors) for adjustment of the applied voltage.

Space Factor. Some space for insulation between turns of a coil is necessary. A greater spacing of the turns may be desirable according to the conditions in each case. The space factor of a coil is the fraction of the length of the coil that is occupied by the coil conductor. The space factors for single-layer coils are

Round conductors,

$$s = \frac{N\pi n}{4l} \tag{40}$$

Rectangular conductors,

$$s = \frac{Nh}{l} \tag{41}$$

where N = number of turns in coil
h = axial dimension of conductor
l = length of coil over turns

The space factor of a coil with an oval conductor must be estimated on the basis of the axial dimension of the conductor.

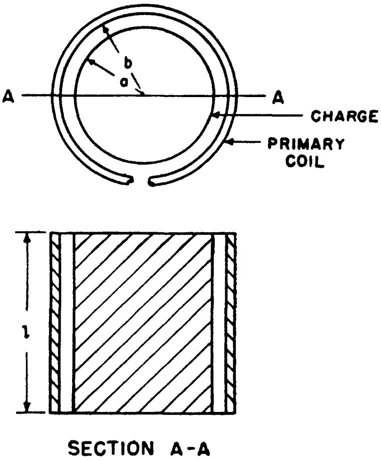

FIG. 49. Air-gap ratio diagram.

Air-gap Ratio. The radial dimension $b - a$ of Fig. 49 is the air gap of the assembly. The ratio b/a (or the ratio of the corresponding dimensions for other than cylindrical charges) is termed the air-gap ratio.

Graded Coils. The general practice is uniform spacing of the turns of a primary coil. With short coils the rate of heat development in the charge is not uniform along the length of the charge. This rate is the maximum opposite the mid-point of the coil winding and decreases toward each end of the charge.

Coils with a graded spacing of turns have been used to obtain a more uniform rate of axial heat development in the charge. However, the axial flow of heat in the charge is usually sufficient compensation for the nonuniformity of heat development with coils that have uniform turn spacing.

Conductor Material. The use of copper for coil conductors is standard practice. There may be cases where some other material is desirable. The assumption here is that copper conductors are used for all primary coils.

Conductor Temperature. The temperature of a primary coil should be kept as low as may be practicable because of the i^2r loss in the coil, the insulation of the coil, the oxidation of the metal of the conductor, deposits from cooling water, and expansion and contraction of the coil. The maximum operating temperature of the coil conductor is below the boiling point of the coolant, usually water. An operating temperature below 80°C (176°F) is considered desirable practice.

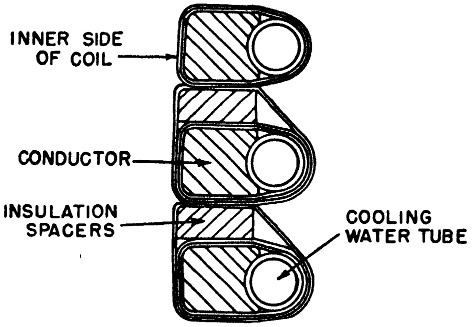

FIG. 50. Part section of a primary coil with a solid rectangular conductor.

Cooling Water. The flow of water through a primary coil must be sufficient to carry away the heat received from the charge and the heat developed by the current in the coil conductor. The rate of flow required is

$$\text{Gallons per minute} = \frac{\text{watts loss}}{264t'} \tag{42}$$

where t' = temperature rise of cooling water, °C

Conductor Shapes. The shape of a conductor for a primary coil may be round, oval, rectangular, or square. The ratio of the shape factors of a square conductor and a round conductor is $4/\pi$. Thus, as regards space utilization, a square or a rectangular conductor is the choice. However, that reason alone is not sufficient to restrict conductors to these shapes.

A primary coil with a hollow rectangular conductor is shown in Fig. 48. A design of a solid rectangular conductor with a tube for cooling water brazed to the outer surface of the conductor is shown in Fig. 50. Coils made of round tubing and of flattened tubing are in

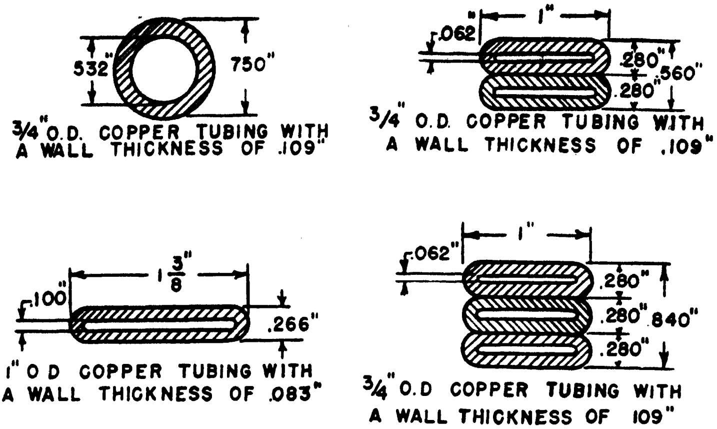

3/4" O.D. COPPER TUBING WITH A WALL THICKNESS OF .109"

3/4" O.D. COPPER TUBING WITH A WALL THICKNESS OF .109"

1" O D COPPER TUBING WITH A WALL THICKNESS OF .083"

3/4" O.D COPPER TUBING WITH A WALL THICKNESS OF 109"

FIG. 51. Examples of designs of conductors of primary coils.

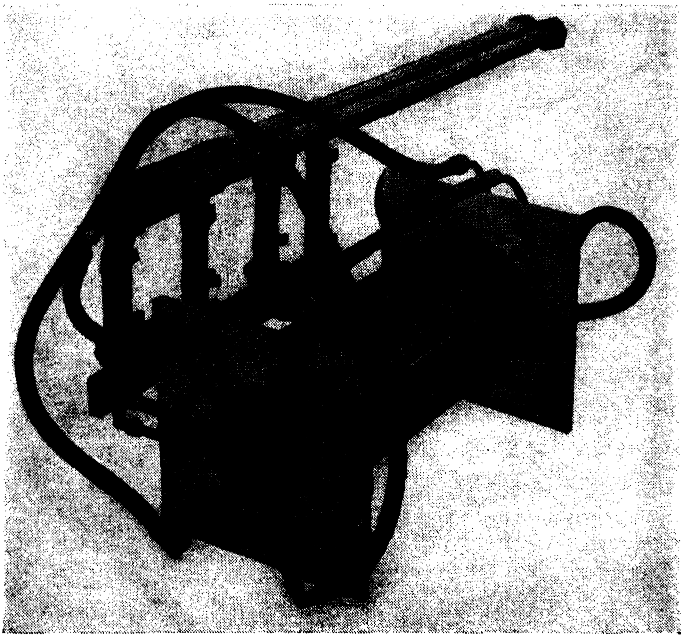

FIG. 52. A multiturn single-layer primary coil. (*The Budd Company.*)

common use. Examples of designs of these shapes of conductors are given in Fig. 51. Conductors in multiple are used as required.

Conductor Dimensions. The axial dimension of a coil conductor is selected with reference to the number of turns in the coil, the desired space factor, the length available for the coil, and the need for insulation between turns.

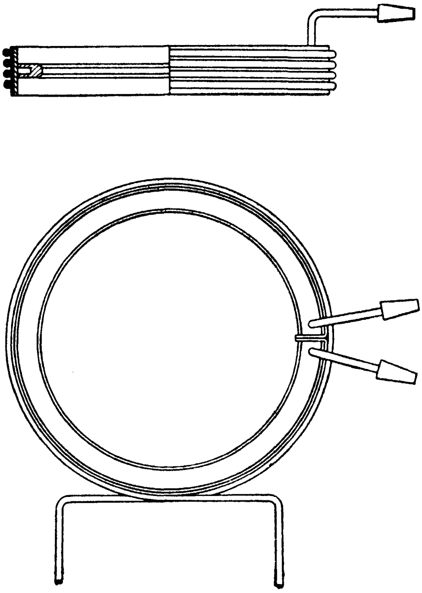

FIG. 53. A combination air-core step-down transformer and primary coil.

The radial dimension is selected with reference to the frequency. This selection will be discussed in the next chapter in connection with the alternating-current resistance of the coil.

EXAMPLES OF COILS

Figure 52 shows a multiturn, single-layer primary coil for either stationary heating or continuous heating. Note the insulation of the coil, the taps in the winding, and the water-cooled supports (stainless steel) for the charge. This is a typical coil for Class A service.

Figure 53 shows a design of a combination air-core, step-down transformer with which the secondary coil serves as the primary coil of an assembly.

Figures 54*a and b* illustrate a split one-turn primary coil for continuous heating and quenching. Note the hinge in the coil, the device

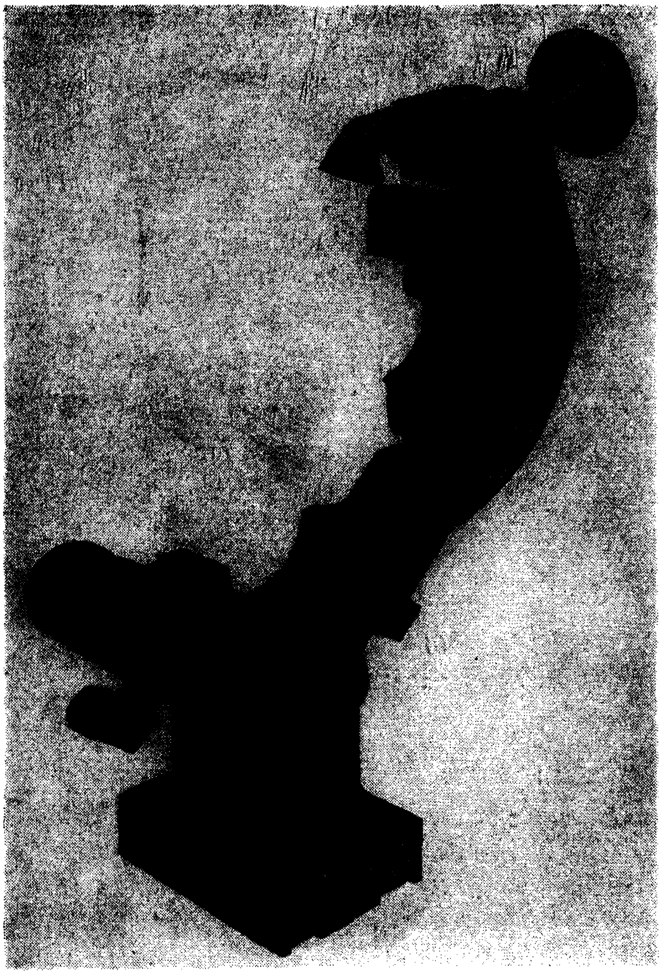

FIG. 54a. A split one-turn primary coil, open. (*The Ohio Crankshaft Company.*)

for holding the halves of the coil in contact, the water-spray openings around the periphery on the outgoing side, and the massive terminals. The water for quenching is forced through the hollow body of the conductor and thus serves also for cooling the coil.

A similar design of split one-turn coil with water-spray openings around the inner face of the coil is used for stationary heating followed by quenching in place. A split primary coil is necessary where the

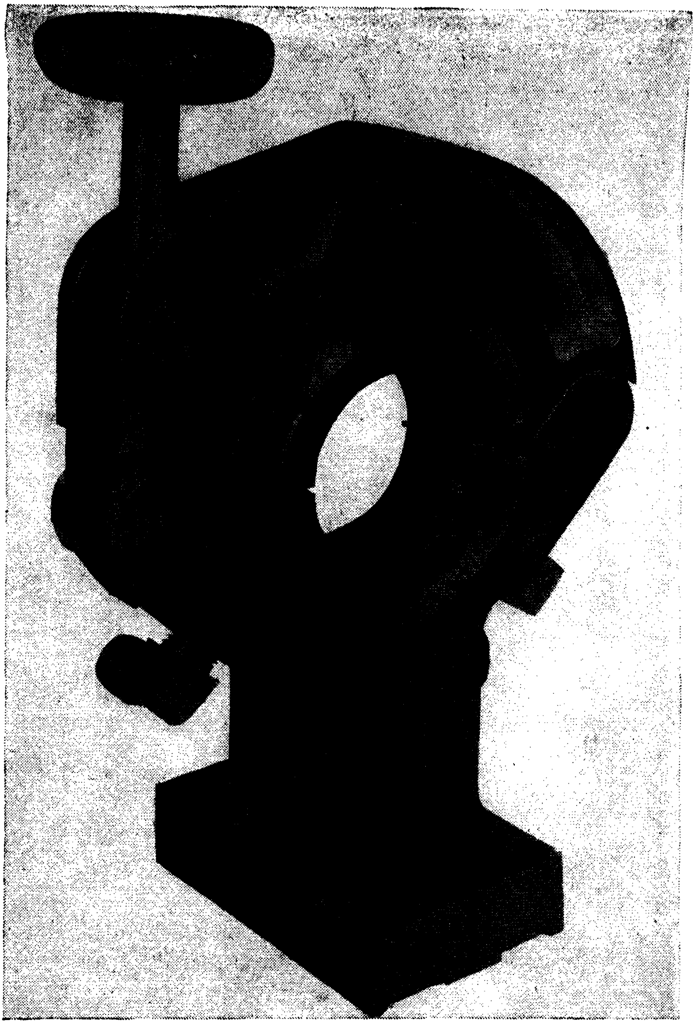

FIG. 54*b*. Primary coil of Fig. 54*a*, closed.

charge cannot be inserted in the coil because of the dimensions on each side of the part of the body to be heated, for example, the bearing journal of a crankshaft. Very small air gaps can be obtained with split primary coils.

Figure 54*c* shows a rectangular primary coil of ½-in. copper tubing. Dimensions: opening 2¾ in.; width, 38 in.; length, 39 in.; 48 turns; 9,600 cycles. This coil is used for continuous heating of sheet steel.

Magnetic Shields. The metal parts of the frame of an assembly can be shielded from the magnetic field of the primary coil by the interposition of a copper sheet so placed that its sides are parallel to the directions of the magnetic flux.

If the thickness of the copper sheet is

$$t \geqslant \frac{35}{\sqrt{f}} \quad \text{cm} \tag{43}$$

the magnetic field on the far side of the sheet will be reduced to 1 per cent or less of its value on the near side. In most cases sufficient shielding is obtained with considerably less thickness of sheet.

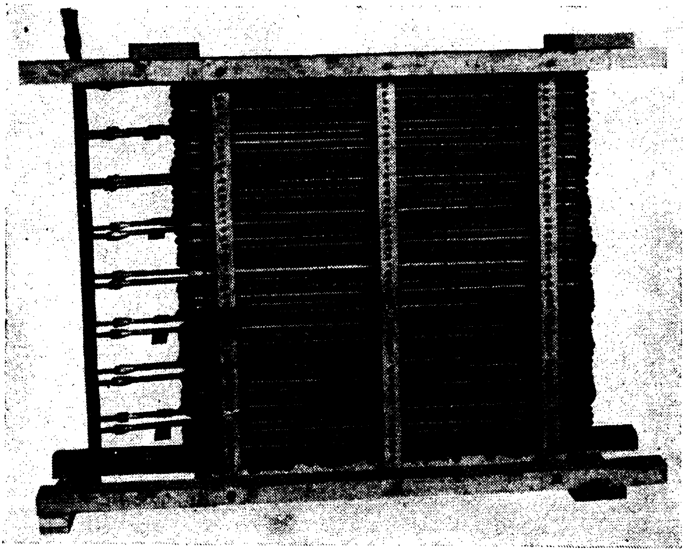

FIG. 54c. A rectangular, multiturn, single-layer primary coil. (*General Electric Company.*)

Instrumentation. Practice in the use of electrical instruments varies to some extent. Ammeters, wattmeters, varmeters, and voltmeters are used as required. Various gauges, according to the service are needed.

Auxiliary Devices. An automatic timer for the control of the heat cycle in stationary heating is standard practice. If there is more than one induction heater at one point, or in a group for a certain operation, a sequence controller to distribute the loading of the circuit is used.

Handling Mechanisms. In most cases the mechanical device for moving the charge into and out of the magnetic field—where such a device is used—is an adaptation of a conventional material-handling mechanism for a similar operation in other classes of service. Some examples of these devices as parts of induction heaters will be noted in illustrations that follow.

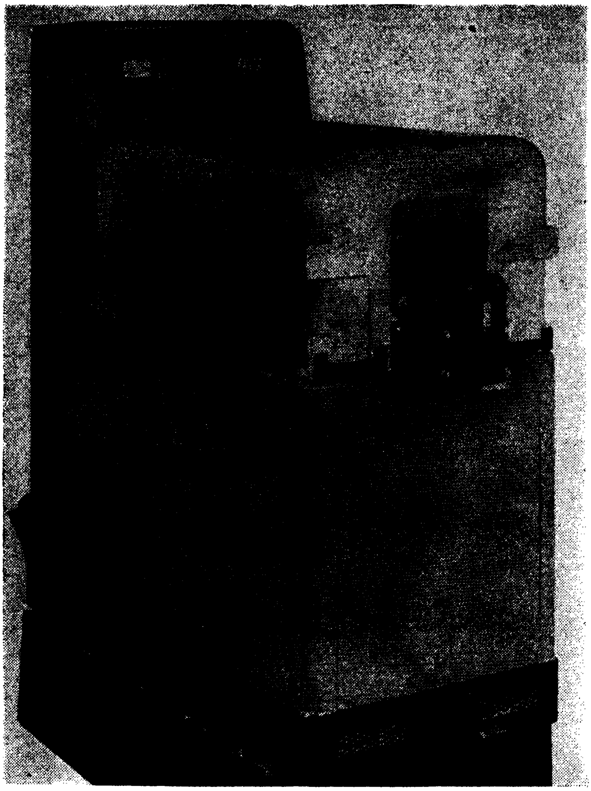

FIG. 55. An assembly for stationary heating. (*The Budd Company.*)

ILLUSTRATIONS

There is much variety in the designs of induction heaters. The details are fitted to the particular requirements in each case. The illustrations that follow, although typical, represent only a small part of these equipments for Class A service.

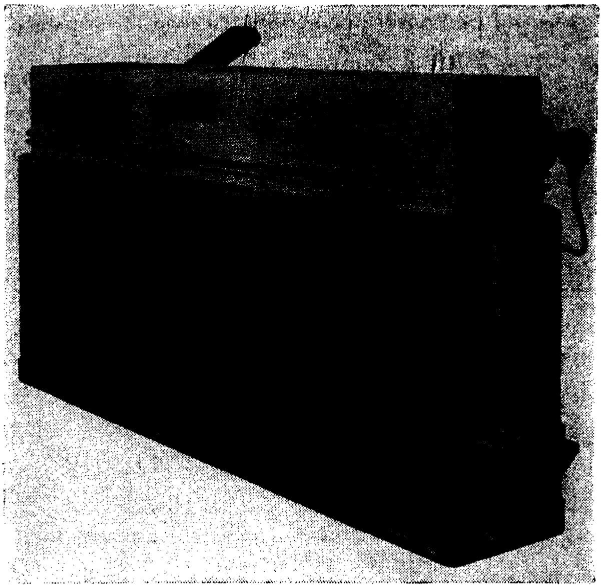

FIG. 56. An assembly for continuous heating. (*The Budd Company.*)

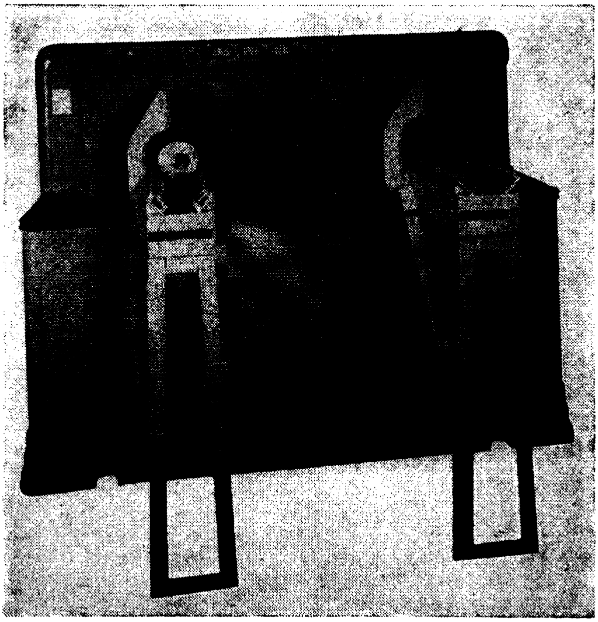

FIG. 57. Front view of unit with two assemblies for heating ends of billets. (*The Ohio Crankshaft Company.*)

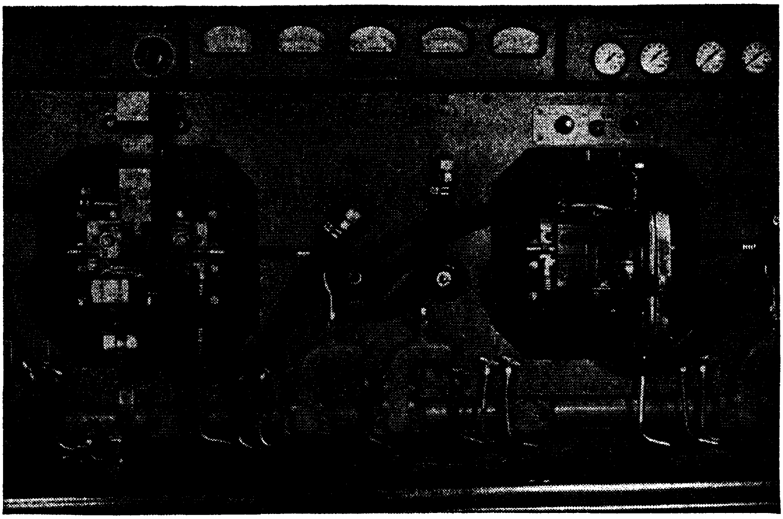

Fig. 58. Front view of unit with two assemblies, each with a split one-turn primary coil. (*The Ohio Crankshaft Company.*)

Figure 55 shows an induction heater for stationary heating.

Figure 56 shows an induction heater for continuous heating of billets.

Figure 57 gives the front view of an induction heater with two primary coils. Note the mechanism for handling the charge.

Figure 58 gives the front view of an induction heater with two split-type primary coils. This coil design is shown in Fig. 54.

CHAPTER IV

CIRCUIT EQUATIONS

The assembly for induction heating is a form of transformer. The coil around the charge forms the primary circuit. The path of the current in the charge is the secondary circuit. This transformer has three peculiar features:

1. A closed secondary circuit without terminals.

2. There is no definite path for the magnetic flux as is provided by the core of a conventional transformer. In some cases a laminated iron section, outside of the coil (or inside of a coil within the bore of a charge), is used to reduce the reluctance of the magnetic circuit.

3. The output is heat, which is absorbed by the charge and dissipated to its surroundings.

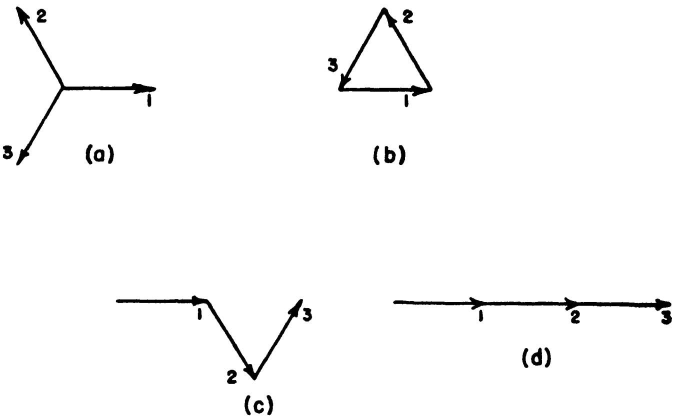

Fig. 59. Vector diagram of phase currents.

Single-phase Load. Suppose that the space available for a primary coil is divided into thirds and that each third is connected to a phase of a three-phase circuit, balanced connection. The phase currents are indicated in Fig. 59*a*. The net sum, which acts to cause secondary currents in the charge, is seen from Fig. 59*b* to be zero. If one phase is reversed, the sum of the three currents is seen from Fig. 59*c* to be twice the current in one coil. If the three sections of the coil are connected single-phase, the currents add to three times the current in one section as shown by Fig. 59*d*.

The conclusions from these diagrams are

1. The balanced three-phase connection gives no current in the charge except that due to leakage of flux.

2. The three-phase connection with one phase reversed draws single-phase power, and causes only two-thirds as much current in the charge as the single-phase connection.

3. For a given coil space and current density the single-phase connection gives the maximum rate of heat development in the charge.

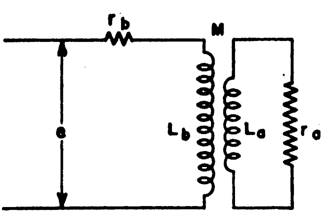

FIG. 60. The circuit diagram of induction heating.

A primary winding composed of three rectangular, or oval, coils, wound lengthwise of the charge and fitted to its contour with axes 120 deg apart, would give a balanced load on a three-phase circuit. That coil arrangement has been used in Europe to some extent for metal-melting furnaces.

Circuits. The diagram of the circuits of an assembly for induction heating is shown in Fig. 60. The symbols are

r_b = resistance of coil around charge
L_b = inductance of this coil
r_a = resistance of path of current in charge
L_a = inductance of this current path
M = mutual inductance of the two circuits
$\omega = 2\pi f$
$\dot{i}_b$ = primary current
$\dot{i}_a$ = secondary current

The equations of the circuits are

$$(r_b + j\omega L_b)i_b + j\omega M i_a = e \qquad (44)$$
$$(r_a + j\omega L_a)i_a + j\omega M i_b = 0 \qquad (45)$$

These equations are combined to give

$$[(r_b + kr_a) + j\omega(L_b - kL_a)]i_b = e \qquad (46)$$

where $k = \omega^2 M^2/(r_a^2 + \omega^2 L_a^2)$
Correspondingly,

$$(R^2 + X^2)^{1/2} i_b = e \qquad (46a)$$

where R = effective resistance
X = effective reactance

Equation (46) shows that the charge is electrically equivalent to a resistance kr_a and a negative inductance kL_a placed in the primary circuit. This is illustrated by the measured values of Table 10. These data were obtained by the use of four assemblies made with one primary coil and four solid cylindrical charges of graphite. The frequency was 960 cycles.

TABLE 10

Coil data: Inside diameter = 24 cm
Length over turns = 35.56 cm
Number of turns = 45

Charge	Diameter, cm	R, ohm	X, ohms
0	.....	0.05	1.58
A	15.24	0.16	1.51
B	17.78	0.23	1.40
C	20.32	0.33	1.30
D	22.86	0.43	1.23

Equations. The equations for circuit values that correspond to the general equations just given are based on the shape factor of the charge—the geometrical relation given in Chap. II. A long solid cylindrical charge, a single-layer primary coil, and a sinusoidal alternating current are assumed as the basis of the equations that follow.

RESISTANCE

Primary Circuit. The alternating-current resistance of a single-layer coil, see Fig. 48, is

$$r_b = \frac{4\pi^2 \sqrt{f}\sqrt{\rho_b 10^9}\, N^2 b' K_r}{l\sqrt{s} \times 10^9} \quad \text{ohms} \tag{47}$$

Equation (47) for a coil with a copper conductor at 80°C

$$(\rho_b = 2.17 \times 10^{-6} \text{ ohm-cm}^3)$$

is

$$r_b = \frac{1.83\sqrt{f}\, N^2 b' K_r}{l\sqrt{s} \times 10^6} \quad \text{ohms} \tag{47a}$$

$$b' = \left(b + \frac{p_b}{\sqrt{2}}\right) \quad \text{cm, effective inner radius of coil} \tag{48}$$

where p_b = reference dimension of coil conductor, Eq. (1)

$$K_r = \text{resistance function, } \frac{\sinh \Lambda + \sin \Lambda}{\cosh \Lambda - \cos \Lambda} \tag{49}$$

$$\Lambda = \text{index ratio of conductor (see Eq. (3))} = \frac{\sqrt{2}\tau}{p_b} \tag{50}$$

where τ = radial thickness of coil conductor (inner wall thickness of a hollow conductor), cm

A graph of Eq. (49) for values of the index ratio is given in Fig. 61

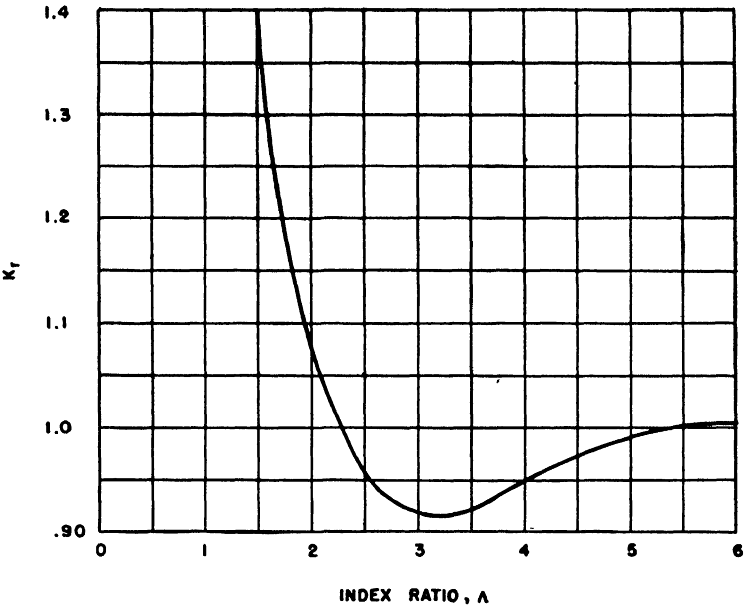

FIG. 61. The resistance function K_r for coil conductors.

Optimum Radial Thickness. The value of the index ratio at the inversion point of the graph of Fig. 61 is π. That value substituted in Eq. (50) gives

$$\tau^0 = 2.22 p_b \quad \text{cm} \tag{51}$$

for the optimum radial thickness of the conductor of a single-layer primary coil.

If the operating temperature of a copper coil conductor is 80°C, its reference dimension is

$$p_b = \frac{5.20}{\sqrt{f}} \quad \text{cm} \tag{52}$$

That value inserted in Eq. (51) gives

$$\tau^0 = \frac{11.54}{\sqrt{f}} \quad \text{cm} \qquad (51a)$$

Values of this optimum dimension for a range of values of frequency are given in Fig. 62.

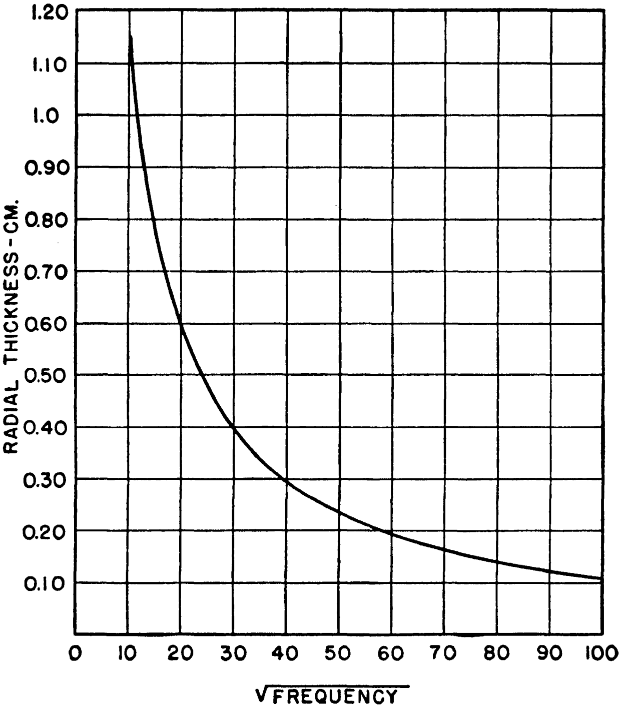

Fig. 62. Radial dimensions of coil conductors by Eq. (51*a*).

The effect of the radial thickness of a coil conductor on the alternating-current resistance of a single-layer coil was investigated experimentally by Polzguter,[9a] who, by using different radial thicknesses of conductors and 1,200 amp, 500 cycles, found the i^2r coil losses to be

	i^2r *Losses, Kw*
With $\tau = 0.25$ cm $= 1.11p_b$, $\Lambda = 1.57$	83
With $\tau = 0.30$ cm $= 1.33p_b$, $\Lambda = 1.88$	80
With $\tau = 0.90$ cm $= 1.78p_b$, $\Lambda = 2.51$	69

Also, in the case of a 3.6-ton steel-melting furnace, Polzguter found that decreasing the radial thickness of the coil conductor from

$\tau = 1.0$ cm ($\Lambda = 6.28$) to $\tau = 0.50$ cm ($\Lambda = \pi$) reduced the melting time from 120 to 100 min and effected some saving in energy consumption.

In practice a value of τ within the range $3p_b$ to $4p_b$ is regarded as good design in that it is on the safe side of the optimum value and does not entail a large decrease of coil efficiency nor an undue waste of conductor material.

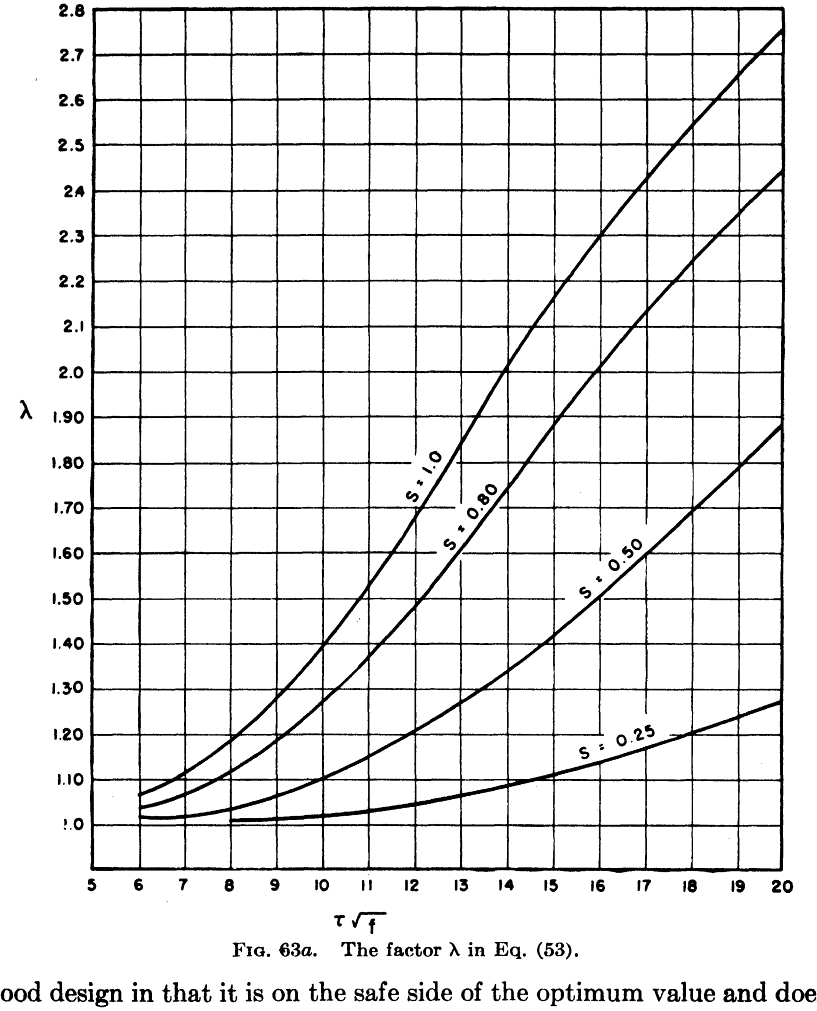

FIG. 63a. The factor λ in Eq. (53).

It should be kept in mind that an increase of the temperature of a conductor increases the value of its reference dimension and thus decreases the value of its index ratio. Hence, referring to Fig. 61, if the temperature of the conductor goes above the value that gives an index ratio less than about 2.50, the efficiency of the coil becomes more and more seriously impaired as the conductor temperature rises.

It may be necessary to design a primary coil to operate at different frequencies. In such cases the lowest frequency is the basis of the selection of the radial thickness of the conductor of the coil.

The consideration of procurable conductor dimensions and the mechanics of coil winding are also factors in the selection of the radial thickness of the coil conductor. These factors usually are not handicaps because of the previously noted freedom in the choice of dimensions.

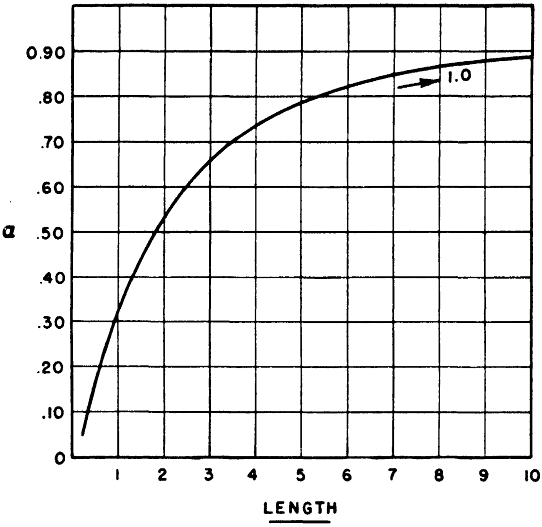

FIG. 63b. The factor α in Eq. (53).

Loaded Coil. The introduction of a charge into a coil decreases the i^2r loss in the coil conductor to some extent by reducing the radial component of the magnetic field. If the ratio of the axial dimension of the coil conductor and the reference dimension of the charge is greater than 1.0, that is, if $(h/p_a) > 1.0$, this effect is negligible. For values of $(h/p_a) < 1.0$, the resistance of the loaded coil is

$$r_b{}^0 = \left(r_b - \frac{r_b}{\lambda}\right)\alpha + \frac{r_b}{\lambda} \quad \text{ohms} \tag{53}$$

where λ = a factor from Fig. 63a by Howe[10]

α = a factor from Fig. 63b by Butterworth[11]

CAPACITANCE

For all frequencies up to its natural frequency a single-layer coil behaves as though it had a uniform current throughout its length and a fixed capacitance across its ends. Hence, the distributed capacitance of the winding can be considered as a capacitance in parallel with the coil. Thus, whatever the value of this capacitance may be, it serves to that extent as compensation for the reactance of the coil.

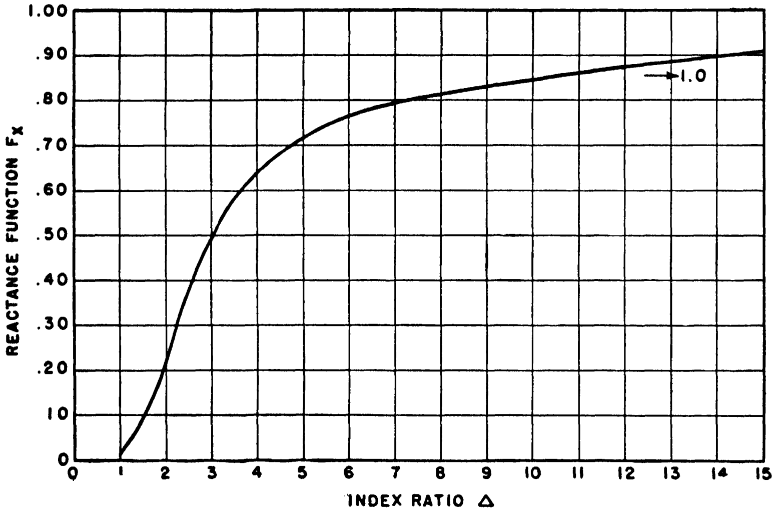

FIG. 64a. The reactance function, F_x, Eq. (58).

Secondary Circuit. The equation for the resistance of the path of the current in the charge—the secondary circuit—which corresponds to the power equation for a solid cylindrical charge, Eq. (15b), is

$$r_a = \frac{4\pi^2 \sqrt{2}\, \sqrt{\mu f}\, \sqrt{\rho_a 10^9}\, N^2 a F_r}{l \times 10^9} \quad \text{ohms} \tag{54}$$

or, referring to Eq. (15c),

$$r_a = \frac{2\pi \rho_a N^2}{l} \Delta F_r \quad \text{ohms} \tag{54a}$$

Effective Resistance, *R*. This is the sum of the primary and secondary resistances, thus

$$R = (r_b + r_a) \quad \text{ohms} \tag{55}$$

REACTANCE

Primary Circuit. The reactance of a long single-layer coil is

$$x_b = \frac{8\pi^3 f N^2 (b')^2}{l \times 10^9} \quad \text{ohms} \tag{56}$$

where b' = effective radius of coil, Eq. (48)

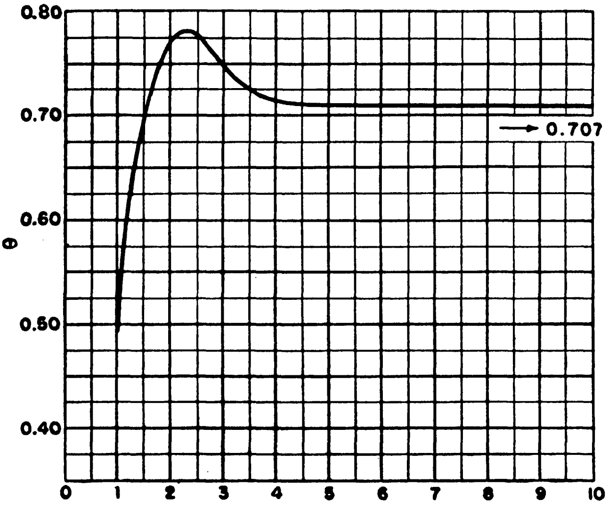

FIG. 64b. The ratio θ, Eq. (59).

Effect of Charge. The change in the reactance, measured at the terminals of the primary coil, caused by the insertion of a charge into the coil is

$$x_a = -\frac{8\pi^3 f N^2 a^2 F_x}{l \times 10^9} \quad \text{ohms} \tag{57}$$

where F_x = reactance function, $1 - (2\mu\theta/\Delta)$ (58)

$$\theta = \frac{(\text{ber}\ \Delta\ \text{bei}'\ \Delta) - (\text{bei}\ \Delta\ \text{ber}'\ \Delta)}{(\text{ber}\ \Delta)^2 + (\text{bei}\ \Delta)^2} \tag{59}$$

A graph of the function F_x for values of the index ratio is given in Fig. 64a. The corresponding graph of the ratio θ is given in Fig. 64b. The value $\Delta = \dfrac{a\sqrt{2}\,2\pi\sqrt{\mu f}}{\sqrt{\rho_a 10^9}}$ inserted in Eq. (58) gives

$$F_x = 1 - \frac{\sqrt{\mu}\sqrt{\rho_a 10^9}\,\theta}{\sqrt{2}\pi a\sqrt{f}} \tag{58a}$$

That expression for F_x is placed in Eq. (57) to obtain

$$x_a = -\frac{8\pi^3 f N^2 a^2}{l \times 10^9} + \frac{4\pi^2\sqrt{2}\sqrt{\mu f}\sqrt{\rho_a 10^9}\,N^2 a\theta}{l \times 10^9} \quad \text{ohms} \quad (57a)$$

The second member of Eq. (57*a*) is Eq. (54) for the secondary resistance multiplied by the ratio (θ/F_r). Hence,

$$x_a = -\frac{8\pi^3 f N^2 a^2}{l \times 10^9} + \frac{r_a\theta}{F_r} \quad \text{ohms} \quad (57b)$$

Effective Reactance, X. This is the sum of Eqs. (56) and (57*b*); thus,

$$X = \frac{8\pi^3 f N^2 (b')^2}{l \times 10^9} - \frac{8\pi^3 f N^2 a^2}{l \times 10^9} + \frac{r_a\theta}{F_r} \quad \text{ohms} \quad (60)$$

Effective Impedance, Z. This is the impedance that corresponds to resistance R and reactance X.

$$Z = (R^2 + X^2)^{1/2} \quad \text{ohms} \quad (61)$$

Power factor,

$$\cos\phi = \frac{R}{Z} \quad (62)$$

Electrical Efficiency. The electrical losses of an assembly are the i^2r watts in the primary coil and the eddy-current watts in any metallic parts of the assembly that are exposed to the alternating magnetic flux. If the latter loss, which should be small, is neglected, the efficiency of the transformation from electric energy to heat in the charge is

$$\eta = \frac{r_a}{r_b + r_a} = \frac{r_a}{R} \quad (63)$$

The importance of this efficiency relates mainly to the effectiveness of the heating operation.

Conversion Efficiency. This is the product of the thermal efficiency and the electrical efficiency. The conversion efficiency of an assembly is expressed as watthours per pound, pounds per kilowatt-hour, or kilowatt hours per ton as may be best suited to the conditions in each case.

Power. The primary power is

$$P_b = \frac{e^2\cos\phi}{Z} = \frac{e^2 R}{Z^2} \quad \text{watts} \quad (64)$$

The corresponding rate of heat development in the charge is the product of the primary power and the electrical efficiency of the assembly; that is,

$$P_a = \frac{e^2 R}{Z^2}\eta = \frac{e^2 r_a}{Z^2} \quad \text{watts} \tag{65}$$

Power Ratio. The ratio R/Z^2 from Eq. (64) is the power ratio of an assembly for a given frequency.

Power Density. The gross power density is expressed as the primary watts per unit area of the lateral surface of the charge. The net power density is the gross power density multiplied by the electrical efficiency of the assembly.

Inasmuch as the electrical efficiencies of assemblies for a given service vary, a comparison of power densities should take this variation into account; that is, such comparisons should be on the basis of net power densities.

Number of Turns. The square of the number of turns in the primary coil appears in the numerator and in both terms of the denominator of the equation for electrical efficiency, Eq. (63). Hence, this efficiency is not affected by the number of turns in the primary coil. This is true also of the power factor.

Therefore, as regards electrical efficiency and power factor, the number of turns of a primary coil can be selected to suit a desired relation of volts and amperes for a given value of volt-amperes. This freedom is subject to whatever conditions may be imposed by the mechanics of coil winding, insulation, and water cooling.

If an arbitrary number of turns is assumed for calculation, the required number of turns to correspond to an available voltage can be determined by the following relation:

$$N_2 = \frac{N_1 e_2}{e_1} \tag{66}$$

where N_1 = number of turns assumed for calculation
e_1 = voltage that corresponds to N_1 turns
e_2 = available voltage
N_2 = number of turns for voltage e_2

Corrective Factors. The circuit equations as given are on the long-coil basis, that is, a length many times the diameter. If an assembly does not meet this condition, these equations must be corrected by the addition of multiplying factors, each less than unity. These factors are given in the paragraphs that follow.

TABLE 11. VALUES OF K_x FOR EQ. (56*a*)

Diameter/Length	K_x	Difference	Diameter/Length	K_x	Difference	Diameter/Length	K_x	Difference
0.00	1.0000	−0.0209	2.00	0.5255	−0.0118	7.00	0.2584	−0.0047
0.05	0.9791	203	2.10	0.5137	112	7.20	0.2537	45
0.10	0.9588	197	2.20	0.5025	107	7.40	0.2491	43
0.15	0.9391	190	2.30	0.4918	102	7.60	0.2448	42
0.20	0.9201	185	2.40	0.4816	97	7.80	0.2406	40
0.25	0.9016	−0.0178	2.50	0.4719	−0.0093	8.00	0.2366	−0.0094
0.30	0.8838	173	2.60	0.4626	89	8.50	0.2272	86
0.35	0.8665	167	2.70	0.4537	85	9.00	0.2185	79
0.40	0.8499	162	2.80	0.4452	82	9.50	0.2106	73
0.45	0.8337	156	2.90	0.4370	78	10.00	0.2033	
0.50	0.8181	−0.0150	3.00	0.4292	−0.0075	10.0	0.2033	−0.0133
0.55	0.8031	146	3.10	0.4217	72	11.0	0.1903	113
0.60	0.7885	140	3.20	0.4145	70	12.0	0.1790	98
0.65	0.7745	136	3.30	0.4075	67	13.0	0.1692	87
0.70	0.7609	131	3.40	0.4008	64	14.0	0.1605	78
0.75	0.7478	−0.0127	3.50	0.3944	−0.0062	15.0	0.1527	−0.0070
0.80	0.7351	123	3.60	0.3882	60	16.0	0.1457	63
0.85	0.7228	118	3.70	0.3822	58	17.0	0.1394	58
0.90	0.7110	115	3.80	0.3764	56	18.0	0.1336	52
0.95	0.6995	111	3.90	0.3708	54	19.0	0.1284	48
1.00	0.6884	−0.0107	4.00	0.3654	−0.0052	20.0	0.1236	−0.0085
1.05	0.6777	104	4.10	0.3602	51	22.0	0.1151	73
1.10	0.6673	100	4.20	0.3551	49	24.0	0.1078	63
1.15	0.6573	98	4.30	0.3502	47	26.0	0.1015	56
1.20	0.6475	94	4.40	0.3455	46	28.0	0.0959	49
1.25	0.6381	−0.0091	4.50	0.3409	−0.0045	30.0	0.0910	−0.0102
1.30	0.6290	89	4.60	0.3364	43	35.0	0.0808	80
1.35	0.6201	86	4.70	0.3321	42	40.0	0.0728	64
1.40	0.6115	84	4.80	0.3279	41	45.0	0.0664	53
1.45	0.6031	81	4.90	0.3238	40	50.0	0.0611	43
1.50	0.5950	−0.0079	5.00	0.3198	−0.0076	60.0	0.0528	−0.0061
1.55	0.5871	76	5.20	0.3122	72	70.0	0.0467	48
1.60	0.5795	74	5.40	0.3050	69	80.0	0.0419	38
1.65	0.5721	72	5.60	0.2981	65	90.0	0.0381	31
1.70	0.5649	70	5.80	0.2916	62	100.0	0.0350	
1.75	0.5579	−0.0068	6.00	0.2854	−0.0059			
1.80	0.5511	67	6.20	0.2795	56			
1.85	0.5444	65	6.40	0.2739	54			
1.90	0.5379	63	6.60	0.2685	52			
1.95	0.5316	61	6.80	0.2633	49			

Equation (56). A factor K_x from Table 11 is added to this equation. Table 11 is Table 10 in Circular No. 74 of the National Bureau of Standards. The value K_x is based on the ratio $2b'/l$ (see Fig. 48). Thus, Eq. (56) becomes

$$x_b = \frac{8\pi^3 f N^2 (b')^2 K_x}{l \times 10^9} \quad \text{ohms} \tag{56a}$$

An alternate method of correcting Eq. (56) for shortness is the following equation:

$$x_b = \frac{8\pi^3 f N^2 (b')^2}{(l + 0.90b)10^9} \quad \text{ohms} \tag{56b}$$

Equations (54) and (57). Methods of deriving corrective factors to be applied to these equations are given by Burch and Davis[12] and by Reche.[13] These methods, although different, give values that are in fair agreement. The corrective factors noted below are based on a modification of the Burch and Davis method.

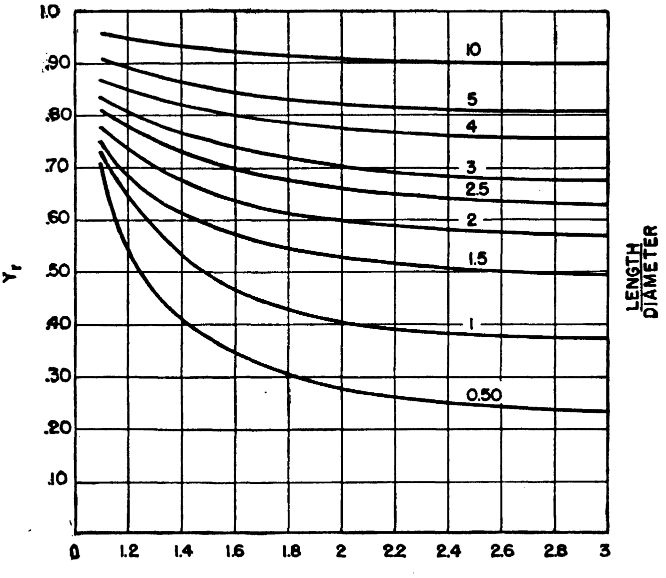

FIG. 65. The corrective factor Y_r for Eq. (54).

Equation (54). Values of the corrective factor Y_r are given in Fig. 65.

Equation (57). Values of the corrective factor Y_x are given in Fig. 66

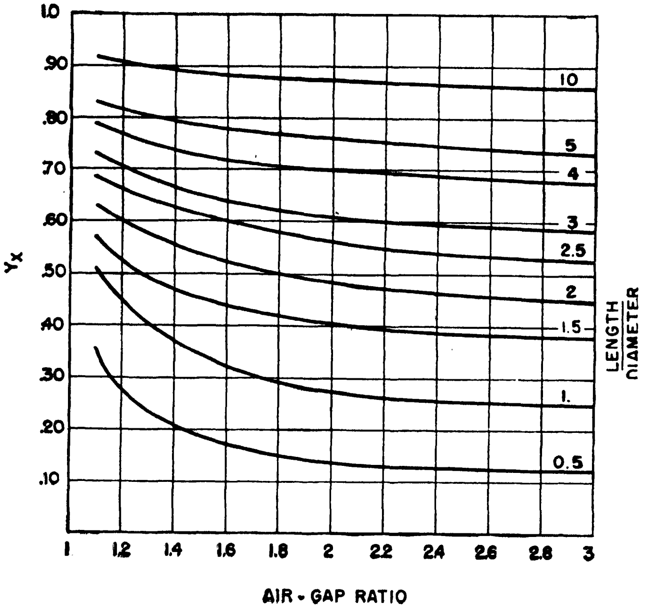

FIG. 66. The corrective factor Y_x for Eq. (57).

In the two examples of the use of Figs. 65 and 66 that follow, the measured values of the corrective factors are in parentheses after the values obtained from the charts in the above noted figures.

Example 3.

$$\frac{l}{2a} = 1.74 \qquad Y_r = 0.63\ (0.67)$$

$$\frac{b}{a} = 1.58 \qquad Y_x = 0.52\ (0.55)$$

Example 4.

$$\frac{l}{2a} = 2 \qquad Y_r = 0.73\ (0.71)$$

$$\frac{b}{a} = 1.23 \qquad Y_x = 0.60\ (0.64)$$

With the additions of the corrective factors, we have

$$r_a = \frac{2\pi\rho_a N^2}{l}\,\Delta F_r Y_r \qquad \text{ohms} \tag{54b}$$

$$x_b = \frac{8\pi^3 f N^2 (b')^2 K_x}{l \times 10^9} \qquad \text{ohms} \tag{56a}$$

$$X = \frac{8\pi^3 f N^2 (b')^2 K_x}{l \times 10^9} - \frac{8\pi^3 f N^2 a^2 Y_x}{l \times 10^9} + \frac{r_a \theta Y_x}{F_r Y_r} \qquad \text{ohms} \tag{60a}$$

Hollow Cylindrical Charge. The equation for the secondary resistance corresponding to the power equation for this shape of charge, Eq. (20*a*) is

$$r_a = \frac{4\pi^2 \sqrt{\mu f}\,\sqrt{\rho_a 10^9}\, N^2 a M_r}{l \times 10^9} \quad \text{ohms} \tag{67}$$

The other circuit equations for an assembly with this shape of charge are the same as for an assembly with a solid cylindrical charge.

Charge with a Rectangular Section. It is assumed that the primary coil is likewise rectangular and that it conforms otherwise to the specification for the primary coil of Eq. (47).

RESISTANCE

Primary Circuit. The alternating-current resistance of a rectangular coil, as noted above, is

$$r_b = \frac{4\pi \sqrt{f}\,\sqrt{\rho_b 10^9}\, N^2(2b + w_b)}{l\sqrt{s} \times 10^9} \quad \text{ohms} \tag{68}$$

where b = one-half the smaller dimension of the coil opening, cm. This dimension corresponds to the inner radius b of a cylindrical coil

w_b = larger dimension of the coil opening, cm

The corresponding resistance of the primary coil with a full charge in place is

$$r_b{}^0 = 0.90 r_b \quad \text{ohms} \tag{69}$$

Secondary Circuit. The equation for the resistance of the secondary circuit which corresponds to the secondary power equation for a charge with a rectangular section, Eq. (23*a*), is

$$r_a = \frac{4\pi \sqrt{\mu f}\,\sqrt{\rho_a 10^9}\, w_a N^2 G_r}{l \times 10^9} \quad \text{ohms} \tag{70}$$

Effective Resistance. This resistance, as before, is the sum of the primary and secondary resistances as expressed by Eq. (55).

VOLT-AMPERES

Primary Circuit. The voltage induced in a rectangular single-layer coil is

$$e_b = \frac{\sqrt{2}\pi f N(2b \times w_b)H}{10^8} \quad \text{volts rms} \tag{71}$$

Equation (71) multiplied by the value of the current in amperes from Eq. (12) gives

$$(va)_b = \frac{fbw_b lH^2}{2 \times 10^7} \quad \text{primary volt-amperes} \tag{72}$$

Secondary Circuit. The voltage induced in a charge with a rectangular section is

$$e_a = \frac{\sqrt{2}\pi fN(2Jp_a w_a \mu H)}{10^8} \quad \text{volts rms} \tag{73}$$

where w_a = width of charge, cm

$$J = \text{function}\left(\frac{\cosh \nabla - \cos \nabla}{\cosh \nabla + \cos \nabla}\right)^{1/2} \tag{74}$$

p_a = reference dimension

Equation (73) multiplied by the value of the current in amperes from Eq. (12) gives

$$(va)_a = \frac{\mu fJp_a w_a lH^2}{2 \times 10^7} \quad \text{secondary volt-amperes} \tag{75}$$

Effective Volt-amperes. This is the sum of the values given by Eqs. (72) and (75); thus,

$$VA = \frac{flH^2}{2 \times 10^7}[(bw_b) + (\mu Jp_a w_a)] \quad \text{volt-amperes} \tag{76}$$

CALCULATIONS

The practical uses of the circuit equations are for calculating values of the watts and volt-amperes that correspond to the rated index ratio of the charge and, for charges of magnetic material, calculating these values at the beginning of the heat cycle.

Inasmuch as there is no way to measure values of charge resistivity and the permeability of a magnetic material during a heat cycle, calculations of intermediate circuit values are problematical. This introduces a difficulty in calculations for continuous heating of magnetic charges as the rated index ratio is based on the mean values of the resistivity and permeability of the charge during the heat cycle. Thus an estimate of these values must be made. However, it is sufficient usually to take the average of the circuit values calculated for the end temperature of the charge and the circuit values calculated for the initial charge temperature. These average values are low but useful.

Measurements. The calorimeter method of measurement of electrical and thermal values is required for laboratory accuracy. Generally, measurements with thermocouple-type voltmeter and ammeter, the electrodynamic-type wattmeter, and thermocouples suffice to obtain data for calculations.

In some cases it is convenient to use a specimen of the material to be heated and 60 cycles for measurements. The base dimension of the specimen should be chosen to given an index ratio reasonably near the rated index ratio desired for the application.

Data. As a rule it is necessary to use typical values, or in some cases estimated values, of electric and magnetic properties for calculations. Hence, assuming that the dimensions of the assembly are known, the accuracy of the calculations depends on the closeness of the approach of the assumed data to the corresponding values of the material of the charge.

Examples. A number of examples of calculations are given as illustrations of the use of the equations in this and the preceding chapters. Measured values, where available, are placed in parentheses after the calculated values.

The arrangement of the examples indicates a convenient method of procedure. First the pertinent data are given. Then follow under Circuit Values the steps in the uses of the circuit equations to obtain the desired end values.

Example 5. *An assembly with a nonmagnetic charge (copper).*
Frequency = 10,000 cycles
Primary coil of round copper tubing: resistivity, $\rho_b = 1.754 \times 10^{-6}$ ohm-cm^3
Solid cylindrical charge; resistivity $\rho_a = 1.754 \times 10^{-6}$ ohm-cm^3

ASSEMBLY DATA

Primary Coil

$p_b = 0.047$ cm, Eq. (1)
$\tau^\circ = 0.104$ cm, Eq. (51)
$\tau = 0.100$ cm
$h = 0.70$ cm
$h/p_a > 1.0$
$\Lambda = 3.0$, Eq. (50)
$K_r = 0.92$, Fig. 61
$b = 9.20$ cm
$b' = 9.23$ cm, Eq. (48)
$l = 30$ cm
$N = 37$
$s = 0.68$, Eq. (40)
$K_x = 0.784$, Table 11

Charge

$p_a = 0.047$ cm, Eq. (1)
$a = 7.50$ cm
$l = 30$ cm
$b/a = 1.225$
$\Delta = 159.5$, Eq. (2)
$F_r = 0.706$, Fig. 31
$\theta = 0.708$, Fig. 64*b*
$Y_r = 0.74$, Fig. 65
$Y_x = 0.60$, Fig. 66

Circuit Values

r_b = 0.078 ohm (0.077), Eq. (47)
x_b = 7.54 ohms (7.46), Eq. (56*a*)
r_a = 0.042 ohm (0.0435), Eq. (54*b*)
R = 0.120 ohm (0.121), Eq. (55)
X = 3.75 ohms (3.25), Eq. (60*a*)

Example 6. *An assembly with a nonmagnetic charge.*
Frequency = 50 cycles
Primary coil with rectangular copper conductor: resistivity = 1.732×10^{-6} ohm-cm^3
Solid cylindrical charge: resistivity = 7.10×10^{-6} ohm-cm^3

ASSEMBLY DATA AND MEASUREMENTS BY BURCH AND DAVIS[12]

Primary Coil	*Charge*
$p_b = 0.725$ cm	$p_a = 1.34$ cm
$\tau^\circ = 1.61$ cm	$a = 7.62$ cm
$\tau = 1.78$ cm	$l = 26.5$ cm
$h = 0.311$ cm	$b/a = 1.58$
$h/p_a < 1.0$	$\Delta = 5.68$
$\lambda = 1.67$, Fig. 63*a*	$F_r = 0.606$
$\alpha = 0.38$, Fig. 63*b*	$\theta = 0.71$
$\Lambda = 3.47$	$Y_r = 0.64$
$K_r = 0.925$	$Y_x = 0.52$
$b = 11.5$ cm	
$b' = 12$ cm	
$l = 26.5$ cm	
$N = 75$	
$s = 0.88$, Eq. (41)	
$K_x = 0.71$	

Circuit Values

r_b° = 0.0217 ohm (0.0221), Eq. (53)
x_b = 0.269 ohm
r_a = 0.021 ohm (0.0217)
R = 0.043 ohm (0.0437)
X = 0.209 ohm (0.206)
Z = 0.211 ohm, Eq. (61)
$\cos\phi$ = 0.20 (0.216), Eq. (62)
η = 0.48 (0.489), Eq. (63)

Example 7. *An assembly with a nonmagnetic charge.*
Frequency = 10,000 cycles
Primary coil with hollow rectangular copper conductor: resistivity = 1.96×10^{-6} ohm-cm^3
Solid cylindrical charge: resistivity 74.42×10^{-6} ohm-cm^3

ASSEMBLY DATA AND MEASUREMENTS BY VAUGHAN AND WILLIAMSON[14]

Primary Coil

$p_b = 0.049$ cm
$\tau^\circ = 0.11$ cm
$\tau = 0.11$ cm
$h = 0.63$ cm
$h/p_a > 1.0$
$\Lambda = 3.17$
$K_r = 0.92$
$b = 1.43$ cm
$b' = 1.46$ cm
$l = 15.10$ cm
$N = 20$
$s = 0.83$
$K_x = 0.92$

Charge

$p_a = 0.307$ cm
$a = 1.27$ cm
$l = 15.10$ cm
$b/a = 1.13$
$\Delta = 4.13$
$F_r = 0.586$
$\theta = 0.713$
$Y_r = 0.92$
$Y_x = 0.85$

Circuit Values

$r_b = 0.0068$ ohm (0.0073)
$x_b = 0.135$ ohm
$r_a = 0.0276$ ohm (0.028)
$R = 0.0344$ ohm (0.0353)

$X = 0.070$ ohm (0.075)
$Z = 0.078$ ohm
$\cos\phi = 0.44$
$\eta = 0.80$

Example 8. *An assembly with a charge of nonmagnetic material.*
Frequency = 10,000 cycles
Primary coil of rectangular copper tubing: resistivity = 1.854×10^{-6} ohm-cm^3
Hollow cylindrical charge: resistivity = 75.95×10^{-6} ohm-cm^3

ASSEMBLY DATA AND MEASUREMENTS BY VAUGHAN AND WILLIAMSON[14]

Primary Coil

$p_b = 0.0486$ cm
$\tau^\circ = 0.108$ cm
$\tau = 0.107$ cm
$h = 0.64$ cm
$\Lambda = 3.10$
$K_r = 0.917$
$b = 3.82$ cm
$b' = 3.86$ cm
$l = 7.62$ cm
$N = 10$
$s = 0.84$
$K_x = 0.688$

Charge

$p_a = 0.31$ cm
$a = 1.27$ cm
$t = 0.343$ cm
$l = 7.62$ cm
$b/a = 3.0$
$M_r = 0.923$, Eq. (18)
$k = 0.47$, Eq. (19)
$Y_r = 0.68$
$Y_x = 0.59$

Circuit Values

$r_b = 0.0086$ ohm (0.0095)
$x_b = 0.333$ ohm
$r_a = 0.011$ ohm (0.0102), Eq. (67)
$R = 0.0196$ ohm (0.0197)

$X = 0.315$ ohm (0.316)
$Z = 0.315$ ohm (0.316)
$\cos\phi = 0.062$
$\eta = 0.56$

Example 9. *An assembly with a charge of magnetic material.*

Frequency = 60 cycles

Primary coil with rectangular copper conductor: resistivity = 1.7241×10^{-6} ohm-cm^3

Solid cylindrical charge of SAE 1045 steel: resistivity = 20×10^{-6} ohm-cm^3

Photomicrograph, Fig. 17*a*

Reference magnetization curve No. 5, Fig. 24.

ASSEMBLY DATA

Primary Coil

$p_b = 0.60$ cm
$\tau^\circ = 1.33$ cm
$\tau = 2.54$ cm
$h = 0.635$ cm
$h/p_a > 1.0$
$\Lambda = 5.9$
$K_r = 1.0$
$b = 4.128$ cm
$b' = 4.55$ cm
$l = 25.4$ cm
$N = 29.50$
$s = 0.75$
$K_x = 0.86$

Charge

$p_a = 0.484$ cm
$a = 3.016$ cm
$l = 25.4$ cm
$b/a = 1.37$
$H = 1{,}200$ oersteds
$\mu = 18$
$\Delta = 6.23$
$F_r = 0.6236$
$\theta = 0.709$
$Y_r = 0.82$
$Y_x = 0.75$

Circuit Values

$r_b = 0.0023$ ohm (0.002)
$x_b = 0.0091$ ohm (0.0092)
$r_a = 0.0137$ ohm (0.0135)
$R = 0.016$ ohm (0.0155)

$X = 0.20$ ohm (0.25)
$Z = 0.026$ ohm (0.029)
$\cos \phi = 0.61$ (0.53)
$\eta = 0.85$ (0.87)

Example 10. *An assembly with a charge of magnetic material.*

Frequency = 4,000 cycles

Primary coil of round copper tubing: resistivity = 1.7241×10^{-6} ohm-cm^3

Solid cylindrical charge of SAE 1045 steel: resistivity = 20.5×10^{-6} ohm-cm^3

Reference magnetization curve No. 5, Fig. 24

ASSEMBLY DATA

Primary Coil

$p_b = 0.0738$ cm
$\tau^\circ = 0.164$ cm
$\tau = 0.22$ cm
$h = 0.95$ cm
$h/p_a > 1.0$
$\Lambda = 4.2$
$K_r = 0.96$
$b = 2.06$ cm
$b' = 2.11$ cm
$l = 58.42$ cm
$N = 61$
$s = 0.78$
$K_x = 0.95$

Charge

$p_a = 0.027$ cm
$a = 1.27$ cm
$l = 58.42$ cm
$b/a = 1.62$
$H = 215$ oersteds
$\mu = 88$
$\Delta = 47$
$F_r = 0.706$
$\theta = 0.708$
$Y_r = 1.0$
$Y_x = 1.0$

Circuit Values

r_b = 0.015 ohm (0.0155)
x_b = 0.267 ohm (0.274)
r_a = 0.272 ohm (0.31)
R = 0.29 ohm (0.32)

X = 0.43 ohm (0.375)
Z = 0.52 ohm (0.492)
$\cos \phi$ = 0.55 (0.65)
η = 0.94 (0.96)

Example 11. *The charge is a solid cylindrical steel billet, stationary heating* (see Table 9).

Charge dimensions: diameter, 2 in.; length, 12¼ in.
Lateral surface area = 77 sq in.
Weight = 11⅞ lb
Temperature 2600°F (1427°C, 1700°K)
Heat cycle = 110 sec
Frequency = 9,600 cycles
Heat content (Fig. 46) = 1,425 watthours
Heat loss, Fig. 47 = 600 watthours
Total heat to charge = 2,025 watthours
Power input to charge = 66.3 kw

ASSEMBLY DATA

Primary Coil

b = 3.20 cm
b' = 3.24 cm
l = 31 cm
N = 20
s = 0.90
K_r = 0.917
K_x = 0.92

Charge

ρ_a = 125 × 10^{-6} ohm-cm³
a = 2.54 cm
b/a = 1.27
l = 31 cm
Δ = 6.15
F_r = 0.623
θ = 0.71
Y_r = 0.90
Y_x = 0.85

Circuit Values

r_b = 0.0071 ohm
x_b = 0.30 ohm
r_a = 0.035 ohm
R = 0.042 ohm

X = 0.140 ohm
Z = 0.146 ohm
$\cos \phi$ = 0.28
η = 0.83

Power, $\frac{66.3}{0.83} = 80$ kw (79)

Gross power density = 1040 watts per sq in.
Voltage required by Eq. (64) is e = 200 volts
Coil current = 1,370 amp
Volt-amperes = 274 × 10^3
For 480 volts,

$$N_2 = \frac{20 \times 480}{200} = 48 \text{ turns, Eq. (66)}$$

Example 12. *Continuous heating of SAE* 1045 *steel, round bar stock, diameter* 1¼ *in., random lengths.*

Through heating to 871°C (1600°F)

Production = 250 lb per hr
Protective gas atmosphere
Frequency = 9,600 cycles
Unit weight of charge = 4.17 lb per ft
Heat content = 250 lb, 18,750 watthours
Conversion efficiency, assumed = 7 lb per kwhr (60 per cent)
Input to primary coil = 35 kw (35)

ASSEMBLY DATA

Primary Coil

Inside diameter = 1.75 in.
Length = 15 in.
Movement of charge = 12 in. per min
Heat cycle = 1.25 min
Power density, gross = 584 watts sq in.
r_b = 0.022 ohm
x_b = 0.589 ohm

Circuit Values

Initial	*End*, 871°C
$\rho_a = 18 \times 10^{-6}$ ohm-cm^3	$\rho_a = 121 \times 10^{-6}$ ohm-cm^3
$\mu = 18$	$\mu = 1.0$
R = 0.197 ohm	R = 0.112 ohm
Z = 0.505 ohm	Z = 0.41 ohm

Average Circuit Values

R = 0.155 ohm (0.18)
Z = 0.46 ohm (0.497)
$\cos \phi$ = 0.34 (0.36)
η = 0.86 (0.88)
i = 495 amp (440)
e = 226 volts (219)
kva = 112 (98)

Example 13. *Continuous heating of sheet steel, SAE* 1020.
Temperature = 1350°F (734°C)
Frequency = 9,600 cycles
Sheet dimensions:
  Thickness = 0.0613 in. (0.156 cm)
  c = 0.078 cm
  Width = 48 in. (122 cm)
Weight = 10 lb per ft length
Production = 20,000 lb per hr

ASSEMBLY DATA

Primary Coil

Length = 50 in. (127 cm)
Width = 50 in. (127 cm)
Opening = 3 in. (7.62 cm)
b = 3.81 cm

Speed of sheet = 33.3 fpm, 0.555 fps
Heat cycle = 7.5 sec
Unit heat content, Fig. 46 = 60 watthours per lb
Total heat content = 1,200 kwhr
Rate of heat loss, Fig. 47 = 30 watts per sq in.
Heat loss = 144 kwhr
Total heat absorption = 1,344 kwhr

Electrical efficiency, assumed = 0.90
Total heat required = 1,490 kwhr
Conversion efficiency = 13.40 lb per kwhr
Power required = 1,490 kw

Mean resistivity of sheet = 75×10^{-6} ohm-cm^3

The example includes all the data required for the calculation of the volt-amperes by Eq. (76) except the values H and μ. It is necessary to assume a value of H and the corresponding value of μ from the magnetization curve of the material for trial.

We find that $H = 400$ oersteds and μ from Fig. 25 substituted in Eq. (23) give a value of power somewhat higher than the required value, 1,490 kw. However, that margin is retained by the use of the above noted values of H and μ in Eq. (76), and we obtain

$$\text{Volt-amperes} = 7{,}364 \times 10^3$$

The power factor is

$$\cos \phi = \frac{1490}{7364} = 0.20$$

CHAPTER V

CIRCUIT ANALYSIS

This chapter is a study of the effects of charge resistivity, air-gap ratio, the magnetic property, and frequency on circuit values.

CHARGE RESISTIVITY

The effects of charge resistivity can be examined by taking this factor as a variable—and the only variable—in the equations of the secondary circuit. The values thus obtained and the corresponding index ratios are coordinates of graphs that show the effects of charge resistivity on circuit values.

Numerical values are an aid in a study of this kind. The following data will be used.

Example 14. *An assembly with a solid cylindrical charge.*

Primary Coil	*Charge*
Inside radius, $b = 3.92$ cm	Radius, $a = 3.56$ cm
Length, $l = 7.12$ cm	Length, $l = 7.12$ cm
Number of turns, $N = 5$	Permeability, $\mu = 1.0$
Space factor, $s = 0.81$	

Secondary Resistance. The equation for the resistance of the secondary circuit can be written

$$r_a = C_r \sqrt{\rho_a} F_r \qquad \text{ohms} \tag{54c}$$

where C_r = a constant for the given conditions

If a frequency is assumed and this equation is examined over a sufficient range of charge resistivity values, it is found that, with increasing resistivity (decreasing index ratio), the secondary resistance increases with increase of charge resistivity until the index ratio becomes 2.50. Thereafter, the secondary resistance decreases with increase of charge resistivity. This characteristic is illustrated for the data of Example 14, the frequency 400 cycles, and the resistivity range 9×10^{-6} to 125×10^{-6} ohm-cm³ by graph A of Fig. 67.

This characteristic for a given range of resistivity may or may not exhibit the inversion point shown by curve A, Fig. 67. That for a given radius of charge depends on the frequency. For illustration, the solid portion of graph *B* of Fig. 67 is based on the data of graph *A* except that the frequency is 900 cycles. The broken portion of graph *B* is for resistivity values above the maximum resistivity value of graph *A*.

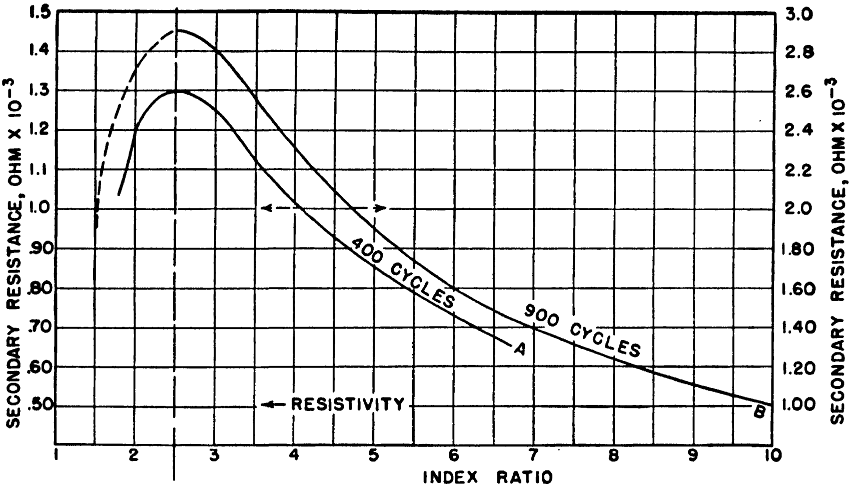

FIG. 67. Effect of charge resistivity on secondary resistance.

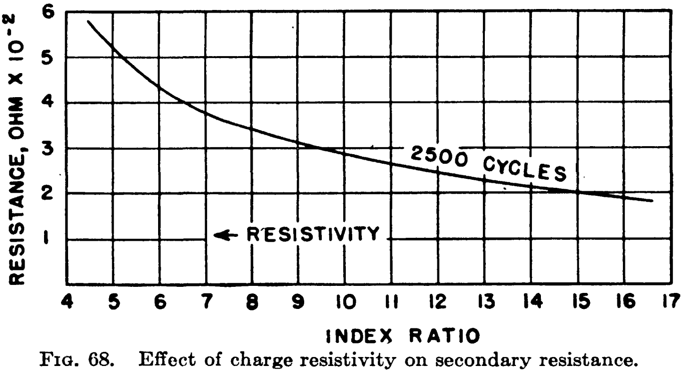

FIG. 68. Effect of charge resistivity on secondary resistance.

This is further illustrated by the use of 2,500 cycles and the other data of graph *A*, Fig. 67, to obtain the graph of Fig. 68.

Effective Values. *Resistance R.* The resistance of the primary circuit is assumed to be constant. Hence, on the basis of charge resistivity as a variable, the graph of the effective resistance values has the shape of the corresponding graph of secondary resistance values. This is illustrated by the graph of Fig. 69 which corresponds to graph *A* of Fig. 67.

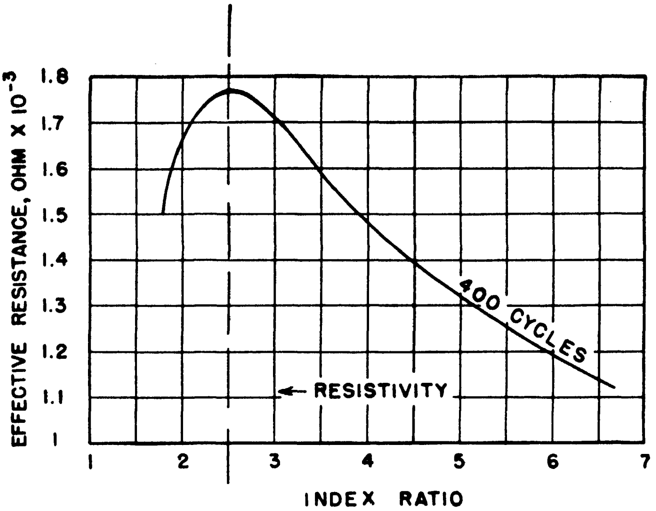

Fig. 69. Effect of charge resistivity on effective resistance.

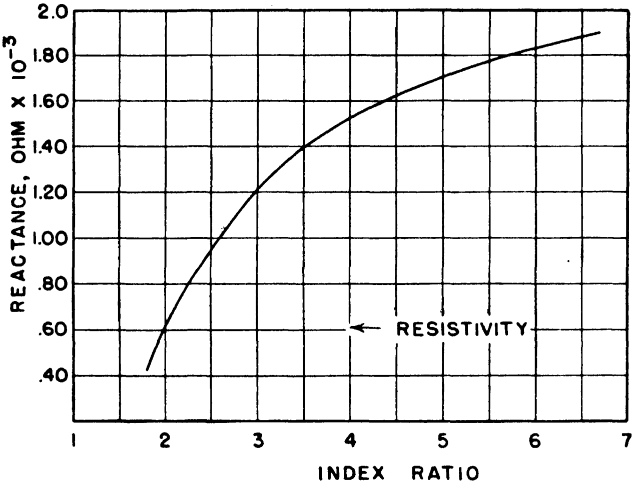

Fig. 70. Effect of charge resistivity on change of reactance due to insertion of a charge in a coil.

Reactance X. The value of the charge resistivity affects only the value of the reactance function F_x, Eq. (58). Hence, Eq. (57) can be written

$$x_a = C_xF_x \qquad \text{ohms} \tag{57c}$$

where C_x = a constant for the given conditions

A graph of Eq. (57*c*) on the basis of the data of graph *A* of Fig. 67 is shown in Fig. 70.

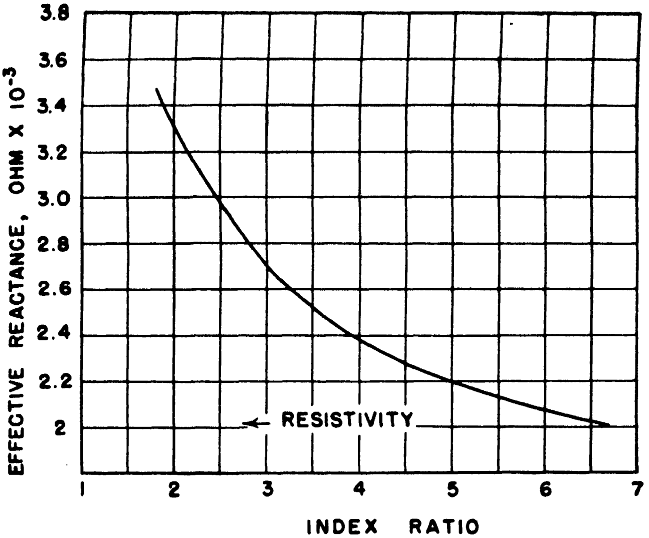

FIG. 71. Effect of charge resistivity on effective reactance.

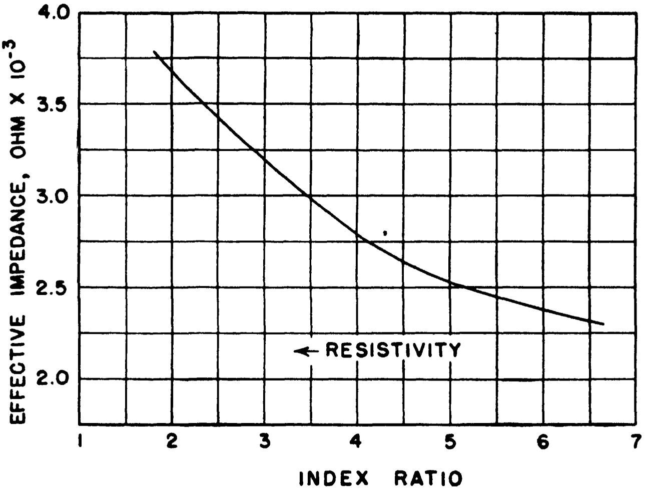

FIG. 72. Effect of charge resistivity on effective impedance.

Thus, with the decreasing value of the reactance function F_x with increasing charge resistivity, the effective reactance X, Eq. (60), increases as shown in Fig. 71.

Effective Impedance, Z. The effective reactance is large in comparison with the effective resistance. Hence, the effective impedance increases with increasing charge resistivity as shown by the graph of Fig. 72. That graph corresponds to the graphs of Figs. 69 and 71.

Power Factor. The graph of Fig. 73 was obtained by taking the ratios of the ordinates of the graphs of Figs. 69 and 72. This graph thus shows the effect of charge resistivity on the power factor of the circuit.

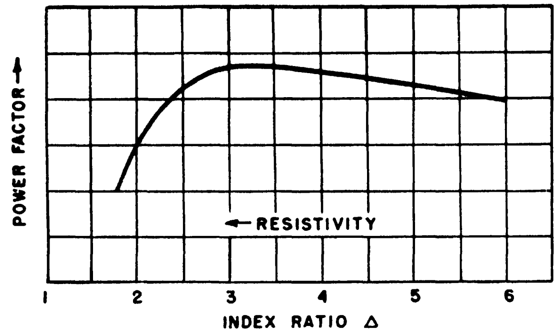

Fig. 73. Effect of charge resistivity on power factor.

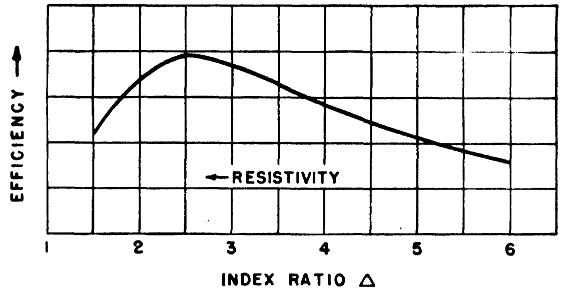

Fig. 74. Effect of charge resistivity on electrical efficiency with a solid cylindrical charge.

Electrical Efficiency. The equation for the electrical efficiency is applicable to an assembly with any shape of charge. Hence, on the basis of charge resistivity as a variable we can write,

$$\eta = \frac{C_r \sqrt{\rho_a} \times \text{resistance function}}{C_b + C_r \sqrt{\rho_a} \times \text{resistance function}} \qquad (63a)$$

and

$$\frac{1}{\eta} = \frac{C_b}{C_r \sqrt{\rho_a} \times \text{resistance function}} + 1 \qquad (77)$$

Hence,

$$\frac{1}{\eta} \simeq \frac{1}{\sqrt{\rho_a} \times \text{resistance function}} + 1 \qquad (78)$$

Solid Cylindrical Charge.

$$\frac{1}{\eta} \simeq \frac{1}{\sqrt{\rho_a} F_r} + 1 \tag{78a}$$

The graph of this relation is shown in Fig. 74. It is obvious that the shape of this graph is the same as that of the graphs of Figs. 67 and 69.

Charge with Rectangular Section.

$$\frac{1}{\eta} \simeq \frac{1}{\sqrt{\rho_a} G_r} + 1 \tag{78b}$$

Example 15. The one-half thickness of the charge is equal to the radius of the charge in Example 14 divided by $\sqrt{2}$; that is,

$$c = \frac{3.56}{\sqrt{2}} = 2.517 \text{ cm}$$

The frequency is 400 cycles, and the range of charge resistivity is 9×10^{-6} to 125×10^{-6} ohm-cm³.

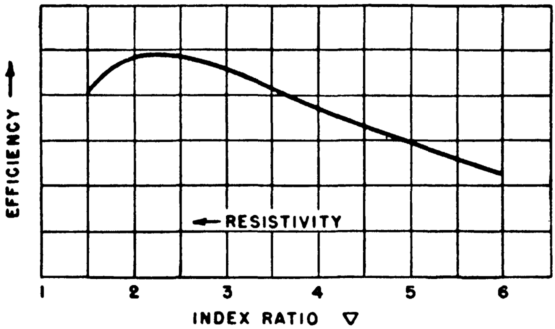

Fig. 75. Effect of charge resistivity on electrical efficiency with a rectangular charge.

The graph of Eq. (78*b*) for these data is given in Fig. 75. Such graphs exhibit maximum values of electrical efficiency with the index ratio value about $\nabla = 2.30$.

Hollow Cylindrical Charge.

$$\frac{1}{\eta} \simeq \frac{1}{\sqrt{\rho_a} M_r} + 1 \tag{78c}$$

There is an individual graph of the relation of Eq. (78*c*) for each set of the radial dimensions *a* and *t*.

Example 16. *An assembly with a hollow cylindrical charge.* The data of the charge are those of graph 1, Fig. 32. Thus, that M graph applies. The frequency is 2,500 cycles. The resistivity range is 36×10^{-6} to 196×10^{-6} ohm-cm^3.

The electrical efficiency—index ratio relation for this example is shown by graph 1 of Fig. 76.

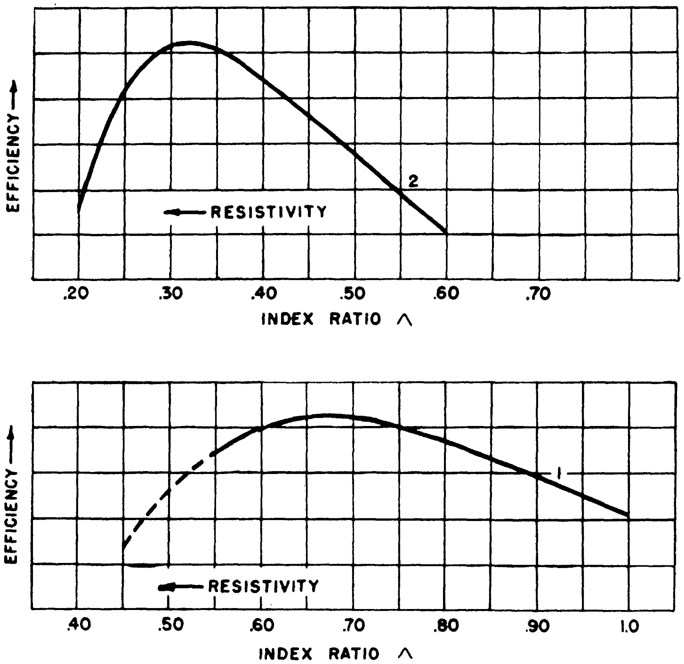

Fig. 76. Effect of charge resistivity on electrical efficiency with a hollow cylindrical charge (see text).

Example 17. *An assembly with a hollow cylindrical charge.* The data of the charge are those of graph 2, Fig. 32. Thus, that M graph applies. The frequency is 8,100 cycles. The resistivity range is 25×10^{-6} to 196×10^{-6} ohm-cm^3.

The electrical efficiency—index ratio relation for this example is shown by graph 2 of Fig. 76.

Power. With a constant current the variation of power with variation of charge resistivity would be shown by a graph that has the shape of the graph of the resistance-index ratio relation. For example, the maximum power with a solid cylindrical charge would occur with the index ratio 2.50.

With constant voltage and charge resistivity as a variable, the current decreases with increase of charge resistivity because of the resultant increase of impedance (see Fig. 72). The graph that shows the relation of power and index ratio may or may not exhibit a maximum value. That with a given assembly depends on the frequency as shown in Fig. 77. The bases of these graphs are the data of Example 14, the resistivity range 9 × 10^{-6} to 125 × 10^{-6} ohm-cm^3 and the frequencies shown on the chart.

The graphs of Fig. 77 also show that the higher the frequency the less is the power affected by a change of charge resistivity.

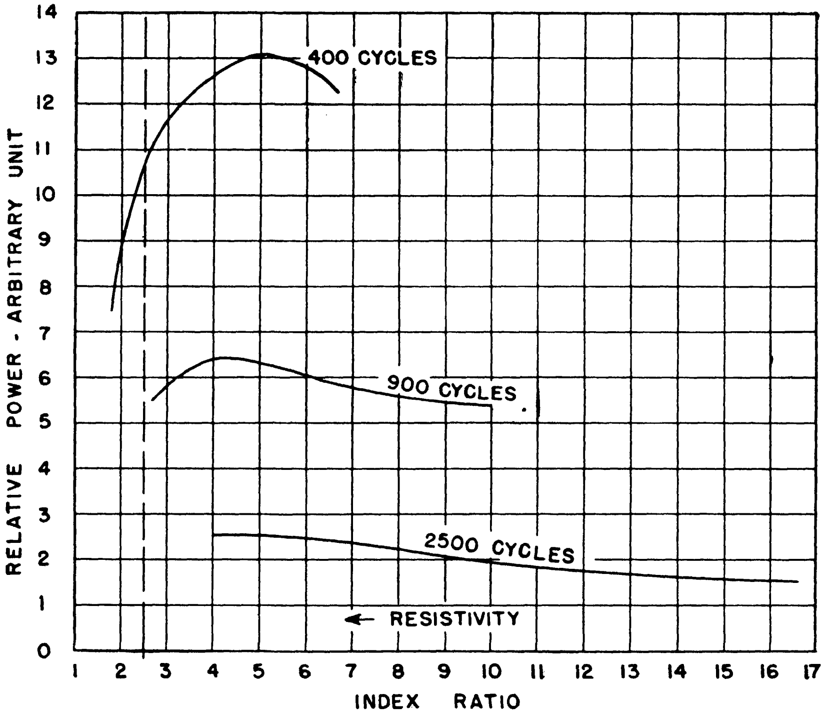

FIG. 77. Effect of charge resistivity on power with constant voltage at different frequencies.

Basic Principle. The graphs so far given in this chapter illustrate a basic principle of the eddy-current phenomenon. This principle is stated thus:

1. An increase of charge resistivity is favorable to heat development if that increase does not decrease the index ratio of the power-index ratio characteristic below the inversion point value.

2. An increase of charge resistivity is unfavorable to heat development if the result of that increase is an index ratio below the inversion point value on the power-index ratio characteristic.

It will be observed that the first condition pertains to the use of eddy currents for heating service and that the second pertains to the minimization of the heating effect of eddy currents.

Heating a Nonmagnetic Charge. The preceding graphs in this chapter were obtained by successively inserting values of charge resistivity—each value higher than the preceding one—in the equation for the resistance of the secondary circuit. This step-by-step procedure corresponds to the initial period of a heat cycle during which the temperature of the annular zone of the charge is raised to the equilibrium temperature.

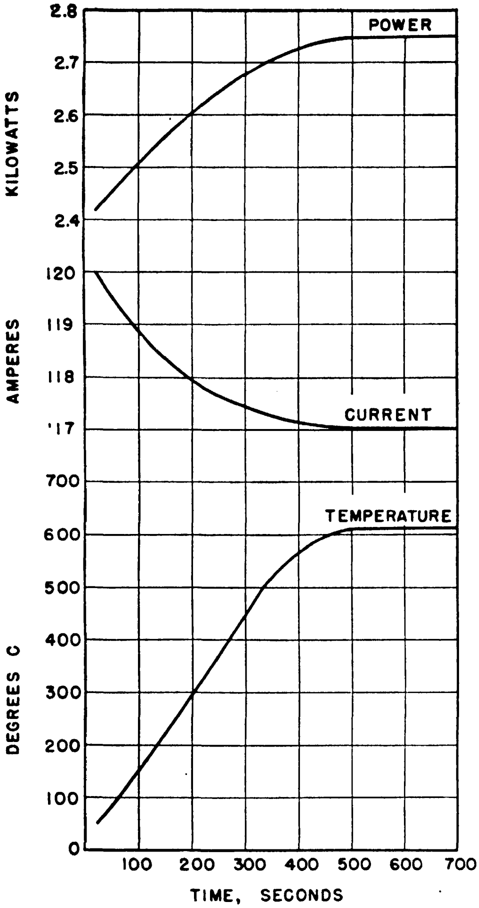

Fig. 78. Records of circuit values and temperature during the heating of a nonmagnetic charge with constant voltage.

For the example that follows a charge of nonmagnetic material was heated slowly to the equilibrium temperature and readings of current, power, and surface temperature were taken at frequent intervals.

Example 18. *An assembly with a solid cylindrical charge of aluminum.* Stationary heating. Constant voltage.

a = 1.27 cm (0.50 in.)
l = 28 cm (11 in.)
f = 9,600 cycles

Temperature range = 20 to 620°C
Initial index ratio = 20
End index ratio = 11

The following graphs are records of this heat cycle:
Figure 78 shows amperes, watts, and surface temperature.

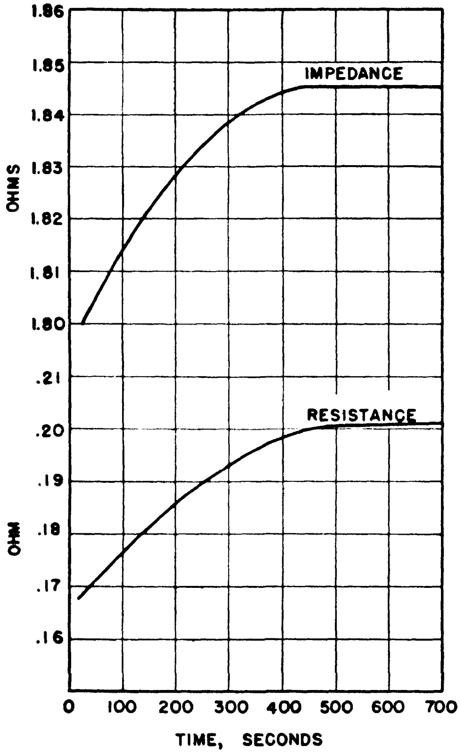

FIG. 79. Values of effective resistance and effective impedance which correspond to the graphs of Fig. 78.

Figure 79 gives the derived values of effective resistance and effective impedance.

A likeness between these graphs and the corresponding calculated graphs, previously given, will be noted if it is kept in mind that the index ratio decreases with rise of temperature.

In practice the temperature rise of the charge is too rapid for observation of circuit values during the temperature rise. With nonmagnetic charges the instruments indicate practically constant current and constant power throughout the heat cycle.

AIR-GAP RATIO

The power is inversely proportional to the square of the effective impedance. The effective impedance, all other conditions being the same, varies with the value of the air-gap ratio. Thus, with a given range of charge resistivity there will be an individual graph of the power and index ratio relation for each air-gap ratio. This is illustrated by the chart of Fig. 80, which repeats the 900-cycle graph of Fig. 77 and includes graphs for the same data except for the air-gap ratios noted on the chart.

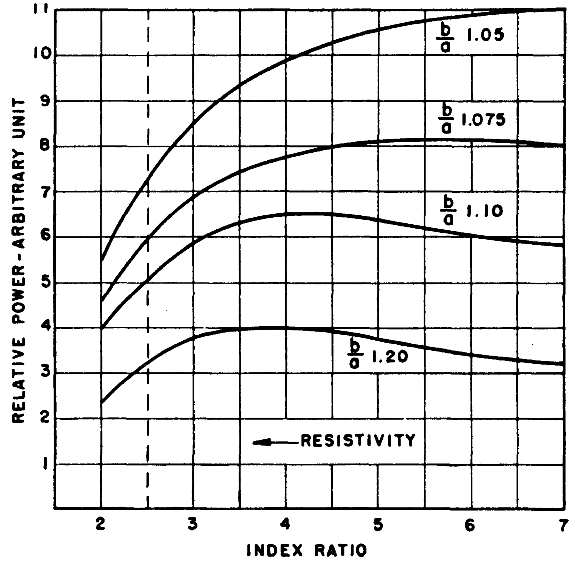

Fig. 80. Effect of the air-gap ratio on power values with increasing charge resistivity. Constant voltage.

THE MAGNETIC PROPERTY

The effects of the magnetic property can be studied by taking a particular material at a temperature below the value at which the permeability is affected and using increasing values of magnetizing current.

Example 19. The data of the assembly for this study are those of Example 9 in Chap. IV. Circuit values were obtained by increasing the magnetizing current in steps. All measurements were made at room temperature.

The following graphs are records of these measurements:

Figure 81 give the effective values of resistance, reactance, and impedance.

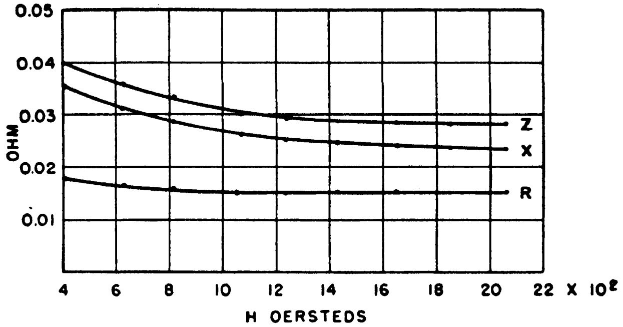

FIG. 81. Effective values of resistance, reactance, and impedance of an assembly with a magnetic charge. Room temperature.

Figure 82 shows the power values. The corresponding calculated power values are included on this chart. An example of these calculations is Example 9, Chap. IV.

It is seen in Fig. 81 that, as saturation is approached—around 1,200 oersteds—the effective values of resistance, reactance, and impedance become constant.

The effect of the magnetizing force on the index ratio is illustrated by the following example.

Example 20. *Continuous heating of SAE* 1020 *sheet steel.*

DATA

Sheet thickness = 0.0613 in. (0.078 cm)
Temperature = 734°C (1350°F)
Resistivity, mean value = 75×10^{-6} ohm-cm^3
Permeability curve, Fig. 25
Index ratio with $H = 1{,}000$ oersteds and $\mu = 21.5$, $\nabla = 1.70$
Corresponding reference dimension = $p = 0.066$ cm, Eq. (1)
Corresponding frequency by Eq. (4) = 10,000 cycles

H	μ	∇
300	65	2.90
400	50.5	2.60
500	41	2.35
700	30	2.0
1,000	21.5	1.70

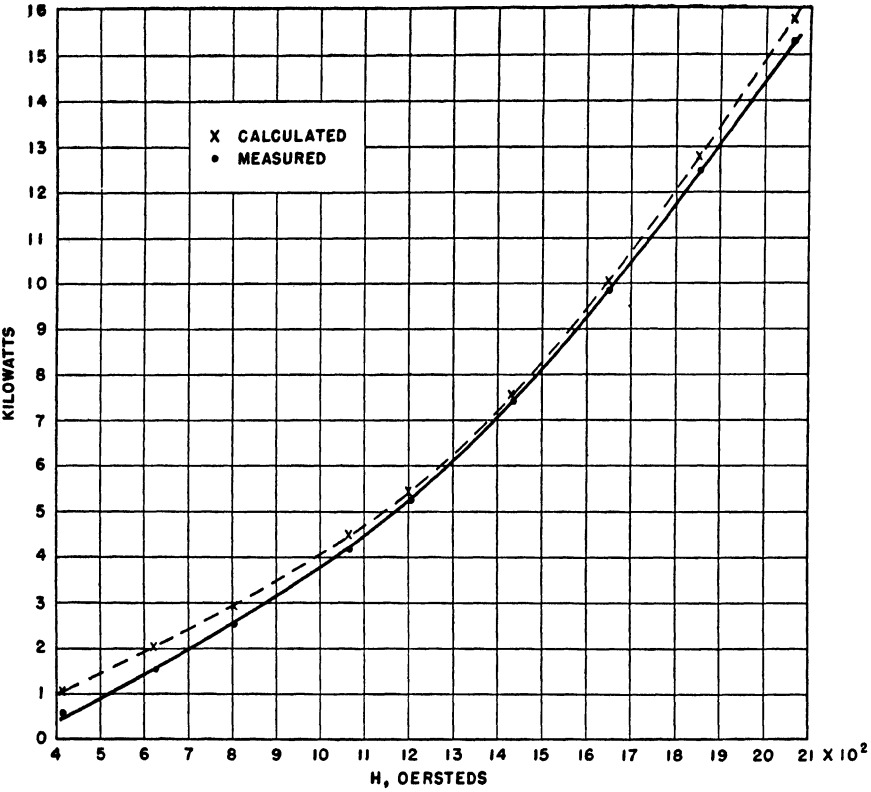

Fig. 82. Measured and calculated values of power input to an assembly with a magnetic charge. Room temperature.

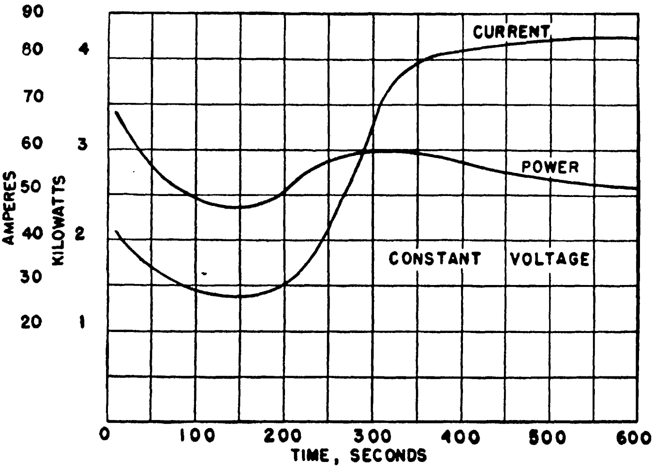

Fig. 83. Circuit characteristics of an assembly with a magnetic charge for the first part of the heat cycle.

Heating Magnetic Charges. The combined effects of charge resistivity and permeability on the effective values of current and power during the first part of the heat cycle are illustrated by the graphs of Fig. 83. These graphs are records of measurements made during the stationary heating of a charge of SAE 1045 steel with constant voltage and constant frequency. The corresponding values of resistance and impedance are shown in Fig. 84.

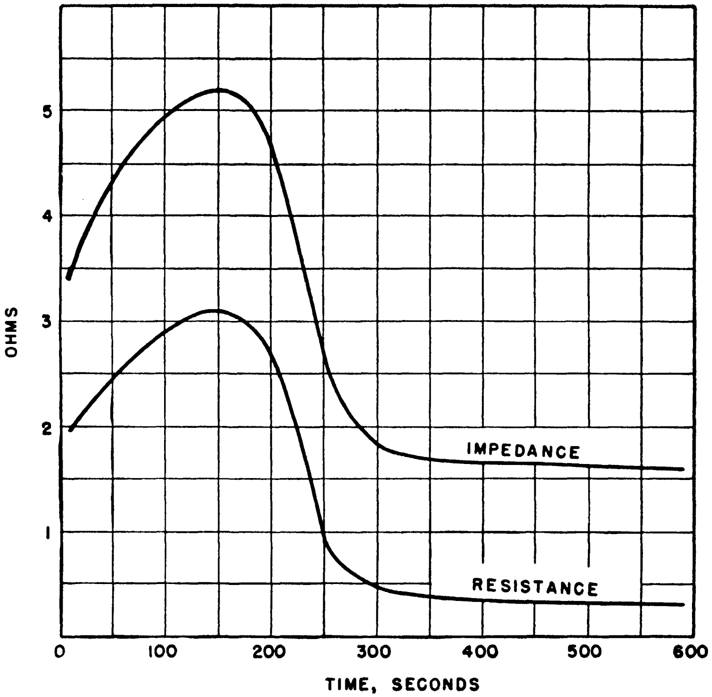

FIG. 84. Values of effective resistance and effective impedance which correspond to the values of Fig. 83.

These records were obtained by using a slow rate of heating so that the changes of circuit values could be recorded. In the corresponding procedure, the initial rate of heat development in the charge is rapid. In such cases the usual instruments indicate that, upon application of voltage, the power rises more or less rapidly to a certain value in each case. The response of these instruments is not fast enough to follow the changes shown in Fig. 84.

With the continuation of the heat cycle the peak power value noted above is followed by a more or less rapid decline of power to a value around 35 to 50 per cent of the peak value of the instrument indication.

Thereafter the power and the current remain practically constant until the end of the heat cycle.

The end period of the heat cycle is the same as would be the case with a charge of nonmagnetic material. However, the core of the charge is heated by thermal conduction, and the transformation of that part of the charge to the nonmagnetic state occurs later than this transformation in the annular zone of the charge.

FREQUENCY

The effects of frequency on circuit values will be considered by taking frequency as a variable—and the only variable—in the circuit equations and using index ratios as abscissas of graphs as was done in the study of the effects of charge resistivity.

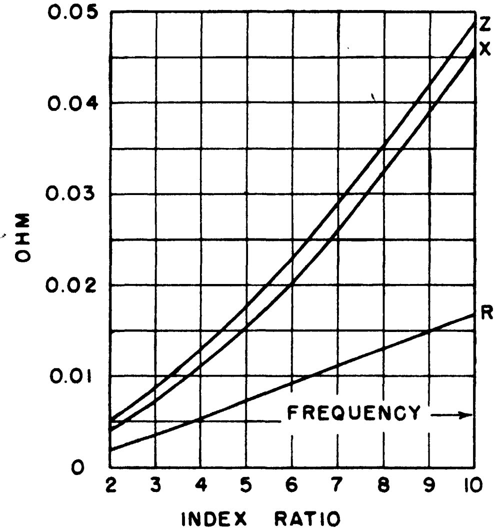

FIG. 85. Effects of frequency on effective values of resistance, reactance, and impedance.

Frequency is a factor in each of the circuit equations. Hence, with frequency as a variable factor, we need consider only the effective circuit values. The example to be used for this purpose is given below.

Example 21. The data of this example are the same as those of Example 14 with the addition of the charge resistivity 100×10^{-6} ohm-cm^3.

Effective Values. The graphs of Fig. 85 illustrate the effects of frequency on the effective resistance, effective reactance, and effective impedance.

Power Ratio. The graph of the power ratio, R/Z^2, which corresponds to Fig. 85 is shown in Fig. 86. With frequencies that give index ratios above 7 or 8, this ratio is practically constant.

Power Factor. The graph of the ratio R/Z from Fig. 85 in Fig. 87 illustrates the effect of frequency on the power factor of an assembly.

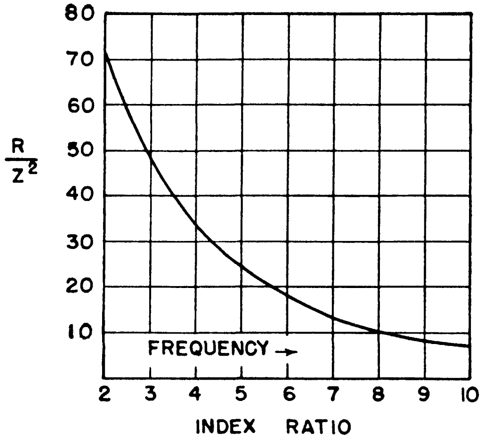

FIG. 86. Effect of frequency on the power ratio of an assembly.

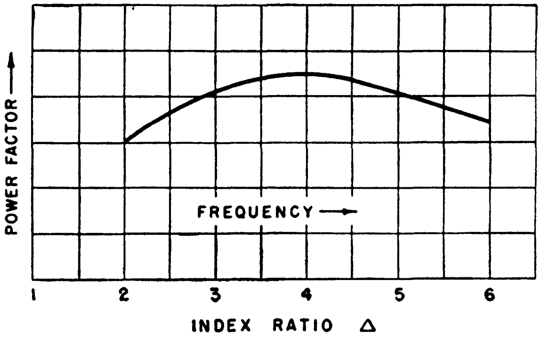

FIG. 87. Effect of frequency on the power factor of an assembly.

Electrical Efficiency. The equation for electrical efficiency on the basis of frequency as a variable can be written,

$$\eta = \frac{C_r\sqrt{f} \times \text{resistance function}}{C_b\sqrt{f} + C_r\sqrt{f} \times \text{resistance function}} \tag{63b}$$

Hence,

$$\frac{1}{\eta} \simeq \frac{1}{\text{resistance function}} + 1 \tag{79}$$

Thus we can insert values of the appropriate resistance function in Eq. (79) to determine the effect of frequency on the electrical efficiency of an assembly with any shape of charge.

Solid Cylindrical Charge. Equation (79) for this shape of charge is

$$\frac{1}{\eta} \simeq \frac{1}{F_r} + 1 \tag{79a}$$

The graph of Eq. (79a) in Fig. 88 shows the relation of the electrical efficiency and the index ratio on the basis of frequency as a variable.

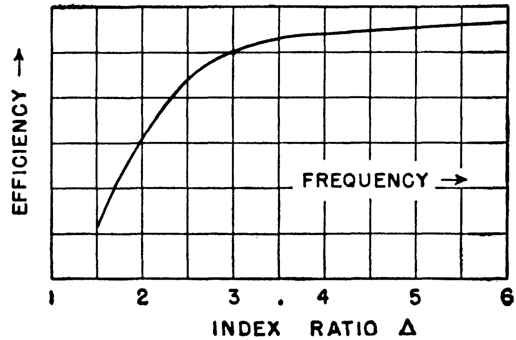

Fig. 88. Effect of frequency on electrical efficiency with a solid cylindrical charge.

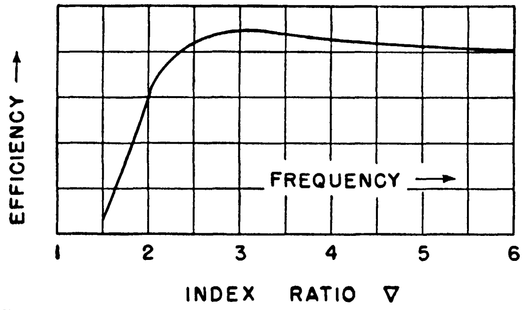

Fig. 89. Effect of frequency on electrical efficiency with a rectangular charge.

This efficiency increases with increase of frequency but approaches a constant value as the resistance function approaches the value 0.707 (see Fig. 31).

The significant feature of the graph of Fig. 88 is that above the frequency giving an index ratio around 5 or 6 the gain in efficiency by increasing the frequency is small.

Charge with Rectangular Section. Equation (78) for this shape of charge is

$$\frac{1}{\eta} \simeq \frac{1}{G_r} + 1 \tag{79b}$$

A graph of this relation with reference to the index ratio is shown in Fig. 89. The electrical efficiency increases with increase of frequency until the index ratio becomes about 3.0. Therefore, the efficiency decreases until it becomes constant with the frequency that gives the index ratio having the value 2π.

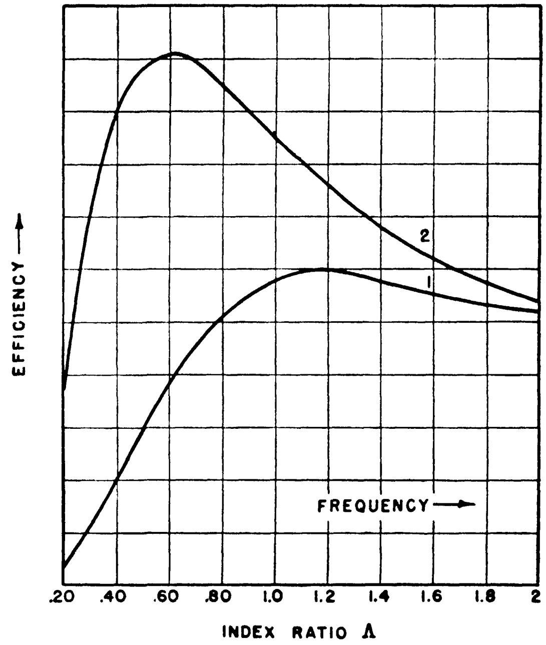

FIG. 90. Effect of frequency on electrical efficiency with a hollow cylindrical charge (see text).

Hollow Cylindrical Charge. Equation (79) for this shape of charge is

$$\frac{1}{\eta} \simeq \frac{1}{M_r} + 1 \tag{79c}$$

The electrical efficiency–index ratio graphs on the basis of frequency as a variable for the relation of Eq. (79*c*) and for the two charges represented by the M graphs of Fig. 32 are shown in Fig. 90, from which we see that the electrical efficiency increases with increase of frequency until the inversion-point value of the index ratio is reached. Thereafter the efficiency decreases until it becomes the value that would be obtained with a solid cylindrical charge of the same material with a radius equal to the outer radius of the hollow charge.

Thin-wall Tubes. *A thin-wall tube is defined by the conditions,*

$$t << p \quad \text{and} \quad \frac{t}{a-t} << 1.0$$

These conditions, although indefinite, are useful for reference.

The maximum electrical efficiency of an assembly with a thin-wall tube as a charge is obtained with the frequency given by the equation,

$$f_o = \frac{44 \times 10^6 \times \rho_a}{(a-t)t} \quad \text{cycles} \tag{80}$$

where ρ_a = resistivity of material of charge, ohm-cm^3
a = outer radius, cm
t = wall thickness, cm

Tubes may, and often do, vary in wall thickness around the perimeter. In such cases the minimum wall thickness is used in Eq. (80).

Example 22.
Tube dimensions: $a = 2$ cm, $t = 0.05$ cm.
Resistivity, $\rho_a = 81 \times 10^{-6}$ ohm-cm^3, $\mu = 1.0$

$$f_o = \frac{44 \times 81}{1.95 \times 0.05} = 36{,}000 \text{ cycles}$$
$$p = 0.17 \text{ cm}$$
$$\frac{t}{a-t} = 0.025$$

Hollow cylindrical charges may not—and often do not—meet the specification for a thin-wall tube. The frequency in such cases that gives the maximum electrical efficiency is higher than the frequency given by Eq. (80). This is illustrated by the two examples that follow.

Example 23. *The hollow cylindrical charge of graph* 1, *Fig.* 32. The frequency by Eq. (80) is

$$f_o = \frac{44 \times 1.905}{(3.175 - 0.333) \times 0.333} = 89 \text{ cycles}$$

The maximum electrical efficiency with this charge occurs with the index ratio 1.20. The corresponding frequency by Eq. (3) is

$$f = \left(\frac{1.20 \times 3560 \sqrt{1.905}}{\sqrt{2} \times 0.333 \sqrt{10^6}}\right)^2 = 156 \text{ cycles}$$

Example 24. *The hollow cylindrical charge of graph* 2, *Fig.* 32. The frequency by Eq. (80) is 1,053 cycles. The maximum electrical efficiency with this charge occurs with the index ratio 0.60. The corresponding frequency by Eq. (3) is 2,079 cycles.

Base Frequency. The assumption of a solid cylindrical charge for illustration is continued. An arbitrary choice of frequency as the basis for a study of the effect of frequency on current and voltage values is the frequency that gives the index ratio 2.50. This frequency is termed the base frequency and is designated by the symbol f_B. As a rule lower frequencies are not desirable for induction heating because of the consequent low electrical efficiencies (see Fig. 88).

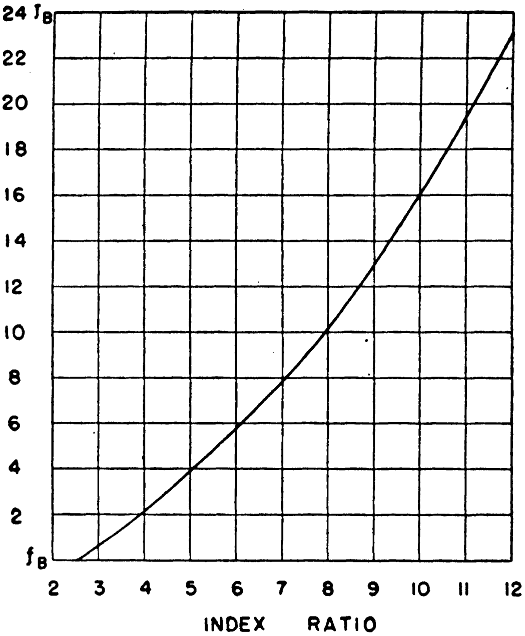

FIG. 91. Values of multiples of the base frequency.

The value of the base frequency is obtained by substituting 2.50 in Eq. (2); thus,

$$f_B = \frac{79 \times 10^6 \times \rho_a}{a^2} \quad \text{cycles} \qquad (81)$$

Values of multiples of the base frequency by Eq. (81) and the corresponding values of the index ratio are given in Fig. 91. For example, the base frequency of a given assembly is 1,000 cycles. The index ratio with 4,000 cycles is $(\sqrt{4} \times 2.50) = 5.0$.

Current. The rate of heat development by eddy currents in a charge with its base frequency is

$$P_B = i_B{}^2 r_{aB} \quad \text{watts} \qquad (82)$$

and with another frequency, f_2,

$$P_2 = i_2^2 r_{a2} \quad \text{watts} \tag{83}$$

For $P_2 = P_B$,

$$i_2 = i_B \left(\frac{r_{aB}}{r_{a2}}\right)^{1/2} \quad \text{amp} \tag{84}$$

The equation for the secondary resistance, Eq. (54*a*) substituted in Eq. (84), gives

$$i_2 = i_B \left(\frac{\Delta_B F_{rB}}{\Delta_2 F_{r2}}\right)^{1/2} = i_B \left(\frac{1.1775}{\Delta_2 F_{r2}}\right)^{1/2} \quad \text{amp} \tag{84a}$$

where Δ_B = index ratio 2.50
F_{rB} = 0.471

A graph of Eq. (84*a*) for values of the index ratio is given in Fig. 92. The ordinates of this graph express the percentages of the current value i_B that are required for the given rate of heat development. For example, if the new frequency gives the index ratio 4, the required current is 71 per cent of the current with the base frequency.

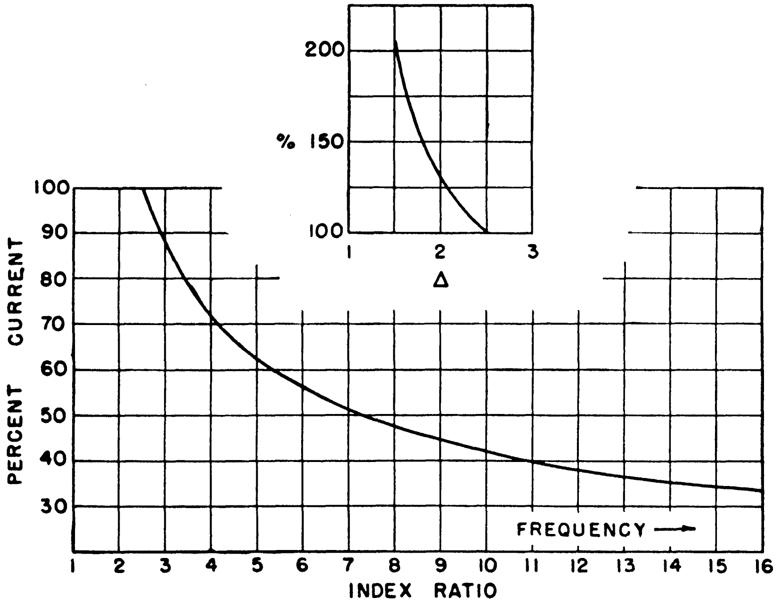

FIG. 92. Percentage values of the current required for constant power and increasing frequency.

Voltage. The voltage required for a given rate of heat development with the base frequency is

$$e_B = i_B Z_B \qquad \text{volts} \tag{85}$$

and with another frequency f_2,

$$e_2 = i_2 Z_2 \qquad \text{volts} \tag{86}$$

for $P_2 = P_B$,

$$e_2 = e_B \left(\frac{r_{aB}}{r_{a2}}\right)^{1/2} \frac{Z_2}{Z_B} \qquad \text{volts} \tag{87}$$

or, corresponding to Eq. (84*a*),

$$e_2 = e_B \left(\frac{1.1775}{\Delta_2 F_{r2}}\right)^{1/2} \frac{Z_2}{Z_B} \qquad \text{volts} \tag{87a}$$

Graphs of Eq. (87*a*) for values of the index ratio and for three air-gap ratios are given in Fig. 93. The ordinates of these graphs are percentage values of voltage e_B which are required for the given rate of heat development with frequencies higher than the base frequency. For example, with the air-gap ratio 1.10, if the new frequency gives the index ratio 7.50, the required voltage is 2.40 times the voltage with the base frequency.

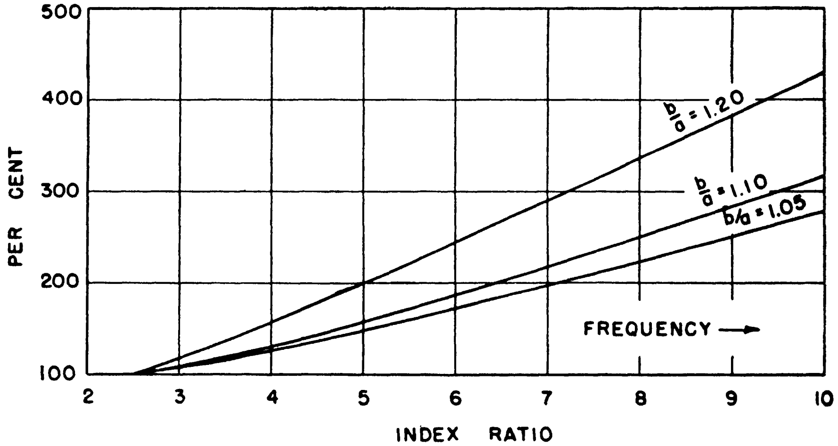

FIG. 93. Percentage values of the voltage required for constant power and increasing frequency with different air-gap ratios.

Volt-amperes. The product of Eqs. (84*a*) and (87*a*) is

$$i_2e_2 = i_Be_B\left(\frac{1.1775}{\Delta_2F_{r2}}\right)\frac{Z_2}{Z_B} \qquad \text{volt-amperes} \qquad (88)$$

Graphs of Eq. (88) that correspond to Figs. 92 and 93 are given in Fig. 94. For example, with the air-gap ratio 1.10 if the new frequency gives the index ratio 7.50, the new value of volt-amperes is 1.20 times the volt-amperes required for the same rate of heat development with the base frequency.

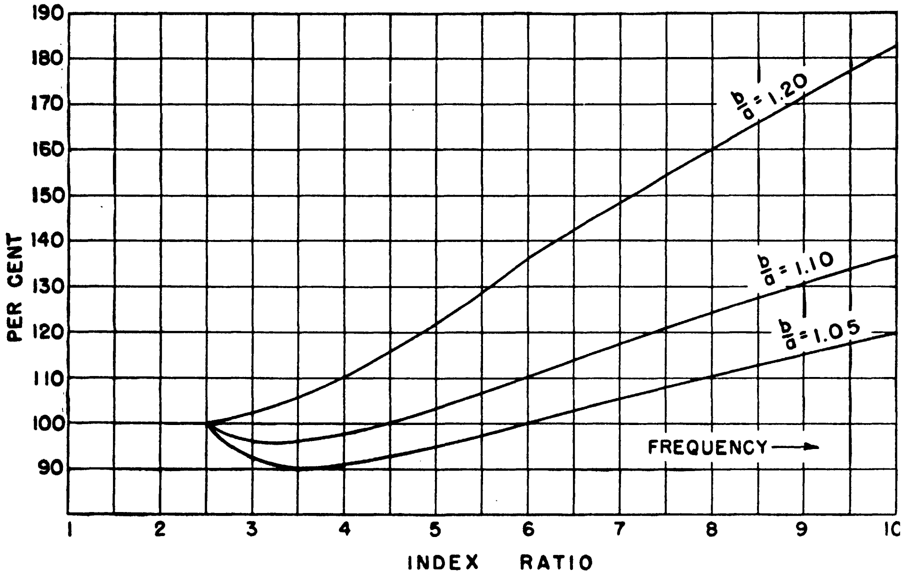

FIG. 94. Percentage values of volt-amperes required for constant power and increasing frequency with different air-gap ratios.

The importance of the relations shown by Fig. 94 is measured by the value of the air-gap ratio. Thus, on the basis of the volt-amperes required for a given rate of heat development, there is considerable freedom in the selection of frequency if the air-gap ratio is small. On the other hand, with large values of the air-gap ratio the volt-amperes increase rapidly with increase of frequency above the base frequency.

CHAPTER VI

APPLICATIONS—CLASS A SERVICE

There is a wide variety of Class A applications. The principal variations are

1. Charges include all materials that are conductive. In addition charges of nonconductive materials are heated indirectly in containers of conductive material, for example, graphite crucibles.
2. Charges are of many shapes and sizes.
3. There is a plurality of objectives and a wide range of specified temperatures.

Two features distinguish induction heating for Class A service:

1. The internal development of heat, which makes rapid heating practicable and economical.
2. The heat placement. The development of heat is confined to the zone of the charge that is exposed to the magnetic flux.

Operating Conditions. The conditions of operation that are peculiar to Class A service are

1. A one-piece charge. The division of the charge into lengths as in the continuous heating of billets does not change this designation.
2. The absence of a heat reservoir (refractory) around the charge.
3. The absence likewise of heat insulation around the charge.

These conditions are best appreciated by a comparison with the conditions of heating by radiation, as in resistor furnaces.

A resistor furnace is an insulated enclosure (heating chamber) with a refractory lining. The source of heat is resistors (heating elements) mounted on the inner surfaces of the chamber. The charge, one-piece or many pieces as the case may be, is heated by radiation from the resistors and by reradiation from the inner surfaces of the chamber. The rate of transformation from electric energy to heat in the charge is determined by the temperature gradient, source to charge surface, and by the emissivity coefficient of the charge surface. A high value of this coefficient is advantageous.

The problem in radiation heating is, thus, to get the heat into the charge. In induction heating the heat is developed within the mass of the charge, and a low value of the emissivity coefficient of the charge surface is advantageous because the loss of heat from the charge by radiation is proportional to the value of this coefficient.

The refractory lining of a resistor furnace is a heat reservoir. As such, it serves as a temperature equalizer and thus is an aid toward the uniform heating of the charge. Uniform heating by the inductive method is accomplished by the distribution of magnetic flux around the charge and by diffusion of heat within its mass.

The resistor furnace requires a heating-up period before it is ready for service. An induction heater is ready for service at any time.

The thermal insulation of a resistor furnace permits the use of the comparatively long heat cycles required for heating by radiation. The heat cycles of induction heating must be short for economy because of the lack of thermal insulation around the charge, and short heat cycles are practicable because of the rapid flow of heat into the mass of the charge.

Thin and Thick Bodies. This is an indefinite thermal distinction which conveys the same thought as the equally indefinite terms "low values" and "high values" of the index ratio noted in Chap. I. That is, a body as a charge is thin, referring to its base dimension, if with a given frequency the electrical efficiency of the assembly is too low for effective heating.

MASS HEATING

Selection of Frequency. A first consideration in each application is the selection of frequency. The technical criterion is electrical efficiency. The frequency must be high enough to make the charge a thick body. It is stated in Chap. I that economics usually dictate the use of a standard frequency. As a general rule, both technical and economic requirements are met as follows:

Solid Cylindrical Charges. The reference is to Fig. 88, Chap. V. A standard frequency is used, which gives a rated index ratio within the range 2.50 to 6.0. The upper limit is generally preferred.

Charges with Rectangular Sections. The reference is to Fig. 89, Chap. V. A standard frequency is used, which gives a rated index ratio within the range 1.70 to 5.0. An intermediate value is usually preferred.

Hollow Cylindrical Charges. The rule for this shape of charge is a standard frequency which gives a rated index ratio somewhat higher than the index ratio corresponding to the frequency given by Eq. (80) for a thin-wall tube.

Miscellaneous Shapes. There are many charges with other than cylindrical or rectangular sections. Some of these are symmetrical, others are asymmetrical. The objective in each case is a frequency which is effective for heating the bulk of the charge but which is ineffective for the development of eddy currents in edges and thin projections. This leaves the latter portions of the charge to be heated by thermal conduction. (The edges and thin projections are considered as thin bodies.)

As with other charges, the leading dimension of the charge is placed parallel to the directions of the alternating magnetic flux. The base dimension of the charge is the radius, or one-half the thickness, of the maximum symmetrical body that could be placed within the perimeter of the median plane of the charge that is normal to its leading dimension. If the lateral surface of the charge is predominantly curvilinear, it is considered as a cylindrical charge; if predominantly planar, as a charge with a rectangular section.

Example 25. Selection of frequency for heating a solid cylindrical charge of steel to forging temperature. See Example 11, Chap. IV.

Charge diameter = 2 in. (5.08 cm)
Charge radius = 2.54 cm
Resistivity = 125×10^{-6} ohm-cm^3
Permeability = 1.0
Assumed rated index ratio = 6.0
Reference dimension, by Eq. (2) = 0.423 cm
Frequency by Eq. (1) = 8,855 cycles
Nearest standard frequency = 9,600 cycles

Lower Limit Frequencies. The graphs of Fig. 95 give values of the lower limit frequencies for solid cylindrical charges for a range of diameters on the basis of the charge resistivity, 125×10^{-6} ohm-cm^3. The lower limit frequencies for solid cylindrical charges shown by Fig. 96 are on the basis of the charge resistivity 10×10^{-6} ohm-cm^3.

The graphs of Fig. 97 give values of lower limit frequencies for charges with thin rectangular sections (plates and sheets) for a range of thicknesses on the basis of the charge resistivity 125×10^{-6} ohm-cm^3.

The technical objections to frequencies below the lower limit values are low electrical efficiencies and high current values. The technical objection to frequencies above the upper limit values is the voltages required with such frequencies with reference to the insulation of the circuits. This objection seldom applies to machine frequencies but may be decisive with spark-gap and electronic frequencies.

In every case the economics of investment and of electrical losses must be taken into account.

Standard Frequencies. Examples of the adaptability of standard frequencies to charge dimensions are given in Tables 12 and 13. For example, a ¾-in.-diameter solid aluminum charge is within the range of three standard frequencies, 960, 3,000, and 9,600 cycles. The choice of one of these frequencies in a given case would be mainly a matter of economics.

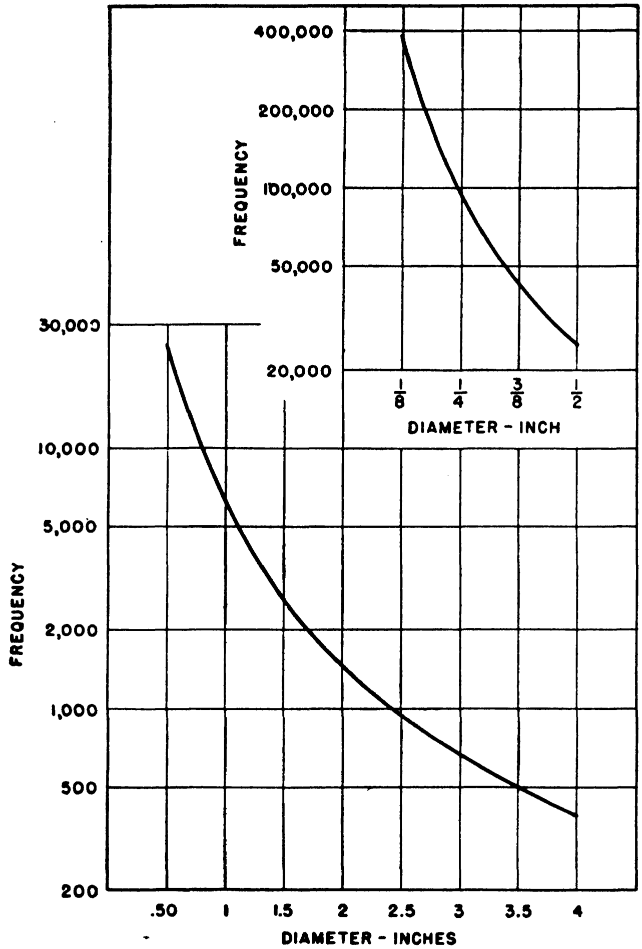

FIG. 95. Lower limit frequencies for solid cylindrical charges; charge resistivity 125 × 10^{-6} ohm-cm³, unit permeability.

In the case of a magnetic material to be heated to a temperature above the Curie point, the initial boosting effect of the magnetic property on the rate of heat development can be considered in the selection of frequency. For example, referring to Table 13, 9,600 cycles is effective for steel charges down to about ½ in. diameter.

Sixty Cycles. There are some uses of 60 cycles for mass heating, as for forging, annealing, and strain relief. The graphs of Fig. 98 show the index ratios for 60 cycles and the corresponding diameters of solid cylindrical charges of aluminum and of steel at the respective forging temperatures of these materials.

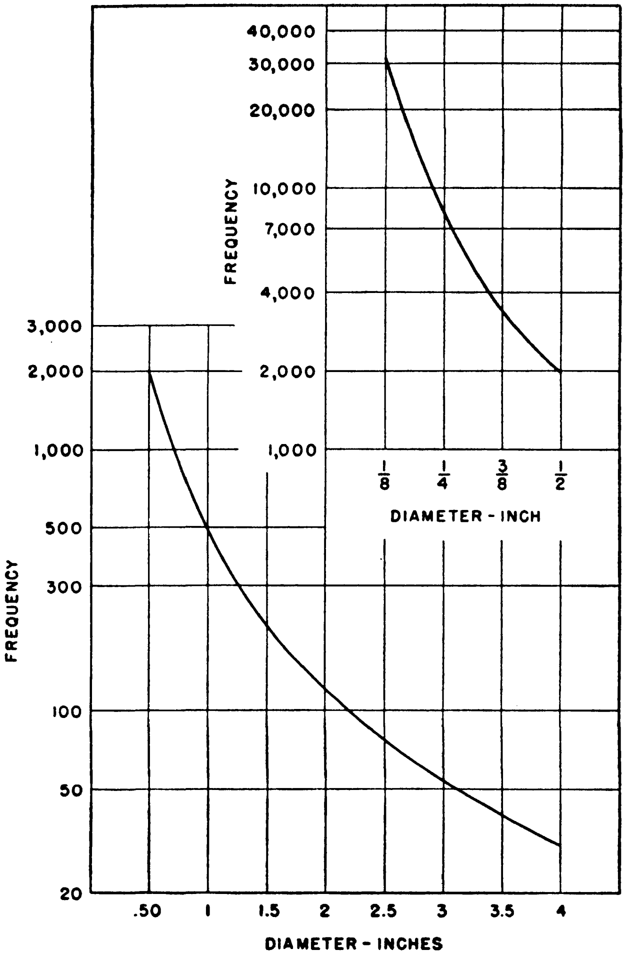

FIG. 96. Lower limit frequencies for solid cylindrical charges; charge resistivity 10 × 10^{-6} ohm-cm^3, unit permeability.

The two technical problems in the use of 60 cycles for induction heating are

1. The effective radius of the primary coil, or inductor [Eq. (48)] is comparatively large. This has adverse effects on the electrical efficiency and power factor.

2. The radial thickness of the conductor of the primary coil by Eq. (51*a*) is 1.48 cm (0.58 in.). That thickness may be a handicap in the water cooling of the coil.

Frequency Combinations. The use of a combination of 60 cycles and a higher frequency for heating charges of magnetic material to a temperature above the Curie point was an early concept. The method has not found favor, mainly because of the complications involved.

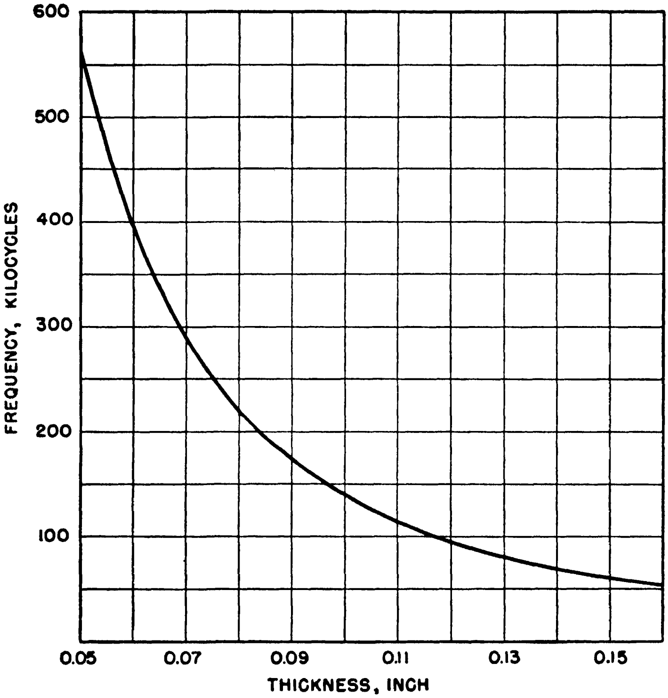

FIG. 97. Lower limit frequencies for charges with rectangular sections; charge resistivity 125 × 10^{-6} ohm-cm³, unit permeability.

Protection. It may be desired that the rated index ratio be a value on the positive or increasing portion of the power-index ratio characteristic based on charge resistivity as a variable (see Figs. 77 and 80). If that is the case and if the power is left on after the rated index ratio is reached, the temperature of the charge will continue to rise. This will continue until the index ratio reaches the inversion point. The charge temperature will then decrease until the equilibrium temperature is attained.

Protection against such rising temperature and possible overheating of the charge is provided by automatic timers for the heat cycle in stationary heating. In continuous heating, a power relay responsive to the movement of the charge gives this protection.

If the rated index ratio is on the negative or decreasing portion of the power-index ratio characteristic, the protection against overheating is inherent. This assumes that the maximum temperature (corresponding to the inversion point) is not harmful.

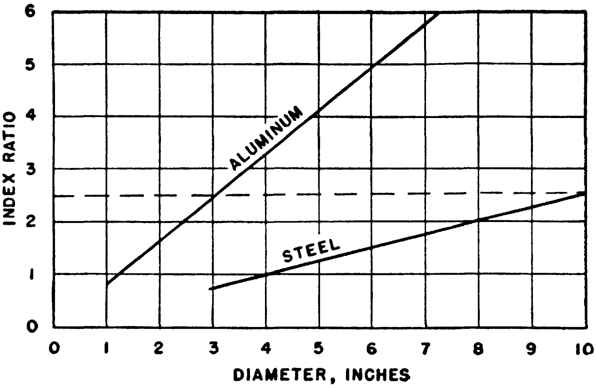

FIG. 98. Index ratios with 60 cycles of solid cylindrical charges of aluminum and carbon steel.

Plant Economics. There may be—and often is—a variety in the heating service of a plant; such as,

1. Charges of different materials
2. A range of diameters (or thicknesses) of charges of a given material
3. Different heat applications
4. Some combination of these conditions

A single standard frequency that is effective for the entire range of work in a plant is desirable. In some cases a preponderance of one service may justify a frequency selected for that service alone.

Heating Rates. The rate of heating for a particular application is generally a matter of economics. As a rule, the best practice in mass heating is a heating rate with which the flow of parts through the plant is continuous during the working period. In some cases storage of heat-treated parts is advantageous.

Internal Stress. During the initial period of heating the outer layer of the charge is trying to expand but is restrained by the core, which being cold has no tendency to expand. The result is a radial tensile stress, which is accompanied by a circumferential compressive stress in the outer zone. The magnitude of these stresses depends on the temperature gradient in the mass, on the natural rate of thermal expansion of the material, on the elastic constants, and on Young's modulus.

TABLE 12. SOLID CYLINDRICAL ALUMINUM CHARGES AT FORGING TEMPERATURE

Diameters		Index ratios		
		Frequencies		
In.	Cm	9,600	3,000	960
0.25	0.635	2.60	1.47	0.83
0.50	1.27	5.25	3.0	1.66
0.75	1.90	7.86	4.4	2.49
1.0	2.54	10.5	5.9	3.30
1.5	3.81	15.7	8.8	5.0
2.0	5.08	20	11.7	6.65
2.5	6.35	26	14.7	8.30
3.0	7.62	31	17.6	10

TABLE 13. SOLID CYLINDRICAL STEEL CHARGES AT FORGING TEMPERATURE

Diameters		Index ratios		
		Frequencies		
In.	Cm	9,600	3,000	960
0.50	1.27	1.58	0.88	0.50
0.75	1.90	2.38	1.32	0.74
1.0	2.54	3.18	1.76	1.0
1.5	3.81	4.76	2.64	1.49
2.0	5.08	6.35	3.52	1.98
2.5	6.35	7.93	4.40	2.48
3.0	7.62	9.52	5.40	2.98

This development of stresses puts a restriction on the permissible rate of heating in some cases. This refers mainly to the initial period of the heat cycle, say up to a core temperature around 500°C. Above that temperature the stress effects are dissipated about as fast as they are set up.

Typical Heating Rates. Ranges of heating rates for steel heated to temperatures above the Curie point that have been observed in practice are shown by the chart of Fig. 99. For example, the range on this chart for the 1½-in.-diameter charge is from 15 to 90 sec.

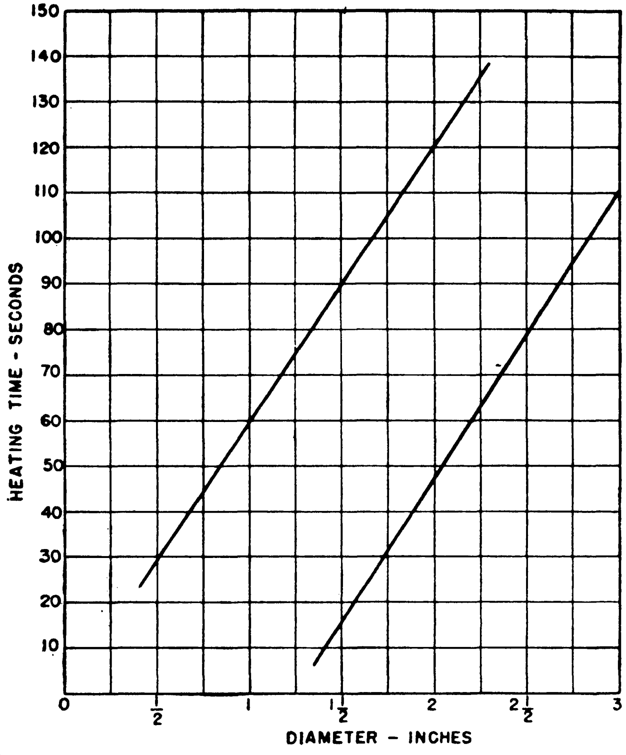

FIG. 99. Ranges of heating rates for mass heating of steel charges.

Power Density. The selection of the rate of heating of a given charge fixes the net power density. The corresponding gross power density is determined by the electrical efficiency of the assembly.

The lower limit of net power density is fixed by the rate of heat dissipation from the surfaces of the charge; the upper limit by the maximum permissible temperature of the near-surface layer of the charge. That temperature must be below the value that, together with the time period of the heat application, would be harmful to the charge.

Values of power density in mass heating vary over a considerable range because of differences in charges, differences in operating conditions, variations of electrical efficiency, and variations in heating practice. Representative values lie between 500 and 2,000 watts per sq in. of the lateral-surface area of the charge.

The power density for a given diameter of charge decreases with increase of frequency because of the corresponding decrease of the volume V_p. An example from practice of the comparatively slow heating of a 3-in.-diameter steel billet to forging temperature is

1,000 cycles	700 watts per sq in.
3,000 cycles	500 watts per sq in.
9,600 cycles	400 watts per sq in.

Heating Metals for Forming. The heating of a charge for such operations as forging and upsetting is preparatory. It is not an end in itself as is the heating phase of a heat-treatment process.

Forging. A large use of mass heating is for the production of steel forgings up to 4 in. in diameter. An analysis of induction heating for that service is given by Strickland.[15] A summary of its merits as stated therein is as follows:

1. Practically no scale. This means a saving of metal and long die life.
2. Close forging tolerances. A minimum amount of machining is required.
3. Rapid heating. Examples from practice are

Diameter, In.	*Heating Time, Sec*
1⅜	8
1¾	20
3	110
5¼	420

4. No heating-up period. Equipment is immediately available for service.
5. Flexibility.
6. Uniformity of temperature.
7. Limitation of the heat effect to the zone desired.
8. Ease of duplication of results.
9. A minimum of skilled labor.
10. Small space.
11. Clean and cool working conditions.

Upsetting. The foregoing comments relative to heating for forging apply also to heating metal parts for upsetting. In addition, the localized heat feature of induction heating has the special usefulness of leaving rigid cold metal adjacent to the heated zone to serve as a backing to resist the flow of metal during the operation.

SURFACE HEATING

This service is essentially a special use of heat concentration and comparatively short heat cycles. Power densities higher than those used for mass heating can be employed because of the short time period of the heat application.

It will be noted by reference to Table 8 that the frequency must be high enough in a given case to obtain an index ratio about 4 or higher for surface heating. With lower frequencies, the surface-heating effect merges into through heating. Another way of defining surface heating is the requirement of a thick body for that effect.

Surface Hardening. This heat-treatment process is defined as hardening an outer layer of a steel part without affecting the crystal structure of its core. This definition leaves the relative radial dimensions of the hardened layer and the core to metallurgical consideration. Three features of induction heating make that method particularly well suited for surface hardening:

1. The heat concentration, that is, the surface heating effect.
2. The more or less abrupt decrease of the rate of heat development with the transformation of the outer layer of the charge to the nonmagnetic state.
3. The axial localization of the heat effect.

General Relations. Provided that the metallurgical conditions and the provision for quenching are correct, the general relations in the use of heat concentration for surface hardening are

1. With a given time period of heat application, the depth or thickness of the hardened layer increases with an increase of net power density.
2. With a given net power density, the depth or thickness of the hardened layer increases with an increase of the time period of the heat application.
3. The depth or thickness of the hardened layer with reference to the first two relations is determined by the frequency; this dimension decreasing with an increase of frequency.

Each application of heat for hardening steel is a part of a metallurgical operation with reference to a particular steel or a particular service. Thus general values of frequency, power density, and the time period of the heat application are not particularly useful. The best technique is developed by experimental studies.

As regards the heating phase of this heat-treatment process, good practice for mass heating is likewise good practice for surface heating. In some cases of surface hardening a frequency higher than normal for mass heating is used as a part of the technique to obtain a very thin hardened layer.

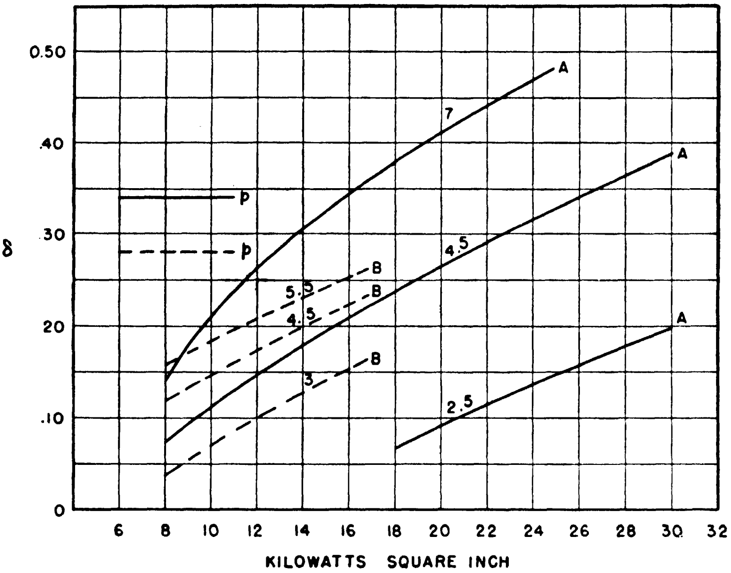

FIG. 100. Comparison of two sets of data of surface hardening of steel (see text).

The two examples of surface hardening given in Fig. 100 and Table 14 are illustrative but do not imply any limitation on this heat-treatment process. Although the conditions stated are not the same, the two sets of data are sufficiently well related for a comparative study.

The curves marked *A* in Fig. 100 are based on data from a paper by Seulen and Voss.[16] The curves marked *B* are from a paper by Vaughn, Farlow, and Meyer.[17] The ordinates of the curves are the depths in fractions of an inch of the layers hardened to 50 Rockwell C. The time periods of the heat applications, in seconds, are noted on the curves. The power densities are gross values. The reference dimensions *p*, in fractions of an inch, which correspond to curves *A* and *B* are marked on the chart.

TABLE 14. DATA PERTAINING TO FIG. 100

	Curves *A*	Curves *B*
Analysis	0.35C, 1.25 Si, 1.25 Mn	SAE 1045
Diameter	2.75 in.	1.5 in.
Frequency	2,000 cycles	3,000 cycles
Reference dimension	0.34 in. (0.87 cm)	0.28 in. (0.71 cm)
Rated index ratio	4.0	2.70

Internal Hardening. The sketches of Fig. 101 illustrate the application of surface hardening to parts with concave surfaces, generally termed internal hardening.

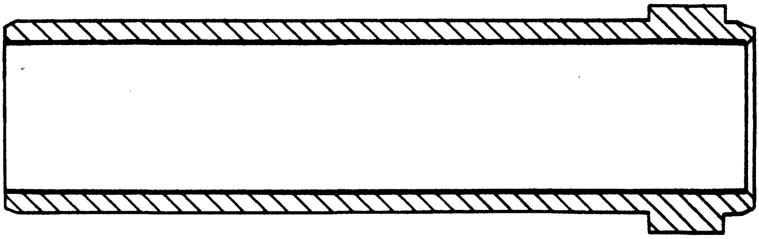

Pump liner

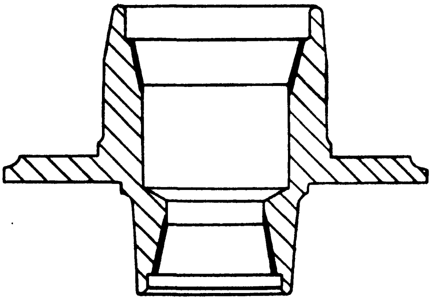

Wheel hub

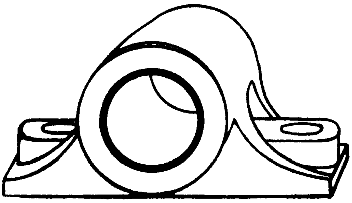

Journal bearing

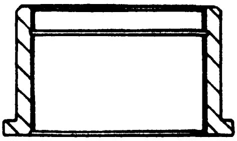

Flanged bushing

FIG. 101. Types of internal surface-hardened parts.

Internal hardening is adapted to parts, or sections thereof, which are substantially cylindrical in form, either straight or tapered sections. This classification includes tubes, oil-well casings, hubs, engine and pump liners, and bearing races. Long lengths of tubes and pipes are heated by the continuous method in which the inductor and a following quenching device travel through the bore.

ILLUSTRATIONS OF SURFACE HARDENING

Figure 102 shows the longitudinal section of a crank pin bearing journal. It is an example of the use of a split-type inductor, similar to that shown in Fig. 55, for heating and quenching. This was one of the first applications of induction heating for surface hardening.

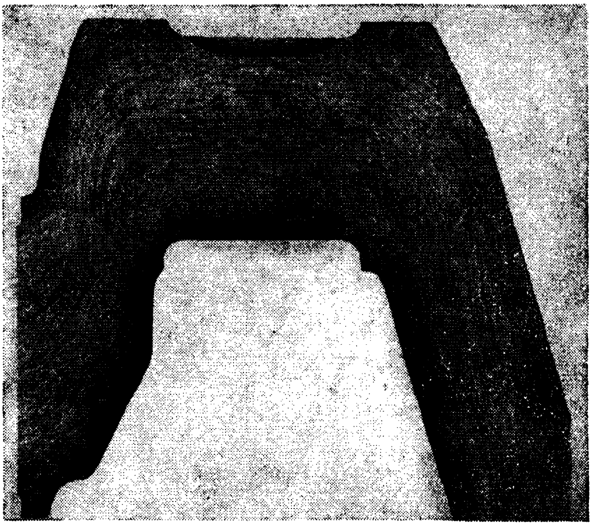

FIG. 102. Longitudinal section of a surface-hardened crankpin bearing journal.

Figure 103 illustrates an SAE 1045 steel brake cam, frequency 1,920 cycles. This is an example of an irregular shape heated in a cylindrical coil and of contour hardening. The rated index ratio of the body of the cam was high enough for effective heating whereas the rated index ratio of the tips was too low for this effect. The tips were heated mainly by thermal conduction.

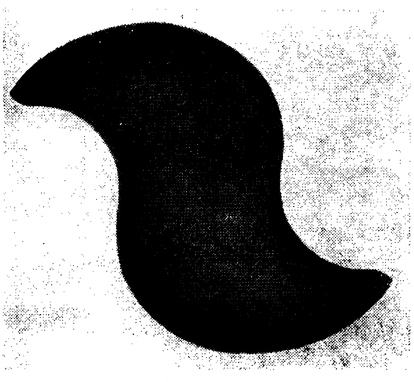

FIG. 103. Steel brake cam, surface-hardened; 4 in. tip to tip.

Figure 104 shows a camshaft with wearing surfaces surface-hardened. The surfaces were hardened by the step-by-step or progressive movement of the inductor and quenching device along the length of the shaft.

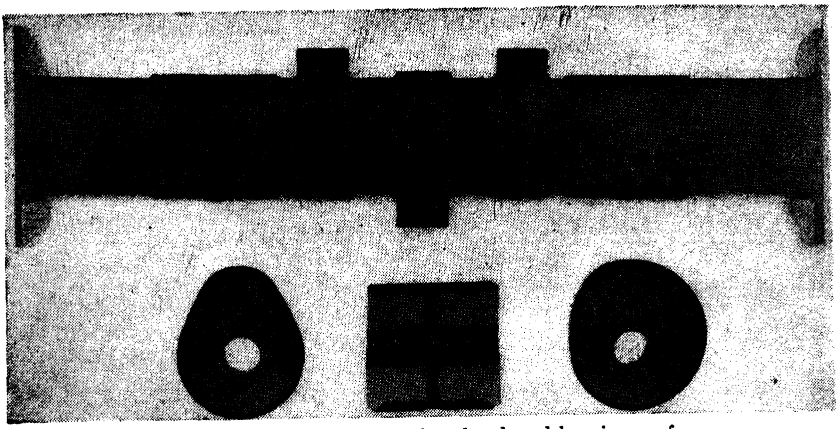

FIG. 104. Camshaft with surface-hardened bearing surfaces.

Figure 105 shows a section of a wheel hub with hardened bearing race. This was one of the first uses of induction heating for internal hardening.

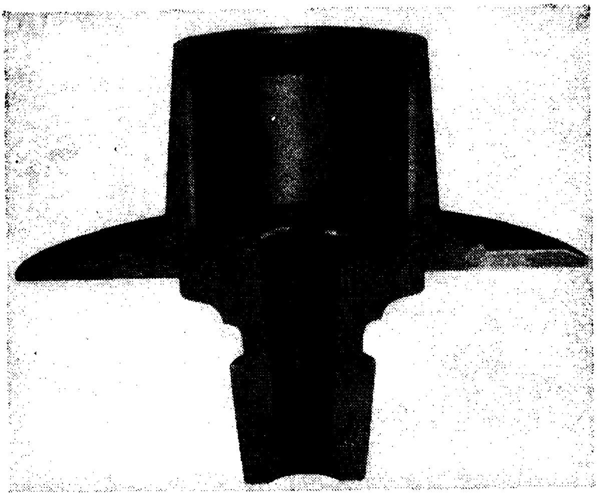

FIG. 105. Section of cast-iron wheel hub with surface-hardened bearing race.

Figure 106 presents typical small machine parts surface-hardened by the induction heating method.

Additional references to the use of induction heating for hardening steel, both surface and through hardening, are papers by Osborn,[18] Riegel,[19] Somes,[20] Babat and Losinsky.[21]

INSTALLATIONS—CLASS A SERVICE

Brazing and Soldering. These processes are uses of surface heating to raise the temperatures of the surface zone of a part and of the brazing or soldering material (a metal or alloy) to its flow point simultaneously. In some cases, through heating of the part is required.

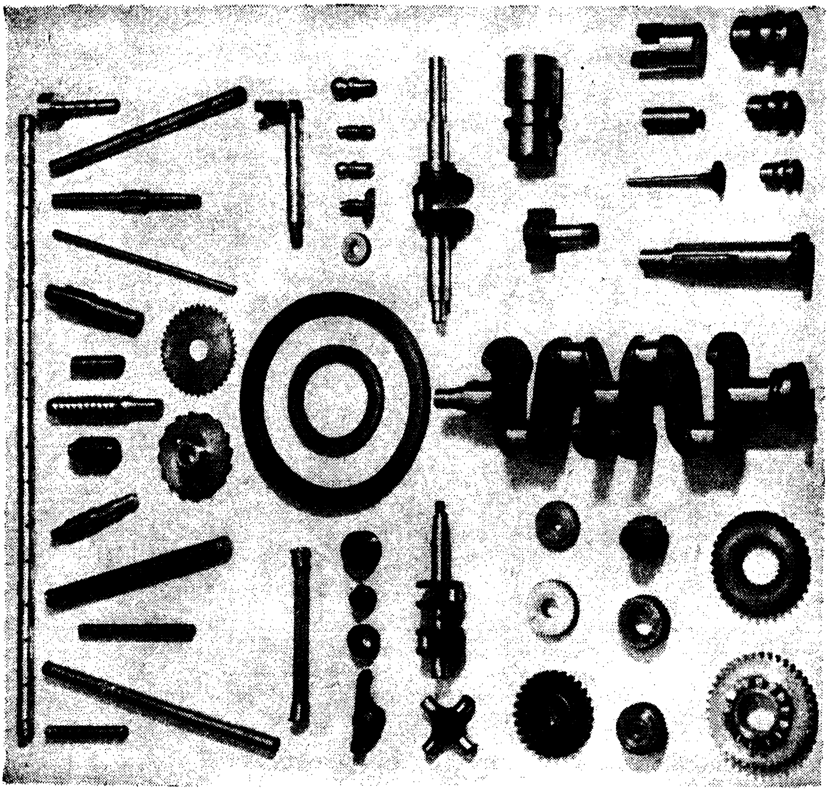

FIG. 106. Typical machine parts, surface-hardened.

There are many and varied uses of induction heating for these services. Many applications include a conveying mechanism for mass production.

The front view of an induction heater for brazing cutting tips on tools is shown in Fig. 107. Note the part turn primary coil or inductor. This operation requires only a few seconds.

Degassing Tubes. In the evacuation of an electron tube it is necessary to include the removal of gases and vapors occluded in the metal parts inside the glass envelope. This is accomplished by heating

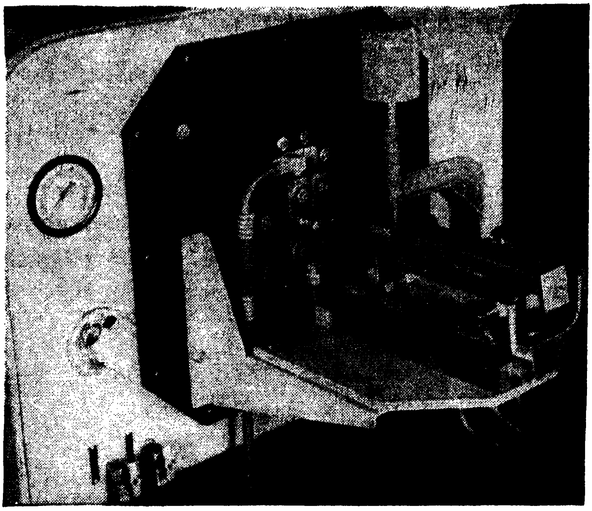

FIG. 107. Front view of an induction heater for brazing cutting tips on tools. (*The Ohio Crankshaft Company.*)

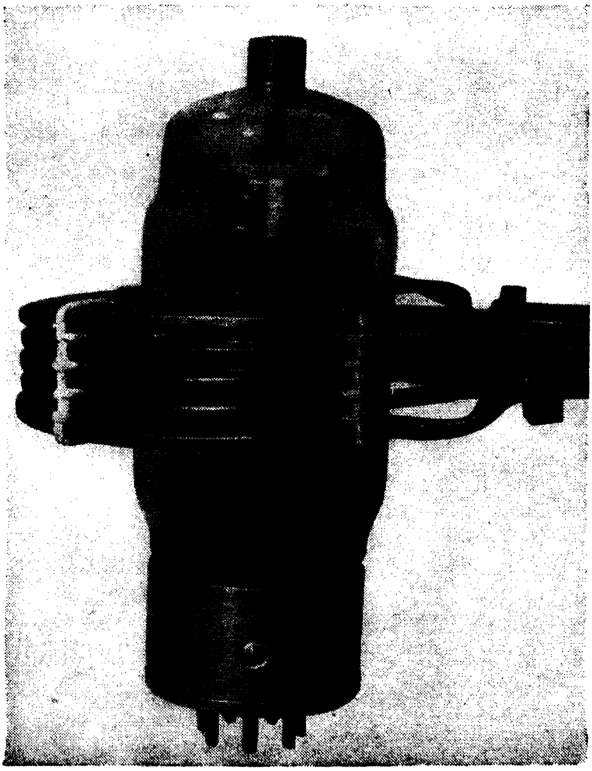

FIG. 108. Assembly of electron tube and primary coil for degassing tubes. (*Radio Corporation of America.*)

these parts by eddy currents during the evacuation operation. An assembly for this service is shown in Fig. 108. An evacuation machine for the quantity production of tubes is shown in Fig. 109.

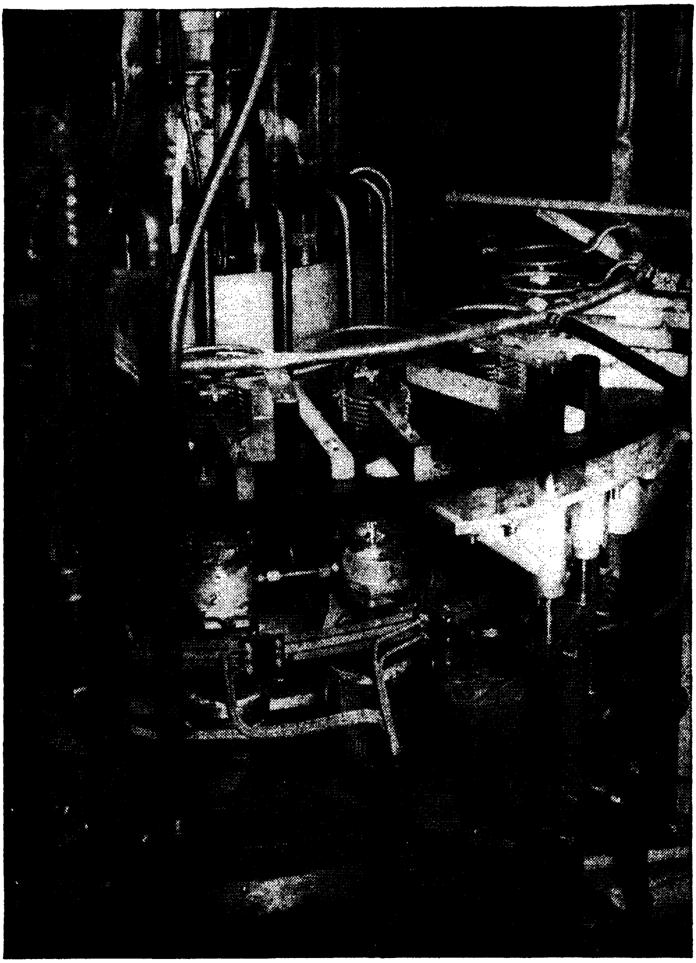

FIG. 109. An automatic electron-tube evacuation machine. (*General Electric Company.*)

Other uses of induction heating in the manufacture of electron tubes are making glass-to-metal joints, brazing, and welding.

Heating Aluminum for Upsetting. An installation for heating solid aluminum propeller blade hubs for upsetting is shown in Fig. 110. This installation contains five induction heaters, each rated 50 kw, 3,000 cycles, 350 volts. The handling mechanism for the charge is of the carriage type. The upsetting machine is in the left background.

A log of temperature measurements, made at the points indicated in Fig. 111 during the heating of a hub and after the heat cycle, is given in Table 15.

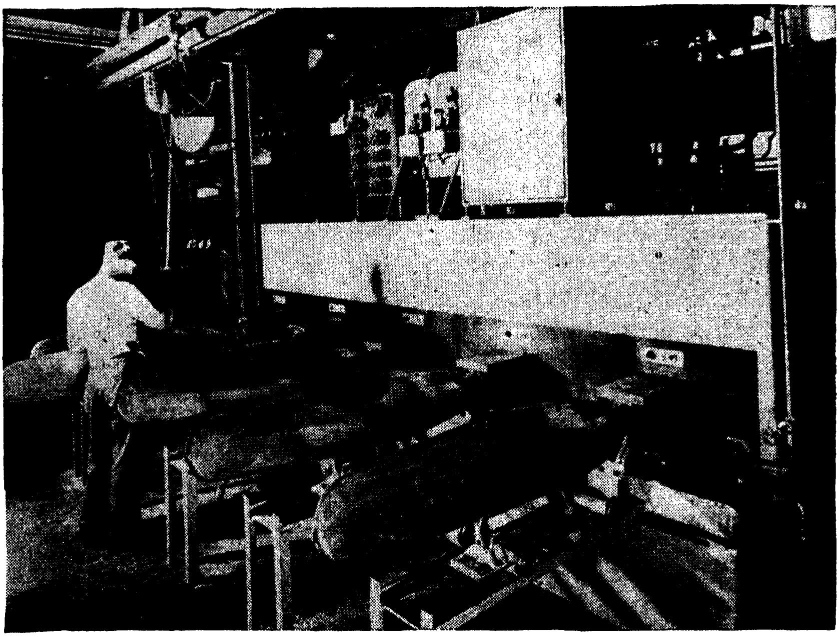

Fig. 110. An installation for forging aluminum propeller-blade hubs. (*The Ohio Crankshaft Company.*)

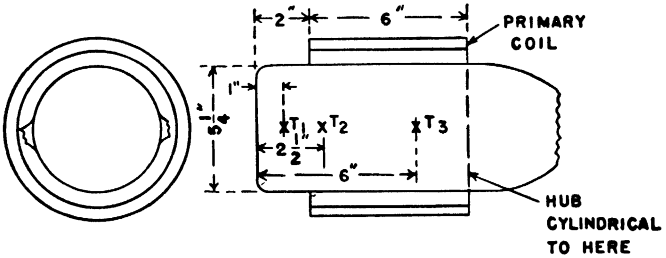

Fig. 111. Temperature-location diagram (Table 15).

The output of this installation in normal production is one blade ready for upsetting every 47 sec; a production of 70 blades per hour.

Heating Steel for Forging. An installation for the production of steel forgings by stationary heating and multiple units is shown in

TABLE 15. LOG OF HEATING ALUMINUM PROPELLER BLADE HUBS (SEE FIG. 110)
(Constant voltage, 3,000 cycles)

Time, sec	Kw	Temperatures		
		T_1	T_2	T_3
0	50	70	70	70
10	. .	. . .	85	
20				
30	50	112		
40	. .	. . .	200	
50	. .	. . .	. . .	200
60	52	200		
70	. .	. . .	258	
80	. .	. . .	. . .	200
90	54	200		
100	. .	. . .	358	
110	. .	. . .	. . .	380
120	55	400		
130	. .	. . .	535	
140	. .	. . .	. . .	610
150	55	560		
160	. .	. . .	673	
170	. .	. . .	. . .	740
180	57	685		
190	. .	. . .	795	
200	. .	. . .	. . .	855
Power off				
210	. .	785		
220	. .	. . .	862	
230	. .	. . .	. . .	890
240	. .	855		
250	. .	. . .	868	
260	. .	. . .	. . .	830

Fig. 112. This installation contains eight units, each with seven induction heaters and an upsetting machine. The charges are billets of round steel bar stock: diameter 3 in., length 19 in., weight 37 lb, temperature 1260°C (2300°F). Each induction heater is rated 100 kw, 960 cycles, 400 volts. Two of these heaters and the common supporting structure are shown in Fig. 113.

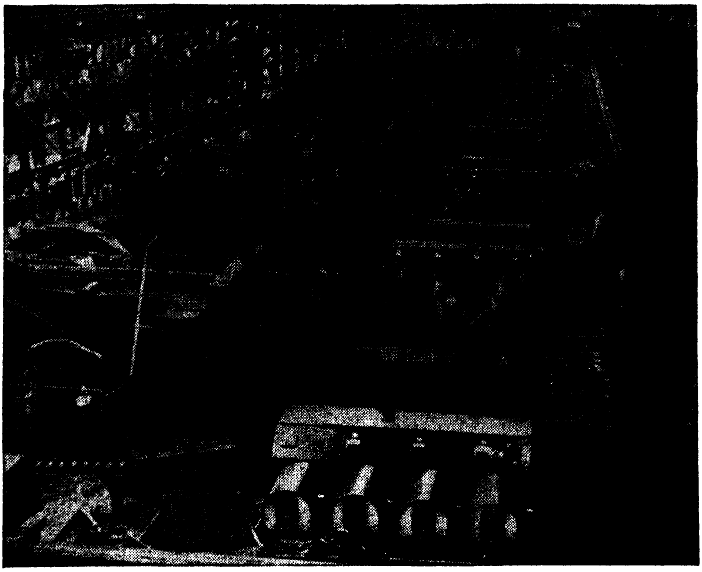

FIG. 112. An installation for forging steel billets. (*Ajax Electrothermic Corporation.*)

Operating Data. The data of the operation of this installation are given in Table 16.

TABLE 16. DATA PERTAINING TO THE INSTALLATION OF FIG. 112

Heating time per charge	4 min
Output per assembly	555 lb per hr
Heat content, 555 lb	59 kwhr
Heat loss, 555 lb	27 kwhr
Thermal efficiency	69 per cent
Input, primary coil, for 555 lb	97.5 kwhr
Electrical efficiency	88 per cent
Conversion efficiency	5.7 lb per kwhr
Over-all efficiency	4.8 lb per kwhr

Heating Steel for Hardening and Tempering. A machine that comprises two induction heaters, a quenching device, and a conveyor for continuous through hardening, followed by tempering, of solid round steel bar stock, diameters ½ to 3 in., random lengths, is shown

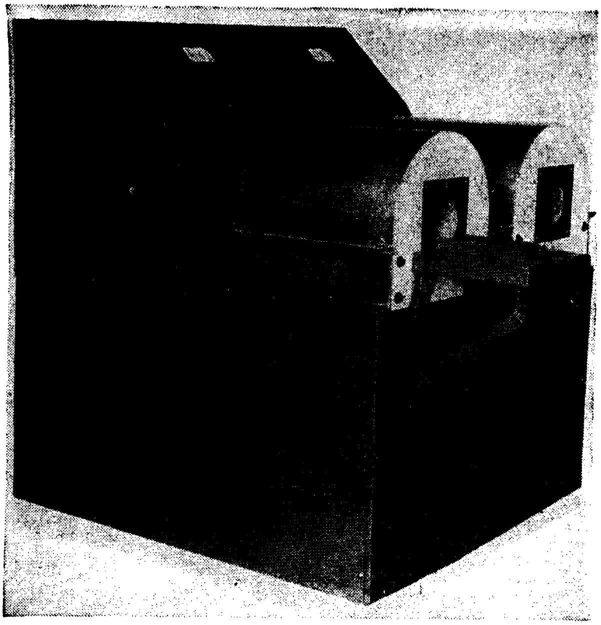

FIG. 113. Two induction heaters of the installation of Fig. 112.

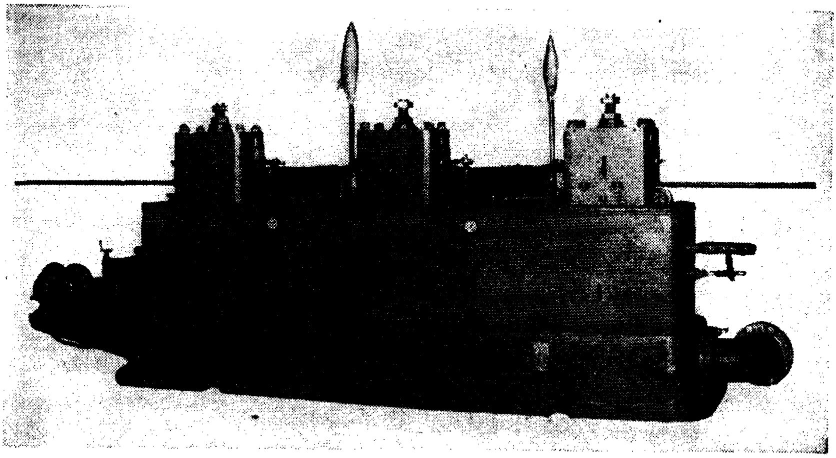

FIG. 114a. An induction-heating machine for continuous hardening and tempering of steel-bar stock. (*The Ohio Crankshaft Company.*)

in Fig. 114*a*. The over-all dimensions are: length 11 ft 6 in., width 37 in., height 39 in. A protective gas atmosphere is used. An installation of these machines is described by Such.[22]

The arrangement of the inductors and of the quenching device and the general designs of the coils are shown in Fig. 114*b*.

The handling mechanism is an adjustable-speed motor-driven roller conveyor.

The data in Table 17 of the performance of this machine, when through-heating carbon steel bar stock, were obtained as a check on its operation. One set of coils and 9,600 cycles were used for all diameters of bars heated. In practice the designs of the inductors, the frequency, and the range of speed adjustment are selected with reference to the class and range of the work to be done.

TABLE 17. DATA OF THE MACHINE SHOWN IN FIG. 114*a*; FREQUENCY 9,600 CYCLES; THROUGH HEATING OF STEEL BAR STOCK

Charge		Heating coil			Reheating coil		
Diameter solid bar, in.	Speed, fpm	Volts	Kw	Rated Δ	Volts	Kw	Rated Δ
½	1.83	220	12	1.6	120	4.5	7
9⁄16	1.83	220	14	1.8	130	6	7.9
⅝	2.0	220	15	1.98	135	7	8.8
¾	1.67	220	22	2.4	170	11	10.5
1	1.50	220	35	3.2	170	17	1.4
	Air-gap ratio	Lb per hr			Conversion efficiency, lb per kwhr		
½	3.5	73			4.40		
9⁄16	3.1	93			4.65		
⅝	2.8	125			5.68		
¾	2.3	150			4.40		
1	1.75	243			5.0		

It will be observed from the data of Table 17 that a good conversion efficiency is obtained with the ½-in.-diameter stock despite the low rated index ratio and the large air-gap ratio. This illustrates the beneficial effect of the magnetic property in induction heating. These data also illustrate the effectiveness of one coil design and one frequency for a wide range of diameters of charges.

This operation is a heat-treatment process, and the quality of the

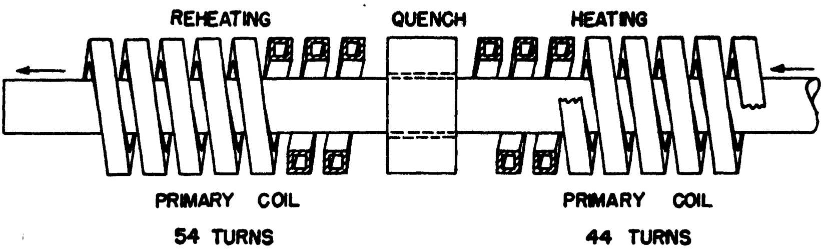

FIG. 114b. General designs and arrangements of the primary coils of the induction heaters of the machine shown in Fig. 114a.

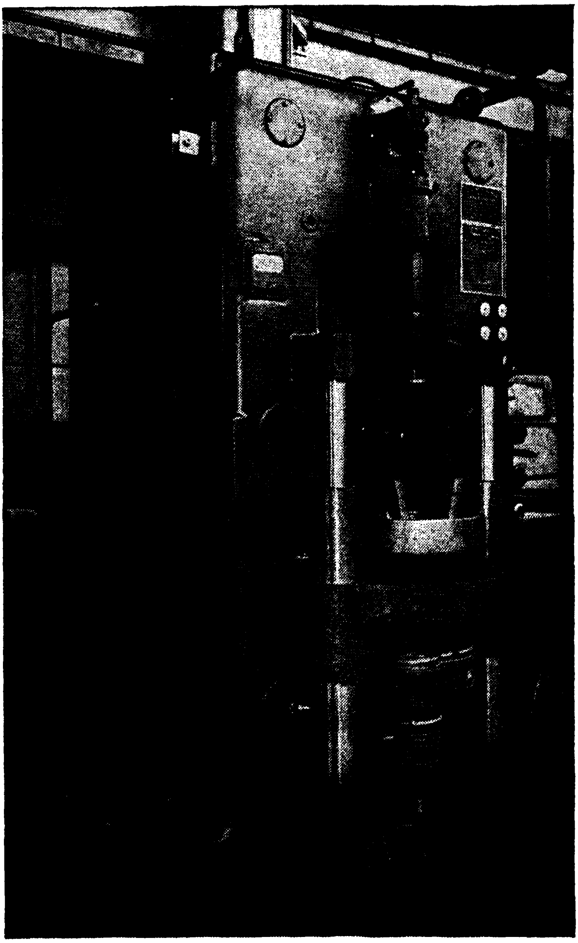

FIG. 115. A typical machine for hardening the internal surfaces of hollow steel parts.

product takes precedence over speed. A normal performance of this machine is 250 lb of SAE 1045 steel hardened to 63-64 Rockwell C and tempered to 30-31 Rockwell C per hour. One operator is sufficient for eight machines in a group. Such an installation would produce 2,000 lb of heat-treated steel per hour.

Internal Heating. A typical machine for hardening the internal surfaces of hollow steel parts is shown in Fig. 115.

CHAPTER VII

MELTING METALS—CLASS B SERVICE

The term melting includes, in addition to the change from the solid to the liquid state, the further heating of the metal to some specified temperature, known as the pouring temperature if the metal is to be poured into molds for ingots or castings, or as the working temperature if the metal is to be used for coating, as in galvanizing, or as a liquid heating bath (for example, the lead bath for heating steel parts for hardening).

The term superheated metal, although indefinite, refers to molten metal heated beyond the temperature at which it is to be used.

Refining a metal or alloy may follow melting. The term denotes the removal of impurities from the molten metal before it is poured. The general method is the use of a blanket of a suitable material over the bath to remove impurities by chemical action. Examples are the production of oxygen-free copper by a blanket of carbon (coke) over the bath, and the refining of steel by a blanket of slag which varies in composition according to the nature of the impurities to be removed.

In melting practice the term holding refers to holding the metal after it is melted, either in the melting furnace or in an auxiliary furnace, for refining, for adjustment of pouring temperature, or simply for regulation of the flow of metal to conform to plant operation.

Metal Classification. A grouping of metals with reference to melting service is given in Table 18. Group I includes the soft metals and Group II the hard metals. An alloy belongs in the group of this table to which its major component belongs.

Another grouping is the classification of the nonferrous metals as light metals, aluminum, magnesium, and alloys of these metals, and heavy metals, mainly copper and its alloys.

Charges. The charge of a melting furnace may be scrap metal only, a mixture of scrap metal and virgin metal, or virgin metal only.

Pouring Temperatures. The pouring temperatures of metals in general range from 100 to 200°C (180 to 360°F) above the melting point. These temperatures vary for each metal and for each alloy with the type of mold, size of casting, and the purpose for which the casting is intended.

Melting Furnaces. There are two types of induction furnaces for metal-melting service: (1) the coreless induction furnace, sometimes referred to as the high-frequency induction furnace, and (2) the submerged resistor furnace which operates with a standard power frequency, usually 60 cycles.

TABLE 18. METAL GROUPS

Metal	Melting point*	
	°C	°F
Group I		
Tin	232	450
Bismuth	271	520
Cadmium	321	610
Lead	327	621
Zinc	420	788
Antimony	630	1166
Magnesium	651	1204
Aluminum	659	1218
Group II		
Silver	961	1761
Copper	1083	1981
Nickel	1452	2646
Cobalt	1480	2696
Iron	1530	2786
Molybdenum	2535	4595
Tungsten	3400	6152

* The melting-temperature range of an alloy must be obtained from the constitution diagram of the alloy system to which the alloy belongs.

CORELESS INDUCTION FURNACE

The general design of this furnace is shown in Fig. 116. The metal is melted by currents induced in the charge. Basically, this furnace differs from an induction heater for Class A service only in the provision of a refractory chamber, or crucible, for the charge.

The development of the coreless induction furnace is described by Clamer.[3]

The main parts of the assembly of a coreless induction furnace are

1. The crucible
2. The primary coil, or inductor

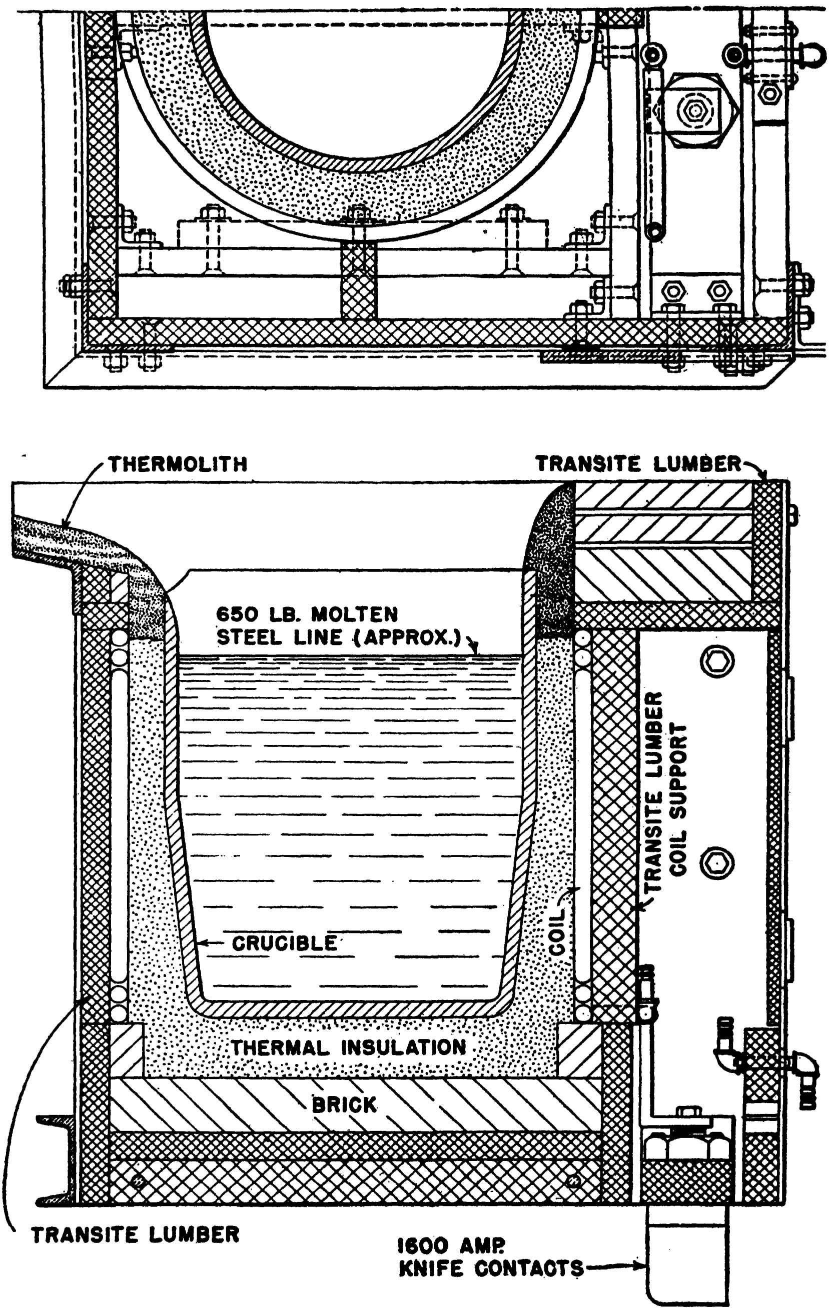

Fig. 116. Sectional view of a coreless induction furnace. (*Ajax Electrothermic Corporation.*)

3. The frame, including its support and a mechanism for tilting the furnace for pouring

Crucibles. Preformed crucibles, as indicated in Fig. 116, are used for small furnaces, up to about 500 lb holding capacity.

Clay crucibles are used for melting nonferrous metals and alloys. Crucibles made of clay and graphite or clay and silicon carbide, and of graphite only, serve for heating charges of nonconducting materials. In these applications the heat is developed by currents induced in the wall of the crucible and transferred to the charge by thermal conduction.

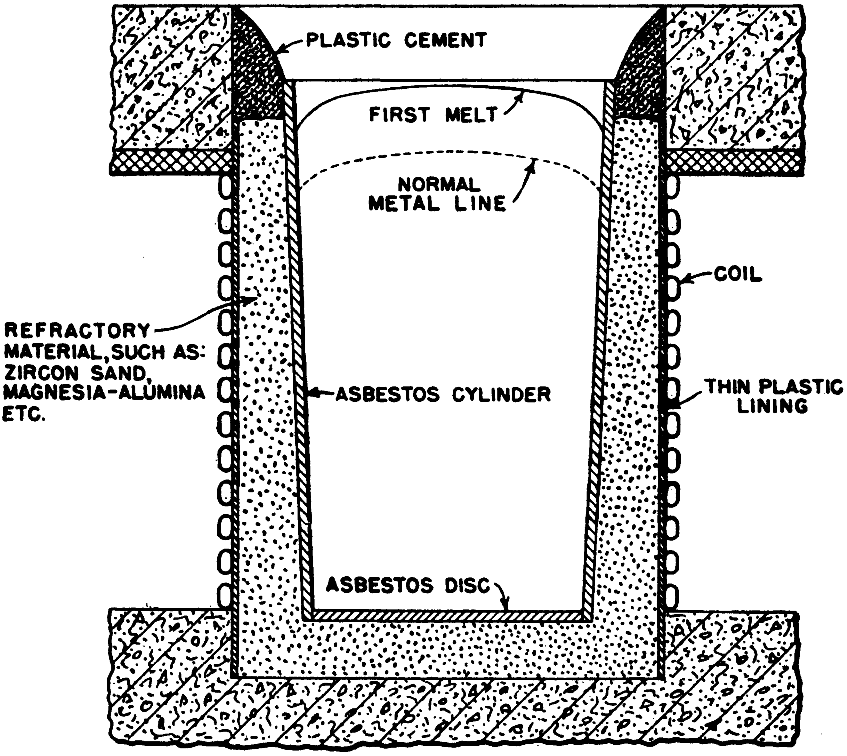

FIG. 117. Diagram showing a method of making a rammed crucible. (*Ajax Electrothermic Corporation.*)

The crucibles of larger furnaces are made in place by ramming a granular refractory material around a hollow form. This construction is indicated in Fig. 117. Acid or basic refractories are used as required. Acid refractories are sized gannister. A mixture of magnesia and alumina is the common basic refractory.

The inner portion of the wall of a rammed crucible—the lining—

becomes sintered with use to a certain depth, ½ in. or more. The outer portion of the wall remains in granular form and serves as a support for the lining, as thermal insulation, and as a barrier against the leakage of molten metal if a crack occurs in the lining.

The life of the lining of a rammed crucible varies with the service. Reference values are 50 melts for acid linings and 90 melts for basic linings. These values are often exceeded.

The useful depth of a crucible is its internal axial dimension from the bottom to the top plane of the primary coil. A common proportion is a useful depth equal to the inside diameter. An example of German practice by Badenheuer[23] is shown in Fig. 118.

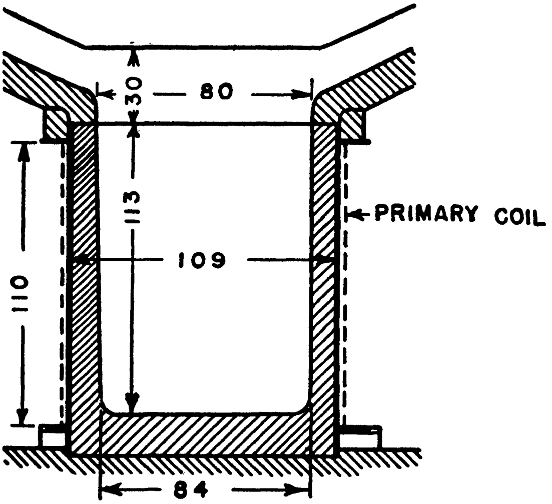

FIG. 118. Proportion of the crucible of a German coreless induction furnace. Dimensions in millimeters.

Primary Coils. The single-layer, water-cooled coil noted in Chap. III is standard practice. A design of a primary coil for a furnace rated 300 kw, 960 cycles, 800 volts is shown in Fig. 119. The view of a partly assembled furnace in Fig. 120 shows the primary coil in place.

Frame. A standard construction is a wood frame, as seen in Fig. 120, with nonmagnetic metal for fastenings. Magnetic shielding is used where needed.

Tilting Mechanism. Conventional types of mechanisms for tilting the furnace for pouring are used. These may be of the hand-, electric-, or hydraulic-operated type.

The general practice is to fit the frame of the furnace with trunnions so placed that the furnace tilts about a horizontal axis that passes through the pouring spout. This maintains the location of the stream of molten metal during pouring.

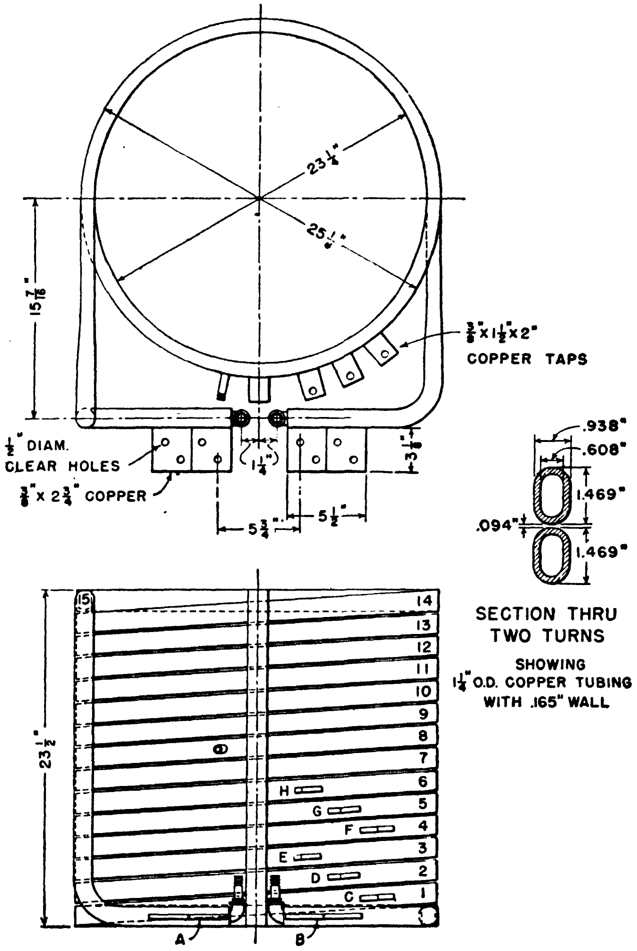

Fig. 119. Design of the primary coil of a 300-kw, 960-cycle, 800-volt coreless induction furnace. (*Ajax Electrothermic Corporation.*)

A typical coreless induction furnace of the standard type is shown in Fig. 121.

A furnace of an English design for large sizes which embodies a structural steel frame with magnetic shields of laminated iron placed between the primary coil and frame is shown in Fig. 122.

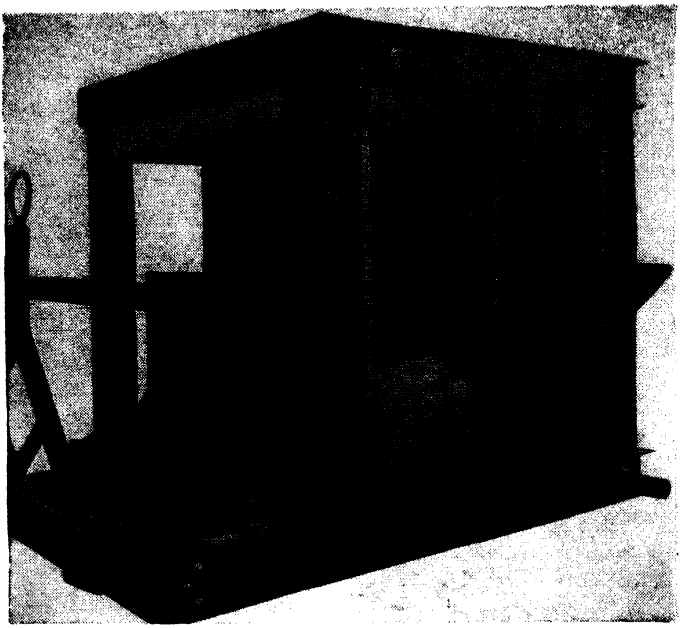

FIG. 120. A partly assembled coreless induction furnace, 3½ tons capacity. (*Ajax Electrothermic Corporation.*)

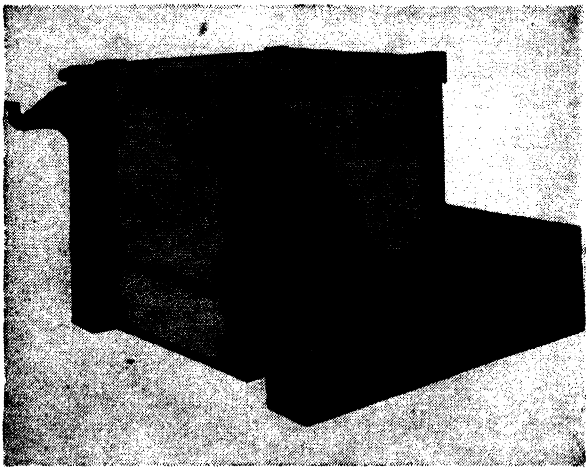

FIG. 121. A typical coreless induction furnace. (*Ajax Electrothermic Corporation.*)

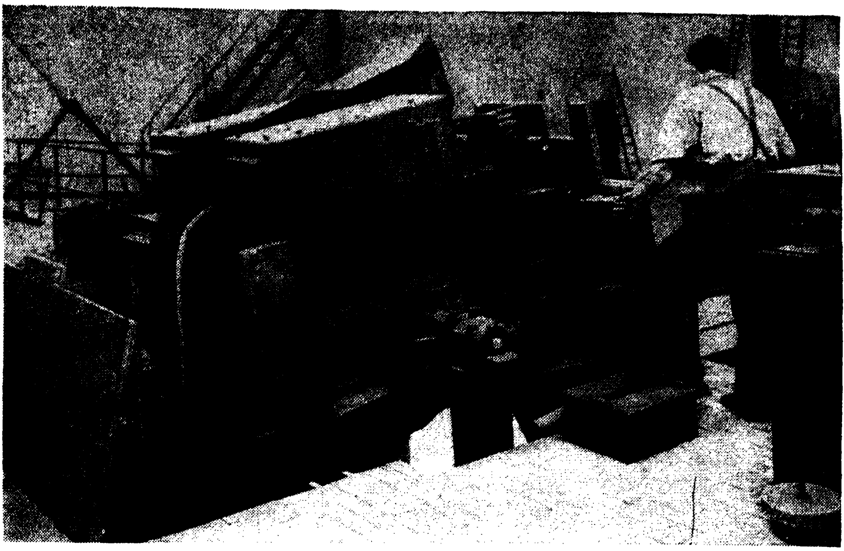

FIG. 122. A coreless induction furnace with steel frame. (*Metropolitan-Vickers Electric Company, Ltd.*)

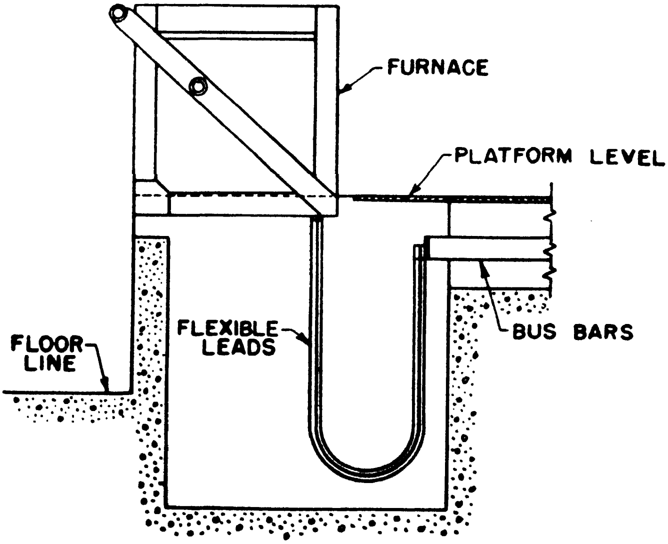

FIG. 123. Platform mounting of coreless induction furnace.

Platform Furnaces. A furnace design for platform mounting is shown in Fig. 123. The electrical connection to the furnace is made with flexible cables. This design provides for maintaining power on the furnace during pouring and is desirable where a number of castings are poured from one heat.

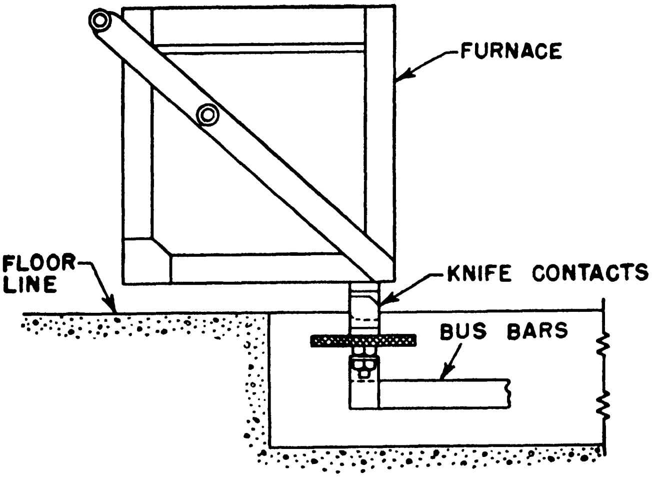

FIG. 124. Floor-level mounting of coreless induction furnace.

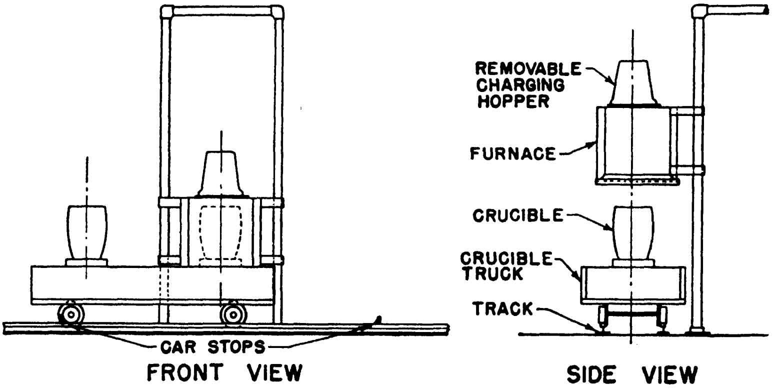

FIG. 125. Lift-coil type of coreless induction furnace.

Floor-level Furnaces. A furnace design for floor-level mounting is shown in Fig. 124. The electrical connection is made with knife contacts. This design permits the use of the furnace as a ladle for pouring.

Lift-coil Furnaces. This design is illustrated by Fig. 125. Preformed crucibles are used. The primary coil is lowered over the loaded

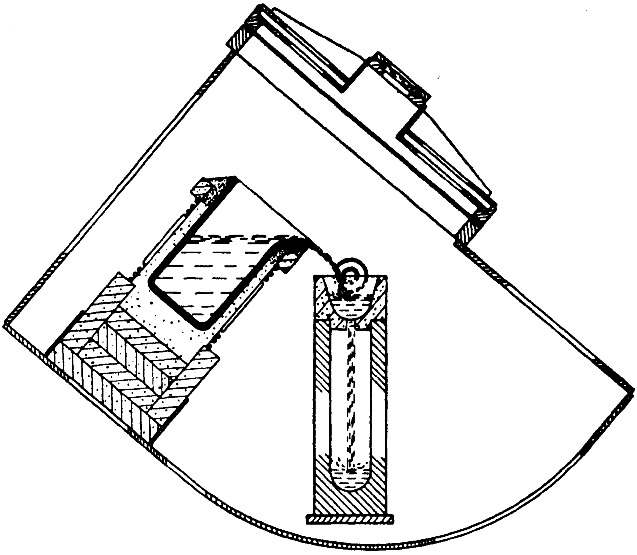

FIG. 126. Sectional view of vacuum-type melting unit.

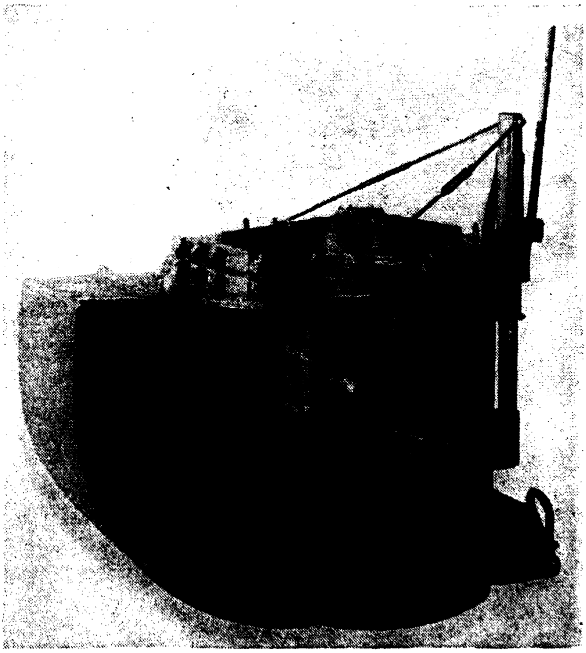

FIG. 127. A vacuum-type melting unit. (*Ajax Electrothermic Corporation.*)

crucible and raised after the charge is melted. This is a popular furnace for melting nonferrous metals and alloys where the quantities are not large.

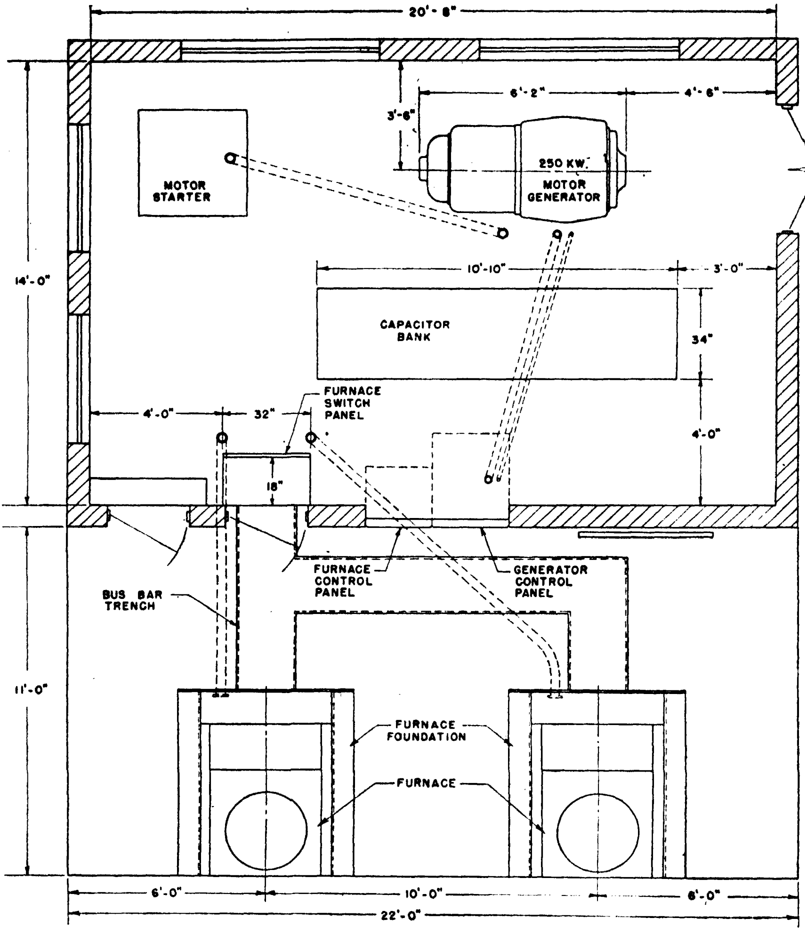

Fig. 128. Typical floor plan of an installation of coreless induction furnaces.

Vacuum Furnaces. An arrangement of a coreless induction furnace and a mold for melting and pouring metals under pressures below 1 atm is shown in Fig. 126. The complete unit is shown in Fig. 127.

Standard Furnaces. The sizes of standard coreless induction furnaces for steel-melting service are listed in Table 19, which also contains average performance data of these furnaces.

Floor Plan. The arrangement of furnace installations varies according to the conditions in each case. One layout, shown in Fig. 128, provides for the alternate use of two furnaces from one power source.

Installations. A typical installation of coreless induction furnaces is shown in Fig. 129. The installation of Fig. 130 is a steel plant in England, described in *Metallurgia,* **9**, 167–170, 1934.

TABLE 19. STANDARD SIZES OF CORELESS INDUCTION FURNACES, STEEL-MELTING SERVICE
(Ajax Electrothermic Corporation)

Size, kw	Size, lb	Steel-melting performance		
		Approx. time to melt	Approx. kwhr per ton over all	Approx. lb per hr
50	50	25 min	850	125
50	100	50 min	850	125
50	150	75 min	850	125
50	200	1 hr, 50 min	850	125
100	100	20 min	800	300
100	200	35 min	800	300
100	300	1 hr	800	300
100	500	2 hr	825	300
175	300	35 min	750	500
175	600	1 hr, 15 min	750	500
175	1,000	2 hr, 15 min	775	450
250	600	50 min	700	750
250	1,000	1 hr, 20 min	700	750
350	600	35 min	700	1,000
350	1,000	1 hr	700	1,000
350	2,000	2 hr, 15 min	725	900
700	1,000	30 min	675	2,000
700	2,000	1 hr	675	2,000
700	4,000	2 hr, 15 min	700	1,800
1,250	2,000	30 min	650	4,000
1,250	4,000	1 hr	650	4,000
1,250	8,000	2 hr, 15 min	675	3,500

Service. The coreless induction furnace is primarily a melting unit. Its special field is the production of high-grade alloys, bronzes, stainless steels, gun steels, magnet steels, tool steels, nickel-chromium alloys, bearing metals, etc.

FIG. 129. A typical installation of coreless induction furnaces. (*Ajax Electrothermic Corporation.*)

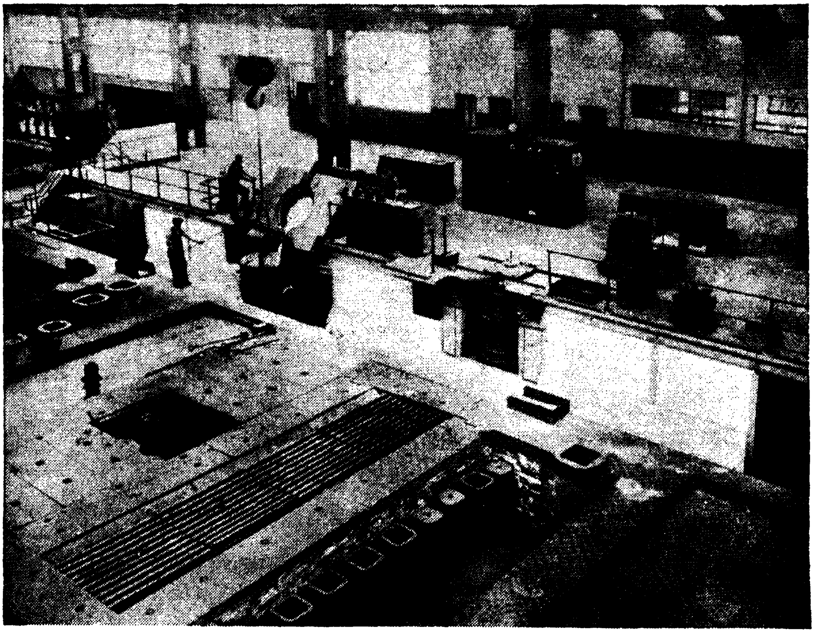

FIG. 130. An installation of coreless induction furnaces, one 5 ton and one 2 ton, in a steel plant in England. (*Metropolitan-Vickers Electric Company, Ltd.*)

The refining of steel, referring particularly to the removal of phosphorous and sulfur, in this furnace has not been developed. Some experimental work has been done. One difficulty is the erosion of the comparatively thin refractory lining of the crucible which does not stand up in refining service. The deoxidation of the melt, for example, by the addition of aluminum prior to pouring, is not refining in the complete sense.

Special Services. Various heat applications other than melting metals are performed in coreless induction furnaces. An example is the graphitization of carbon shapes. This requires a graphite crucible sealed against the entrance of air.

Very high temperatures can be obtained by the use of a graphite crucible which is insulated with graphite in powder form. The upper limit of temperature is the volatilization temperature of the material of the charge.

Artificial Atmospheres. A sealed cover for the crucible provides for the use of any desired artificial atmosphere over the charge.

OPERATION

Operating Periods. The operation of a melting furnace is divided into four periods:

1. Charging time
2. Melting time
3. Holding time
4. Pouring time

There may or may not be an idle period after pouring.

Charging. Inasmuch as the secondary circuit of the furnace is formed in the annular zone of the charge, which initially is composed of pieces of metal, the manner of charging the furnace (sizes of pieces and placement) has much to do with the performance of the furnace circuit during the initial period of the heat cycle. A careful placement of the charge to give a favorable secondary circuit is advisable.

Filling Coefficient. This term denotes the percentage of the internal volume of the crucible occupied by cold scrap metal when the crucible is filled to the top plane of the primary coil. Values of this coefficient range from 40 to 90 per cent; the latter value is infrequent. The average value is around 50 per cent.

Aftercharging. The volume of the charge shrinks as it melts. A full charge of molten metal is obtained by adding cold metal after a portion of the initial charge is melted. This addition may be at any time after enough of the initial charge is melted to provide room for more cold metal.

Stirring. A unique feature of the coreless induction furnace is the automatic stirring of the molten metal, as indicated in Fig. 131. This movement is the result of the interaction of the magnetic fields of the primary and secondary currents. The effect is proportional to the square of the ampere-turns and inversely proportional to the density of the molten metal. The action is measured by the height to which the metal rises along the vertical axis.

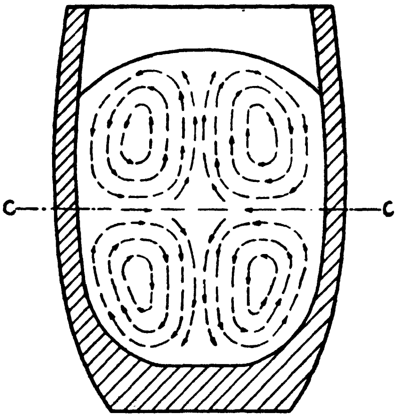

FIG. 131. Diagram of the stirring effect within a mass of molten metal being heated by eddy currents.

This stirring of the molten metal with the consequent mixing of the components of an alloy is an important factor in the production of high-grade alloys.

Melting Rates. In practice the rates of melting are established mainly by rates at which molten metal can be used. Hence, there is considerable variation in this rate. The average practice for steel is indicated in Table 19. There are some limitations on the melting rate. These are

1. The initial physical condition of the charge is not favorable to the conduction of heat into its mass.
2. Bridging may occur. This prevents the top solid metal from dropping into the central zone of the charge where the rate of heat development is the maximum. Consequently a high rate of heat development may cause the metal at the center of the charge to be superheated. This promotes oxidation of that portion of the charge and affects adversely the life of the lining of the crucible.
3. There is an unwarranted loss of heat caused by melting metal faster than it can be used.
4. The higher the melting rate, the higher is the investment charge of the installation.

Losses. The energy losses from a metal-melting furnace are

1. The heat absorbed by the structure of the furnace. The large part of this loss is the heat absorbed by the refractory. This heat is lost when the furnace is allowed to cool. In continuous operation this item of loss is comparatively small. However, idle periods after pouring may entail a considerable loss as the heat lost from the furnace structure during such a period must be restored during the succeeding heats.

2. The heat flow through the furnace wall. This heat is removed by the water flowing through the conductor of the primary coil.
3. The heat dissipated from the surfaces of the furnace.
4. The i^2r loss of the primary coil.

Conversion Efficiency. The unit energy value (kilowatt-hours per ton) required for melting a metal in a coreless induction furnace varies with the following factors:

1. The metal
2. Size of furnace
3. Weight of charge
4. Filling coefficient
5. Electrical efficiency of furnace
6. Rate of melting
7. Maximum temperature
8. Cold or hot crucible
9. Holding time
10. Idle time

As previously noted, the main use of the coreless induction furnace is for melting steels. The heat content value 360 kwhr per ton (2,000 lb) of molten iron from Fig. 46 is used as a reference value for all steels. Also for reference the conversion efficiency 70 per cent is assumed. These values give 514 kwhr per ton as the energy input to the furnace.

TABLE 20. OPERATING DATA OF CORELESS INDUCTION FURNACE IN STEEL-MELTING SERVICE

Melt No.	Charge, lb	Filling coefficient	Melting time, min	Lb per hr	Kwhr per 2,000 lb
I	1,100	0.44	60	1,100	660
II	1,650	0.47	85	1,165	607
III	2,200	0.51	100	1,320	585
IV	1,650	0.66	81	1,218	587
V	1,650	0.58	102	970	742
VI	1,650	0.77	97	1,020	660

TABLE 20A. ALLOCATION OF LOSSES, KWHR PER 2,000 LB

Melt No.	Cooling water	Radiation	Electrical apparatus	Total
I	163.60	17.60	138.90	320.10
II	138	22.10	124.90	285
III	131.30	9.87	121.83	263
IV	117.70	9.20	120.10	247
V	172	82	153	407
VI	161.80	22.85	135.35	320

Over-all Efficiency. The conversion efficiency multiplied by the efficiency of the special electrical apparatus required for this service gives the over-all efficiency of the installation. The efficiency of the electrical apparatus varies with the type, size, frequency, and loading. The value 80 per cent is assumed for reference. Thus the reference value for the over-all efficiency in steel-melting service is 56 per cent, that is, 642 kwhr per ton (2,000 lb). That value may be compared with the corresponding values in Table 19 which are somewhat more conservative.

TABLE 21. LOG OF 1,250-KW, 960-CYCLE, METAL-MELTING FURNACE
(Initial charge 4,930 lb C steel scrap)

Time	Volts	Kw	Power factor,* per cent
1:40	800	1,050	30.5
1:45	860	1,150	29
1:50	700	750	24
1:55	1,000	950	13
2:00	1,060	900	10
2:05	1,200	1,000	8.7
2:10	1,250	1,075	8.4
2:15	1,150	1,050	9.0
2:20	1,200	950	6.7
Power off to add 500 lb to charge			
2:30	1,200	1,050	7.15
2:35	1,050	800	7.0
2:40	1,150	900	6.4
2:45	1,150	1,100	7.5
2:50	1,150	1,000	6.8
2:55	1,100	950	7.0
3:00	1,100	925	5.9
3:05	1,200	1,000	6.1
3:10	1,200	1,000	6.0
3:15	1,200	1,000	6.0
Power off 20 min			
3:35	One-half power 15 min		
3:50	875	600	6.7
3:55	1,175	1,025	6.4

* Power-factor correction by capacitors.

Operating Data. The data of Table 20 by Badenheuer[23] are typical of medium-size furnaces in steel-melting service. The figures relate to the melting period only. The log of a heat cycle of a 1,250-kw coreless induction furnace is given in Table 21.

ELECTRICAL FEATURES

Circuit. A simplified diagram of the circuits of a coreless induction furnace, including the connections of the capacitors for power-factor correction, is shown in Fig. 132. This diagram indicates the use of the primary coil as an autotransformer with taps in the winding for adjustment of furnace power. These features may or may not be used according to the conditions in each case.

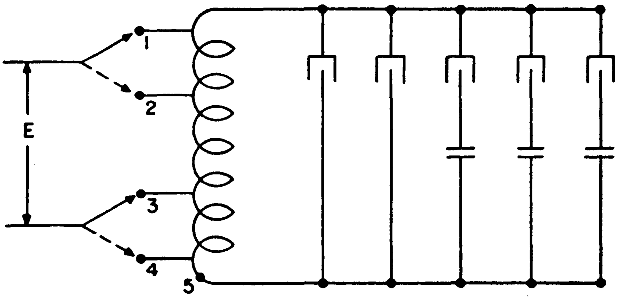

FIG. 132. Circuit diagram of a coreless induction furnace including capacitors for power-factor correction.

Special Features. The furnace assembly is the form of transformer noted in Chap. IV. The special electrical features of these assemblies are

1. A comparatively large air gap, necessary because of the wall of the crucible. Consequently the power factor is low.

2. Initially the secondary circuit is formed by the pieces of the charge adjacent to the wall of the crucible and by the contacts between these pieces. As the metal melts, the resistances introduced by these contacts disappear, and the height of the charge decreases. Thereafter the secondary circuit is a path of current flow in molten metal.

3. The effect of the filling coefficient is equivalent to an increase of charge resistivity in inverse proportion to the value of that coefficient. This effect continues as the charge melts. After charging offsets this effect by increasing the height of the charge.

4. The stirring action in the molten metal.

Frequency. The primary technical factor in the selection of frequency for a metal-melting furnace is the desired degree of stirring of the molten metal. Inasmuch as the current required for a given power value decreases with an increase of frequency and as the stirring action is proportional to the square of the ampere-turns, a too violent stirring action is avoided by limiting the ampere-turns by the selection of frequency. If this is done, it will be found that the requirement of a frequency with reference to the electrical efficiency has been met.

No specification of the degree of stirring that is desirable in a given case can be given. The effect should be moderate, and there is much leeway. Consequently the selection of frequency can be, and is, considered jointly with the economics of the service.

There is a secondary technical factor with reference to frequency to be considered. The frequency that may satisfy the aforesaid technical and economic requirements imposes a limit on the fineness of the assortment of scrap metal for the charge. The index ratio on which the initial electrical efficiency is based is determined for a given metal by the average base dimension of the pieces of the charge and by the frequency. This efficiency may be too low with charges of finely divided material for starting the melting operation. That would mean a higher frequency than might otherwise be desirable. This condition is not frequent in practice.

Standard Frequencies. The considerations outlined in the preceding paragraphs early led to the adoption in this country of 960 cycles as the standard frequency for steel-melting furnaces above 100 kw, electrical rating. As a rule, this frequency is also suitable for melting nonferrous charges, although 480 cycles is favored in some cases. The corresponding standard frequency for industrial furnaces below 100 kw is 3,000 cycles. Various higher frequencies are used for laboratory furnaces. European practice for steel-melting furnaces has ranged from 450 to 2,000 cycles.

Rated Index Ratios. The frequencies noted in the preceding paragraphs give rated index ratios higher than are used generally in Class A service with machine frequencies.

Power-time Relation. The time period here considered is the length of the heat cycle. A general representation of the power-time relation of a metal-melting furnace that starts with a cold charge of scrap metal is shown in Fig. 133.

The initial power-ratio R/Z^2 is usually the maximum value of this ratio. This is due to the high value of the resistance of the secondary circuit caused by the contacts between the pieces of the charge that are in the path of the current. All other conditions being the same, the initial power will be higher with a charge of magnetic material than with a charge of nonmagnetic material.

The extent of the decrease of power with time as indicated by Fig. 133 depends on the conditions of the charge and on bridging if any. The rate of increase of power after its minimum value and the maximum power thereafter are dependent on the material of the charge, the filling coefficient, and aftercharging, if any.

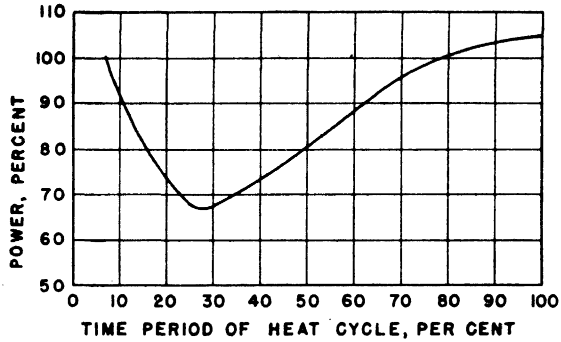

FIG. 133. Power-time characteristic of a coreless induction furnace.

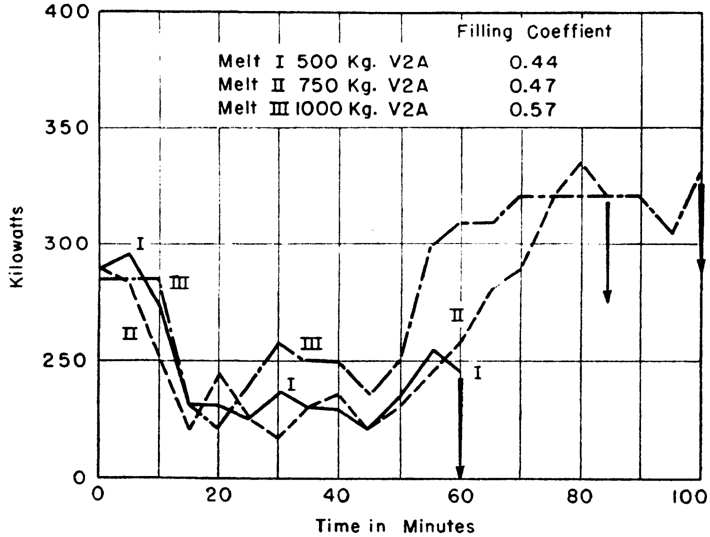

FIG. 134. Power-time records of a coreless induction furnace during the melting of steel charges.

There are many erratic variations from the general power-time relation of Fig. 133. Some examples of records of this kind from a steel-melting furnace, given by Badenheuer,[23] are shown in Fig. 134. The data pertaining to these graphs are included in Table 20. In each case, the conditions of the charge permitted aftercharging after 45 min from the start of the heat cycle.

Example 26. *Metal-melting furnace.* A record of the operation of this furnace with a charge of steel is given in Table 21. The frequency is 960 cycles. The basis of the calculation of the circuit values is a full charge of steel at pouring temperature. Resistivity 166×10^{-6} ohm-cm^3. The circuit values derived from the instrument readings at 3:15 in Table 21 are given in parentheses after the calculated values.

ASSEMBLY DATA

Primary Coil

$p_b = 0.162$ cm
$\tau^{\circ} = 0.36$ cm
$\tau = 0.56$ cm
$b/p_a > 1.0$
$\Lambda = 4.88$
$K_r = 0.99$
$b = 46.99$ cm
$b' = 47$ cm
$l = 95$ cm
$N = 6$
$s = 0.84$
$K_x = 0.69$

Charge

$p_a = 1.47$ cm
$a = 35$ cm
$l = 78.74$ cm
$b/a = 1.34$
$\Delta = 23.7$
$F_r = 0.706$
$\theta = 0.708$
$Y_r = 0.58$
$Y_x = 0.40$

Circuit Values

$r_b = 0.0011$ ohm, Eq. (47*a*)
$x_b = 0.137$ ohm, Eq. (56*a*)
$r_a = 0.0046$ ohm, Eq. (54*b*)
$R = 0.0057$ ohm, Eq. (55) (0.0053)
$X = 0.087$ ohm, Eq. (60*a*)
$Z = 0.087$ ohm, Eq. (61) (0.087)
$\cos \phi = 0.066$, Eq. (62) (0.061)
$\eta = 0.82$, Eq. (63)

For $e = 1200$ volts, $P_b = 1{,}080$ kw, Eq. (64) (1000),
Coil current = 13,793 amp
Volt-amperes = $16{,}552 \times 10^3$
Gross power density = 405 watts per sq in. (373)

SUBMERGED RESISTOR FURNACE

The general design of this furnace is illustrated by Fig. 135. The history of its development is given by Clamer.[24] The furnace has two main parts: (1) a refractory-lined chamber, or crucible, and (2) a transformer heating unit mounted underneath the crucible.

The heat is developed in the secondary circuit of the heating unit. This circuit is formed by a loop of molten metal in a vertical, refractory-lined channel below and connected to a bath of molten metal in the chamber. A laminated iron core with a primary winding thereon completes an otherwise conventional air-cooled transformer for a standard frequency—usually 60 cycles—power circuit.

The current induced in the secondary circuit forces by electrodynamic action a movement of the molten metal in the channel, as indicated by the white arrow in Fig. 135. Thus the heat developed in the secondary circuit is transferred to the mass of the metal in the crucible. Metal is melted by feeding cold metal in the bath of molten metal in the crucible.

The starting of the furnace requires a priming charge of molten metal sufficient in quantity to close the loop of the secondary circuit. For day-by-day operation the furnace is left charged—or partly charged—at the end of the working period, and a reduced voltage is applied to hold the metal liquid during the idle period.

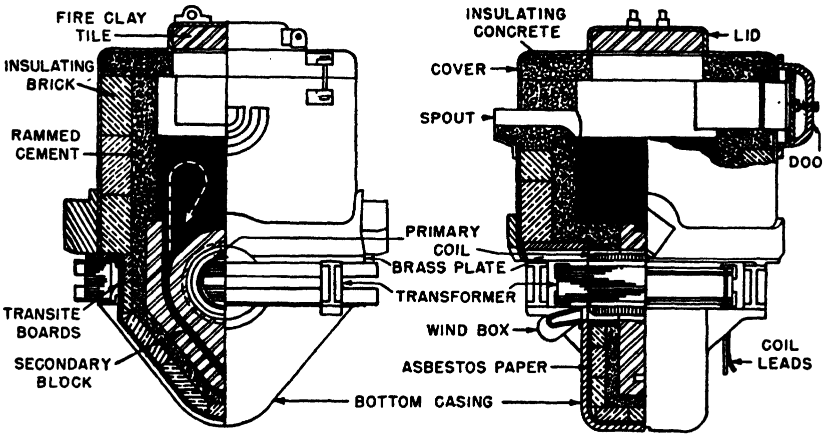

Fig. 135. Sectional views of a submerged resistor furnace for melting brass and similar alloys. (*Ajax Electric Furnace Corporation.*)

The cross-sectional area of the channel of the secondary circuit that is normal to its length and the length of the secondary circuit are chosen with reference to the resistivity of the molten metal. Thus the comparatively high secondary resistance necessary for effective operation is obtained.

The maximum rate of melting in a furnace of this type is obtained with the resistivity value with which the power factor of the furnace circuit is 0.707. The general practice is the use of capacitors to raise the power factor of the load to aproximate unity.

The design of the furnace with a V-shaped channel for the secondary circuit, shown in Fig. 135, was developed for melting the heavy nonferrous metals and alloys, such as copper, brass, and bronze. Standard sizes of this furnace for batch melting range up to 300 kw, single-phase, standard power frequencies and standard low voltages.

An installation of the two of these furnaces—one melting and one being charged—is shown in Fig. 136.

Operation Data. The values of Table 22 are representative for the class of metals and alloys for which the furnace of Fig. 135 is designed. A feature of its operation is the low metal loss by volatilization during melting; a feature of much importance in melting zinc and alloys that contain zinc.

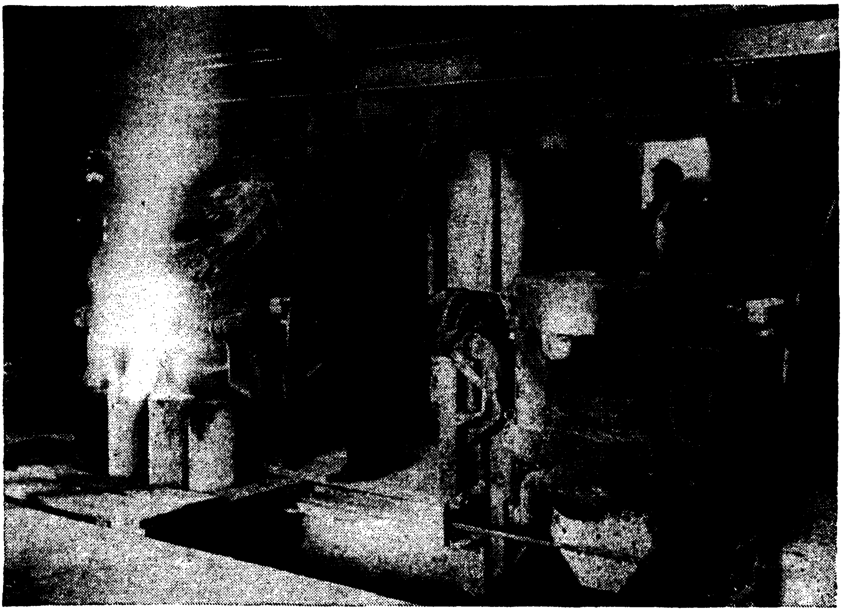

FIG. 136. Installation of submerged resistor furnaces of the design shown in Fig. 135. (*Ajax Electric Furnace Corporation.*)

TABLE 22. OPERATION DATA OF SUBMERGED RESISTOR FURNACES

Charge	Kwhr per ton	Kw, to hold overnight	Net metal loss, per cent
Red brass	252	11	0.40
Yellow brass	195	8	0.30–0.60
Alloy: 75 Cu, 2 Sn, 3 Pb, 20 Zn	200	8	0.50 Zn
Nickel silver	275	8	0.50 Zn
Alloy: 87 Cu, 6 Sn, 5 Zn, 2 Pb	260	12	0.50 Zn
Bronze	285	12	0.70 gross
Copper	310	13	
Zinc	90	4.5	0.25

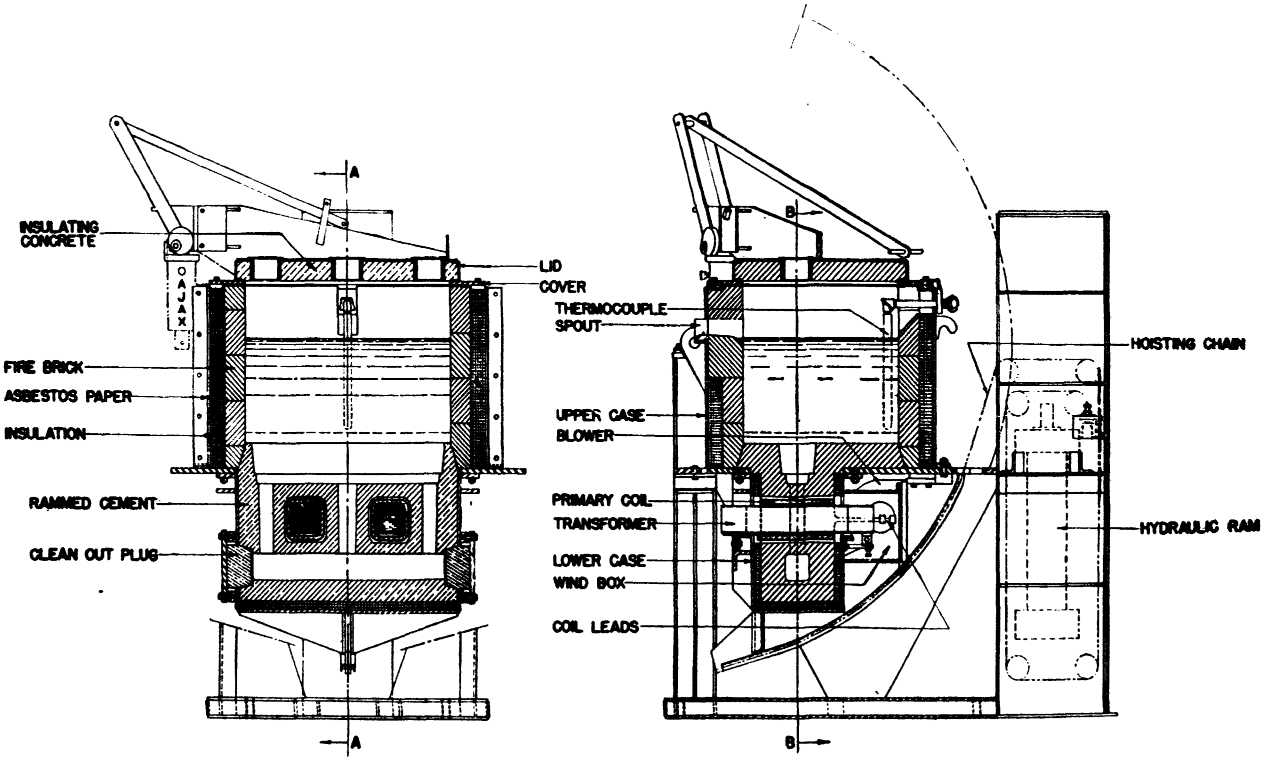

FIG. 137. Sectional views of a submerged resistor furnace for melting aluminum. (*Ajax Engineering Corporation.*)

Melting Aluminum. The design of a submerged resistor furnace for batch melting of aluminum and its alloys is described by Tama.[25] This design is illustrated by Fig. 137. A complete furnace is shown in Fig. 138.

The basic consideration of this design is that the slag particles of the light metals have about the same specific gravity as—or are heavier than—the molten metal. Thus these particles tend to sink and clog the channel of the secondary circuit. It will be noted in Fig. 137 that the vertical channels are connected at the bottom ends by a horizontal channel of larger cross-sectional area. With this construction the slag particles that accumulate in the channels can be removed from time to time with a scraping tool without interfering with the operation of the furnace.

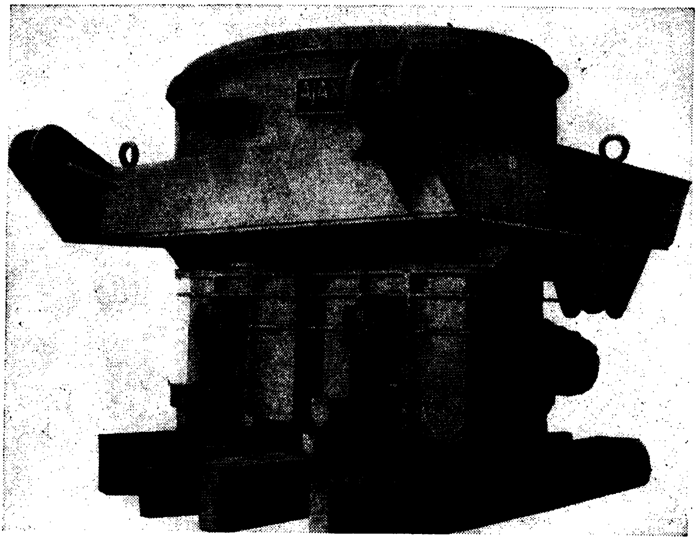

FIG. 138. A submerged resistor furnace of the design shown in Fig. 137. (*Ajax Engineering Corporation.*)

The energy required for melting aluminum in this furnace is around 440 kwhr per ton (2,000 lb). Standard sizes range up to 250 kw, 60 cycles, single phase. A standard 500-kw furnace has two transformer heating units connected for three-phase service.

Continuous Melting Furnaces. The transformer heating unit of the submerged resistor furnace—either the unit of Fig. 135 for heavy metals or the unit of Fig. 137 for light metals—can be arranged as shown in Fig. 139 for attachment, in any number, to large heating chambers for continuous melting (charging and pouring simultaneously) of nonferrous metals and alloys.

This use of multiple heating units is shown in the general design of a continuous melting furnace (Fig. 140). A photograph of a furnace of this type during assembly is shown in Fig. 141. The designations of parts are explained in the caption.

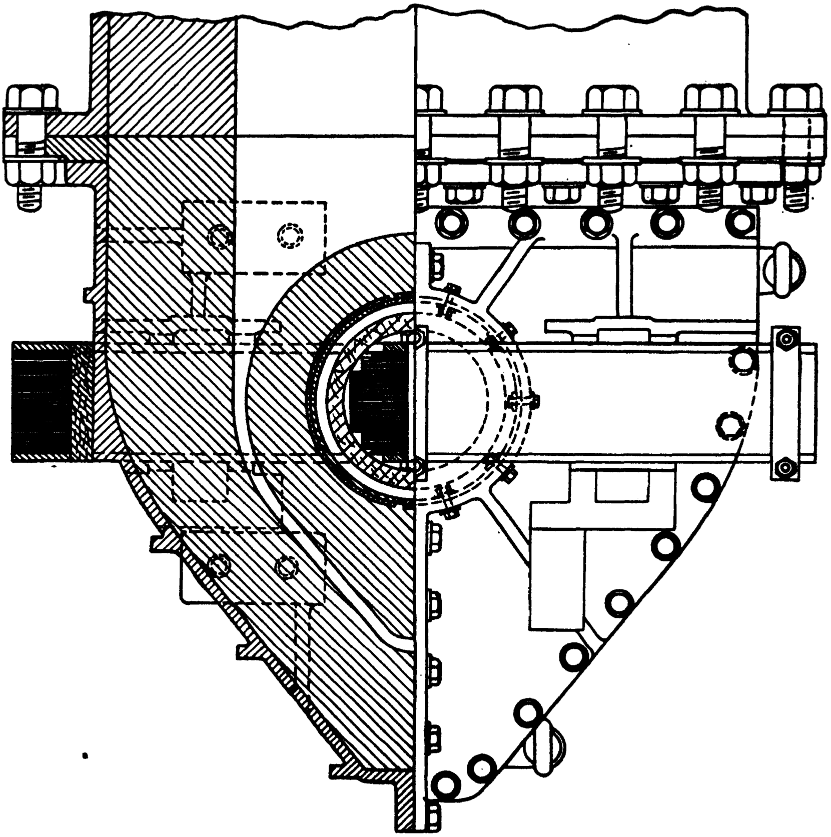

FIG. 139. A transformer heating unit for bolting to the shell of a continuous melting furnace.

General Construction. The cylindrical steel shells of this type of furnace have refractory linings and are mounted on cradles supported by roller-bearing idlers. One of the cradles is geared to a motor-driven tilting mechanism. The charging doors are in the top of the shell. The arrangement for pouring the molten metal through a closed launder is seen in Fig. 141. The spout *B* is located on the horizontal axis of the chamber. This feature provides for accurate control of the stream of metal. The operator raises and lowers the outlet from the chamber according to the rate at which cold metal is fed into the furnace.

A thermocouple in the stream of outgoing metal serves through relays for automatic regulation of the temperature of the molten metal by control of the power input. The openings in the shell of the furnace and the launder are sealed so that a gas atmosphere can be maintained in the chamber and in the launder to prevent the access of oxygen (air) to the molten metal.

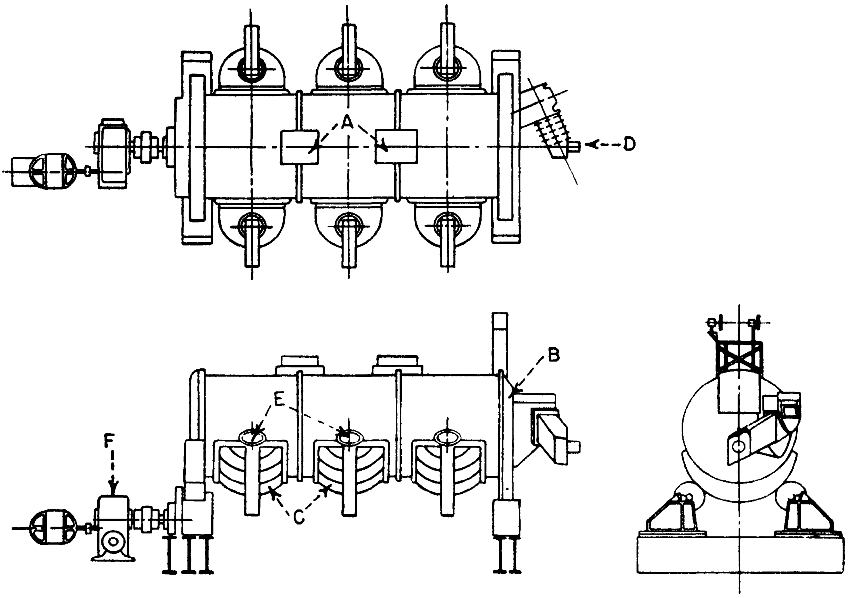

FIG. 140. General design of a type 3F Scomet continuous melting furnace. (*Scomet Engineering Company.*) (*A*) Charging door. (*B*) Door for skimming. (*C*) Transformer heating units, each 150 kw. (*D*) Pouring spout. (*E*) Openings for cooling air for transformers. (*F*) Reducing gear.

Holding or Pouring Furnace. A common plant arrangement, where two or more melting furnaces are used, is the delivery of the metal from the melting furnaces to a holding or pouring furnace and thence to the molds.

Standard Sizes. The standard sizes of the type of furnace shown in Figs. 140 and 141 are given in Table 23.

Energy and Rate of Melting. The energy required for melting copper in the furnaces of Table 23 is about 250 kwhr per ton. The corresponding melting rate is 1,200 lb per hr per 150-kw heating unit.

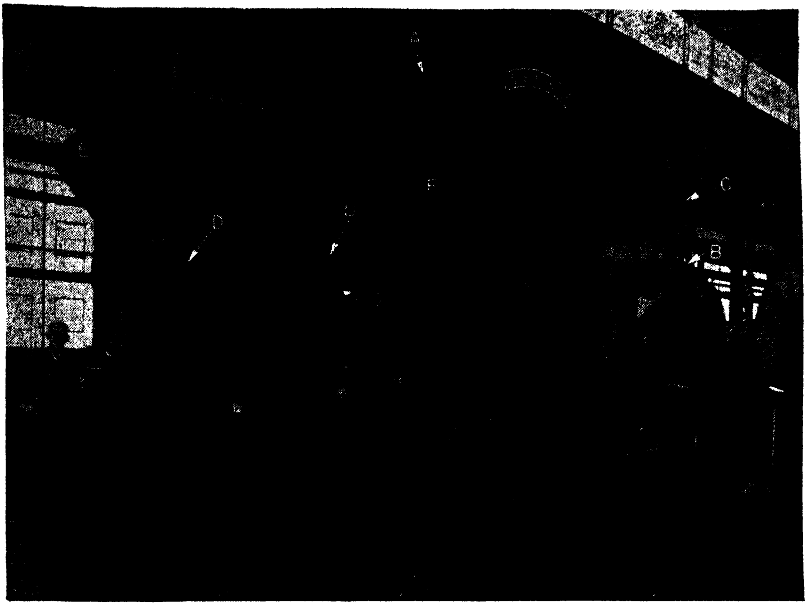

FIG. 141. A type 2F Scomet continuous melting furnace during assembly. (*Scomet Engineering Company.*) (*A*) Charging doors. (*B*) Discharge spout. (*C*) Door for access to throat and to launder between *B* and *C*. (*D*) Openings in shell for transformer heating units. Two similar openings on opposite side. (*F*) Shell of furnace.

For example, the melting rate of the type 3F furnace is approximately 3.6 tons of copper per hour.

Service. The general service of these furnaces is in melting nonferrous metals and alloys. A particular service is melting cathode copper in the production of oxygen-free, high-conductivity (OFHC) copper. In this operation, a blanket of carbon in granular form over the bath serves as the reducing agent to remove copper oxide from the metal. A protective gas atmosphere, for example, producer gas, is used in the chamber and launder.

TABLE 23. CONTINUOUS MELTING FURNACES
(Scomet Engineering Company)

Type	Service*	Nominal capacity, tons of copper, melting service	Kilowatt rating for melting service
G	P	. .	150 (one unit)
IF	P or M	4	300 (two units)
2F	P or M	11	600 (four units)
3F	M	20	900 (six units)

* P = holding or pouring service; M = melting service.

CHAPTER VIII

POWER CIRCUIT CONDUCTORS—MACHINE FREQUENCIES

The installation of power apparatus for machine frequencies up to 10,000 cycles, at some distance from induction-heating loads, is often desirable; in some cases distant locations are necessary.

The design of a power circuit for induction-heating loads differs from that of a conventional 60-cycle power circuit mainly in that there is more emphasis on the reactance of the circuit. This reactance is offset to the degree desired by the use of capacitors.

The conductors can be either aluminum or copper. Copper conductors are assumed for this discussion. The conditions may permit the use of bare conductors or may require that the conductors be insulated. Usually bare conductors are rigid, and there is a choice of shapes. As a rule, insulated conductors are round and flexible.

The shapes of conductors in general use for indoor circuits are solid round, hollow round, hollow square, and rectangular. The term solid as used herein includes both one-piece (or homogeneous) conductors and stranded conductors without cores.

Heating of Conductors.

Bare Conductors. The advisable maximum temperature of a bare copper conductor in air is about 80°C, because above that temperature the rate of oxidation of copper increases rapidly. The conditions assumed herein are horizontal conductors in still air and 40°C temperature rise above 30°C ambient.

Insulated Conductors. The assumed conductor temperature is 85°C.

Equations for the direct-current carrying capacity of bare copper conductors mounted horizontally, under stable conditions in still air, with normally oxidized surfaces, and for the range of temperatures usually met in service, were derived experimentally by the Copper Development Association, London.[26] The measurements were made with single rectangular bars ranging from 1 by ⅛ in. to 4 by ¼ in. in section and with round solid bars and round tubular conductors from ½ to 1½ in. in diameter. These equations are given on the following page.

Flat bars on edge—single bar,

$$i_{dc} = \frac{24.9\sqrt{A_h}\,(2h + 2t)^{0.39}(t')^{0.61}}{\sqrt{\rho_m}} \quad \text{amp} \qquad (89)$$

Round bars, either solid or hollow—single bar,

$$i_{dc} = \frac{25.9\sqrt{A_h}\,(2\pi a)^{0.36}(t')^{0.61}}{\sqrt{\rho_m}} \quad \text{amp} \qquad (90)$$

where h = width of rectangular bar, cm
t = thickness of rectangular bar, cm
a = radius of round bar, cm
A_h = cross-sectional area of metal of conductor normal to its length, sq cm
t' = temperature gradient between conductor and surrounding air, °C
ρ_m = resistivity of copper at temperature of conductor, microhm-cm^3

These equations on the basis of the resistivity of copper at 20°C (1.724 microhm-cm^3) for 70°C conductor temperature become
Flat bars on edge,

$$i_{dc} = 164\sqrt{A_h}\,(2h + 2t)^{0.39} \quad \text{amp} \qquad (89a)$$

Round bars, either solid or hollow,

$$i_{dc} = 171\sqrt{A_h}\,(2\pi a)^{0.36} \quad \text{amp} \qquad (90a)$$

where a = radius, cm (outside radius for hollow conductor)

The direct-current densities (amperes per square inch) of several sizes of rectangular bars and of a range of diameters of solid round bars in accordance with Eqs. (89*a*) and (90*a*) are given in Fig. 142.

Another equation for hollow copper conductors is

$$i_{dc} = 467\sqrt{w}(2a_1)^{0.36} \quad \text{amp} \qquad (90b)$$

where w = weight per foot, lb
$2a_1$ = outside diameter, in.

There is a wide range of standard dimensions—outside and inside diameters—of tubular conductors, both round and square. An example of the use of Eq. (90*a*) for this type of conductor follows.

Example 27. Copper pipe, standard 1-in. size. Outside diameter, 1.315 in. (3.35 cm); wall thickness, 0.1265 in. (0.32 cm); area of cross section of wall, 0.472 sq in. (3.045 sq cm).

$$i_{dc} = 700 \text{ amp}$$

The rate of heat dissipation from a normally oxidized copper surface in still air for 40°C rise above 30°C is about equally divided between radiation and natural convection. The surface finish affects the radiation component but not the natural convection component.

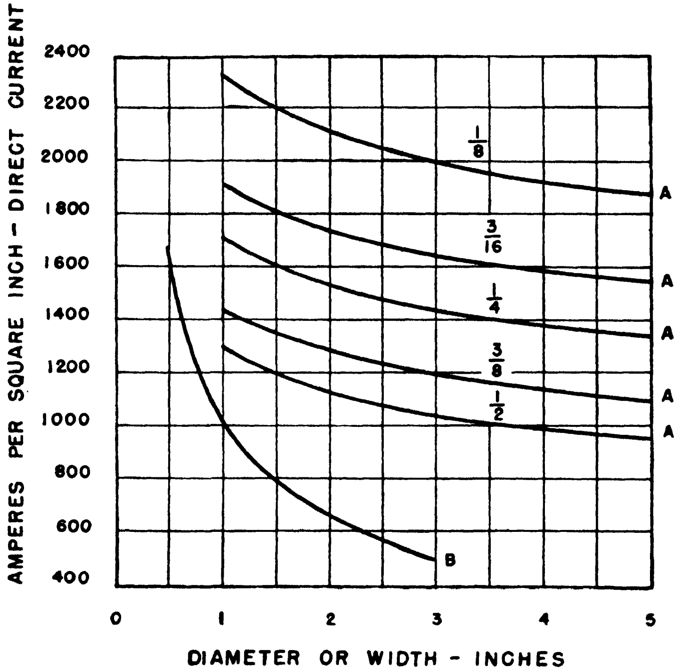

FIG. 142. Direct-current densities in rectangular copper conductors and in round solid copper conductors by Eqs. (89*a*) and (90*a*). Thicknesses of rectangular conductors in fractions of an inch.

The emissivity coefficients (radiation) of copper surfaces at around 70°C are about as follows:

Polished surfaces = 0.03
Scraped surfaces, shiny = 0.09
Slightly oxidized surfaces = 0.30
Normally oxidized surfaces = 0.50
Heavily oxidized surfaces = 0.70
Shiny paint surfaces = 0.80 to 0.95
Flat paint surfaces = 0.90 to 0.98

These values of the emissivity coefficient indicate the extent to which the total rate of heat dissipation from a copper conductor can be increased by painting the surface.

If the conductor is so located that there is an artificial movement of air across its surface, for example, by chimney action, the convection component of the rate of heat dissipation is increased.

One or both of these conditions can in some cases be the basis of a higher current rating than is expressed by the preceding equations.

Alternating-current Ratings. The alternating-current carrying capacity of a given conductor is

$$i_{ac} = i_{dc} \sqrt{\frac{R_{dc}}{R_{ac}}} \quad \text{amp} \qquad (91)$$

where R_{ac} = alternating-current resistance, ohms
R_{dc} = direct-current resistance, ohms

Insulated Conductors. The current-carrying capacity of an insulated conductor depends on the kind and thickness of the insulation, the voltage, the frequency, and the nature of its surroundings. Examples of current ratings of coaxial conductors with varnished-cambric insulation for installation in still air of 40°C are given in Table 24. The decrease of current ratings with increase of voltage with 9,600 cycles is due to dielectric loss. The current ratings in the table are representative only. Installation conditions vary so widely that each case should be referred to the manufacturer for advice regarding the current rating of the conductor.

TABLE 24. CURRENT RATINGS OF COAXIAL CONDUCTORS, ⅛-IN. VARNISHED-CAMBRIC INSULATION, LEAD SHEATH, FOR INSTALLATION IN STILL AIR AT 40°C

Frequency	Volts	Size of conductor, circular mils × 1,000					
		40	70	100	200	400	700
		Amperes*					
60	1,200	100	155	175	265	400	560
960	1,200	100	150	165	225	300	390
3,000	1,200	90	120	135	180	240	310
9,600	400	76	100	110	140	185	230
9,600	900	70	92	100	130	165	205
9,600	1,200	66	80	88	110	145	175

* Multiplying factors for installation in underground conduits:
Up to and including 9,600 cycles, 400 volts.............................. 0.80
9,600 cycles above 400 volts.............................. 0.71

RESISTANCE AND INDUCTANCE

Either single-phase or polyphase power circuits can be used for induction-heating service. Generally a single-phase circuit with one conductor per leg of the circuit is sufficient. That type of circuit is assumed for this discussion.

Resistivity of Copper. The resistivity of 100 per cent conductivity copper at 20°C is 1.724×10^{-6} ohm-cm^3. Multipliers of that value for conductivities from 95 to 101 per cent and for temperatures from 0 to 100°C are given in Table 25. Direct interpolation for intermediate values can be made.

Example 28. Temperature of conductor, 70°C; conductivity, 98 per cent.

$$\rho_{70^\circ\text{C}} = \frac{1.724}{10^6} \times 1.2168 = 2.10 \times 10^{-6} \text{ ohm-cm}^3$$

TABLE 25. MULTIPLIERS TO OBTAIN RESISTIVITIES OF COPPER WITH VARIOUS CONDUCTIVITIES AND AT VARIOUS TEMPERATURES*

Temperature, °C	Conductivity, per cent						
	95	96	97	98	99	100	101
0	0.9741	0.9631	0.9524	0.9418	0.9315	0.9214	0.9115
10	1.0134	1.0024	0.9917	0.9811	0.9708	0.9607	0.9508
20	1.0526	1.0417	1.0309	1.0204	1.0101	1.0000	0.9901
25	1.0722	1.0612	1.0505	1.0400	1.0297	1.0196	1.0097
30	1.0919	1.0809	1.0702	1.0597	1.0494	1.0393	1.0294
40	1.1312	1.1202	1.1095	1.0990	1.0887	1.0786	1.0687
50	1.1704	1.1595	1.1488	1.1484	1.1280	1.1179	1.1080
60	1.2097	1.1987	1.1880	1.1775	1.1673	1.1572	1.1473
70	1.2489	1.2380	1.2273	1.2168	1.2066	1.1965	1.1866
80	1.2882	1.2773	1.2666	1.2561	1.2459	1.2358	1.2259
85	1.3078	1.2969	1.2862	1.2757	1.2655	1.2455	1.2455
90	1.3275	1.3166	1.3059	1.2954	1.2852	1.2751	1.2653
100	1.3667	1.3558	1.3452	1.3347	1.3244	1.3144	1.3045

* Values in this table are from the Chase Electrical Handbook.

Alternating-current Resistance. The resistance of an isolated conductor for alternating current is usually greater than for direct current. This is caused by the crowding of the current in the conductor toward its surface in all radial directions; a symmetrical concentration of current in the annular zone of the conductor which is termed skin effect. With low values of the index ratio of the conductor, the skin effect is negligible.

If the conductor is near another conductor carrying current, the currents are crowded toward adjacent conductor surfaces with unlike polarity and away from adjacent conductor surfaces with like polarity

—the proximity effect. This effect increases with decrease of the distance between the conductors.

We are concerned particularly with the proximity effect in a go and return (single-phase) circuit in which the conductors are not coaxial. The result in this case is an increase of resistance which is superimposed on the increase caused by skin effect, if any.

Comprehensive treatments of skin effect and of proximity effect are given by Dwight[27] and by Arnold.[29,30]

Inductance. The inductance of a go and return circuit is determined by the shape and size of the conductors and by the distance between them, the inductance decreasing with decrease of that distance.

Inasmuch as proximity effect reduces the effective distance between the paths of the currents in the conductors of a go and return circuit, that effect reduces the inductance of the circuit.

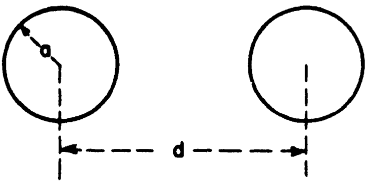

FIG. 143. Single-phase circuit with solid round conductors.

Solid Round Conductors (Fig. 143). *Direct-current Resistance.*

$$R_{dc} = \frac{\rho}{\pi a^2} \quad \text{ohms per cm length of conductor} \tag{92}$$

where ρ = resistivity, ohm-cm^3
a = radius of conductor, cm

Alternating-current Resistance with No Proximity Effect.

$$R_s = \frac{\rho U_r}{2\pi a p} \quad \text{ohms per cm length of conductor} \tag{93}$$

where p = reference dimension, Eq. (1)

$$U_r = \text{function } \frac{(\text{ber } \Delta \text{ bei}' \Delta) - (\text{bei } \Delta \text{ ber}' \Delta)}{(\text{ber}' \Delta)^2 + (\text{bei}' \Delta)^2} \tag{94}$$

Δ = index ratio, a/p, Eq. (2)

A graph of values of the function U_r for values of the index ratio is given in Fig. 144. The derivation of Eq. (93) is given by Grover.[28]

Alternating-current Resistance with Proximity Effect. If there is proximity effect, the alternating-current resistance of a solid round conductor (Fig. 143) is

$$R_{ac} = \frac{R_s}{\sqrt{1 - \alpha^2 a_0 + \dfrac{\alpha^4 b_0}{1 - \alpha^2 c_0}}} \quad \text{ohms per cm length of conductor} \tag{95}$$

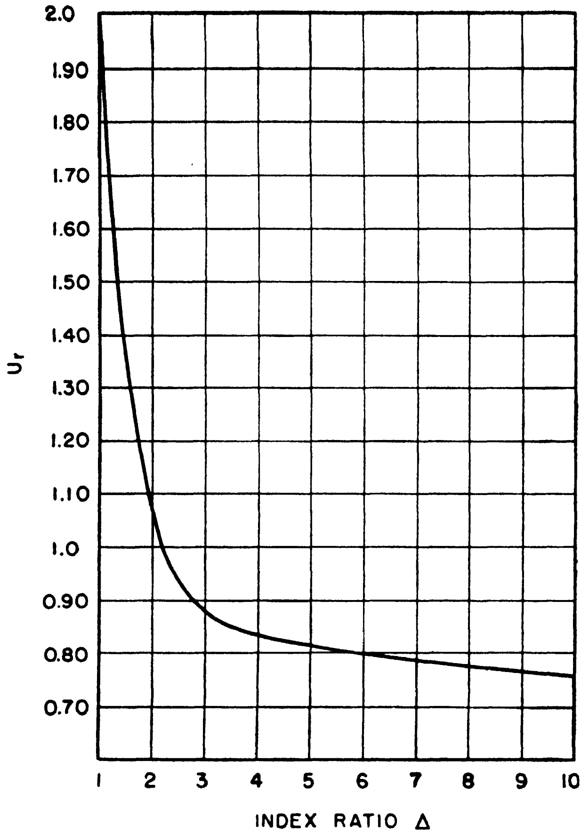

FIG. 144. Values of the function U_r, Eq. (94).

R_s is from Eq. (93)

$$\alpha = \frac{2a}{d} \qquad \text{see Fig. 143} \tag{96}$$

$$\chi = 2\sqrt{\frac{2\pi f}{R_{dc}10^9}} \tag{97}$$

R_{dc} is from Eq. (92). Values of a_0, b_0, and c_0 are given in Table 26. If α is less than 0.50,

$$R_{ac} = \frac{R_s}{\sqrt{1 - \alpha^2 a_0}}$$

The proximity effect factor included in Eq. (95) is given by Arnold.[29] The skin effect with frequencies above about 1,000 cycles in a stranded conductor of conventional construction is greater than in a

TABLE 26. FACTORS IN EQS. (95), (105), (106), AND (107)

χ	a_0	b_0	c_0	χ	a_0	b_0	c_0
0	0	0	0.09	3.4	0.661	0.060	0.24
0.20	0	0	0.09	3.6	0.675	0.053	0.29
0.40	0.001	0	0.09	3.8	0.687	0.046	0.35
0.60	0.004	0	0.08	4	0.696	0.039	0.41
0.80	0.013	0	0.08	5	0.739	0.018	0.64
1.0	0.030	0.001	0.06	6	0.778	0.012	0.72
1.2	0.061	0.001	0.02	7	0.809	0.009	0.76
1.4	0.106	0	0	8	0.832	0.007	0.79
1.6	0.167	0.003	0.02	9	0.849	0.006	0.83
1.8	0.240	0.011	0.05	10	0.864	0.005	0.85
2.0	0.320	0.022	0.07	15	0.908	0.002	0.89
2.2	0.399	0.037	0.08	20	0.931	0.001	0.93
2.4	0.470	0.051	0.08	30	0.953	0.001	0.95
2.6	0.530	0.062	0.10	40	0.965	0	0.96
2.8	0.578	0.068	0.12	50	0.972	0	0.97
3.0	0.614	0.069	0.15	Above 50	$1 - \sqrt{2}/\chi$	$1/2\chi^2$	$1 - \sqrt{2}/\chi$
3.2	0.641	0.066	0.19				

one-piece conductor with the same cross-sectional area. This is caused by the spiraling of the strands and is approximately inversely proportional to the pitch. This effect is partly offset by the segmental construction of a stranded conductor illustrated by Fig. 145. The number of segments may be three, four, or more, depending on the frequency and size of the conductor.

The proximity effect, if any, in a stranded conductor is somewhat less than in a one-piece conductor of equal cross-sectional area. This difference varies with the construction of the stranded conductor.

Inductance. The inductance of a go and return circuit with solid round conductors, Fig. 143.

$$L = 4\left(\log_e \frac{d}{a} + \frac{1}{4}\right) \times 10^{-9} \tag{98}$$

henrys per cm length of circuit (for circuits where the length l is large in comparison with the distance d)

where $\log_e$ = natural (hyperbolic or Napierian) logarithms

NOTE 5. The inductance of a stranded round conductor is about the same as the inductance of a one-piece round conductor of the same diameter, but it is less than that of one-piece round conductor of the same cross-sectional area.

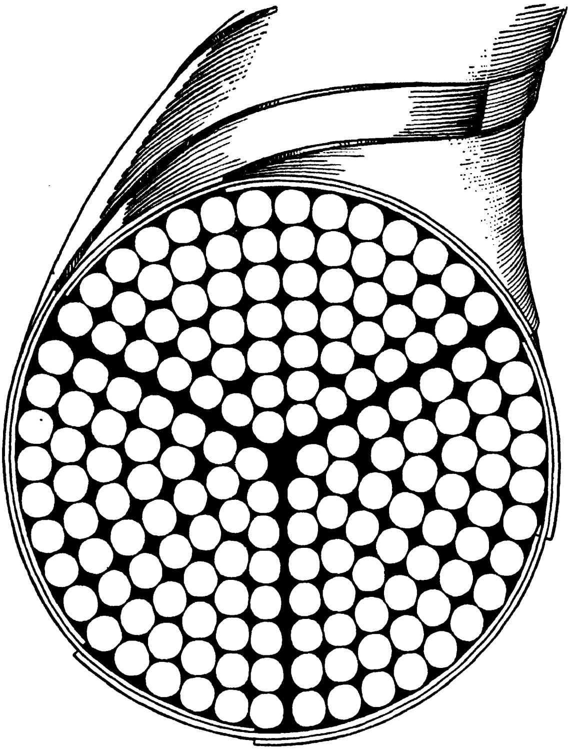

FIG. 145. Section of a cable with segmental conductor.

Hollow Round Conductors (Fig. 146). *Direct-current Resistance.*

$$R_{dc} = \frac{\rho}{\pi t(2a_1 - t)} \quad \text{ohms per cm length of conductor} \qquad (99)$$

Alternating-current Resistance with No Proximity Effect. If there is no proximity effect and if the outside radius of the conductor is not less than about $2.5p$,

$$R_s = \frac{\rho K_r}{2\pi\sqrt{2}pa_1'} \quad \text{ohms per cm length of conductor} \qquad (100)$$

$$a_1' = a_1 - \frac{p}{\sqrt{2}} \quad \text{cm} \qquad (101)$$

$$\text{where } K_r = \text{function } \frac{\sinh \Lambda + \sin \Lambda}{\cosh \Lambda - \cos \Lambda} \qquad (102)$$

Λ = index ratio, $\sqrt{2}t/p$ Eq. (3)
t = wall thickness, cm
p = reference dimension, Eq (1)

A graph of values of the function K_r for values of the index ratio is given in Fig. 147.

NOTE 6. Equation (102) is a repetition of Eq. (49) in Chap. IV.

For $p \geqslant t$, $R_s = R_{dc}$. This equality occurs with values of the index ratio $\leqslant 2$. Values of the resistance ratio R_s/R_{dc} of hollow round conductors for values of a selected parameter are given in Figs. 160*a* and 160*b*, Appendix *E*.

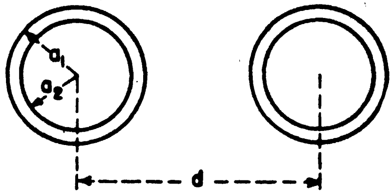

FIG. 146. Single-phase circuit with hollow round conductors.

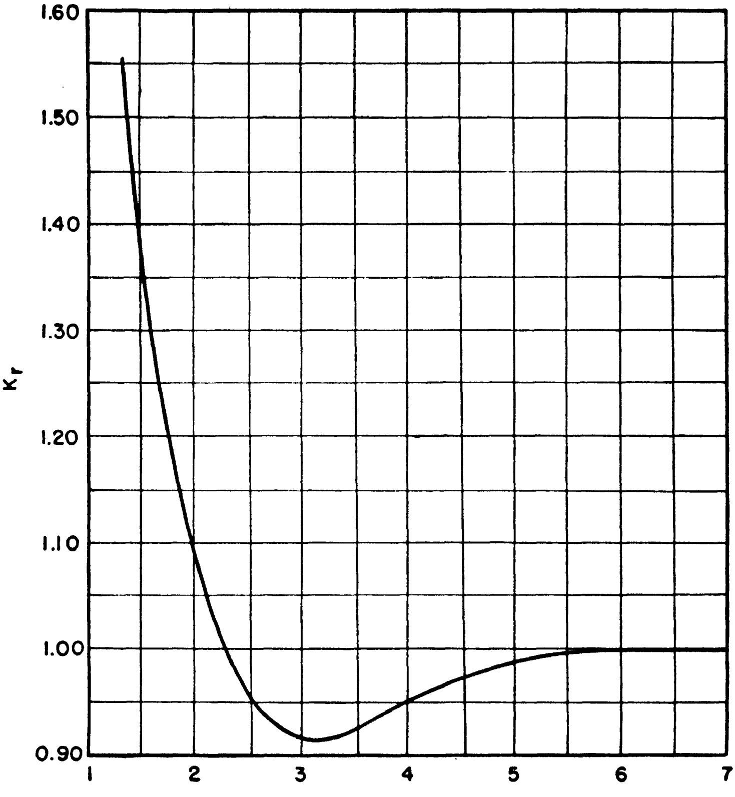

FIG. 147. Values of the function K_r, Eq. (102).

If the wall thickness *t* of a hollow round conductor with a given outside diameter $2a$ is progressively increased and if all other conditions are the same, the graph of the alternating-current resistance due to skin effect [Eq. (100)] exhibits a minimum value with the wall thickness which gives the index ratio $\Lambda = \pi$. An example is shown in Fig. 148. The corresponding graph of the direct-current resistance is included in this illustration.

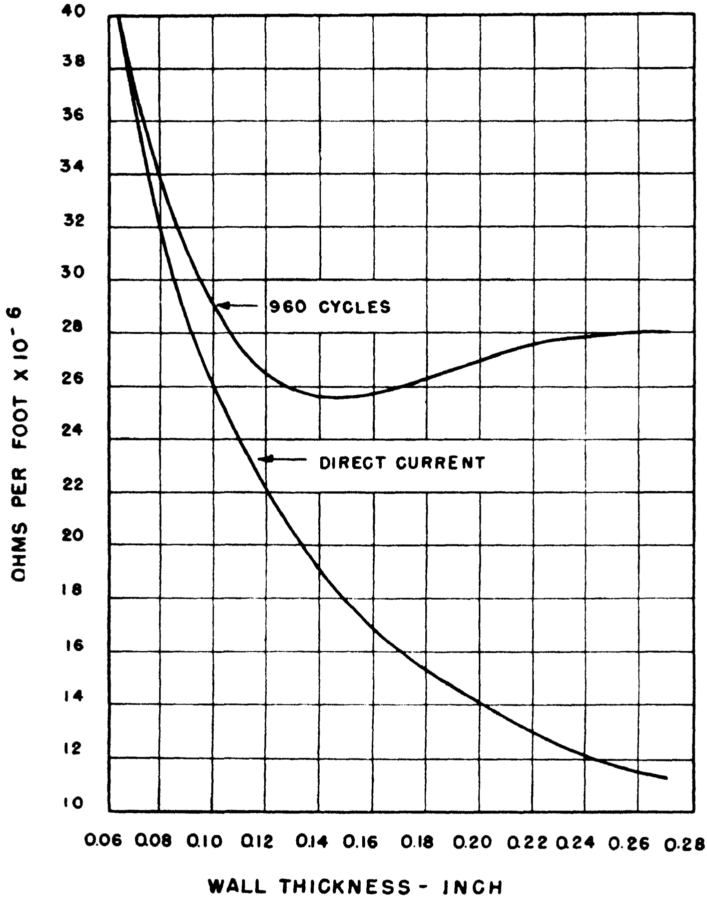

FIG. 148. Alternating-current, 960 cycles, resistances at 70°C of isolated round hollow copper conductors over a range of wall thicknesses. Outside diameter 1.315 in. The lower curve shows the corresponding direct-current resistances.

Alternating-current Resistance with Proximity Effect. If there is proximity effect, the alternating-current resistance of a hollow round conductor (Fig. 146) is

$$R_{ac} = \frac{R_s}{\sqrt{1 - \alpha^2 A_0 + \dfrac{\alpha^4 B_0}{1 - \alpha^2 C_0}}} \quad \text{ohms per cm length of conductor} \qquad (103)$$

R_s is from Eq. (100).

$$\alpha = \frac{2a_1}{d} \qquad \text{see Fig. 146} \tag{104}$$

$$A_0 = a_0 + p_0\left[1 - \psi^2 - \frac{\psi(1-\psi)\chi^3}{400 + \chi^3}\right] \tag{105}$$

$$B_0 = b_0 + (1 - \psi^2)q_0 \tag{106}$$

$$C_0 = c_0 + (1 - \psi)r_0 \tag{107}$$

$$\chi = 2\sqrt{\frac{2\pi f}{R_{dc}10^9}} \tag{108}$$

R_{dc} is from Eq. (99).

$$\psi = \frac{2}{d}\sqrt{t(d-t)} \qquad \text{(109}$$

Values of a_0, b_0, c_0, p_0, q_0, and r_0 are given in Tables 26 and 27 The proximity effect factor in Eq. (103) is by Arnold.[29]

TABLE 27. FACTORS IN EQS. (105), (106), AND (107)

χ	p_0	q_0	r_0	χ	p_0	q_0	r_0
0	0	0	0.03	3.4	0.233	−0.030	0.42
0.20	0	0	0.03	3.6	0.238	−0.026	0.39
0.40	0.001	0	0.03	3.8	0.242	−0.021	0.36
0.60	0.004	0	0.02	4	0.245	−0.017	0.33
0.80	0.012	−0.001	0.02	5	0.236	−0.007	0.19
1.0	0.029	−0.002	0	6	0.209	−0.006	0.14
1.2	0.054	−0.003	0	7	0.185	−0.006	0.13
1.4	0.088	−0.005	0	8	0.165	−0.005	0.11
1.6	0.123	−0.006	0	9	0.148	−0.005	0.08
1.8	0.156	−0.007	0	10	0.135	−0.004	0.07
2.0	0.180	−0.010	0.44	15	0.092	−0.002	0.03
2.2	0.196	−0.015	0.44	20	0.069	−0.001	0
2.4	0.205	−0.022	0.44	30	0.047	−0.001	0
2.6	0.210	−0.028	0.44	40	0.035	0	0
2.8	0.215	−0.033	0.44	50	0.028	0	0
3.0	0.221	−0.034	0.44	Above 50	$\frac{\sqrt{2}}{\chi}$	$-1/2\chi^2$	$\rightarrow\sqrt{2}/\chi$
3.2	0.227	−0.033	0.43				

Inductance. **Inductance of a go and return circuit with hollow round conductors, Fig. 146.**

$$L = 4\left(\log_e \frac{d}{a_1} + \log_e \zeta\right)10^{-9} \quad \text{henry per cm length of circuit} \qquad (110)$$

Values of $\log_e \zeta$ are from Table 28.

TABLE 28. VALUES OF $\log_e \zeta$, EQS. (110), (123), AND (124)

$\frac{a_2}{a_1}$	$\log_e \zeta$	$\frac{a_2}{a_1}$	$\log_e \zeta$
0	0.25	0.55	0.1456
0.05	0.2488	0.60	0.1304
0.10	0.2452	0.65	0.1148
0.15	0.2395	0.70	0.0989
0.20	0.2320	0.75	0.0827
0.25	0.2248	0.80	0.0663
0.30	0.2123	0.85	0.0479
0.35	0.2007	0.90	0.0333
0.40	0.1880	0.95	0.0167
0.45	0.1745	1.10	0
0.50	0.1603		

Hollow Square Conductors (Fig. 149). *Direct-current Resistance.*

$$R_{dc} = \frac{\rho}{A_h} \quad \text{ohms per cm length of conductor} \qquad (111)$$

A_h = the cross-sectional area of the metal of the conductor in square centimeters. Values of the areas of standard hollow conductors, in square inches, are given in Tables 40 and 41, Appendix *E*.

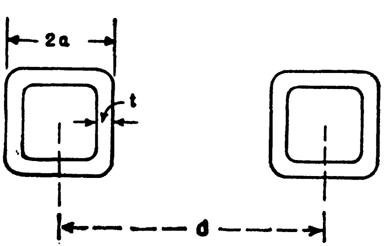

FIG. 149. Single-phase circuit with hollow square conductors.

Alternating-current Resistance with No Proximity Effect. If there is no proximity effect and for values of the index ratio not less than about $\sqrt{2.0}$,

$$R_s = \frac{\rho K_r}{2\pi \sqrt{2pa'}} \quad \text{ohms per cm length of conductor} \qquad (112)$$

where $a' = a - \frac{p}{\sqrt{2}}$, cm

a = one-half the dimension between opposite faces of the conductor, cm

K_r is from Eq. (102) or Fig. 147. Values of the resistance ratio R_s/R_{dc} of standard hollow square conductors for values of a selected parameter are given in Fig. 161, Appendix *E*.

NOTE 7. Equations (100) and (112) are applicable to nearly all cases in practice. The corresponding general equations are given by Dwight[27] and Arnold.[29,30]

Alternating-current Resistance with Proximity Effect. If there is proximity effect, the alternating-current resistance of the hollow square conductor (Fig. 149) is

$$R_{\mathrm{ac}} = R_s + \left(\frac{\alpha^2 D_0 F_0}{1 - \alpha^2 E_0}\right) R_{\mathrm{dc}} \qquad \text{ohms per cm length of conductor} \qquad (113)$$

R_{dc} is from Eq. (111); R_s from Eq. (112). $\alpha = \frac{2a}{d}$, see Fig. 149.

$$D_0 = 0.50\sqrt{\frac{2\pi f}{R_{\mathrm{dc}}10^9}} - 0.27 \qquad (114)$$

$$E_0 = 0.707\left(\frac{20\sqrt{\frac{2\pi f}{R_{\mathrm{dc}}10^9}} - 3.0}{20\sqrt{\frac{2\pi f}{R_{\mathrm{dc}}}} + 30}\right) \qquad (115)$$

The second term of this equation is omitted.

$$F_0 = \frac{2 - \frac{2t}{a} + \left(\frac{t}{a}\right)^2 + \left(\frac{2\pi f}{R_{\mathrm{dc}}10^9}\right)\frac{t}{a}\sqrt{2 - \frac{t}{a}}}{1 + \frac{2\pi f}{R_{\mathrm{dc}}10^9}\sqrt{\frac{t}{a}}} \qquad (116)$$

For $\frac{t}{a} = 1.0$ (solid square conductor), $F_0 = 1.0$. The proximity factor in Eq. (113) is given by Arnold.[30]

Inductance. The inductance of a single-phase circuit with hollow square conductors, Fig. 149.

$$L = 4\left(\log_e \frac{d}{G_s}\right)10^{-9} \qquad \text{henry per cm length of circuit} \qquad (117)$$

where G_s = self-geometric mean distance of the conductor

Values of G_s, in inches, of standard hollow square conductors are given in Tables 40 and 41, Appendix *E*.

Comparison of Hollow Round Conductors and Hollow Square Conductors. For the same direct-current resistance and the same separation of live parts:

1. The skin effect and the proximity effect are greater with hollow square conductors.

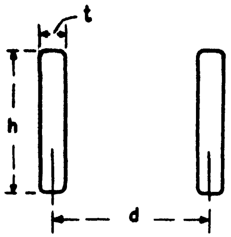

FIG. 150. Single-phase circuit with solid rectangular conductors.

2. The alternating-current carrying capacity decreases with increase of frequency more rapidly with hollow square conductors.

3. The circuit inductance is somewhat less with hollow square conductors.

Flat Bars on Edge (Fig. 150). *Direct-current Resistance.*

$$R_{dc} = \frac{\rho}{A_h} \quad \text{ohms per cm length of conductor} \tag{118}$$

where A_h = area of cross section of conductor normal to its length, sq cm

If the bar has sharp edges, $A_h = ht$. If the bar has round edges, the area to be deducted from the product ht is

$$\begin{aligned} a_h &= 4r_h^2 - \pi r_h^2 \\ &= 0.8584 r_h^2 \end{aligned} \tag{119}$$

where r_h = radius of the round edges, cm

Alternating-current Resistance with No Proximity Effect. If there is no proximity effect, the alternating-current resistance is

$$R_s = \frac{2\Phi \sqrt{f} \sqrt{\rho 10^9}}{\sqrt{\pi} \sqrt{ht} \times 10^9} \quad \text{ohms per cm length of conductor} \tag{120}$$

Φ is a factor related to the width-thickness ratio of the conductor. Values of this factor are given in Fig. 151.

The basis of Eq. (120) is the equation for the resistance ratio of rectangular conductors given by Cockcroft.[31] A discussion of the Cockcroft equation by Dwight[32] includes a summary of the data of alternating-current resistances of rectangular conductors obtained by several investigators. The most complete of these groups of measured values is the work of Forbes and Gorman.[33]

The data noted above show that the Cockcroft equation gives correct values of the alternating-current resistance of isolated rectangular conductors, provided that the width-thickness ratio of the conductor is greater than about 3.0 and that the index ratio of the conductor

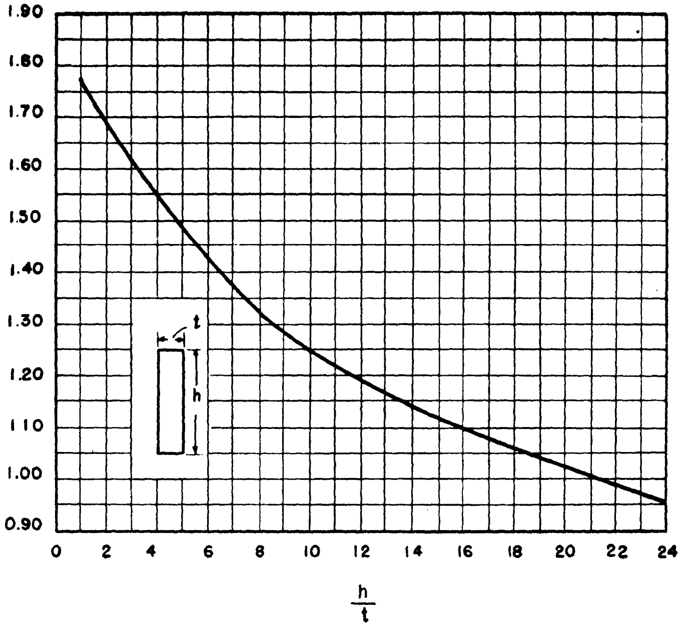

Fig. 151a. Values of the factor Φ, Eq. (120).

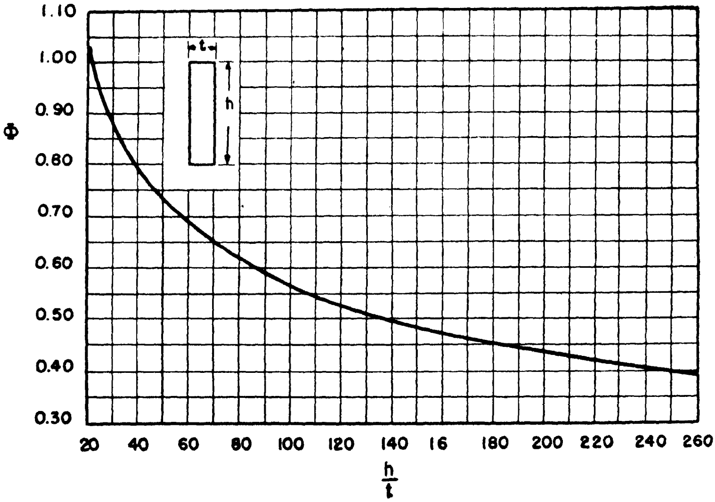

Fig. 151b. Values of the factor Φ, Eq. (120).

[Eq. (4)] is above about 3.0. Below these limit values, Eq. (120) gives resistance values lower than the corresponding measured values. This difference increases with decrease of the width-thickness ratio and with decrease of the index ratio below the limit values noted.

Cockcroft shows that the effect of rounding the edges of rectangular conductors with a radius of curvature equal to one-fortieth of the perimeter of the section of the conductor is only to decrease the alternating-current resistance about 5 per cent. The corner radius of standard rectangular conductors usually is less than the radius noted above, and little, if any, correction of Eq. (120) is needed for round edges.

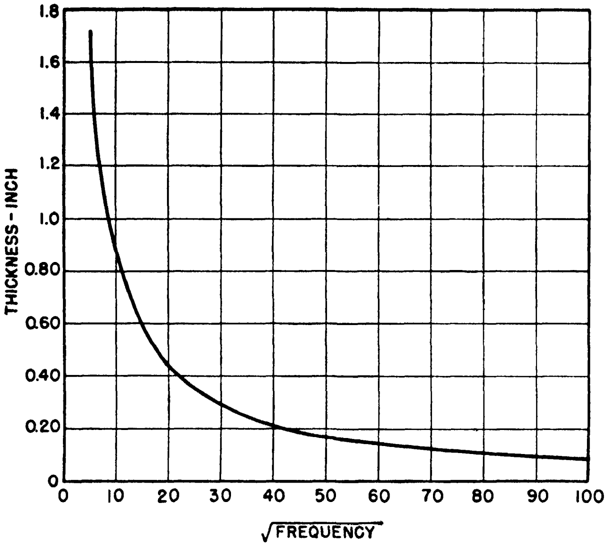

FIG. 152. Thickness of rectangular copper conductors which for 70°C correspond to the index-ratio value 3.0 for a range of frequencies.

The thicknesses of rectangular conductors, which for 70°C correspond to the index-ratio value 3.0 with machine frequencies, are shown in Fig. 152.

The thickness of a rectangular conductor for a power circuit with a machine frequency usually will be equal to or larger than the value from Fig. 152, and the width-thickness ratio of the conductor as a rule will be above 3.0.

With a constant cross-sectional area and progressive increase of the width-thickness ratio of a rectangular conductor from its minimum value 1.0—a square conductor—the alternating-current resistance with a given frequency decreases at the same rate as that of the factor Φ, Fig. 151, down to the thickness of the conductor that gives the critical index-ratio value 3.0.

The perimeter of the section of a rectangular conductor for a given cross-sectional area increases with increase of the width-thickness ratio. Thus, as is stated by Eq. (89), the current-carrying capacity of a rectangular conductor for a given cross-sectional area increases with increase of the width-thickness ratio. This statement corresponds to the statement of the preceding paragraph.

TABLE 29. VALUES OF $\log_e k$, EQ. (121)

$\frac{h}{d}$	t/h										
	0	0.1	0.2	0.3	0.4	0.5	0.6	0.7	0.8	0.9	1.0
0	0	0	0	0	0	0	0	0	0	0	0
0.1	0.0008	0.0008	0.0008	0.0008	0.0007	0.0006	0.0005	0.0004	0.0003	0.0002	0.0000
0.2	0.0033	0.0033	0.0032	0.0030	0.0028	0.0025	0.0021	0.0017	0.0012	0.0007	0.0000
0.3	0.0074	0.0073	0.0071	0.0067	0.0062	0.0056	0.0048	0.0038	0.0027	0.0015	0.0001
0.4	0.0129	0.0128	0.0124	0.0118	0.0109	0.0098	0.0084	0.0068	0.0050	0.0027	0.0003
0.5	0.0199	0.0197	0.0191	0.0182	0.0169	0.0152	0.0131	0.0106	0.0077	0.0043	0.0005
0.6	0.0281	0.0278	0.0271	0.0258	0.0240	0.0216	0.0185	0.0152	0.0111	0.0064	0.0011
0.7	0.0374	0.0371	0.0361	0.0344	0.0320	0.0290	0.0251	0.0206	0.0155	0.0090	0.0019
0.8	0.0477	0.0473	0.0461	0.0440	0.0411	0.0373	0.0321	0.0268	0.0200	0.0129	0.0031
0.9	0.0589	0.0584	0.0569	0.0544	0.0506	0.0464	0.0404	0.0338	0.0254	0.0158	0.0046
1.0	0.0708	0.0702	0.0685	0.0655	0.0614	0.0560	0.0492	0.0406	0.0313	0.0199	0.0065
0.9	0.0847	0.0841	0.0821	0.0787	0.0738	0.0675	0.0596	0.0501	0.0382	0.0250	
0.8	0.1031	0.1023	0.0999	0.0959	0.0903	0.0829	0.0745	0.0622	0.0485		
0.7	0.1277	0.1268	0.1240	0.1192	0.1125	0.1037	0.0925	0.0788			
0.6	0.1618	0.1607	0.1573	0.1507	0.1436	0.1329	0.1194				
0.5	0.2107	0.2094	0.2053	0.1984	0.1886	0.1754					
0.4	0.2843	0.2826	0.2776	0.2691	0.2567						
0.3	0.4024	0.4003	0.3942	0.3831							
0.2	0.6132	0.6105	0.6021								
0.1	1.0787	1.1075									
$\frac{d}{h}$	t/h										

There are no available experimental data which show the effect of proximity on the alternating-current resistance of rectangular conductors which are within the range of practice. An estimate of the proximity effect can be made by using Eq. (113) for a solid square conductor.

Inductance. The inductance of a go and return circuit with rectangular conductors, Fig. 150.

$$L = 4\left(\log_e \frac{d}{h+t} + 1.5 + \log_e k - \log_e e\right) 10^{-9} \qquad (121)$$

henry per cm length of circuit

Values of $\log_e k$ are given in Table 29. Values of $\log_e e$ are given in Table 30.

TABLE 30. VALUES OF $\log_e e$, EQ. (121)

$\frac{h}{t}$ or $\frac{t}{h}$*	$\log_e e$	$\frac{h}{t}$ or $\frac{t}{h}$*	$\log_e e$
0	0	0.50	0.00211
0.025	0.00089	0.55	0.00203
0.05	0.00146	0.60	0.00197
0.10	0.00210	0.65	0.00192
0.15	0.00239	0.70	0.00187
0.20	0.00249	0.75	0.00184
0.25	0.00249	0.80	0.00181
0.30	0.00244	0.85	0.00179
0.35	0.00236	0.90	0.00178
0.40	0.00228	0.95	0.00177
0.45	0.00219	1.0	0.00177

* Use h/t or t/h, whichever is smaller.

Coaxial Conductors (Fig. 153). *Direct-current Resistance.* The direct-current resistances of the conductors are obtained by the use of Eqs. (92) and (99).

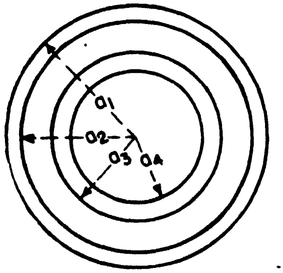

FIG. 153. A single-phase circuit with coaxial conductors.

Alternating-current Resistances.

1. Inner conductor, if hollow, use Eq. (100).
2. Inner conductor, if solid, use Eq. (93).
3. Outer conductor,

$$R_{ac} = \frac{\rho K_r}{2\pi \sqrt{2} p a'_2} \text{ ohms per cm length of conductor} \qquad (122)$$

where

$$a_2' = a_2 + \frac{p}{\sqrt{2}} \qquad \text{cm}$$

K_r is from Eq. (102) or Fig. 147.

The alternating-current resistances with various frequencies of coaxial conductors with stranded innerconductors without cores, at 85°C, per 1,000 ft length of circuit are given in Fig. 154. The corresponding resistances of coaxial conductors with segmental innerconductors (Fig. 145) are somewhat lower than these values.

Inductance of a circuit with coaxial conductors, Fig. 153.

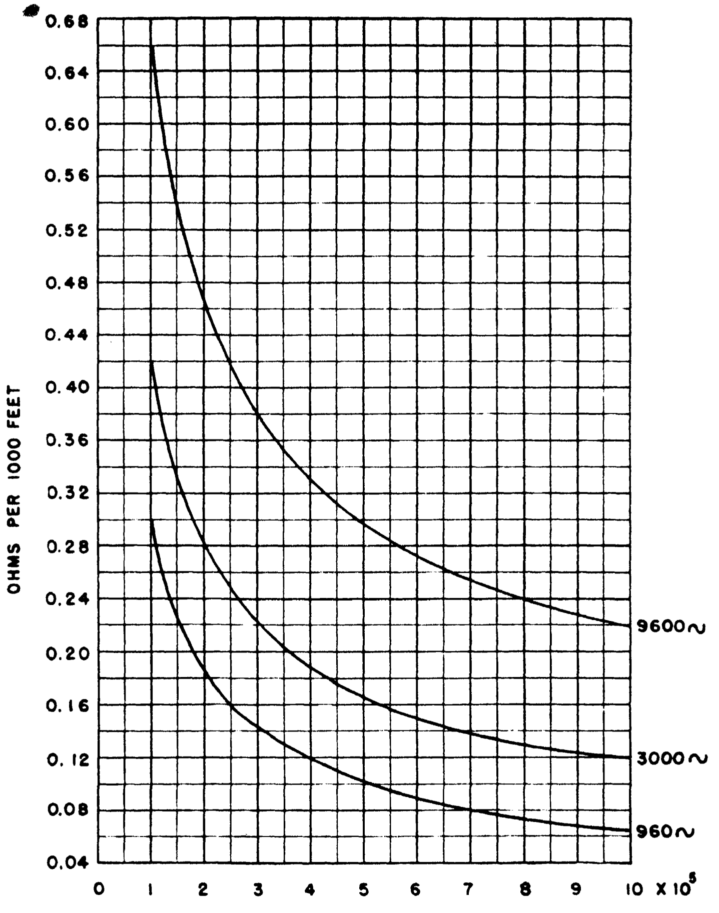

FIG. 154. Alternating-current resistances of standard coaxial cables with 960, 3,000, and 9,600 cycles. Values are the sum of the resistances of the two conductors per 1,000 ft length of circuit.

Inductance with Hollow Inner Conductor.

$$L = 2\left[\log_e \frac{a_1}{a^3} + \frac{2(a_2/a_1)^2}{1 - (a_2/a_1)^2} + \log_e \frac{a_1}{a_2} - 1 + \log_e \zeta_1 + \log_e \zeta_3\right] 10^{-9}$$

henrys per cm length of circuit (123)

$\log_e \zeta_1$ for a_2/a_1; $\log_e \zeta_3$ for a_4/a_3.

Inductance with Solid Inner Conductor.

$$L = 2\left[\log_e \frac{a_1}{a_3} + \frac{2(a_2/a_1)^2}{1 - (a_2/a_1)^2} \times \log_e \frac{a_1}{a_2} - 0.75 + \log_e \zeta_1\right] 10^{-9}$$

henrys per cm length of circuit (124)

Values of $\log_e \zeta_1$ and $\log_e \zeta_3$ are obtained from Table 28.

NOTE 8. Equations (98), (110), (121), (123), and (124) for values of the inductances of circuits are from "Inductance Calculations," by F. W. Grover.[34]

Electrical Separation of Bare Conductors. Values for the minimum distances between live parts of the bare conductors in air and between live parts of bare conductors and ground for various voltages are given in Table 31.

TABLE 31. SEPARATION OF BARE CONDUCTORS IN AIR (SEMIRIGID CONSTRUCTION*) UP TO 3,300 FT ALTITUDE
(Above 3,300 ft, add 4 per cent for each additional 1,000 ft)

Voltage, a-c	Between conductors, in.	To ground, in.
125	0.75	0.75
250	1	1
500	1.5	1.375
600	1.75	1.50
1,200	2	2
2,500	3	2.75
3,500	3.5	3
4,500	4	3.5
5,000	4.25	4

* Semirigid construction means supporting the live part so that the maximum possible mechanical and magnetic loading cannot reduce the separation by more than 25 per cent.

Example 29. Single-phase circuit, 960 cycles, 1,200 volts. Length, 1,000 ft. Hollow round conductors, bare (Fig. 146). Conductors, standard copper pipe, 1 in. nominal diameter. Weight, 1.83 lb per ft. Temperature 70°C, 98 per cent conductivity. Resistivity ρ, 2.10×10^{-6} ohm-cm[3].

DIMENSIONS

OD = 1.315 in.	a_1 = 1.67 cm
ID = 1.062 in.	a_2 = 1.35 cm
t = 0.1265 in.	t = 0.32 cm
Area = 600,000 cir mils	Area = 3.044 sq cm
= 0.472 sq in.	

Separation of conductors, Table 31 = 2 in. (5.08 cm)
Spacing of conductors, d = 8.42 cm
i_{dc}, Eq. (90*b*) = 696 amp

R_{dc}, Eq. (99) $= 0.69 \times 10^{-6}$ ohm per cm
Index ratio, Eq. (3), $\Lambda = 2.71$
K_r, Fig. 147 $= 0.935$
R_s, Eq. (100) $= 0.854 \times 10^{-6}$ ohm per cm
R_{ac}, Eq. (103) $= 0.924 \times 10^{-6}$ ohm per cm
i_{ac}, Eq. (91) $= 600$ amp
L, Eq. (110) $= 6.72 \times 10^{-9}$ henry per cm

$$\text{Circuit resistance, ac} = \frac{0.924 \times 2.54 \times 12 \times 1{,}000 \times 2}{10^6} = 0.056 \text{ ohm}$$

$$\text{Circuit inductance} = \frac{6.72 \times 2.54 \times 12 \times 1{,}000}{10^9} = 205 \text{ microhenrys}$$

$$\text{Circuit reactance} = \frac{2\pi \times 960 \times 205}{10^6} = 1.237 \text{ ohms}$$

Example 30. This example is the same as Example 29 with the exceptions of insulated conductors and the conductor spacing, $d = 4$ cm.

$$R_{ac} = 1.38 \times 10^{-6} \text{ ohm per cm}$$
$$L = 3.75 \times 10^{-9} \text{ henry per cm}$$

Circuit resistance, ac = 0.084 ohm
Circuit inductance = 114 microhenrys
Circuit reactance = 0.69 ohm

Example 31. *Single-phase circuit with coaxial conductors.* Inner conductor solid (stranded without core). Frequency 960 cycles, 1,200 volts. Length 1,000 ft. Area of each conductor 600,000 circular mils (same as the conductor area of Example 29). Temperature 85°C. Conductivity 98 per cent. Resistivity $\rho = 2.22 \times 10^{-6}$ ohm-cm³. i_{ac}, Table 24, 360 amp.

DIMENSIONS (SEE FIG. 153)

$a_1 = 1.67$ cm
$a_2 = 1.35$ cm
t, outer conductor $= 0.32$ cm
$a_3 = 0.984$ cm

Circuit resistance, dc, Eqs. (92) and (99) = 0.044 ohm
Circuit resistance, ac, Eqs. (93) and (122) = 0.085 ohm
Circuit inductance, Eq. (124) = 41 microhenrys
Circuit reactance = 0.247 ohm

Example 32. Single-phase circuit, 9,600 cycles, 1200 volts. Length 1,000 ft. Hollow round conductors, bare, Fig. 146. Thin-wall copper pipe. Weight 1.83 lb per ft. Resistivity 2.10×10^{6} ohm-cm³.

DIMENSIONS

OD = 2.375 in.
ID = 2.245 in.
$t = 0.065$ in.
Area = 600,000 cir mils

$a_1 = 3.016$ cm
$a_2 = 2.851$ cm
$t = 0.165$ cm
Area = 3.044 sq cm

Separation of conductors = 2 in. (5.08 cm)
Spacing of conductors $d = 11.11$ cm

$i_{dc} = 860$ amp
$R_{dc} = 0.69 \times 10^{-6}$ ohm per cm
Index ratio $= 4.40$
$K_r = 0.97$
$R_s = 1.45 \times 10^{-6}$ ohm per cm
$R_{ac} = 1.72 \times 10^{-6}$ ohm per cm
$i_{ac} = 544$ amp
$L = 5.29 \times 10^{-9}$ henry per cm
Circuit resistance, ac $= 0.105$ ohm
Circuit inductance $= 161$ microhenrys
Circuit reactance $= 9.7$ ohms

Selection of Conductors. Local conditions usually dictate the choice between bare and insulated conductors. If either type of circuit can be used, the selection is based mainly on the comparative costs of the installations, including the costs of the capacitors.

Hollow round conductors and hollow square conductors are the best shapes as regards the electrical characteristics for bare conductors. Generally the surface areas of these shapes are sufficient for heat dissipation from the conductor. The square hollow conductor is better in this respect, and the ventilated conductor (Fig. 158 and Table 41) provides additional current-carrying capacity where that is needed. Also hollow conductors, both round and square, are well suited to the mechanical design of the circuit.

The coaxial arrangement of conductors (Fig. 153) is usually a good choice with reference to the electrical characteristics for a circuit with insulated conductors. This arrangement, referred to generally as coaxial cable, has the additional merit of easy installation but is handicapped by the lower current-carrying capacity of insulated conductors.

REFERENCES

General

Russell, A.: "The Theory of Alternating Currents," Vol. 1, 2d Ed., Cambridge University Press, Cambridge, England, 1914.

LaCour and Bragstad: "Theory and Calculation of Electric Currents," Longmans, Green & Co., Inc., New York, 1913.

Benische, G.: "Scientific Bases of Electrical Engineering," in German, Verlag Julius Springer, Berlin, 1914.

Stansel, N. R.: "Industrial Electric Heating," John Wiley & Sons, Inc., New York, 1933.

Knowlton, A. E.: "Standard Handbook for Electrical Engineers," 8th ed., McGraw-Hill Book Company, Inc., New York, 1949.

References Cited

1. Heaviside, O.: The Induction of Currents in Cores, *Electrician*, **12**, 583, 1884.
2. Thomson, J. J.: On the Heat Produced by Eddy Currents in an Iron Plate Exposed to an Alternating Magnetic Field, *Electrician*, **28**, 599, 1892.
3. Clamer, G. H.: The Development of the Coreless Induction Furnace, *Metals & Alloys*, **6**, 119, 1935.
4. Ewing, J. A.: On magnetic screening, eddy currents, and hysteresis, *Electrician*, **28**, 631, 1892.
5. Tama, M.: Present Status of Electric Melting Furnaces (in German), *Z. Metallhunde*, **18**, **7**, 1926.
6. Northrup, E. F.: Resistivity of Brass, *Met. Chem. Eng.*, **12**, 161, 1914.
7. Vosburgh, F. J.: Carbon and Graphite for Mechanical and Electrical Parts, *Metals & Alloys*, **22**, 721, 1945.
8. Guyer, E. M.: Electrical Glass, Proc. *IRE*, **32**, 743, 1944.
9. Oatley, C. W.: The Power Loss and Electromagnetic Shielding Due to the Flow of Eddy Currents in Thin Cylindrical Tubes, *Phil. Mag.*, **22**, 7th series, 445, 1936.

9*a*. Polzguter, F.: Economical Operation of Induction Furnaces (in German), *Stahl u Eisen*, **29**, 773, 1935.

10. Howe, G. W. O.: The High-frequency Resistance of Wires and Coils, *J.IEE*, **58**, 152, 1920.
11. Butterworth, J.: On the Alternating-current Resistance of Solenoid Coils, *Proc. Roy. Soc. (London)*, **107**, Series A, 693, 1925.
12. Burch and Davis: "Theory of Eddy-current Heating," Ernest Benn, Ltd., London, 1928.
13. Reche, K.: Theoretical and Experimental Investigation of the Coreless Induction Furnace (in German), *Wiss. Veröffentl. Siemens-Konzern*, **12**, 1, 1933.
14. Vaughan, J. T., and J. W. Williamson: Design of Induction Heating Coils for Cylindrical Nonmagnetic Loads, *Elec. Eng.* **64**, 587, 1945.

15. STRICKLAND, H. A., JR.: Induction Heating for Forging, *Metals & Alloys*, **21,** 719, 1945.
16. SEULEN, G., and H. VOSS: Medium Frequency Hardening (in German), *Stahl u Eisen*, **63,** 929, 1943.
17. VAUGHN, F. F., V. R. FARLOW, and E. R. MEYER: Metallurgical Control of Induction Hardening, *Trans. ASM*, **30,** 516, 1942.
18. OSBORN, H. B., JR.: "Principles and Theory of High-frequency Heating. Induction Heating," American Society for Metals, 1946.
19. RIEGEL, G. C.: Case Hardening of Large Gears with High-frequency Current, *Metal Progress*, **44,** 78, 1943.
20. SOMES, H. E.: The Development of High-speed Induction Heating for the Hardening of Internal Diameters, *Trans. Electrochem. Soc.*, **79,** 45, 1941.
21. BABAT, G., and M. LOSINSKY: Heat Treatment of Steel by High-frequency Currents, *J.IEE*, **86,** 161, 1940.
22. SUCH, I. H.: Continuous Heat Treatment of Steel, *Steel*, **115,** 94, 1944.
23. BADENHEUER, F.: Operation of Large-size Coreless Induction Furnaces (in German), *Stahl u Eisen*, **55,** 821.
24. CLAMER, G. H.: The Development of the Submerged Resistor Furnace, *Metals & Alloys*, **5,** 240, 1934.
25. TAMA, M.: Induction Furnace for Melting Aluminum, *Mech. Eng.*, **66,** 731, 1944.
26. "Copper for Bus-bars," The Copper Development Association, London, 1936.
27. DWIGHT, H. B.: "Electrical Coils and Conductors," McGraw-Hill Book Company, Inc., New York, 1945.
28. GROVER, F. W.: *Nat. Bur. Standards Sci. Paper* 169.
29. ARNOLD, A. H. M.: Proximity Effects in Solid and Hollow Round Conductors, *J.IEE*, **88,** Part 2, 349, 1941.
30. ARNOLD, A. H. M.: Alternating-current Resistance of Hollow Square Conductors, *J.IEE*, **82,** 537, 1938.
31. COCKCROFT, J. D.: Skin Effects in Rectangular Conductors at High Frequencies. *Proc. Roy. Soc. (London)*, **122,** Series A, 533, 1929.
32. DWIGHT, H. B.: Effective Resistance of Isolated Nonmagnetic Rectangular Conductors, *AIEE Tech. Paper*, 47-88, December, 1946.
33. FORBES, H. B., and L. J. GORMAN: Skin Effect in Rectangular Conductors, *Trans. AIEE*, **52,** 516, 1933.
34. GROVER, F. W.: "Inductance Calculations," D. Van Nostrand Company, Inc., New York, 1946.

Additional references are given in the Appendixes.

APPENDIXES

A. Electrical Resistivities of Metals
B. Electrical Resistivities and Thermal Conductivities of Nonferrous Alloys
C. Electrical Resistivities and Thermal Conductivities of Ferrous Alloys
D. Heat Contents of Carbon Steels
E. Hollow Copper Conductors

APPENDIX A

ELECTRICAL RESISTIVITIES OF METALS

Table 32 was compiled mainly from "International Critical Tables," "Handbook of Chemistry and Physics," and "Smithsonian Physical Tables."

TABLE 32. RESISTIVITIES OF METALS
(ρ = ohm-cm[3])

Metal	Temperature, °C	$\rho \times 10^{-6}$
Bismuth	18	119
	100	160.2
	200	214.5
	300 (liquid)	128.9
	500 (liquid)	139.9
	700 (liquid)	150.8
Cadmium	18	7.54
	100	9.82
	300	16.5
	400 (liquid)	33.7
	500 (liquid)	35.12
	700 (liquid)	35.78
Gold	20	2.44
	100	2.97
	200	3.83
	1000	12.52
	1500 (liquid)	37.0
Lead	20	22
	100	27.8
	200	38
	319	50
	400 (liquid)	98.3
	600 (liquid)	107.2
	800 (liquid)	116.2
Magnesium	20	4.46
	100	6
	400	11.9

TABLE 32. RESISTIVITIES OF METALS—(*Continued*)

Metal	Temperature, °C	$\rho \times 10^{-6}$
Mercury	20 (liquid)	95.78
	50 (liquid)	98.5
	100 (liquid)	103.25
	200 (liquid)	114.27
	300 (liquid)	127
Molybdenum	20	8
	200	10
	400	13
	600	17
	800	22
	1000	28
	1200	34
	1400	40
	1600	47
	1800	54
	2000	60
Platinum	20	10
	100	14.1
	200	17.9
	400	25.4
	800	40.3
	1000	47
	1200	52.7
	1400	58
	1600	63
Silver	18	1.63
	100	2.15
	200	2.80
	400	3.46
	750	6.65
	1000 (liquid)	11.30
	1500 (liquid)	15.3
Tin	20	11.5
	91.45	18.2
	200	20.3
	225	22
	235 (liquid)	47.6
	750 (liquid)	61.22

TABLE 32. RESISTIVITIES OF METALS—(*Continued*)

Metal	Temperature, °C	$\rho \times 10^{-6}$
Tungsten	20	5.51
	727	25.3
	1227	41.4
	1727	59.4
	2727	98.9
	3237	118
Zinc	20	6
	100	7.95
	191.5	10.37
	300	13.25
	415	17
	427 (liquid)	37.3
	500 (liquid)	36.60
	600 (liquid)	35.90
	700 (liquid)	35.60
	800 (liquid)	35.60
	850 (liquid)	35.74

APPENDIX B

ELECTRICAL RESISTIVITIES AND THERMAL CONDUCTIVITIES OF NONFERROUS ALLOYS

Nickel-chromium Alloys. The effects of heat on two nickel-chromium alloys, B82 and B83 (ASTM designations) are shown in Fig. 155.

The nominal compositions of these alloys are

B82—80 per cent Ni, 20 per cent Cr

B83—60 per cent Ni, 15 per cent Cr, 25 per cent Fe

Average resistivities at 20°C:

B82—108 × 10^{-6} ohm-cm^3

B83—112 × 10^{-6} ohm-cm^3

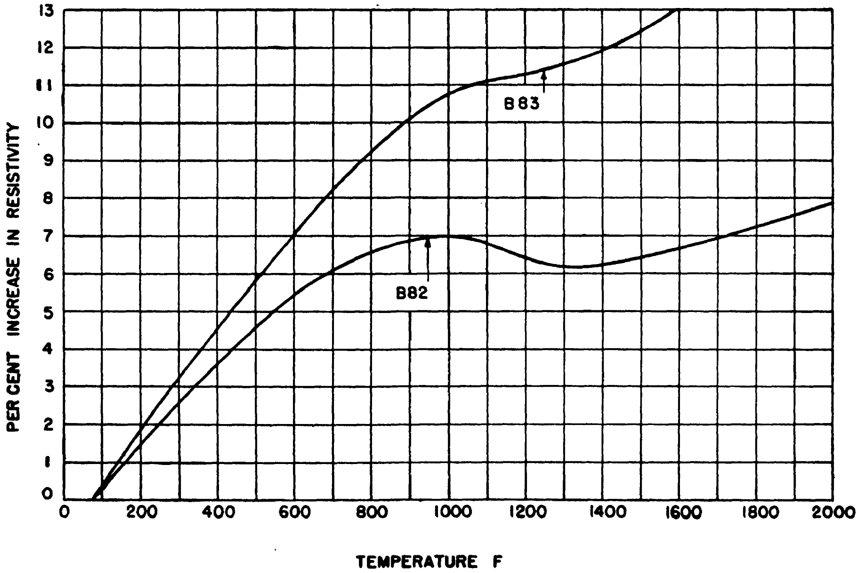

FIG. 155. Resistivity-temperature characteristics of two nickel-chromium alloys.

Monel Metal. A natural nickel-copper alloy. Average composition: 67 per cent Ni, 28 per cent Cu, 5 per cent of other metals such as iron, manganese, and nickel.

Values of resistivities in Table 33 are from *Circular No.* 100, 2d ed., National Bureau of Standards.

TABLE 33. ELECTRICAL RESISTIVITIES OF MONEL METAL, OHM-CM[3] × 10^{-6}

	Temperature, °C										
	0	100	200	300	400	500	600	700	800	900	1000
ρ	42.5	51	54	57	58.5	60	61	63	67	69	72

Copper Alloys. The data of Table 34 are from Thermal Conductivities of Copper Alloys by C. S. Smith and E. W. Palmer, *Trans. of AIMME, Institute of Metals Division,* **117**, 225, 1935.

TABLE 34. ELECTRICAL AND THERMAL CONDUCTIVITIES OF MISCELLANEOUS COPPER ALLOYS

Bar No.	Composition, per cent by weight									Heat-treatment*		Elec. cond., λ ohm⁻¹ per cm × 10⁴		Temp. coef. of elect. resist. (20°–200°) at 20°C	Thermal conductivity K, cal. per cm² per cm per sec per °C		Temp. coefficient of thermal cond. (20°–200°C) at 20°C
	Cu	Zn	Sn	Pb	Al	Fe	Ni	Mn	Other elements	°C	Hours	20°C	200°C		20°C	200°C	
2	99.986	.....	....	.....	....	0.0016	.....	.....	O, 0.022 S, 0.001	550	1	58.96	34.16	+0.00392	0.941	0.934	−0.00004
19	66.24	33.72	....	0.33	....	0.01	.....	.....	....	650	¾	15.62	12.24	0.001591	0.287	0.349	+0.00120
12	96.94	3.04	....	0.00	....	0.02	.....	.....	....	700	¾	36.607	25.21	0.002505	0.640	0.690	0.00043
13	95.21	4.77	....	0.00	....	0.02	.....	.....	....	700	¾	33.062	23.31	0.002312	0.579	0.650	0.00068
140	97.49	.....	....	.....	....	0.06	0.27	.....	Be, 2.24	815	½Q	11.16	(8.645)	(0.001061)	0.205	0.249	0.00119
140	97.49	.....	....	.....	....	0.06	0.27	.....	Be, 2.24	QR300	2	12.760	10.38	0.001268	0.245	0.280	0.00080
141	97.49	.....	....	.....	....	0.06	0.27	.....	Be, 2.24	815	½QD	9.694	(8.184)	(0.000975)	0.177	0.221	0.00138
141	97.49	.....	....	.....	....	0.06	0.27	.....	Be, 2.24	QDR275	2	10.444	8.935	0.000933	0.196	0.240	0.00125
97	85.10	12.97	....	1.88	....	0.05	.....	.....	....	700	2	20.64	15.79	0.001702	0.383	0.444	0.00088
96	61.85	34.79	....	3.29	....	0.07	.....	.....	....	....	....	13.82	10.93	0.001467	0.258	0.317	0.00127
129	65.99	29.18	....	4.02	....	0.01	0.80	.....	....	700	2	14.78	11.28	0.001715	0.264	0.315	0.00106
98	88.07	3.70	3.77	3.83	....	0.03	0.60	.....	....	700	2	11.53	9.80	0.000980	0.215	0.276	0.00159
133	88.08	4.09	3.76	3.80	....	0.02	0.00	.....	P, 0.25	700	2	7.082	6.304	0.000682	0.133	0.182	0.00206
132	60.41	37.09	1.03	1.12	0.18	0.02	.....	.....	Si, 0.15	Chill cast		13.56	10.22	0.001810	0.240	0.286	0.00107
23	64.14	17.06	....	0.00	....	0.19	18.38	0.30	C, 0.023	750	½	3.399	3.249	0.000257	0.080	0.100	0.00142
24	56.01	25.93	....	0.00	....	0.08	17.95	0.18	C, 0.020	750	½	3.251	3.080	0.000306	0.071	0.098	0.00217
28	63.76	19.79	....	.....	....	0.14	16.29	0.18	....	750	1	3.633	3.417	0.000352	0.081	0.107	0.00178
26	65.51	23.86	....	0.00	....	0.08	10.36	0.18	C, 0.011	750	½	4.947	4.590	0.000430	0.110	0.146	0.00182
126	59.76	29.88	....	.....	....	0.04	10.13	0.15	Mg, 0.04	750	4	4.938	4.532	0.000495	0.101	0.135	0.00191
127	64.04	30.50	....	.....	....	0.05	5.41	.....	....	750	4	7.278	6.440	0.000721	0.140	0.185	0.00178
5	56.57	17.65	2.23	10.44	....	0.10	13.24	.....	....	Sand cast		3.398	3.089	0.000553	0.073	0.102	0.00218
6	63.37	8.22	2.31	5.40	....	0.14	19.89	0.23	....	Sand cast		2.916	2.742	0.000350	0.066	0.088	0.00181
66	96.05	.....	....	.....	....	0.04	3.01	.....	Si, 0.88	870	3Q	9.775	9.140	0.000384	0.181	0.256	0.00230
66A	96.05	.....	....	.....	....	0.04	3.01	.....	Si, 0.88	QR500	2	20.69	16.38	0.001460	0.378	0.454	0.00112
66B	96.05	.....	....	.....	....	0.04	3.01	.....	Si, 0.88	870	3SC	22.60	17.34	0.001681	0.403	0.487	0.00116
67	89.08	.....	....	.....	5.11	0.08	4.98	.....	Si, 0.74	850	4Q	5.135	4.755	0.000442	0.107	0.158	0.00265
67A	89.08	.....	....	.....	5.11	0.08	4.98	.....	Si, 0.74	QR500	2	7.087	6.378	0.000617	0.135	0.189	0.00222
67B	89.08	.....	....	.....	5.11	0.08	4.98	.....	Si, 0.74	850	4SC	6.964	6.244	0.000637	0.158	0.214	0.00197
32	74.07	5.31	0.00	.....	....	0.09	19.96	0.57	....	750	1½	3.575	3.431	0.000230	0.092	0.116	0.00145

35	64.15	5.69	....	0.00	....	0.07	29.44	0.52	....	750	....	2.642	2.581	0.000128	0.068	0.086	0.00143
61	56.13	42.34	....	....	....	0.49	1.02	....	....	....	....	14.40	10.77	0.001872	0.272	0.310	0.00078
49	89.38	0.00	0.38	....	9.41	0.52	0.31	....	....	750	3½VSC	7.314	6.364	0.000829	0.144	0.192	0.00185
122	75.79	22.22	....	....	1.98	0.01	....	....	....	700	2	13.08	10.58	0.001310	0.240	0.298	0.00133
59	59.35	38.36	0.98	0.13	....	1.06	....	0.12	....	650	3VSC	13.73	10.58	0.001650	0.241	0.295	0.00124
86	99.654	....	....	0.00	....	0.032	....	....	Si, 0.32 P, 0.00	700	1	21.71	16.98	0.001541	0.394	0.487	0.00131
64	95.61	....	....	....	....	0.11	....	4.51	....	700		5.95	5.798	0.000146	0.111	0.176	0.00325
134	99.21	....	....	....	....	0.007	....	....	Si, 0.009 Cd, 0.85	700	2	50.561	31.19	0.003448	0.824	0.841	0.00012
70	98.41	....	0.59	....	....	0.02	....	....	Si, 0.02 Cd, 1.07	750	1½	32.74	23.30	0.002244	0.556	0.643	0.00087
60	72.49	17.76	....	....	4.44	1.78	....	3.34	....	650	3VSC	5.811	5.310	0.000521	0.120	0.162	0.00195
7	94.00	0.00	....	....	....	0.08	....	1.03	Si, 4.68	Sand cast		2.487	2.698	0.000307	0.060	0.086	0.00239
72	95.69	....	....	....	....	0.16	....	0.99	Si, 3.23	750	1½	3.773	3.611	0.000248	0.078	0.107	0.00208
136	98.10	0.00	0.00	....	0.00	0.06	0.00	0.30	Si, 1.50	700	2	6.611	6.022	0.000530	0.129	0.175	0.00200
131	81.55	14.21	....	....	....	0.04	....	0.20	Si, 4.00	Chill cast		3.518	3.261	0.000433	0.068	0.096	0.00228
135	95.83	1.12	0.00	....	....	0.02	....	....	Si, 3.11	700	2	4.586	4.228	0.000469	0.089	0.124	0.00220
8A	78.30	....	8.04	13.32	....	....	0.20	....	P, 0.10	Sand cast		5.712	4.921	0.000886	0.101	0.146	0.00247
9	87.86	3.05	8.87	....	....	0.03	....	....	....	Sand cast		6.741	5.975	0.000711	0.129	0.171	0.00181
19A	88.36	1.90	9.55	....	....	0.07	....	....	....	Sand cast		6.369	5.670	0.000686	0.120	0.166	0.00213
10	60.54	36.46	1.48	....	0.04	0.73	....	0.21	....	Sand cast		12.54	9.81	0.001544	0.230	0.277	0.00114
69	99.04	....	....	0.00	....	0.07	....	....	Cd, 0.90	750	1½	38.87	26.56	0.002574	0.660	0.745	0.00072
137	50.75	....	....	....	....	48.69	....	0.471	Si, 0.047 C, 0.023	800	1½VSC	12.325	8.98	0.002074	0.237	0.271	0.00081

---

* All alloys, except those in the cast condition, were hot-rolled or cold-rolled from castings 2¼ in. diameter or larger, to 1¼ in. diameter, annealed and cold-drawn to ⅞ in. diameter before final heat-treatment as stated. This was followed by air-cooling unless otherwise noted.

Q = quenched
SC = slowly cooled in furnace.
VSC = very slowly cooled, including holding 18 hr at 450°C.
QR = bar was quenched from same temperature as preceding bar and reheated at temperature stated.
QD = cold-drawn after quenching.

Supplementary Notes.—Table 34.

$$\text{Electrical resistivity} = \frac{10^2}{\lambda 10^6} \quad \text{ohm-cm}^3$$

Example 32. *Bar* 129.

$$\rho,\ 20°\text{C} = \frac{10^2}{14.78 \times 10^6} = \frac{6.76}{10^6},\ \text{ohm-cm}^3$$

Thermal Conductivity. For watts per square centimeter per degree C for 1 cm length of path, multiply values in Table 34 by 4.186.

References Given by Smith and Palmer.

SMITH, C. S.: *Trans. AIME* **89**, 84, 1930.
SMITH, C. S.: *Trans. AIME,* **93**, 176, 1931.
HANSON, D., and C. E. ROGERS: *J. Inst. Metals,* **48**, 37, 1932.
BAILEY, L. C.: *Proc. Roy. Soc.,* **A134**, 57, 1931.
LEES, C. H.: *Trans. Roy. Soc.,* **A208**, 381, 1908.
SAGER, G. H.: *Rensselaer Polytech. Inst. Bull.* 27, 1930.
GRIFFITHS, E., and F. H. SCHOFIELD: *J. Inst. Metals,* **39**, 337, 1928.
SCHOFIELD, F. H.: *Proc. Roy. Soc.,* **A107**, 206, 1925.
MEISSNER, W.: *Ann. Physik,* **47**, 1001, 1915.
GRUNEISEN, E., and A. GOENS: *Z. Physik,* **44**, 615, 1927.
SMITH, A. W.: *Ohio State Univ. Eng. Bull.* 31, 1925.
MASUMOTO, H.: *Tôhoku Imp. Univ. Science Repts.* **13**, 229, 1925.
MANNCHEN W.: *Z. Metallukunde,* **23**, 191, 1931.

APPENDIX C

ELECTRICAL RESISTIVITIES AND THERMAL CONDUCTIVITIES OF FERROUS ALLOYS

The data in Tables 35 to 38, inclusive, are from papers in Special Report No. 24 of the Iron and Steel Institute, London, issued in 1939. Table 35 is from "The Physical Properties of a Series of Steels," The National Physical Laboratory. Tables 36 and 37 are from "Thermal Conductivity and Electrical Resistivity" by R. W. Powell and M. J. Hickman. Table 38 and Fig. 156 are from "A Survey of Existing Data on the Thermal and Electrical Conductivities of Irons and Steels" by R. W. Powell.

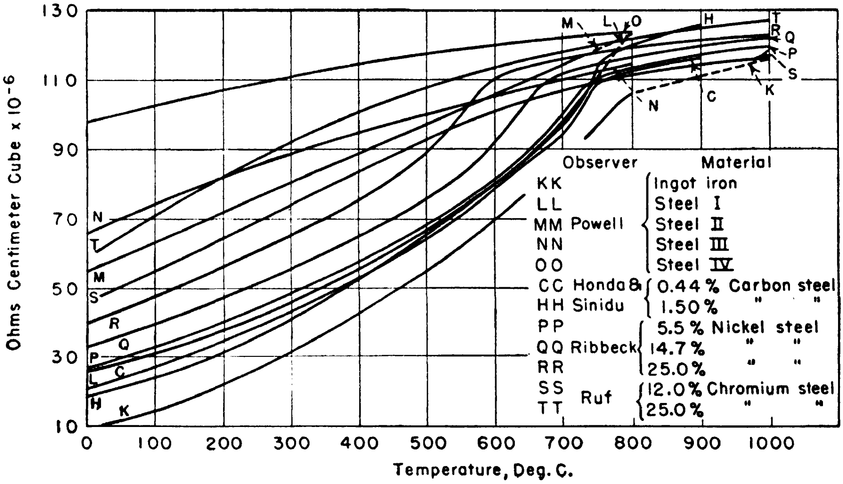

FIG. 156. Resistivity-temperature curves of steels.

References of Fig. 156.

POWELL, R. W.: *Proc. Phys. Soc.* (*London*), **46**, 659, 1934.
HONDA, K., and T. SIMIDU: *Tôhoku Imp. Univ. Sci. Repts.*, **6**, 219, 1917.
RIBBECK, F.: *Z. Physik*, **39**, 787, 1926.
RUF, K.: *Z. Elektrochem.*, **34**, 813, 1928.

Powell comments as follows on the data of Fig. 156:

"Only a few compositions are included in this figure, but, in practice, the amount of added element rarely exceeds 25 per cent of either nickel or chromium and the curves for lower amounts in general fall between those for the 25 per cent

TABLE 35. COMPOSITION OF STEELS REFERRED TO IN TABLES 36 AND 37

Identification No.	C %	Si %	Mn %	S %	P %	Cr %	Ni %	W %	Mo %	V %	Cu %	Al %	As %	Treatment	Density at 15°C
Carbon steels															
1	0.06	0.01	0.38	0.035	0.017	0.022	0.55	Nil	0.030	Nil	0.08	0.001	0.039	Annealed at 930°C	7.871
2	0.08	0.08	0.31	0.050	0.029	0.045	0.07	Nil	0.020	Nil	Trace	0.002	0.032	Annealed at 930°C	7.856
3	0.23	0.11	0.635	0.034	0.034	Trace	0.074	Nil	Nil	Nil	0.13	0.010	0.036	Annealed at 930°C	8.859
5	0.415	0.11	0.643	0.029	0.031	Trace	0.063	Nil	Nil	Nil	0.12	0.006	0.033	Annealed at 860°C	7.854
6	0.435	0.20	0.69	0.038	0.037	0.03	0.04	Nil	0.01	Nil	0.060	0.006	0.024	Annealed at 860°C	7.844
7	0.80	0.13	0.32	0.009	0.008	0.11	0.13	Nil	<0.01	Nil	0.070	0.004	0.021	Annealed at 800°C	7.851
101	0.84	0.13	0.24	0.014	0.014	Trace	Trace	Nil	Nil	Nil	0.02	0.004	0.009		
8	1.22	0.16	0.35	0.015	0.009	0.11	0.13	Nil	0.01	Nil	0.077	0.006	0.025	Annealed at 800°C	7.830
Alloy steels															
4	0.23	0.12	1.51	0.038	0.037	0.06	0.04	Nil	0.025	Nil	0.105	0.015	0.033	Annealed at 860°C	7.849
9	0.325	0.18	0.55	0.034	0.032	0.17	3.47	Nil	0.04	0.01	0.086	0.006	0.023	Annealed at 860°C	7.855
10	0.33	0.17	0.53	0.033	0.031	0.80	3.38	Nil	0.07	0.01	0.053	0.006	0.028	Annealed at 860°C, then reheated to 640°C and cooled in furnace	7.847
11	0.325	0.25	0.55	0.025	0.018	0.71	3.41	Nil	0.06	0.01	0.120	0.008	0.023		7.848
12	0.34	0.27	0.55	0.003	0.024	0.78	3.53	Nil	0.039	Nil	0.050	0.007	0.037		7.859
19	0.315	0.20	0.69	0.036	0.039	1.09	0.073	Nil	0.012	Nil	0.066	0.005	0.028	Annealed at 860°C	7.842
20	0.35	0.21	0.59	0.031	0.028	0.88	0.26	Nil	0.20	Trace	0.12	0.004	0.039	Annealed at 860°C, then reheated to 640°C and cooled in furnace	7.845
21	0.485	1.98	0.90	0.047	0.044	0.04	0.156	Nil	Nil	Nil	0.637	0.007	0.029	Annealed at 930°C	7.725
High-alloy steels															
13	1.22	0.22	13.00	0.010	0.038	0.03	0.07	Nil	Nil	Nil	0.070	0.004	0.038	Heated to 1050°C and cooled in air	7.870
14	0.28	0.15	0.89	0.003	0.009	Trace	28.37	Nil	Nil	Nil	0.030	0.012	0.027	Heated to 950°C and cooled in water	8.161
15	0.08	0.68	0.37	0.011	0.022	19.11	8.14	0.60	Nil	Nil	0.030	0.004	0.025	Heated to 1100°C and cooled in water	7.916
16	0.13	0.17	0.25	0.024	0.018	12.95	0.14	Nil	Nil	0.012	0.060	0.034	0.015	Heated at 960°C in air, T. 2 hr at 750°C and air-cooled	7.745
17	0.27	0.18	0.28	0.022	0.022	13.69	0.20	0.25	0.01	0.022	0.074	0.031	0.003		7.741
18	0.715	0.30	0.25	0.028	0.018	4.26	0.067	18.45	Trace	1.075	0.064	0.004	0.035	Annealed at 830°C	8.691

alloy and pure iron. Iron-vanadium alloys have been shown by Ruf to give similar curves, which tend to the same common value at high temperatures. A class of iron alloys, however, for which the specific resistance (resistivity) at high temperatures is much in excess of that of most steels are alloys of iron and aluminum. The properties of these alloys have been studied by Sykes and Bampfylde, who, for a 15.9 per cent alloy, obtained a specific resistance of 168 × 10^{-6} at 800°C. These iron-aluminum alloys have been omitted in the present treatment." (Resistivity-temperature curves from the Sykes and Bampfylde paper are given in Fig. 157 of this appendix.)

Table 36. Electrical Resistivities of the Steels Listed in Table 35, Microhms-cm[3]
(Extrapolated values at 0°C)

Group	Steel No.	Temperature, °C							
		0	50	100	150	200	250	300	350
Carbon steels	1	(11.9)	14.6	17.8	21.1	24.9			
	2	(12.8)	15.9	19.2	22.5	26.1	30.2	34.7	39.7
	3	(16.2)	18.5	21.7	25.2	29.0	33.1	37.6	
	5	(16.1)	19.3	22.6	26.0	29.7	33.9	38.4	43.3
	6	(18.1)	21.2	24.5	27.9	31.5	35.5	40.0	44.8
	7	(17.1)	19.8	23.3	27.1	30.6	35.2	39.7	45.1
	8	(18.4)	21.6	25.0	28.8				
Alloy steels	4	(19.6)	22.8	26.0	29.2				
	9	(25.5)	28.4	31.5	34.9	38.5	42.5	46.8	
	10	(26.8)	22.9	33.1	36.5	40.3	44.1		
	11	(28.5)	31.4	34.5	37.9	41.5	45.5	49.9	
	12	(29.3)	32.4	35.6	38.8	42.4	46.3	50.6	
	19	(19.9)	22.9	26.2	29.8	33.6	37.7	42.0	
	20	(21.3)	24.3	27.5	30.9	34.7	38.8	43.3	47.9
	21	(41.9)	44.2	46.8	49.6	52.7	56.3	60.1	64.1
High-alloy steels	13	(67.0)	71.5	75.8	80.2	84.4	88.5	92.4	96.0
	14	(84.0)	86.8	89.9	92.9	95.9	98.9	102.0	104.8
	15	(69.9)	74.0	78.3	82.4	86.3	89.8	92.8	95.7
	16	(50.0)	54.4	58.9	63.6	68.2	72.6	77.1	81.3
	17	(50.4)	55.0	59.5	64.2	68.8	73.4	78.0	
	18	(42.2)	45.6	49.1	52.6	56.3	60.2	64.1	

"It will be seen that pure iron has the lowest, and Steel IV the highest resistivity. This steel contained the greatest amount (47.8 per cent) of other elements, and it appears that the resistivity increases as the impurity, or quantity of additional elements, increases. The main fact to which attention should be directed is the manner in which the resistivities of all the metals considered converge to a more or less common value at high temperatures."

TABLE 37. THERMAL CONDUCTIVITIES OF THE STEELS LISTED IN TABLE 35, CALORIES PER SQ CM PER SEC PER °C FOR 1 CM LENGTH OF PATH
(For watts per square centimeter for 1 cm length of path, multiply values in table by 4.186)
(Extrapolated values at 0°C)

Group	Steel No.	Temperature, °C							
		0	50	100	150	200	250	300	350
Carbon steels	1	(0.156)	0.150	0.144	0.138				
	2	(0.142)	0.140	0.138	0.132	0.127	0.123	0.188	0.114
	3	(0.124)	0.123	0.122	0.119	0.116	0.111	0.106	
	5	(0.124)	0.123	0.121	0.119	0.115	0.112	0.109	0.106
	6	(0.115)	0.115	0.115	0.114	0.111	0.108	0.105	0.103
	7	(0.119)	0.118	0.115	0.112	0.108	0.103	0.099	0.096
	8	(0.108)	0.107	0.107	0.107				
Alloy steels	4	(0.110)	0.110	0.110	0.109				
	9	(0.087)	0.089	0.090	0.091	0.093	0.094	0.094	
	10	(0.082)	0.084	0.086	0.087	0.088	0.088		
	11	(0.080)	0.083	0.085	0.086	0.087	0.087	0.087	
	12	(0.079)	0.080	0.081	0.083	0.084	0.085	0.085	
	19	(0.116)	0.114	0.111	0.108	0.106	0.104	0.101	
	20	(0.102)	0.102	0.102	0.101	0.100	0.099	0.097	0.095
	21	(0.060)	0.064	0.068	0.070	0.072	0.074	0.074	0.074
High-alloy steels	13	(0.031)	0.033	0.035	0.037	0.039	0.041	0.043	0.045
	14	(0.030)	0.033	0.035	0.037	0.039	0.040	0.042	0.044
	15	(0.038)	0.038	0.039	0.040	0.041	0.042	0.043	0.045
	16	(0.064)	0.065	0.066	0.066	0.066	0.066	0.067	0.067
	17	(0.060)	0.062	0.063	0.064	0.065	0.065	0.066	
	18	(0.058)	0.060	0.062	0.063	0.065	0.066	0.067	

TABLE 38. COMPOSITIONS OF IRON AND STEELS DESIGNATED BY POWELL IN FIG. 156

Material	Analysis, per cent								
	Fe	C	Ni	Cr	Mn	Si	W	S	P
Ingot iron	99.918*	0.023	.....	.....	0.025	0.007	....	0.020	0.007
Steel I. O.H. and T. 830–600°C	94.36*	0.39	3.55	0.85	0.64	0.21	....	?	?
Steel II. A.H. 940°C, T. 725°C	85.15*	0.27	0.37	13.65	0.29	0.27	....	?	?
Steel III. Softened 1150–1200°C	73.49*	0.15	8.04	17.87	0.26	0.19	....	?	?
Steel IV. Forged steel.	52.2*	0.46	26.86	15.20	1.18	1.30	2.77	0.014	0.018

* Derived by difference.

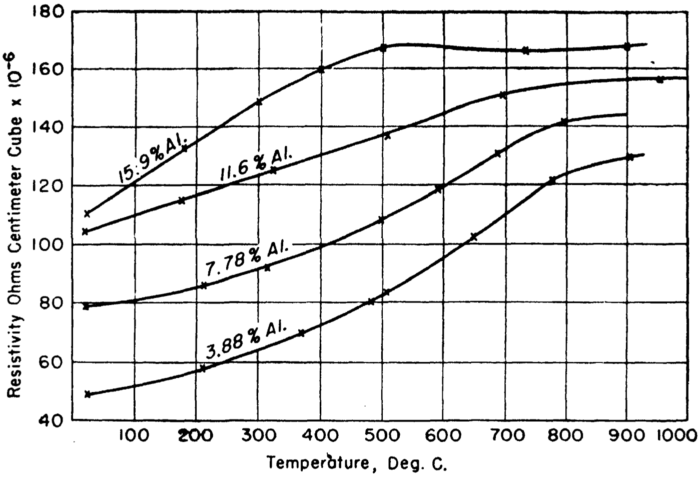

FIG. 157. Resistivity-temperature curves of iron-aluminum alloys.

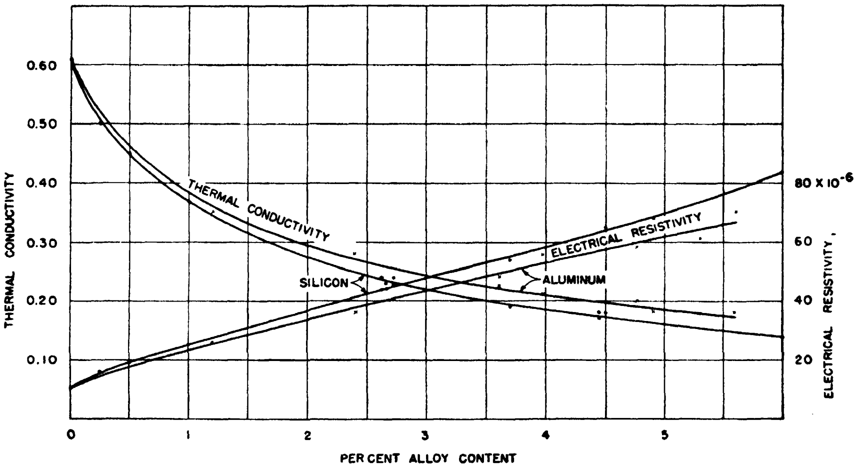

FIG. 158. Electrical resistivities and thermal conductivities of iron-silicon and iron-aluminum alloys. Resistivities of 30°C in ohm-centimeters cube. Conductivities in watts per square centimeter per degree C for 1 cm length of path.

Iron-aluminum Alloys. The chart of Fig. 157 is from The Physical Properties of Iron-aluminum Alloys, by C. Sykes and J. W. Bampfylde, *J. Iron Steel Inst. (London)*, **130**, 389, 1934.

Iron-silicon and Iron-aluminum Alloys. A comparison of the electrical resistivities and the thermal conductivities of these two alloy systems at 30°C is shown in Fig. 158.

APPENDIX D

HEAT CONTENTS OF CARBON STEELS

The data in this appendix are from the paper, Total Heat at Various Temperatures up to 950°C, by J. H. Awbery and A. Snow, in *Iron Steel Inst. Spec. Rept.* 24, Sect. IX, 1939.

TABLE 39. HEAT CONTENTS OF THE CARBON STEELS LISTED IN TABLE 35 OF APPENDIX C, CAL PER GRAM
(For watthours per pound, multiply values in table 39 by 0.5275)

Temp., °C	Steel No.								
	1	2	3	5	5*	6	7	101	8
50	0	0	0	0	0	0	0	0	0
100	5.75	5.75	5.78	5.78	5.86	5.72	5.84	5.96	5.80
150	11.77	11.76	11.81	11.79	12.01	11.80	12.02	12.21	12.01
200	17.95	17.99	18.02	17.93	18.28	18.01	18.36	18.70	18.47
250	24.35	24.47	24.39	24.24	24.72	24.41	24.89	25.24	24.99
300	30.96	31.11	31.02	30.79	31.36	31.02	31.66	31.98	31.66
350	37.82	37.93	37.87	37.61	38.25	37.87	38.66	38.94	38.56
400	44.94	45.03	45.00	44.62	45.41	44.95	45.91	46.16	45.70
450	52.39	52.49	52.46	51.92	52.88	52.31	53.43	53.71	53.06
500	60.28	60.38	60.36	59.67	60.78	59.99	61.41	61.67	60.66
550	68.72	68.69	68.75	67.90	69.13	68.04	69.73	70.14	68.56
600	77.73	77.55	77.69	76.37	77.93	76.58	78.25	79.11	76.91
650	87.27	86.98	87.10	85.10	87.07	85.74	86.87	88.41	85.82
700	97.60	97.22	97.21	94.31	96.83	95.90	96.06	98.35	95.57
750	110.80	110.81	114.32	113.20	116.71	117.77	120.91	124.47	120.53
800	121.25	122.27	125.69	120.65	124.70	128.12	128.25	132.04	128.29
850	130.75	132.60	134.49	126.66	130.78	135.37	136.10	139.42	136.14
900	140.83	142.33	......	133.23	136.78	142.40	......	146.81	
950	148.01	149.92	......	140.18	142.59				

* Second specimen.

APPENDIX E

HOLLOW COPPER CONDUCTORS

The material in this appendix is from the Chase Electrical Handbook issued by the Chase Brass and Copper Company, Waterbury, Conn.

In Tables 40 and 41, R_{20} is the direct-current resistance for 98 per cent conductivity at 20°C. The corresponding direct-current resistance at 70°C is $R_{20} \times 1.1925$.

R_{70}' is the 60-cycle resistance of an isolated conductor, 98 per cent conductivity at 70°C.

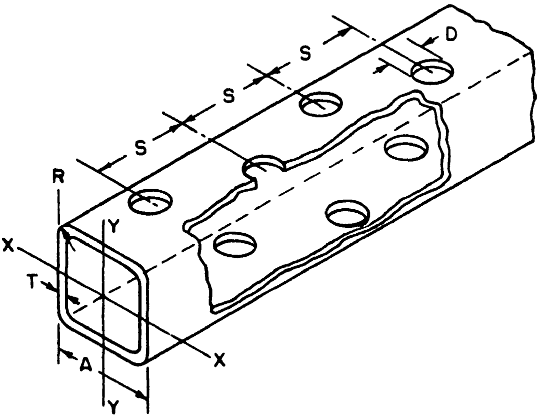

FIG. 159. Hollow square copper conductor with openings in top and bottom walls for ventilation (see Table 41).

$\frac{R'}{R}$ is the 60-cycle resistance ratio at 70°C due to skin effect. The resistance ratios for ventilated conductors, Table 41, are the same as for unventilated conductors, Table 40.

Ampere ratings are for still air indoors, without special enclosures and a 40°C ambient temperature.

Self GMD is self-geometric mean distance, a function of the size and shape of the conductor.

TABLE 40. UNVENTILATED HOLLOW SQUARE CONDUCTORS
(Chase electrical copper)

Square side A, in.	Wall thickness T, in.	Outside corner radius R, in.	Perimeter, in.	Cross section		Weight lb per, ft	On X-X axis and Y-Y axis			Self GMD, in.	R_{20}, microhms/ft	R'/R	R'_{70}, microhms/ft	Capacity at 100 % load factor			
				Sq in.	1,000 cm		Moment of inertia, in.	Section modulus, in.	Radius of gyration, in.					DC	60 cycles		
														Temperature rise			
														30°C amp	30°C amp	40°C amp	50°C amp
1	1/8	1/4	3.57	0.397	505	1.54	0.048	0.024	0.348	0.529	20.79	1.000	24.79	545	545	640	720
1	3/16	1/4	3.57	0.559	712	2.17	0.061	0.030	0.330	0.514	14.75	1.008	17.73	645	640	750	850
1	1/4	1/4	3.57	0.696	886	2.70	0.068	0.034	0.313	0.500	11.86	1.020	14.42	720	710	835	945
1½	1/8	3/8	5.36	0.620	789	2.40	0.188	0.251	0.551	0.809	13.34	1.004	15.97	800	800	935	1,060
1½	3/16	3/8	5.36	0.894	1,138	3.46	0.252	0.336	0.531	0.794	9.25	1.014	11.18	960	955	1,120	1,270
1½	1/4	3/8	5.36	1.143	1,455	4.43	0.302	0.403	0.514	0.779	7.23	1.034	8.91	1,090	1,070	1,250	1,420
1½	5/16	1/2	5.14	1.30	1,655	5.04	0.306	0.408	0.485	0.751	6.35	1.060	8.02	1,160	1,130	1,320	1,490
1½	3/8	1/2	5.14	1.49	1,892	5.76	0.328	0.437	0.470	0.738	5.56	1.103	7.31	1,240	1,180	1,380	1,560
2	1/8	3/8	7.36	.87	1,108	3.37	0.498	0.498	0.756	1.103	9.50	1.008	11.42	1,080	1,080	1,260	1,430
2	3/16	3/8	7.36	1.27	1,616	4.92	0.688	0.688	0.736	1.087	6.51	1.020	7.92	1,310	1,300	1,520	1,720
2	1/4	3/8	7.36	1.64	2,092	6.37	0.846	0.846	0.717	1.071	5.03	1.048	6.29	1,490	1,450	1,700	1,930
2	5/16	1/2	7.14	1.93	2,451	7.46	0.92	0.92	0.691	1.043	4.29	1.08	5.53	1,610	1,550	1,820	2,060
2	3/8	1/2	7.14	2.24	2,847	8.67	1.02	1.02	0.674	1.028	3.69	1.13	4.97	1,740	1,640	1,920	2,170
2½	1/8	3/8	9.36	1.12	1,426	4.34	1.03	0.83	0.961	1.397	7.42	1.01	8.94	1,360	1,350	1,590	1,790
2½	3/16	3/8	9.36	1.64	2,091	6.36	1.43	1.14	0.932	1.380	5.06	1.03	6.21	1,650	1,620	1,900	2,160
2½	1/4	3/8	9.36	2.14	2,729	8.31	1.82	1.46	0.922	1.363	3.88	1.056	4.89	1,880	1,830	2,140	2,430
2½	5/16	1/2	9.14	2.55	3,247	9.88	2.11	1.69	0.909	1.336	3.26	1.10	4.28	2,050	1,950	2,290	2,600
2½	3/8	1/2	9.14	2.99	3,802	11.57	2.30	1.84	0.878	1.320	2.78	1.16	3.85	2,220	2,060	2,420	2,740
2½	1/2	3/4	8.71	3.57	4,547	13.84	2.42	1.94	0.823	1.265	2.33	1.305	3.64	2,420	2,120	2,490	2,820
3	1/8	3/8	11.36	1.37	1,744	5.31	1.86	1.24	1.17	1.690	6.07	1.015	7.35	1,640	1,620	1,900	2,160
3	3/16	3/8	11.36	2.02	2,568	7.82	2.61	1.74	1.14	1.672	4.12	1.037	5.09	1,910	1,950	2,280	2,600
3	1/4	3/8	11.36	2.64	3,365	10.24	3.35	2.23	1.13	1.655	3.14	1.07	4.00	2,270	2,200	2,580	2,920
3	5/16	1/2	11.14	3.18	4,043	12.31	3.92	2.61	1.11	1.628	2.62	1.11	3.46	2,500	2,360	2,760	3,140
3	3/8	1/2	11.14	3.74	4,757	14.48	4.37	2.91	1.08	1.612	2.22	1.185	3.14	2,700	2,480	2,920	3,300
3	1/2	3/4	10.71	4.57	5,820	17.72	4.83	3.22	1.03	1.557	1.82	1.353	2.94	3,000	2,560	3,010	3,410
4	1/8	1/2	15.14	1.84	2,348	7.15	4.54	2.27	1.57	2.265	4.51	1.025	5.51	2,150	2,120	2,500	2,820
4	3/16	1/2	15.14	2.73	3,473	10.57	6.54	3.27	1.55	2.247	3.05	1.051	3.82	2,620	2,550	2,990	3,380
4	1/4	1/2	15.14	3.59	4,570	13.91	8.37	4.19	1.53	2.230	2.32	1.09	3.02	3,000	2,870	3,360	3,800
4	5/16	1/2	15.14	4.43	5,634	17.15	10.05	5.03	1.51	2.213	1.88	1.15	2.58	3,320	3,100	3,640	4,100
4	3/8	1/2	15.14	5.24	6,667	20.29	11.6	5.80	1.49	2.195	1.59	1.22	2.32	3,620	3,270	3,840	4,350
4	1/2	3/4	14.7	6.57	8,366	25.47	13.6	6.78	1.44	2.142	1.26	1.445	2.17	4,070	3,380	3,970	4,490

TABLE 40. UNVENTILATED HOLLOW SQUARE CONDUCTORS—(*Continued*)

Square side *A*, in.	Wall thickness *T*, in.	Outside corner-radius *R*, in.	Perimeter, in.	Cross section		Weight, lb per ft	On X-X axis and Y-Y axis			Self GMD, in.	R_{20}, microhms/ft	*R'/R*	R'_{70}, microhms/ft	Capacity at 100 % load factor			
				Sq in.	1,000 cm		Moment of inertia, in.	Section modulus, in.	Radius of gyration, in.					DC	60 cycles		
														Temperature rise			
														30°C amp	30°C amp	40°C amp	50°C amp
5	1/8	3/4	18.7	2.29	2,916	8.88	8.84	3.54	1.96	2.828	3.63	1.035	4.48	2,620	2,580	3,020	3,420
5	3/16	3/4	18.7	3.40	4,326	13.17	12.8	5.14	1.94	2.811	2.45	1.065	3.11	3,200	3,150	3,620	4,100
5	1/4	3/4	18.7	4.48	5,707	17.37	16.6	6.63	1.92	2.794	1.85	1.105	2.44	3,670	3,500	4,100	4,620
5	5/16	3/4	18.7	5.54	7,055	21.48	20.1	8.02	1.90	2.777	1.50	1.165	2.08	4,080	3,790	4,430	5,010
5	3/8	3/4	18.7	6.58	8,372	25.48	23.3	9.33	1.88	2.760	1.264	1.242	1.87	4,450	4,000	4,660	5,290
5	1/2	3/4	18.7	8.57	10,913	33.32	29.1	11.66	1.84	2.726	.970	1.48	1.71	5,075	4,180	4,870	5,540
6	1/8	3/4	22.7	2.79	3,552	10.81	15.7	5.24	2.37	3.42	2.979	1.043	3.70	3,150	3,080	3,620	4,100
6	3/16	3/4	22.7	4.15	5,281	16.08	23.0	7.65	2.35	3.40	2.004	1.08	2.58	3,840	3,700	4,320	4,900
6	1/4	3/4	22.7	5.48	6,980	21.25	29.8	9.93	2.33	3.38	1.416	1.13	2.04	4,410	4,150	4,860	5,510
6	5/16	3/4	22.7	6.79	8,647	26.32	36.3	12.09	2.31	3.36	1.224	1.19	1.74	4,910	4,500	5,290	5,975
6	3/8	3/4	22.7	8.08	10.281	31.30	42.4	14.13	2.29	3.35	1.029	1.27	1.56	5,370	4,750	5,575	6,300
6	1/2	3/4	22.7	10.57	13,549	40.97	53.6	17.86	2.25	3.31	.786	1.51	1.415	6,140	5,000	5,850	6,620
7	3/16	3/4	26.7	4.90	6,236	18.98	37.3	10.67	2.76	3.98	1.697	1.097	2.196	4,510	4,310	5,050	5,710
7	1/4	3/4	26.7	6.48	8,253	25.12	48.7	13.90	2.74	3.97	1.282	1.15	1.758	5,160	4,810	5,640	6,390
7	5/16	3/4	26.7	8.04	10,238	31.17	59.5	16.99	2.72	3.95	1.034	1.212	1.494	5,750	5,220	6,110	6,940
7	3/8	3/4	26.7	9.58	12,191	37.11	69.8	19.94	2.70	3.93	.868	1.30	1.345	6,280	5,500	6,450	7,300
7	1/2	3/4	26.7	12.57	16,006	48.73	88.9	25.40	2.66	3.89	.661	1.545	1.217	7,200	5,800	6,770	7,690
8	3/16	3/4	30.7	5.65	7,191	21.89	56.7	14.19	3.17	4.57	1,472	1.11	1.948	5,150	4,880	5,710	6,450
8	1/4	3/4	30.7	7.48	9,526	29.00	74.2	18.54	3.15	4.55	1.111	1.165	1.544	5,920	5,500	6,420	7,250
8	5/16	3/4	30.7	9.29	11,830	36.01	90.9	22.73	3.13	4.53	.895	1.23	1.312	6,600	5,950	6,960	7,860
8	3/8	3/4	30.7	11.08	14,101	42.93	107.0	26.74	3.11	4.51	.750	1.32	1.180	7,200	6,270	7,350	8,300
8	1/2	3/4	30.7	14.57	18,552	56.46	137.1	34.27	3.07	4.48	.567	1.575	1.065	8,280	6,600	7,740	8,740
9	3/16	1	34.3	6.32	8,044	24.48	80.4	17.86	3.57	5.13	1.308	1.122	1.750	5,740	5,410	6,350	7,160
9	1/4	1	34.3	8.37	10,662	32.45	105.2	23.39	3.55	5.12	.987	1.18	1.389	6,600	6,080	7,110	8,030
9	5/16	1	34.3	10.41	13,250	40.33	129.3	28.73	3.52	5.10	.794	1.25	1.184	7,360	6,580	7,710	8,700
9	3/8	1	34.3	12.41	15,806	48.10	152.4	33.87	3.50	5.08	.666	1.34	1.064	8,040	6,950	8,140	9,190
9	1/2	1	34.3	16.36	20,825	63.38	196.2	43.59	3.46	5.04	.505	1.58	.951	9,240	7,350	8,600	9,700
10	3/16	1	38.3	7.07	8,999	27.39	111.7	22.33	3.97	5.72	1.169	1.13	1.575	6,380	6,000	7,050	7,950
10	1/4	1	38.3	9.37	11,935	36.32	146.5	29.31	3.95	5.70	.881	1.195	1,256	7,350	6,710	7,900	8,900
10	5/16	1	38.3	11.66	14,842	45.17	180.3	36.06	3.93	5.68	.709	1.265	1.069	8,200	7,290	8,550	9,650
10	3/8	1	38.3	13.91	17,716	53.92	213	42.60	3.91	5.66	.594	1.35	.956	8,950	7,700	9,025	10,200
10	1/2	1	38.3	18.36	23,372	71.13	275	55.02	3.87	5.63	.450	1.607	.863	10,250	8,100	9,500	10,700
11	3/16	1	42.3	7.82	9,954	30.3	150	27.31	4.38	6.30	1.057	1.14	1.436	7,000	6,560	7,700	8,700
11	1/4	1	42.3	10.37	13,209	40.2	197	35.89	4.36	6.28	.796	1.21	1.148	8,080	7,350	8,625	9,750
11	5/16	1	42.3	12.91	16,434	50.0	243	44.23	4.34	6.27	.640	1.28	.977	9,000	7,960	9,350	10,600
11	3/8	1	42.3	15.41	19,626	59.7	288	52.32	4.32	6.25	.536	1.367	.873	9,840	8,420	9,900	11,200
11	1/2	1	42.3	20.36	25,918	78.9	373	67.78	4.28	6.21	.406	1.615	.782	11,300	8,900	10,500	11,800

TABLE 41. VENTILATED HOLLOW SQUARE CONDUCTORS
(Fig. 159. Chase electrical copper)

Square side A, in.	Wall thickness T, in.	Outside corner radius R, in.	Perimeter, in.	Av. cross-section		Weight, lb per ft	Ventilation			On X-X axis			On Y-Y axis			Self GMD, in.	R_{20}, microhms per ft	R'_{20}, microhms per ft	Capacity at 100% load factor			
				Sq. in.	1,000 cm		Holes per ft	Diameter D, in.	Spacing S, in.	Moment of inertia, in.	Section modulus, in.	Radius of gyration, in.	Moment of inertia, in.	Section modulus, in.	Radius of gyration, in.				DC	60 cycles		
																			Temperature rise			
																			30°C amp	30°C amp	40°C amp	50°C amp
2	1/8	3/8	7.36	0.82	1,044	3.18	8	7/8	3	0.453	0.453	0.734	0.491	0.491	0.773	1.103	10.068	12.10	1,320	1,310	1,540	1,750
2	3/16	3/8	7.36	1.19	1,519	4.62	8	7/8	3	0.624	0.624	0.723	0.678	0.678	0.754	1.087	6.930	8.43	1,590	1,570	1,850	2,100
2	1/4	3/8	7.36	1.54	1,965	5.98	8	7/8	3	0.766	0.766	0.704	0.833	0.833	0.735	1.071	5.394	6.74	1,800	1,760	2,060	2,340
2	5/16	1/2	7.14	1.80	2.292	6.98	8	7/8	3	0.825	0.825	0.677	0.909	0.909	0.710	1.043	4.587	5.91	1,950	1,880	2,200	2,500
2	3/8	1/2	7.24	2.09	2,656	8.09	8	7/8	3	0.909	0.909	0.660	1.004	1.004	0.694	1.028	3.958	5.33	2,100	1,980	2,325	2,640
2 1/2	1/8	3/8	9.36	1.05	1,332	4.05	8	1 1/16	3	0.930	0.744	0.943	1.015	0.812	0.985	1.397	7.946	9.56	1,640	1,630	1,930	2,170
2 1/2	3/16	3/8	9.36	1.53	1,949	5.93	8	1 1/16	3	1.306	1.045	0.923	1.405	1.124	0.958	1.380	5.429	6.66	1,990	1,960	2,300	2,600
2 1/2	1/4	3/8	9.36	2.00	2,540	7.73	8	1 1/16	3	1.627	1.302	0.903	1.783	1.426	0.945	1.363	4.166	5.25	2,260	2,200	2,580	2,940
2 1/2	5/16	1/2	9.14	2.37	3,011	9.17	8	1 1/16	3	1.876	1.501	0.891	2.074	1.659	0.936	1.336	3.514	4.61	2,460	2,350	2,760	3,140
2 1/2	3/8	1/2	9.14	2.76	3,519	10.71	8	1 1/16	3	2.032	1.625	0.857	2.256	1.805	0.903	1.320	3.007	4.16	2,670	2,480	2,900	3,300
2 1/2	1/2	3/4	8.71	3.28	4,171	12.70	8	1 1/16	3	2.102	1.682	0.801	2.397	1.918	0.855	1.265	2.537	3.95	2,900	2,540	2,980	3,380
3	1/8	3/8	11.36	1.29	1,646	5.01	6	1 1/4	4	1.667	1.111	1.135	1.824	1.216	1.188	1.690	6.428	7.78	1,970	1,950	2,300	2,600
3	3/16	3/8	11.36	1.90	2,422	7.37	6	1 1/4	4	2.369	1.579	1.116	2.556	1.704	1.159	1.672	4.370	5.40	2,400	2,350	2,760	3,120
3	1/4	3/8	11.36	2.49	3,170	9.65	6	1 1/4	4	2.987	1.991	1.095	3.270	2.180	1.146	1.655	3.338	4.26	2,740	2,640	3,100	3,520
3	5/16	1/2	11.14	2 98	3,798	11.56	6	1 1/4	4	3.483	2.322	1.080	3.839	2.559	1.134	1.628	2.786	3.69	3,000	2,840	3,340	3,780
3	3/8	1/2	11.14	3.51	4,464	13.59	6	1 1/4	4	3.864	2.576	1.050	4.272	2.848	1.104	1.612	2.371	3.35	3,240	2,980	3,500	3,960
3	1/2	3/4	10.71	4.26	5,429	16.53	6	1 1/4	4	4.217	2.811	0.994	4.765	3.177	1.057	1.557	1.949	3.14	3,580	3,080	3,600	4,090
4	1/8	1/2	15.14	1.73	2,206	6.72	6	1 1/2	4	4.042	2.021	1.527	4.437	2.218	1.600	2.265	4.796	5.86	2,580	2,550	2,980	3,380
4	3/16	1/2	15.14	2.56	3.262	9.93	6	1 1/2	4	5.817	2.908	1.507	6.390	3.195	1.579	2.247	3.244	4.06	3,140	3,060	3,580	4,050
4	1/4	1/2	15.14	3.37	4,288	13.05	6	1 1/2	4	7,442	3.721	1.486	8.178	4.089	1.558	2.230	2.468	3.21	3,600	3,440	4,030	4,560
4	5/16	1/2	15.14	4.15	5,283	16.08	6	1 1/2	4	8.923	4.461	1.466	9.810	4.905	1.538	2.213	2.003	2.75	3,980	3,720	4,350	4,925
4	3/8	1/2	15.14	4.91	6,245	19.01	6	1 1/2	4	10.27	5.137	1.447	11.302	5.651	1.518	2.195	1.695	2.46	4,340	3,930	4,600	5,200
4	1/2	3/4	14.7	6.13	7,804	23.75	6	1 1/2	4	11.90	5.948	1.393	13.286	6.643	1.472	2.142	1.356	2.34	4,830	4,030	4,720	5,350
5	1/4	3/4	18.7	2.16	2,750	8.37	6	1 5/8	4	7.94	3.18	1.917	8.685	3.474	2.005	2.828	3.848	4.75	3,160	3,100	3,620	4,100
5	3/16	3/4	18.7	3.20	4,078	12.42	6	1 5/8	4	11.5	4.61	1.896	12.600	5.044	1.984	2.811	2.595	3.30	3,840	3,720	4,350	4,930
5	1/4	3/4	18.7	4.22	5,377	16.37	6	1 5/8	4	14.9	5.94	1.875	16.261	6.504	1.962	2.794	1.968	2.59	4,410	4,200	4,900	5,550
5	5/16	3/4	18.7	5.22	6.642	20.22	6	1 5/8	4	17.9	7.18	1.855	19.675	7.870	1.942	2.777	1.593	2.21	4,900	4,550	5,300	6,010
5	3/8	3/4	18.7	6.19	7,876	23.98	6	1 5/8	4	20.8	8.34	1.835	22.851	9.140	1.922	2.760	1.344	1.99	5,340	4,800	5,600	6,350
5	1/2	3/4	18.7	8.05	10,252	31.21	6	1 5/8	4	26.0	10.40	1.797	18.527	11.411	1.882	2.726	1.032	1.82	6,100	5,000	5,850	6,640

TABLE 41.—VENTILATED HOLLOW SQUARE CONDUCTORS—(*Continued*)

Square side *A*, in.	Wall thickness *T*, in.	Outside corner radius *R*, in.	Perimeter, in.	Av. cross-section		Weight, lb per ft	Ventilation			On *X-X* axis			On *Y-Y* axis			Self GMD in.	R_{20} microhms per ft	R'_{70}, microhms per ft	Capacity at 100% load factor			
				Sq. in.	1,000 cm		Holes per ft	Diameter *D*, in.	Spacing *S*, in.	Moment of inertia, in.	Section modulus, in.	Radius of gyration, in.	Moment of inertia, in.	Section modulus, in.	Radius of gyration, in.				DC	60 cycles		
																			Temperature rise			
																			30°C amp	30°C amp	40°C amp	50°C amp
6	1/8	3/4	22.7	2.64	3,361	10.23	6	1 3/4	4	14.4	4.81	2.337	15.464	5.155	2.420	3.42	3.148	3.91	3,800	3,720	4,360	4,950
6	3/16	3/4	22.7	3.92	4,995	15.20	6	1 3/4	4	21.0	7.01	2.315	22.579	7.526	2.399	3.40	2.119	2.73	4,640	4,460	5,220	5,925
6	1/4	3/4	22.7	5.18	6,597	20.08	6	1 3/4	4	27.3	9.09	2.295	29.292	9.764	2.378	3.38	1.604	2.16	5,330	5,020	5,890	6,650
6	5/16	3/4	22.7	6.42	8,168	24.87	6	1 3/4	4	33.2	11.06	2.274	35.642	11.881	2.357	3.36	1.296	1.83	5,940	5,450	6,390	7,250
6	3/8	3/4	22.7	7.62	9,707	29.55	6	1 3/4	4	38.8	12.92	2.254	41.633	13.878	2.337	3.35	1.090	1.65	6,460	5,750	6,750	7,620
6	1/2	3/4	22.7	9.97	12,694	38.64	6	1 3/4	4	49.0	16.31	2.215	52.577	17.525	2.296	3.31	0.834	1.50	7,390	6,000	7,050	8,000
7	3/16	3/4	26.7	4.64	5,906	17.98	6	1 7/8	4	34.3	9.80	2.719	36.692	10.483	2.812	3.98	1.792	2.344	5,410	5,170	6,050	6,870
7	1/4	3/4	26.7	6.14	7,814	23.79	6	1 7/8	4	44.7	12.77	2.699	47.796	13.656	2.791	3.97	1.354	1.857	6,250	5,800	6,800	7,700
7	5/16	3/4	26.7	7.61	9,689	29.50	6	1 7/8	4	54.6	15.59	2.678	58.386	16.682	2.770	3.95	1.092	1.578	6,950	6,300	7,380	8,380
7	3/8	3/4	26.7	9.06	11,532	35.11	6	1 7/8	4	64.0	18.28	2.658	68.472	19.563	2.750	3.93	0.918	1.423	7,570	6,650	7,760	8,800
7	1/2	3/4	26.7	11.88	15,127	46.05	6	1 7/8	4	81.4	23.27	2.618	87.163	24.904	2.709	3.89	0.700	1.290	8,675	6,975	8,160	9,250
8	3/16	3/4	30.7	5.35	6,816	20.75	6	2	4	52.2	13.05	3.123	55.705	13.926	3.266	4.57	1.553	2.056	6,200	5,890	6,900	7,800
8	1/4	3/4	30.7	7.09	9,026	27.48	6	2	4	68.2	17.05	3.102	72.783	18.196	3.204	4.55	1.172	1.629	7,150	6,610	7,750	8,750
8	5/16	3/4	30.7	8.80	11,204	34.11	6	2	4	83.5	20.89	3.081	89.172	22.293	3.183	4.53	0.945	1.386	7,950	7,170	8,400	9,500
8	3/8	3/4	30.7	10.49	13,351	40.64	6	2	4	98.3	24.57	3.061	104.887	26.222	3.163	4.51	0.793	1.249	8,675	7,550	8,850	10,000
8	1/2	3/4	30.7	13.79	17,552	53.43	6	2	4	125.8	31.45	3.021	134.311	33.578	3.121	4.48	0.603	1.132	9,950	7,950	9,300	10,500
9	3/16	1	34.3	5.99	7,620	23.20	6	2 1/8	4	73.8	16.4	3.513	78.995	17.554	3.633	5.13	1.389	1.858	6,890	6,500	7,640	8,600
9	1/4	1	34.3	7.93	10,098	30.74	6	2 1/8	4	96.7	21.5	3.492	103.438	22.986	3.611	5.12	1.048	1.475	7,930	7,300	8,560	9,650
9	5/16	1	34.3	9.85	12,545	38.19	6	2 1/8	4	118.7	26.4	3.471	127.004	28.223	3.590	5.10	0.843	1.256	8,850	7,900	9,260	10,500
9	3/8	1	34.3	11.75	14,959	45.54	6	2 1/8	4	140	31.1	3.451	149.717	33.270	3.570	5.08	0.707	1.130	9,650	8,350	9,750	11,000
9	1/2	1	34.3	15.47	19,696	59.96	6	2 1/8	4	180	40.0	3.410	192.541	42.787	3.528	5.04	0.537	1.011	11,100	8,800	10,300	11,700
10	3/16	1	38.3	6.70	8,524	25.95	6	2 1/4	4	103	20.5	3.915	109.678	21.936	4.047	5.72	1.241	1.672	7,650	7,200	8,450	9,550
10	1/4	1	38.3	8.88	11,303	34.41	6	2 1/4	4	135	26.9	3.894	143.878	28.776	4.026	5.70	0.936	1.334	8,800	8,050	9,450	10,700
10	5/16	1	38.3	11.04	14,051	42.77	6	2 1/4	4	166	33.1	3.873	176.983	35.397	4.005	5.68	0.753	1.136	9,800	8,750	10,250	11,600
10	3/8	1	38.3	13.17	16,766	51.04	6	2 1/4	4	195	39.1	3.853	209.015	41.803	3.984	5.66	0.631	1.015	10,700	9,250	10,900	12,200
10	1/2	1	38.3	17.36	22,106	67.29	6	2 1/4	4	252	50.5	3.812	269.812	53.962	3.942	5.63	0.479	0.917	12,300	9,700	11,400	12,900
11	3/16	1	42.3	7.40	9,426	28.69	6	2 3/8	4	138	25.1	4.318	147.404	26.801	4.462	6.30	1.123	1.526	8,400	7,850	9,300	10,400
11	1/4	1	42.3	9.82	12,503	38.06	6	2 3/8	4	181	33.0	4.296	193.562	35.209	4.445	6.28	0.846	1.221	9,650	8,800	10,350	11,700
11	5/16	1	42.3	12.22	15,553	47.34	6	2 3/8	4	223	40.6	4.276	238.570	43.376	4.419	6.27	0.680	1.038	10,800	9,550	11,250	12,700
11	3/8	1	42.3	14.58	18,568	56.52	6	2 3/8	4	264	48.0	2.255	282.166	51.303	4.399	6.25	0.570	0.930	10,800	11,050	11,900	13,406
11	1/2	1	42.3	19.25	24,507	74.61	6	2 3/8	4	342	62.1	4.214	365.334	66.424	4.357	6.21	0.432	0.832	13,500	10,600	12,550	14,200

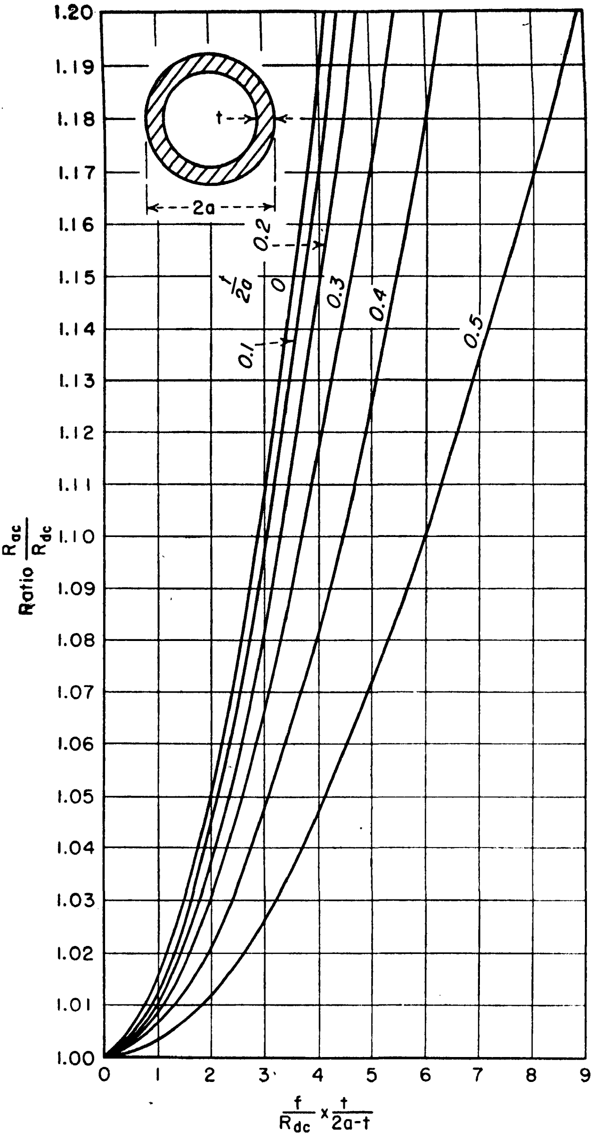

FIG. 160*a*. Resistance ratios of isolated hollow round copper conductors at 70°C. Resistances in microhms per foot.

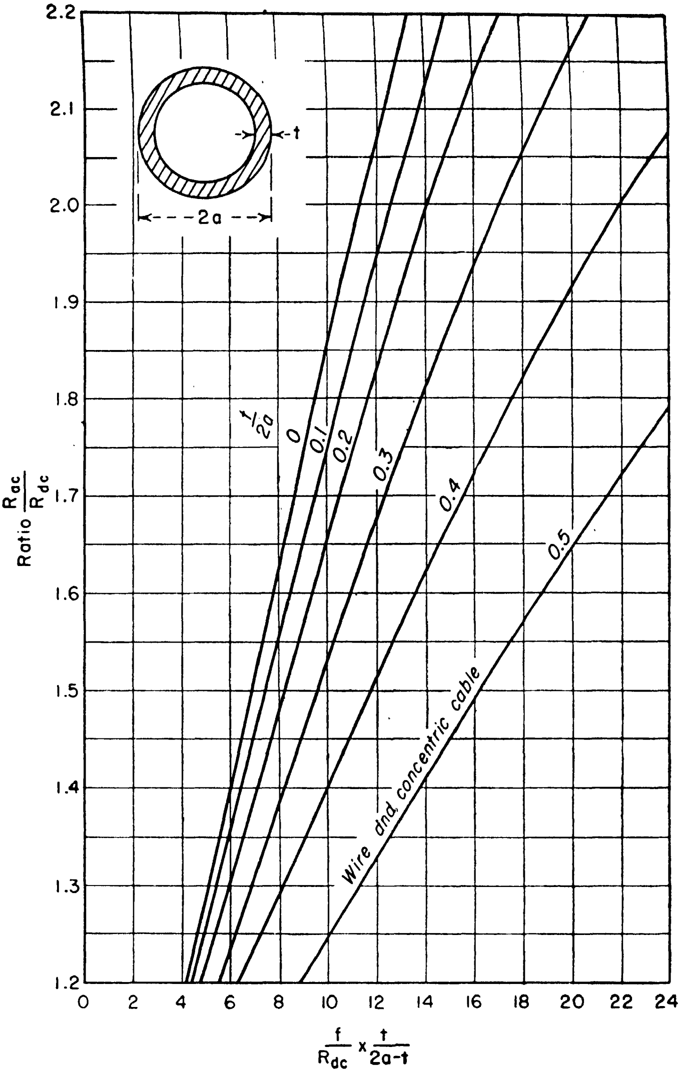

FIG. 160*b*. Resistance ratios of isolated hollow round copper conductors at 70°C. Resistances in microhms per foot.

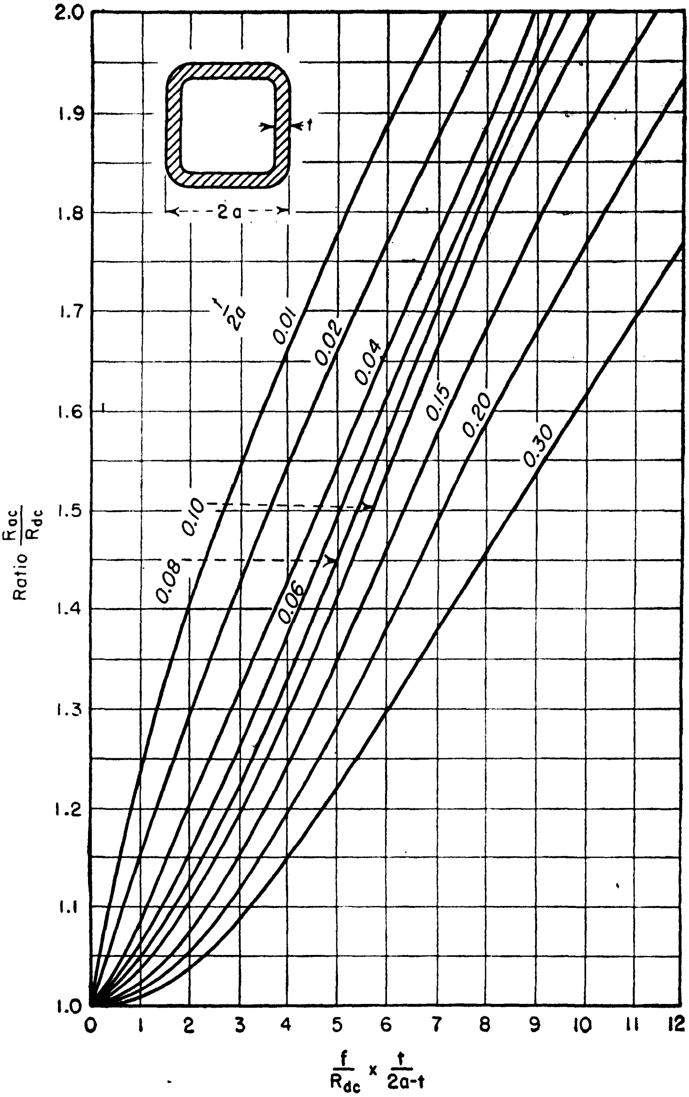

FIG. 161. Resistance ratios of isolated hollow square copper conductors at 70°C. Resistances in microhms per foot.

INDEX

A

Air gap, 51
Air-gap ratio, 51
Alloys, 14–15
Alternating-current resistance, 164
  (*See also* Resistance, power circuits)
Appendixes, 185
Applications, Class A service, 107
Assemblies, 2, 61
Auxiliary devices, 57

B

Base dimension, 6
Base frequency, 103
Basic principle, 91
Brazing, 122

C

Calculations, 76
Capacitance, 68
Cardinal relations, 6
Charges, 2, 28, 48, 107, 108, 132
Circuit analysis, air-gap ratio as a variable, 94
  charge resistivity as a variable, 84–94
    basic principle, 91
    effective impedance, 87
    effective reactance, 86
    effective resistance, 85
    efficiency, electrical, 88–89
    power, 90
    power factor, 88
    secondary resistance, 84
  frequency as a variable, 98–106
    base frequency, 103
    current, 103
    effective impedance, 98
    effective reactance, 98
Circuit analysis, frequency as a variable, effective resistance, 98
    efficiency, electrical, 98–101
    power factor, 99
    power ratio, 99
    voltage, 105
    volt-amperes, 106
  magetizing current as a variable, 94–97
    effective impedance, 95
    effective reactance, 62, 95
    effective resistance, 62, 95
    index ratio, 95
    power, 95
Circuit equations, induction heating, 61–76
    hollow cylindrical charge, 75
    rectangular charge, 75–76
    solid cylindrical charge, 63–74
  power circuits, 160–182
    coaxial conductors, 178–180
    hollow round conductors, 168–172
    hollow square conductors, 172–174
    rectangular conductors, 174–178
    solid round conductors, 165–167
Circuits, 62, 149
Class A service, 9, 107
Class B service, 9, 132
Comparison of hollow round and hollow square conductors, 174
Conductivity, electrical, 10
  thermal (*see* Thermal conductivity)
Conductors, for coils (*see* Primary coils)
  for power circuits, 160
Continuous heating, 10
Convection, 46
Coreless induction furnace, 2, 133–152
  artificial atmospheres, 145
  circuit, 149
  crucibles, 135
  floor plan, 142
  frame, 136

Coreless induction furnace, frequency, 149
  installations, 143
  operation, aftercharging, 145
    charging, 145
    efficiency, 147–148
    filling coefficient, 145
    losses, 146
    melting rates, 146
    stirring, 146
  power-time relation, 150
  primary coils, 136
  rated index ratio, 150
  service, 143
  special features, 149
  standard furnaces, 142
  types, 140–142
Cross-flux watts, 36
Curie point, 25
Current density, charges, 37
  power conductors, 161
Current distribution, charges, 3
Current ratings, bare power conductors, 160–163
  insulated power conductors, 163

D

Degassing tubes, 122
Diffusivity, thermal, 27
Direct-current resistance (*see* Resistance, power circuits)
Directional effect, 35

E

Eddy-current watts, 7, 30
Effects of heat, 10
Efficiency, conversion, 70, 147
  electrical, 70
  over-all, 148
  thermal, 47
Electrical separation of power conductors, 180
Electronic oscillators, 8
Equations (*see* Circuit equations)
Equilibrium temperature, 42
Excitation curves, alternating current, 19

F

Flux distribution, 3
Frequencies, lower limit, 109
  selection of, 108–114
  standard, 8, 109, 150
Frequency, 8, 103, 111, 149
  60 cycles, 111
Frequency combinations, 112

G

Glass, 18
Grain size in steel, 15

H

Hardening and tempering steel, 127
Hardness in steel, 26
Heat, 10
Heat concentration, 37–39
Heat content, 44
Heat contents, of carbon steels, 200
  of metals, 45
Heat cycle, 10, 42
Heat development, 28
  in volume V_p, 39
Heat loss, 46–47, 146
Heating, magnetic charges, 97
  nonmagnetic charges, 92
  of power conductors, 160
Heating aluminum, 124
Heating density, charges, 37
Heating metals, brazing, 122
  forging, 116, 125
  soldering, 122
  surface hardening, 117
  upsetting, 116, 124
Heating rates, 113, 115
Heating steel, 125, 127
Historical note, 1
Hysteresis, 28
  and frequency, 28
  and temperature, 30

I

Impedance (*see* Circuit equations, induction heating)

Index ratio, 6, 48, 150
Inductance, power circuits, 163, 167, 171, 173, 177, 179, 180
Induction furnaces, 133
Induction heaters, 48, 58
Induction heating, 1
Inductors (*see* Primary Coils)
Instrumentation, 57
Internal hardening, 119
Internal heating, 131
Internal stress, 113
Iron, 15

L

Long charge, 48
Longitudinal flux, 3

M

Magnetic charges, 28
Magnetic fields, 2
Magnetic property, 19, 94
Magnetic shields, 57
Magnetization curves, 19
Mass effect, 40
Mass heating, 108
Melting furnaces, 133
Melting metals, 132
Metal classification, 132
Methods of heating, 10

O

Operating conditions, Class A service, 107
Operation, coreless induction furnace, 145
  submerged resistor furnace, 152
Optimum radial thickness, coil conductor, 64

P

Permeability, 24
  and temperature, 25
Plant economics, 113
Pouring temperatures, 132
Power-circuit conductors, 160
Power density, 115
Primary coils, 49–56, 130, 136
  air-gap ratio, 51
  capacitance, 68
  coil dimensions, 50
  conductor dimensions, 54, 64
  conductor material, 51
  conductor shapes, 52
  conductor temperature, 52
  cooling water, 52
  graded coils, 51
  loaded coil, 67
  number of turns, 50, 71
  space factor, 51
  taps, 51
  types, 50
Protection, 112
Proximity effect, 165

R

Radiation, 46, 162
Rated index ratio, 48, 150
Ratings of power conductors, 161–163
Reactance (*see* Circuit equations, induction heating)
Reference dimension, 6
References, 183
Resistance, induction heating (*see* Circuit equations)
  power circuits, 163–179
    alternating-current resistance, 164, 165, 168, 170, 172–174, 178
    direct-current resistance, 165, 168, 172, 174
Resistivity, alloys, 14
  ferrous alloys, 15, 195–199
    alloy steels, 197
    carbon steels, 15, 195, 197
    iron-aluminum, 199
    liquid steel, 16
    silicon steels, 15, 199
    stainless steel, 15
  metals, 12, 187–189
    copper, 164
    iron, 15
  nonferrous alloys, 14, 190–194
    copper, 14, 191–193
    monel metal, 190

Resistivity, nonferrous alloys, nickel-chromium, 190
Rotating machines, 8

S

Selection, of frequency, 108–114
  of power conductors, 182
Service, 8, 9, 107, 132, 143, 159
Shape effect, 35
Shape factors, 31–33
Shape of charge, 2
Short charge, 48
Single-phase load, 61
Skin effect, 164
Soldering, 122
Spark-gap apparatus, 8
Standard frequencies, 8, 109, 150
Stationary heating, 10
Submerged resistor furnace, batch type, 152
    design for melting aluminum, 156
    design for melting brass, bronze, copper, 153
    operation data, 154
  continuous type, 156
    energy required, 158
    general construction, 157
    holding or pouring furnace, 158
    rate of melting, 158
    service, 159
    standard sizes, 158
Surface hardening, 117, 123
Surface heating, 117
Surface-volume ratio, 41

T

Temperature, coil conductors, 52
  power conductors, 160
Temperature equilibrium, 42
Temperature gradient, 40
Temperature rise, charges, 40
Temperature scales, 10
Temperatures, absolute, 10
Thermal conductivity, 26
  alloy steels, 198
  carbon steels, 198
  copper alloys, 191
  iron-aluminum alloys, 199
  iron-silicon alloys, 199
Thermal diffusivity, 27
Thermal efficiency, 47
Thermal properties, 26
Thick and thin bodies, 108
Thin-wall tubes, 102

V

Vacuum furnaces, 142
Volt-amperes (*see* Circuit equations, induction heating)
Volume V_p, 37